Faculty of Engineering, Computer and Mathematical Sciences

School of Mechanical Engineering

Brace for it: assessing lumbar spinal loads for a braced arm-to-thigh lifting and bending technique using a musculoskeletal modelling approach

Erica Beaucage-Gauvreau

A thesis submitted in fulfilment of the requirements for the degree of Doctor of Philosophy

June 2019

Declaration

I certify that this work contains no material which has been accepted for the award of any other degree or diploma in my name, in any university or other tertiary institution and, to the best of my knowledge and belief, contains no material previously published or written by another person, except where due reference has been made in the text. In addition, I certify that no part of this work will, in the future, be used in a submission in my name, for any other degree or diploma in any university or other tertiary institution without the prior approval of the University of Adelaide and where applicable, any partner institution responsible for the joint-award of this degree.

I acknowledge that copyright of published works contained within this thesis resides with the copyright holder(s) of those works.

I also give permission for the digital version of my thesis to be made available on the web, via the University's digital research repository, the Library Search and also through web search engines, unless permission has been granted by the University to restrict access for a period of time.

I acknowledge the support I have received for my research through the provision of an Endeavour Postgraduate Scholarship.

21/03/2019

_____ _____

Signed Dated

Acknowledgements

I would like to acknowledge the Endeavour Postgraduate Scholarships, SafeWork SA, and AOSpine Australia and New Zealand for providing the financial resources required to support this project. There is also a small army behind the work for this PhD thesis, and I would like to thank the following people for their help and support with this project:

First and foremost, I would like to thank my principal supervisor Dr Claire Jones. When I think about our first encounters at UBC (circa 2006-2008), you a PhD candidate/teaching assistant and myself a naive undergraduate student, it's hard to believe that we have ended up here more than a decade later! The last four years of working under your mentorship have been incredibly formative, learning from your intellectual curiosity and rigour in every aspect of research. Thank you for you open door policy, continuous support, and friendship throughout this whole process. You have given me every opportunity to succeed over the past four years and for the next phase of my career.

To Dr Dominic Thewlis, thank you for being so involved with this project. I am particularly grateful for your help with data collection and patience dealing with all the unexpected issues along the way! Thank you for your hard work and encouragement that made this thesis possible. I will always remember your endless positivity!

To Professor Brian Freeman, thank you for giving clinical meaning to my research; it is easy to get caught up with numbers and modelling issues. Thank you for your ongoing encouragement and support throughout this project.

To Professor Robert Fraser, thank you for trusting me to investigate the braced arm-to-thigh technique. Your clinical practice and interest in research have without a doubt positively impacted this project.

To my Canadian collaborators: Dr Ryan Graham and Dr Scott Brandon. Who would have thought that my PhD and Master's acknowledgments would be so similar with respect to both of you? Thank you for your interest in this project. Ryan, thank you for welcoming me into your lab and answering ALL my questions about lifting and spine modelling. Scott, thank you for teaching me everything about

OpenSim, and then some! I always looked forward to your replies to my (many!) emails and was always motivated by your enthusiasm in solving every challenge encountered along the way (we both know there were many)!

Thank you to the current and past members of the Adelaide Spinal Research Group and other collaborators who have made a difference in this project, particularly Adnan Mulaibrahimovic, Dr. Namal Thibbotuwawa, Dr. Will Robertson, and Professor Peter Cripton. Thank you to my summer and honour students, Amie van Antwerpen, Danika Hunt, Zern Lee, and Mingyue Liu for your contributions to this project and for giving me an insight into the rigours of student supervision. Thank you to the electrical and mechanical machine shop staff, especially Pascal Symmonds, for assisting with the design and build of various components needed for this project. Thank you to Suzanne Edwards and Jana Bednarz for helping me to demystify statistics.

To the Adelaide Biomechanics crew, including Flinders Uni and UniSA members, (Amy Lewis, Jas Bahr, Dhara Amin, Dermot O'Rourke, Bryant Roberts, Arj Sivakumar, Jordan Yeomans, Kieran Bennet, Tommy Grace) for providing a stimulating environment and attending Journal Club! Thank you to Sam Sobey, Dave Haydon, Parham Foroutan, and Ryan Quarrington for endless banter at Friday lunches, ISB in Brisbane, and every other event that made this PhD journey much more enjoyable. A special VIP mention to Dr Ryan Q for your teachings over the last four years, despite your young age (!). I could not have asked for a better lab mate, always ready to help me resolve technical issues, while also providing balance to the hard work with footy games, beers, and showing me the real Aussie way!

To the Adelaide Running Crew and WoW ladies, for your friendship and making Adelaide feels like home so quickly. The last four years have been an incredible experience and you are a big reason for it. To all my friends back home, for ignoring the distance between us and keeping in touch, despite long silences between conversations. You have helped me preserve (some of) my sanity!

To my family, thank you for always rooting for me, even from the other side of world. Denis, a special thanks for your contagious excitement about "innovation" and ultimately preparing me for this experience in academia. Mom, for always being a source of comfort, even through Skype. Thank you

for flying here to help me finish this PhD, while caring for a newborn. Thanks to my little bro Franky for distracting me from my work with Facetime calls that I enjoyed more than you probably know. To Dave, for endless laughers and showing me that not everything needs to be planned in life to succeed. To Sarah for being such a good role model, and always providing encouraging words! To the Hum-Pattersons for welcoming me into the family since the very first day I met you.

Finally, and most importantly, I would like to thank my husband, Sean. From leaving the comfort of Canada to the complete unknowns of Australia for this PhD, to welcoming our first child a few weeks ago, and cheering me on through all the highs and lows in between, I cannot imagine this journey without your unconditional support. Thank you for always making everything better. To our little Britta, the last 10 months have been a wild ride, but ultimately you gave me the strength to keep going.

Abstract

Manual material handling activities that involve forward bending and lifting have been identified as risk factors for the development of low back pain, due to the spinal loads and postures experienced during these tasks. Several activities of daily living, such as lifting light-to-moderate objects, gardening, and cleaning, require forward bending and lifting. Many of these tasks can be performed with one hand, therefore allowing for trunk support by placing the free hand on the ipsilateral thigh. This "braced arm-to-thigh technique" (BATT) could especially benefit individuals with low back pain (LBP). However, the BATT has not been evaluated biomechanically in this specific population, and has not been evaluated when applied to tasks other than lifting. The overall goal of this thesis was to evaluate the effect of a bracing force, applied by the hand on the ipsilateral thigh, on lumbar spine loading and trunk kinematics for symmetrical and asymmetrical bending and lifting tasks, using a newly developed and validated full-body musculoskeletal model with a detailed lumbar spine.

In Study 1 (Chapter 4), an OpenSim full-body model was developed and validated by adapting an existing OpenSim jogging model to be suitable for lifting motions. Muscle activations predicted by the resulting Lifting Full-Body (LFB) model were directly compared to muscle activations measured with electromyography (EMG), during various lifting tasks. Good agreement, both with respect to pattern and timing, was observed for the back musculature. Comparison between model estimates of intradiscal pressures (IDP) and *in vivo* IDP measurements also showed strong agreement. The spinal loads estimated by the model matched the trends reported for vertebral body replacement (VBR) measurements in older individuals for similar lifting tasks. This study demonstrated that the LFB model is suitable to evaluate changes in lumbar loading during symmetrical and asymmetrical lifting.

In Study 2 (Chapter 5), trunk kinematics and L4/L5 spine loading for the BATT were compared to those of three common unsupported two-handed and one-handed lifting techniques for two loading conditions (2 kg and 10 kg), in 20 healthy participants (30-70 years old) matched in age and gender to 18 participants. The thigh bracing force, measured by a load cell secured to the thigh with a custom apparatus, significantly reduced L4/L5 extension moments, compressive and antero-posterior (AP)

shear forces, compared to unsupported lifting techniques. However, the BATT technique also increased asymmetrical L4/L5 moments and trunk angles.

In Study 3 (Chapter 6), the BATT was adapted to three activities of daily living (ADLs) to understand the effect of thigh bracing on lumbar loading and spine kinematics in tasks other than lifting. These three tasks, namely weeding (gardening), reaching for objects in low cupboards, and car egress, were simulated in the laboratory, using custom apparatus, by ten healthy young males. The BATT reduced L4/L5 extension moments, compressive and AP shear forces compared to self-selected techniques.

This thesis presents the first validated full-body OpenSim model suited to estimating lumbar spine loading in symmetrical and asymmetrical lifting tasks, with or without external loads. Using this LFB model, it was demonstrated that the BATT reduces lumbar extension moments, compression and AP shear forces for lifting tasks and other ADLs, compared to unsupported techniques, for healthy and LBP populations.

Table of Contents

List of Tables

List of Figures

List of Abbreviations

1ST	One-handed stoop
2SQ	Two-handed squat
2ST	Two-handed stoop
3D	Three-dimensional
ε^T	Tendon strain
ADL	Activity of daily living
AP	Antero-posterior
API	Application program interface
AR	Axial rotation
ASIS	Anterior superior iliac spine
BATT	Braced arm-to-thigh technique
BMI	Body mass index
CE	Contractile element
CF	Correction factor
CSA	Cross-sectional area
DOF	Degree-of-freedom
EMG	Electromyography
EO	External obliques
ES	Erector spinae
F^T	Tendon force
F^M	Muscle force
FABQ	Fear-avoidance belief questionnaire
FABQpa	Fear-avoidance belief questionnaire physical activity
FABQw	Fear-avoidance belief questionnaire work
FBLS	Full-body lumbar spine
FE	Flexion-extension
FP	Force platform
GUI	Graphical user interface
IAR	Instantaneous axis of rotation
IAP	Intra abdominal pressure
IDP	Intradiscal pressure
ILpL	Iliocostalis lumborum pars lumborum
ILpT	Iliocostalis lumborum pars thoracis
IO	Internal obliques
l^M	Fibre length
l^M_o	Optimal fibre length
l^T	Tendon length
LB	Lateral bending
LBP	Low back pain
LBwrap	Lower back wrapping surface
LC	Loadcell
LD	Latissimus dorsi
LFB	Lifting full-body
LTpL	Longissimus thoracis pars lumborum
LTpT	Longissimus thoracis pars thoracis
MF	Multifidus

ML	Medio-lateral
MMS	Maximum muscle stress
MVC	Maximum voluntary contraction
NIOSH	National Institute for Occupational Safety and Health
ODI	Oswestry disability index
OFL	Optimal fibre length
QE	Quadratic equation
QL	Quadratus lumborum
PCSA	Physiological cross-sectional area
PS	Psoas major
PE	Passive element
RA	Rectus adominus
RMQ	Rolland-Morris questionnaire
RMS	Root mean square
ROM	Range of motion
TSL	Tendon slack length
TTA	Transtibial amputation
VAS	Visual analog scale
VBR	Vertebral body replacement
v^M	Fibre velocity
v_{max}	Maximum shortening velocity
WLT	Weight lifters technique

Publications

A version of Chapter 4 was published in Computer Methods in Biomechanics and Biomedical Engineering: Beaucage-Gauvreau, E., Robertson, W.S.P., Brandon, S.C.E., Fraser, R., Freeman, B.J.C., Graham, R.B., Thewlis, D., Jones, C.F., 2019, https://doi.org/10.1080/10255842.2018.1564819. *Validation of an OpenSim full-body model with detailed lumbar spine for estimating lower lumbar spine loads during symmetric and asymmetric lifting tasks*. Ethical approval was granted by the Royal Adelaide Hospital Research Ethics Committee under Protocol R20170816.

Chapter 1 Introduction

1.1 Low Back Pain

Low back pain (LBP) is a widespread problem that affects more than 80% of the population at some point during their lives (Balague et al., 2012, Jeffries et al., 2007, Auvinen et al., 2009, Rubin, 2007). It is the highest non-fatal burden (years lived with disability) globally (Global Burden of Disease Study, 2015) and the leading cause of work absence, loss of productive life years, and receipt of disability benefits (Brage et al., 2010, Costa-Black et al., 2010, Schofield et al., 2015). In Australia alone, 1 in 6 people had chronic back pain problems in 2014-2015, with 77% of them of working age (15-64 years old) (Australian Institute of Health and Welfare, 2016). The health care costs associated with LBP are substantial (Dagenais et al., 2008, Becker et al., 2010, Gore et al., 2012), encompassing both direct costs (physician services, medications, hospital services, diagnostic testing, etc.) and indirect costs (work absence, reduced productivity, etc.) (Dagenais et al., 2008). Total health-care expenditure attributed to back pain in Australia in 2008-2009 was of $1.2 billion (Australian Institute of Health and Welfare, 2016), with similar figures reported in other Western countries, such as the United Kingdom (£1.632 billion in 1998) (Maniadakis and Gray, 2000) and the United States (>$100 billion in 2006) (Katz, 2006).

Most individuals suffering from LBP return to work reasonably quickly after an acute episode of LBP (Croft et al., 1998). However, 11% of the affected population will go on to develop chronic LBP (pain lasting for 3 months or longer), resulting in a long term disability with little chance to returning to work at all (Airaksinen et al., 2006, Waddell and Schoene, 2004). In addition, recurrence rates of LBP are high, especially in the year after the first acute episode, thus resulting in a burden for society and patients suffering from recurrent disabling episodes (Hides et al., 2001).

1.2 Risk factors for low back pain

The majority of LBP cases are classified as non-specific, meaning that the specific diagnosis has an unknown underlying pathology (Balague et al., 2012, Krismer et al., 2007). The causes of LBP are known to be multifaceted, involving both biomechanical (Marras et al., 1995, Norman et al., 1998, Driscoll et al., 2014) and psychological factors (Bigos et al., 1986). Biomechanical factors are linked to

the initial injury and subsequent episodes of back pain, while psychological factors appear to be more related to subsequent episodes after the initial back pain episode (McGill, 2007).

High loads experienced in the spine can cause injuries to the spinal structures (Ferguson et al., 2002, Waters et al., 1993, Norman et al., 1998) that can take years to recover (Woo et al., 1985). Biomechanical risk factors for the development of LBP include high work intensity, frequent bending, axial rotation, lifting, pushing or pulling, and repetition (Marras et al., 1995). Amongst those risk factors, lifting has received considerable attention in the biomechanics literature, in an effort to prevent manual material handling injuries and reduce subsequent related costs (e.g. work days lost, rehabilitation treatments, etc.) (Wrigley et al., 2005). Interventions in the workplace have focused on the "correct" lifting techniques, despite a lack of convincing efficacy of these measures (Nygård et al., 1998), due to the complexity of lifting (Hsiang et al., 1997).

The squat and stoop lifting techniques have been studied extensively in the literature as they are commonly used in industrial settings for heavy lifting tasks requiring both hands (Figure 1.1). However, one-handed lifts are commonly performed for a number of daily occupational tasks and offer the advantage of trunk support by the free hand. Despite the potential biomechanical advantages of one-handed supported lifting techniques, they have only been evaluated in a limited number of studies (Cook et al., 1990, Kingma and van Dieen, 2004, Ferguson et al., 2002, Wilson et al., 1997). More specifically, the braced arm-to-thigh technique (BATT) (Figure 1.1), in which the individual supports the trunk by applying a bracing force with the free hand on the ipsilateral thigh, has only been evaluated in young healthy males (Kingma et al., 2016). A biomechanical study of the BATT is required to understand its effect on spinal loads and trunk movements for healthy individuals and individuals suffering from chronic LBP, in the adult population. Moreover, several activities of daily living (ADLs) require frequent forward bending, and the BATT technique may be applied to these. However, it has never been evaluated for tasks other than lifting. A biomechanical investigation is necessary to understand the applicability of the BATT to other ADLs, and to evaluate its effect on spinal loading and trunk kinematics.

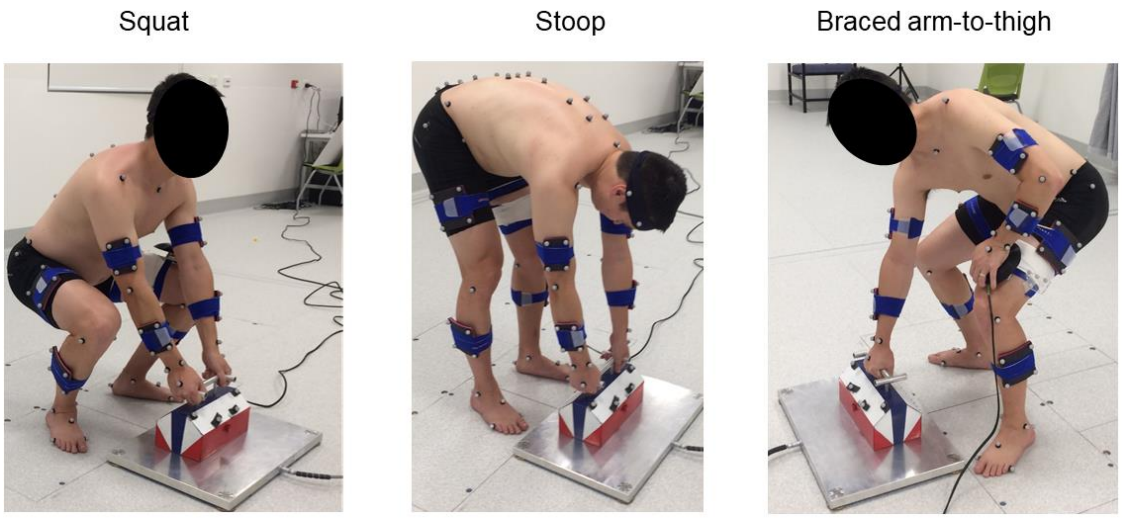

Figure 1.1 Two-handed squat, two-handed stoop, and braced arm-to-thigh lifting techniques.

1.3 Musculoskeletal Models

Knowledge of spinal loading during lifting and forward bending is essential to improve the understanding of the injury mechanisms and to develop guidelines that will reduce the risk of injury at home and in the workplace. However, one of the main challenges when studying the spine is that loads, strains, and stresses experienced by its various components cannot be measured directly unless invasive techniques are used (Dreischarf et al., 2015, Wilke et al., 2001, Sato et al., 1999, Takahashi et al., 2006). Alternatively, musculoskeletal models are a non-invasive mathematical method to estimate joint loading using experimental data inputs. Models are widely used in the field of biomechanics to simulate and analyse various lifting tasks (Bassani et al., 2017, Potvin et al., 1991, Kingma and van Dieen, 2004). Over the years, model complexity has increased to better represent the various anatomical structures of the lumbar spine, thus improving the evaluation of joint loads compared to simple static rigid body models (Bogduk et al., 1992a, Cholewicki et al., 1995, de Zee et al., 2007, Abouhossein et al., 2011). However, these models are generally not widely available to the biomechanics community as many laboratories develop their own simulation software and retain proprietary rights (Delp et al., 2007).

In an attempt to accelerate the development and sharing of simulation technology, a freely available open-source modelling and simulation software called OpenSim (SimTK, Stanford, CA) was created in 2007 (Delp et al., 2007). Despite the large database, none of the models currently available on the public OpenSim directory were developed or validated for the evaluation of spinal loading during symmetrical

and asymmetrical lifting tasks. Appropriate validation for specific activities is needed for modelling studies to help prevent erroneous conclusions.

Consequently, there is a need for a validated full-body OpenSim model appropriate to perform a biomechanical analysis of one-handed and two-handed lifting techniques.

1.4 Aims

The central aim of this thesis was to perform a biomechanical investigation of a braced arm-to-thigh technique during lifting and other activities of daily living, using a musculoskeletal modelling approach. Three interrelated studies were undertaken in this thesis to address this central aim. The specific aims and hypotheses for these three studies were:

Aim 1*: To develop and validate a full-body model in the open-source modelling software OpenSim, capable of estimating lumbar spinal loads during symmetrical and asymmetrical lifting tasks.*

Aim 2a*: To compare trunk kinematics and L4/L5 spinal loads for the BATT to common unsupported squat and stoop lifting techniques for a LBP and healthy group, aged 30-70 years old.*

Hypothesis 2a: The hand support on the thigh will reduce spinal loads at L4/L5, compared to unsupported lifting techniques, for healthy and LBP groups

Aim 2b*: To compare the magnitude of the bracing force applied by the LBP and healthy groups.*

Hypothesis 2b: Participants with LBP will use a higher bracing force than healthy participants during BATT lifting.

Aim 3a*: To design and construct apparatus to compare trunk kinematics and L4/L5 spinal loads between self-selected techniques and the BATT, when adapted to common ADLs simulated in the laboratory.*

Hypothesis 3a: The hand support on the thigh will reduce spinal loads at L4/L5, compared to unsupported techniques for the simulated ADLs.

Aim 3b*: To investigate the effect of the bracing force magnitude on spinal loading.*

Hypothesis 3b: Higher bracing forces will be associated with lower spinal loading for simulated ADLs using the BATT.

1.5 Thesis Structure

The chapters of this thesis comprise both traditional thesis chapters and independent manuscripts. Figure 1.2 illustrates the overall structure of this thesis.

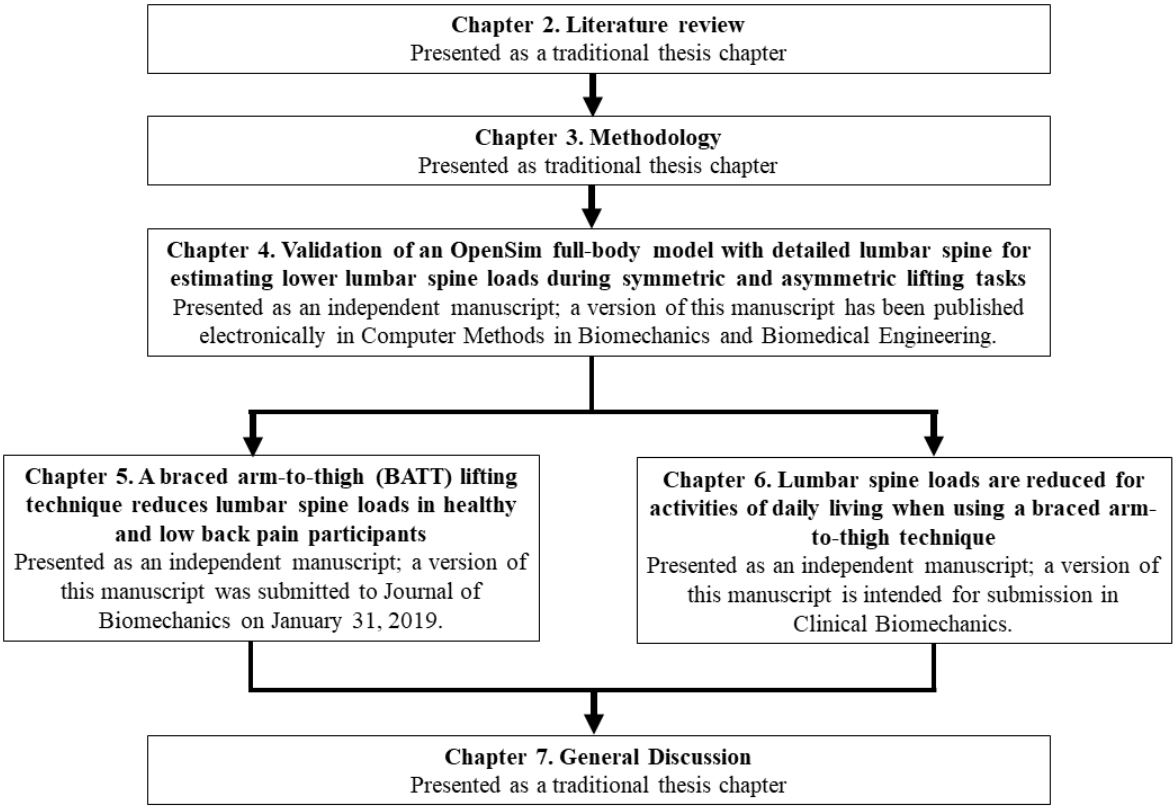

Figure 1.2 Structure of the chapters included in this thesis.

Chapter 2 Literature Review

This literature review provides an overview of musculoskeletal modelling of the lumbar spine, and how such modelling has been used to study different lifting tasks and activities of daily living with respect to biomechanical risk factors. This chapter is divided into four sections. First, a basic anatomical review of the lumbar spine, including its main components and movements, is given. This is followed by a description of how these components are modelled in lumbar musculoskeletal models, and a discussion of the main modelling approaches used to contend with the indeterminacy caused by the large number of spinal structures that can counteract the external moments about an intervertebral joint. This modelling section also includes a critical review of several lumbar spine models in the biomechanics literature. Next, the outcomes of biomechanical studies of one-handed lifts and other activities of daily living are reviewed. The chapter concludes with an overview of the thresholds used to evaluate injury risk associated with manual material handling tasks.

2.1 Anatomy and function of lumbar spine

The lumbar spine is composed of five vertebral bodies, named numerically as one to five from cranial to caudal, i.e. L1, L2, L3, L4, and L5 (Figure 2.1). Adjacent vertebrae are separated by an intervertebral disc, forming an intervertebral joint numbered according to the adjacent vertebrae. The most cranial joint (T12/L1) is called the thoraco-lumbar joint, while the most caudal joint (L5/S1) is called the lumbosacral joint. The lumbar spine is curved in the sagittal plane between the superior endplate of the L1 vertebra and the superior endplate of the sacrum creating the lumbar lordosis, with typical angles of 49-61° in the upright standing posture (Adams et al., 2006) (θ in Figure 2.1B). As a result of the lordosis, the L4/L5 and L5/S1 intervertebral joints are at 45° to the horizontal (Bogduk, 2005).

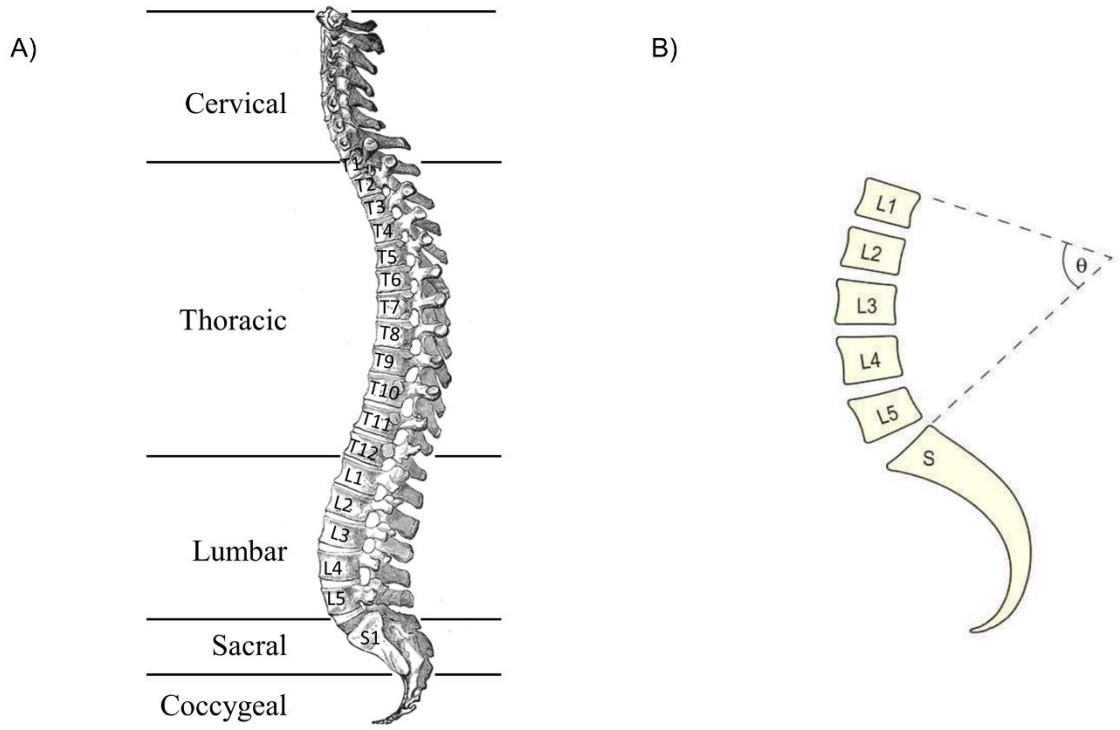

Figure 2.1 A) There are 33 vertebrae in the vertebral column, classified into five distinct regions: 1.Cervical (neck): 7 vertebrae; 2.Thoracic: 12 vertebrae; 3.Lumbar: 5 vertebrae; 4.Sacral: 5 fused vertebrae; 5. Coccygeal: 4 typically fused vertebrae. Image adapted from Gray (1918) (Copyright expired); B) The angle between the upper surface of the L1 vertebra and the top of the sacrum, θ, is typically within 49-61° for standing postures. Image adapted from Adams et al. (2006) with permission from Copyright Elsevier.

Each vertebra is composed of three functional components: vertebral body, pedicles, and posterior elements (Figure 2.2). The vertebral body can withstand large loads in compression; it is formed by an outer shell of cortical bone, reinforced internally by narrow struts of trabeculae, and vertebral end plates (thin plates of cortical bone perforated by many small holes) at the top and bottom of the vertebral body. The pedicles connect the vertebral body to the posterior elements, transmitting both tension and bending forces. The pedicles are stout pillars of bone designed to sustain these forces. The posterior elements comprise the laminae and spinous processes. The laminae are a plate of bone extending from each pedicle towards the midline, where they fuse seamlessly to form the roof of the vertebral foramen, a channel behind the vertebral body. As such, the laminae offer a bony protection to the neural contents of the vertebral canal. The articular processes provide an important locking mechanism between consecutive vertebrae (zygapophyseal/facet joint) that limits forward sliding during flexion and

excessive axial rotation. The spinous, transverse, accessory, and mammillary processes provide areas for muscle attachments.

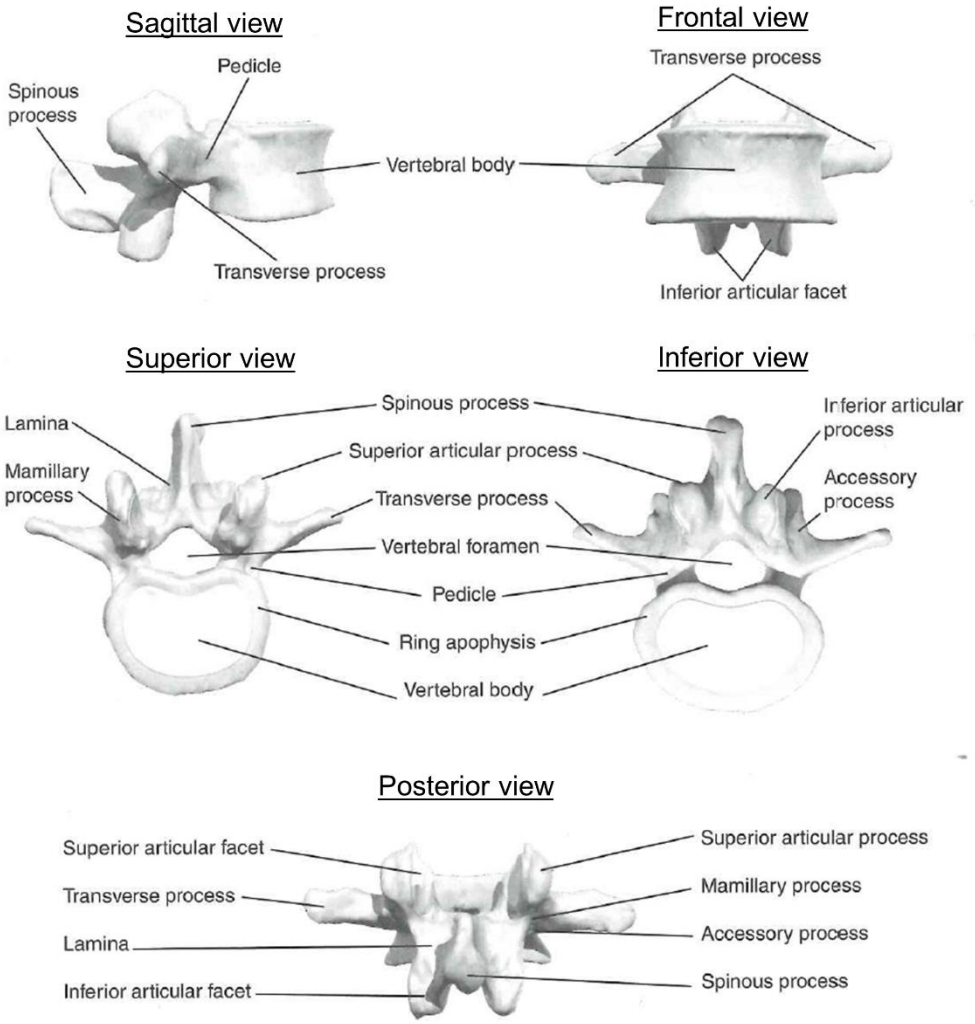

Figure 2.2 Anatomy of a typical lumbar vertebra, with its various components. Image adapted from Figure 4.2 from McGill (2007) (Copyright Restrictions).

The intervertebral disc interfaces with the vertebral end plates from the inferior and superior vertebra. The disc consists of the nucleus pulposus, a gel-like substance in the central portion of the disc, and the annulus fibrosus, a ring of fibrous tissue and fibrocartilage surrounding the nucleus. The disc is capable of withstanding compressive forces, as well as torsional and bending moments, applied to the column. The load through the intervertebral discs is distributed uniformly over the vertebral end plates of the inferior vertebrae. The intervertebral discs in the lumbar region have greater height in comparison to

other regions, with the highest found at the L4/L5 and L5/S1 joints, in a wedge shape that is thicker ventrally than dorsally (Hamill and Knutzen, 2006).

2.1.1 Muscles

Muscles are the only active force generating component of the lumbar spine, and are typically composed of several fascicles. The force produced by a fascicle depends on its fibre architecture, orientation, and physiological cross-sectional area (PCSA), calculated as $\frac{Muscle\ volume}{Muscle\ length}$ and representing an average cross-sectional area of a muscle. The maximum isometric force produced by a muscle fascicle is represented by $F_{max} = K \times PCSA$, where K is the maximum muscle stress (MMS) (Bogduk et al., 1992a). The true value for K is unknown, with estimates varying between 30-140 MPa (Bogduk et al., 1992b, Holzbaur et al., 2005). PCSA is difficult to obtain with few studies reporting the experimental data. As such, cross-sectional area (CSA) obtained from magnetic resonance imaging (MRI) or computed tomography (CT) imaging have been used to determine the force a muscle can produce (Granata and Marras, 1993). However, using *only* CSA can lead to underestimation or overestimation of forces, rather than an average (Gatton et al., 1999).

The line of action and moment arm of a fascicle is determined by its attachment points, thus affecting its capacity to produce a moment. The attachment sites and anatomical description of each spinal muscle fascicle is typically gathered from several anatomical studies that performed detailed cadaveric dissections (Bogduk, 2005, Macintosh et al., 1986, Phillips et al., 2008, Bogduk et al., 1992b, Bogduk et al., 1998). However, these data are a small, heterogenous sample, often not representative of a broader population, especially given that the number and positions of muscle fascicles are not consistent across individuals. In addition, such dissections are performed with the body prone or supine, while moment arms change with posture and therefore need to be adjusted for upright and flexed postures.

The main trunk muscles in the lumbar region are the erector spinae (composed of longissimus thoracis and iliocostalis lumborum), multifidus, quadratus lumborum, psoas major, latissimus dorsi, rectus abdominus, internal obliques, and external obliques. The fascicles of the erector spinae, multifidus,

psoas major, quadratus lumborum are illustrated in Figure 2.3, while the attachment points for the trunk muscles are described in Table 2.1.

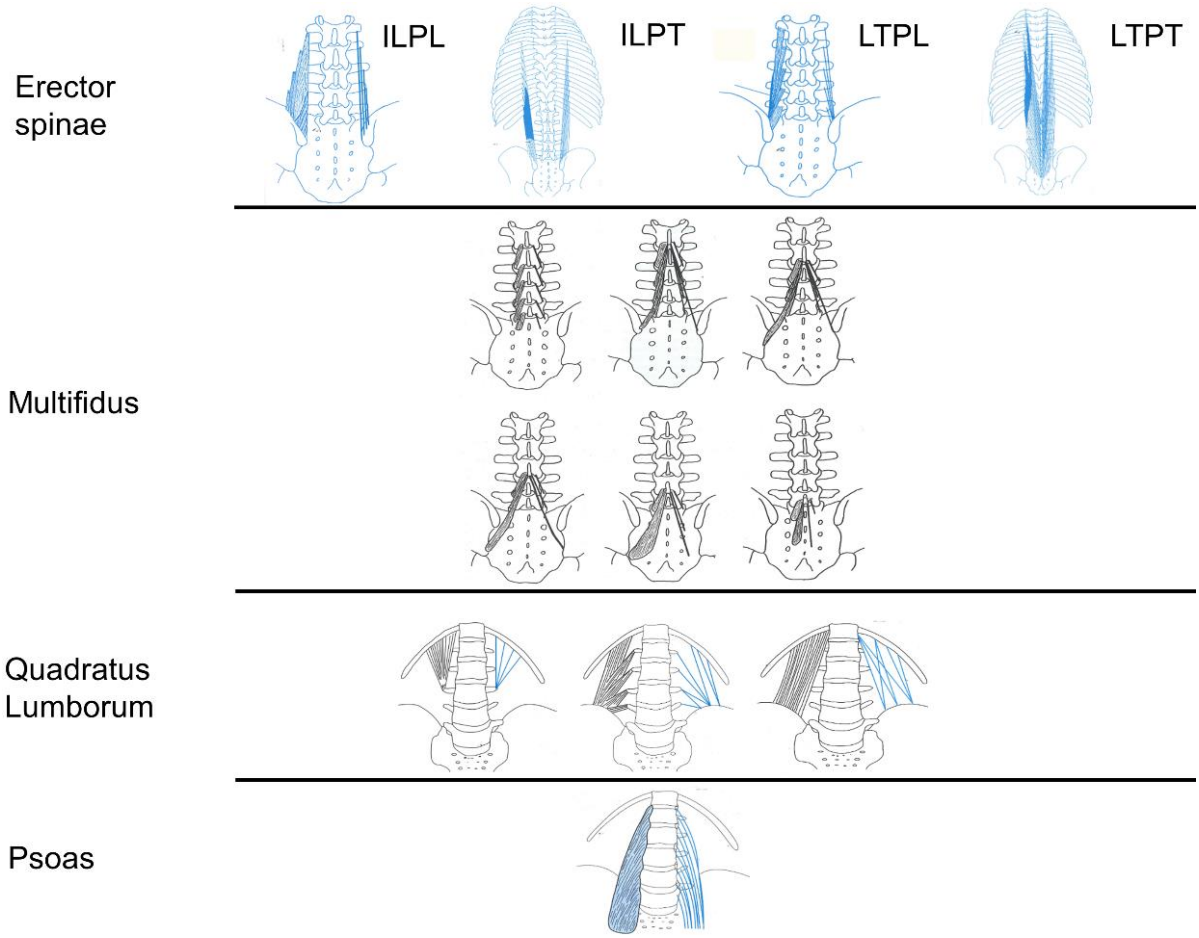

Figure 2.3 The lumbar fibres (left) and corresponding muscle fascicles (right) for Longissimus thoracis pars lumborum (LTpT), Longissimus thoracis pars thoracis (LTpL), Iliocostalis lumborum pars lumborum (ILpL), Iliocostalis lumborum pars thoracis (ILpT), Psoas Major, Quadratus Lumborum, Multifidus. The quadratus lumborum fascicles are arranged in three layers:posterior layer, middle layer, and anterior layer. Images adaped from Bogduk (2005) with permission from Copyright Elsevier.

Table 2.1 Muscles acting on the lumbar spine with their respective attachment points and number of fascicles, as well as their primary actions (Hamill and Knutzen, 2006). The primary action of the Latissimus Dorsi remains controversial.**

Muscle	Attachments	# of fascicles/ side	Primary action
Longissimus thoracis pars lumborum	Transverse processes of L1-L5 to iliac crest	5	Extension Lateral bending
Longissimus thoracis pars thoracis	Ribs; transverse processes of T1 or T2 to T12	11 or 12	Extension
Iliocostalis lumborum pars lumborum	Sacrum; spinous processes of L1-L5, T11, T12; iliac crest to lower 6^{th} or 7^{th} ribs	4	Extension Lateral bending
Iliocostalis lumborum pars thoracis	Lower 7-8 ribs to iliac crest; sacrum	8	Extension Lateral bending
Psoas major	Bodies of T12; L1-L5; transverse processes of L1-L5; inner surface of ilium, sacrum to lesser trochanter	10-11	Hip flexor
Quadratus lumborum	Iliac crest; transverse process of L2-L5 to transverse process of L1-L2; last rib	18	Lateral bending
Multifidus	Sacrum, iliac spine; transverse processes to spinous processes of L1-L5	22	Extension Lateral bending
Latissimus dorsi	Spinous processes of T8-L5; ribs, iliac crest to humerus	13	**
Rectus abdominus	5^{th}-7^{th} costal cartilage and xiphoid process to pubic crest and syphysis	1	Flexion
External obliques	9^{th}-12^{th} ribs to anterior superior spine; pubic tubercle; anterior iliac crest	6	Flexion Lateral bending Axial rotation
Internal Obliques	Iliac crest, lumbar fascia to ribs 8-10, linea alba	6	Flexion Lateral bending Axial rotation
Transverse abdominus	Last 6 ribs; iliac crest; inguinal ligament; lumbodorsal fascia to linea alba; pubic crest	N/A	Stabiliser

While the function of the erector spinae and multifidus as extensors of the trunk is well established, the roles of other muscles in the lumbar spine, and their resulting action on the intervertebral joints, remain controversial. The psoas major is thought to act as a flexor of the hip, whereby the lumbar spine provides a solid base (Adams et al., 2006, Bogduk et al., 1992b) and to provide stability to the lumbar spine through bilateral activation and compressive loading (Santaguida and McGill, 1995). The precise function of the quadratus lumborum remains undetermined due to the small size of its fascicles and their limited number, but it is thought to act as a stabiliser of the lumbar spine (McGill et al., 1996). The function of the latissimus dorsi on the lumbar spine is controversial, some believe that it acts as

major stabiliser, while others believe it does not exert any forces on the lumbar spine since very few fascicles cross the lumbar spine (Adams et al., 2006, McGill, 2007).

The intersegmental muscles (interspinales, intertransversarii mediales, intertransversarii laterals dorasales, and intertransversarii lateral ventrales) are very small muscles that attach on various processes of adjacent vertebrae (Adams et al., 2006) (Figure 2.4). Due to their small size, these muscles are not responsible for the execution of movements of the lumbar spine; they are believed to only serve a sensory role (McGill, 2007).

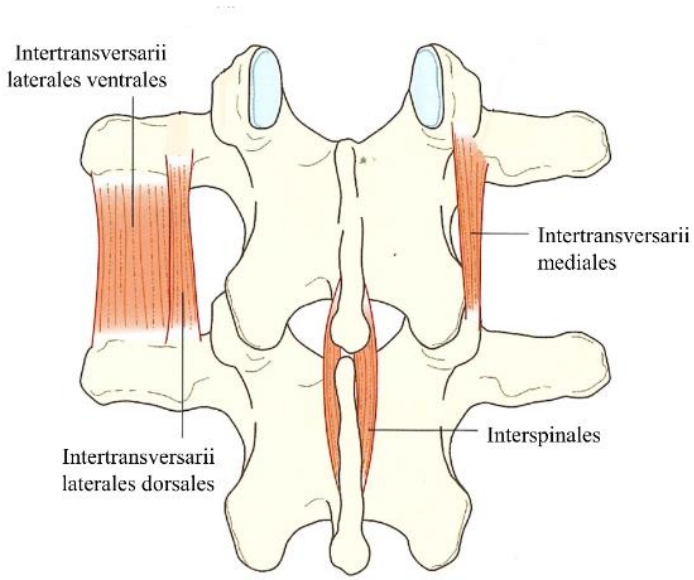

Figure 2.4 The short intersegmental muscles: interspinales, intertransversarii mediales, intertransversarii laterals dorasales, and the intertransversarii lateral ventrales. Image adapted from Adams et al. (2006) with permission from Copyright Elsevier.

2.1.2 Ligaments

Spinal ligaments are passive structures, exhibiting nonlinear viscoelastic mechanical properties. They can sustain high tensile forces when stretched beyond their slack length. There is limited information on their mechanical properties available in the literature (de Zee et al., 2007, Hansen et al., 2006, Christophy et al., 2012). Consequently, the contribution of ligaments to extension moments in the lower back is difficult to estimate as the forces depend on a highly non-linear behaviour as a function of angles, that varies considerably across individuals (Dolan and Adams, 1993). Nonetheless, their contribution to the extension moment is low compared to muscles (Potvin et al., 1991). Their

contribution is higher in a round-back posture (such as stoop lifts) than in a flat-back posture (such as squat lifts) (Potvin et al., 1991), as they are stretched beyond their slack length.

The ligaments in the lumbar spine are the ligamentum flavum, capsular, posterior longitudinal, anterior longitudinal, interspinous and supraspinous ligaments (Figure 2.5). These ligaments, with the exception of the anterior longitudinal ligament, lie posterior to the centre of rotation in the sagittal plane, and therefore, their primary action is to prevent excessive lumbar flexion. Conversely, the anterior longitudinal ligament helps to resist extension movements.

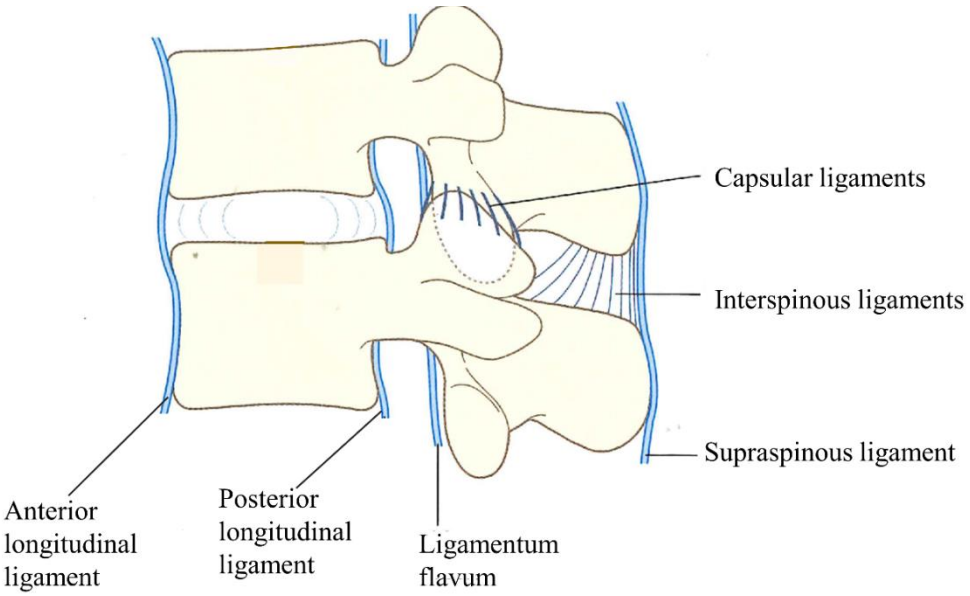

Figure 2.5 Ligaments in the lumbar spine between two adjacent vertebrae. Image adapted from Adams et al. (2006) with permission from Copyright Elsevier.

2.1.3 Trunk movement

Human movements are described with respect to three perpendicular planes intersecting at the centre of mass of the body (Figure 2.6). Trunk movement can be described as a whole, or it can be examined within regions of the vertebral column or movements at the individual vertebral level.

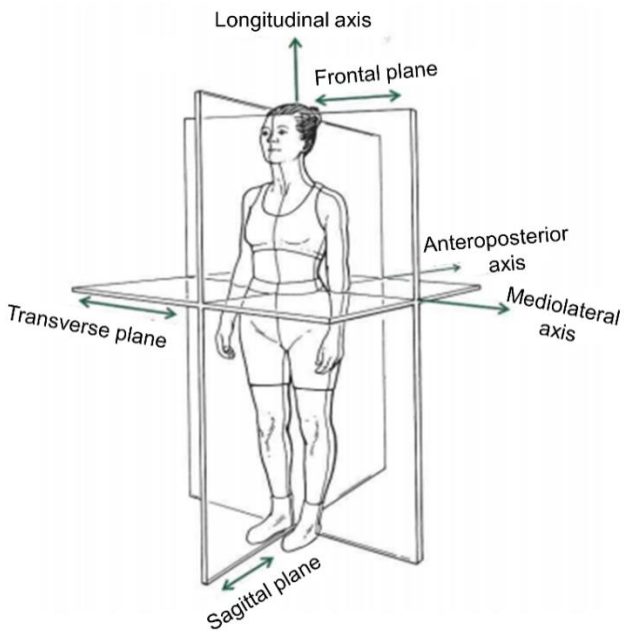

Figure 2.6 Anatomical planes (Frontal, Transverse, Sagittal) and anatomical axes (Longitudinal, antero-posterior, mediolateral). The sagittal plane divides the body into right and left, and trunk movements in this plane are described as flexion (forward bending) and extension (backward bending), about the mediolateral axis. The frontal plane divides the body into front and back, and trunk movements in this plane are described as right and left lateral bending (leaning towards the right and left side, respectively), about the antero-posterior axis. The transverse plane divides the body into top and bottom with trunk movements taking place about the longitudinal axis and described as right and left axial rotation. Image adapted from Figure 1.15 from Hamill and Knutzen (2006) (Copyright restrictions).

Motion at the individual vertebral level is described at the intervertebral joint between adjacent vertebrae, and involves both small translations (<3 mm) and rotations along all three anatomical axes (Ochia et al., 2006, Pearcy, 1985). The intervertebral rotational range of motion of the adult lumbar spine, about the three anatomical axes, has been measured *in vivo* in several studies using radiography, computed tomography (CT), and magnetic resonance imaging (MRI) (Pearcy et al., 1984, Pearcy and Tibrewal, 1984, Stokes et al., 1981, Dvorak et al., 1991, Fujii et al., 2007). Although the reported range of motion at each level varies slightly, sagittal plane motion (i.e. total flexion-extension) is approximately 14° at most lumbar intervertebral levels, while lateral bending angles are slightly less than those in the sagittal plane. In lateral bending, the L4/L5 and L5/S1 levels are significantly less mobile than upper levels (Pearcy and Tibrewal, 1984). Intervertebral axial rotation in the lumbar spine is small, with reported angles less than 4° (Fujii et al., 2007, Ochia et al., 2006).

Axial rotation and lateral bending are coupled in the lumbar spine (Pearcy and Tibrewal, 1984), resulting in lateral bending angles typically about twice those in axial rotation towards the same side

(Ochia et al., 2006) and axial rotation to the opposite side of lateral bending (Oxland et al., 1992). In contrast, there is little coupled motion associated with the flexion-extension motion (Ochia et al., 2006). The facet joints and intervertebral discs between adjacent vertebrae cause these coupled motions in the lumbar spine, while the ligaments play no role (Oxland et al., 1992, Kingma et al., 2018).

2.2 Modelling of the lumbar spine

Loads applied to the spine during lifting and bending tasks may be sufficient to cause injuries and subsequent LBP (Norman et al., 1998). Although spinal loads have been measured *in vivo* using instrumented vertebral body replacements (VBR), these implants required invasive surgeries and are only used in patients with spinal disorders or injuries. In addition, the spinal loads measured in these patients are associated with several limitations such as load sharing between the VBR and other structures (internal fixation device or remaining bone), and a small patient cohort (Rohlmann et al., 2014a). Accordingly, these measurements are likely not indicative of the spinal loads experienced by healthy individuals. Spinal loads have also been evaluated indirectly by measuring intradiscal pressure using needles instrumented with pressure transducers (Wilke et al., 2001, Sato et al., 1999, Takahashi et al., 2006, Polga et al., 2004). However, this method is also invasive and does not directly relate to spinal loads. Consequently, musculoskeletal models represent an alternative method to non-invasively describe the behaviours of the lumbar spine in a wide range of activities to estimate muscle forces and joint loads.

Musculoskeletal models represent the human body using rigid bodies, corresponding to bones, connected by joints, muscles, and occasionally ligaments. As opposed to finite element modelling, the rigid bodies (vertebrae and other bones) neglect deformability. Consequently, musculoskeletal models do not aim to evaluate the stress-displacement and shear distributions of the bony and soft tissues of the lumbar spine; rather, they describe the motion and loads acting on the segments as a whole.

Although the general principles discussed in this section apply to other joints, this section focuses on the lumbar spine. Sections 2.2.1 to 2.2.3 describe the common modelling methods for the constitutive elements of models (joints, muscles, ligaments), while Sections 2.2.4 and 2.2.5 present an overview of

the modelling approaches used to contend with mechanical indeterminacy at the lumbar joints, and a review of biomechanical lumbar spine models used to evaluate lifting and bending tasks, respectively.

2.2.1 Joints

During spinal motion, adjacent vertebrae do not simply rotate about the centre of the disc, but rather they translate with respect to each other, as they rotate. This complex movement can be described as rotation only, about an instantaneous axis of rotation (IAR). This IAR is the centre of the arcuate motion exhibited by each vertebra, where the arc is defined by the start and end position of each vertebra with respect to the inferior adjacent vertebra (Figure 2.7 A). The location of the IAR can be calculated for small incremental movements; however, for larger motions, it is difficult to locate this moving centre. As such, the location of the IAR for large motions is defined as an ellipse containing the entire path of the IARs (the individual values of IAR at each increment) and a single value for the centre of rotation is then obtained by averaging this ellipsoidal data over a group of healthy participants. According to experimental data obtained in healthy volunteers using stereo radiography, the locations of IARs of the lumbar spine in the sagittal plane (i.e. for flexion-extension) fall within a tightly clustered zone near the superior endplate of the inferior vertebra at each intervertebral joint (Pearcy and Bogduk, 1988) (Figure 2.7 B). Consequently, intervertebral joints are commonly modelled by spherical joints with three rotational degrees-of-freedom (DOFs), neglecting intervertebral translations due to their small magnitude and associated *in vivo* measurement difficulties. The locations of the IARs in the other planes have not been measured experimentally and are therefore generally assumed to be in the centre of the disc (in the coronal and transverse planes).

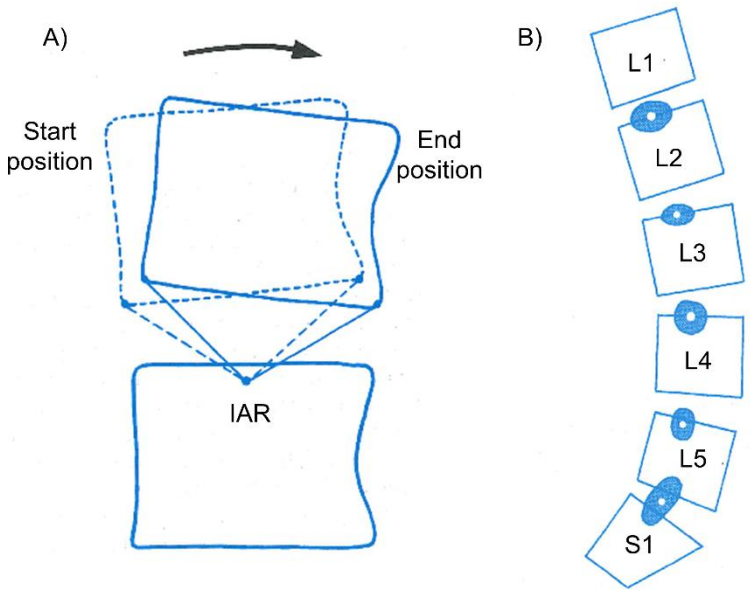

Figure 2.7 A) Arcuate motion of the superior vertebrae with respect to the inferior vertebrae in the sagittal plane, with the centre of the arc known as the instantaneous axis of rotation (IAR); B) Mean location (white dots) and distribution (shaded ellipses) of IARs. Both images adapted from Bogduk (2005) with permission from Copyright Elsevier.

Motion of each lumbar vertebrae is often assumed to be a fixed proportion of the trunk or lumbar rotation in the three planes of motion (flexion-extension, axial rotation, and lateral bending), where the distribution of the vertebral motion angles is based on ratios reported in the literature (Dvorak et al., 1991, Wong et al., 2006, Fujii et al., 2007).

2.2.2 Ligaments

Although ligaments have been included in finite element models (Naserkhaki et al., 2018), they are not always included in musculoskeletal models of the lumbar spine due the lack of available experimental information about their mechanical properties and slack lengths. Consequently, modelling of ligaments is not reviewed in this thesis nor included in the model developed in Chapter 4.

2.2.3 Muscles and tendons

The Hill-type muscle model is the most prevalent model used to describe the complex and nonlinear force output (Hill, 1938, Zajac, 1989, Robertson et al., 2013). In this model, the muscle is represented by a contractile element (CE) in parallel with an elastic passive element (PE), while the tendon is represented by an elastic component, placed in series with the muscle, at an angle (α, pennation angle) with the muscle (Robertson et al., 2013, Rajagopal et al., 2016) (Figure 2.8).

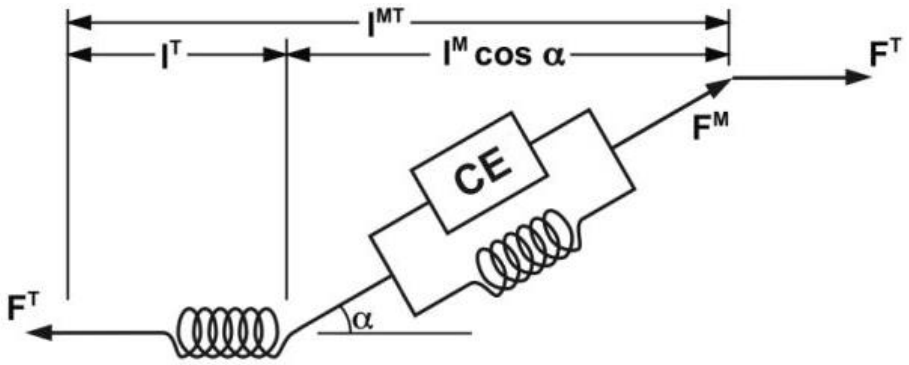

Figure 2.8 Hill-type Model for the muscle-tendon unit to represent its force generating capacity. The force generated by a muscles is based on its muscle fibre length (l^M), muscle pennation angle (α), and tendon length (l^T). F^M represents the force generated by a muscle, while F^T is the force through the tendon. The total muscle-tendon length is represented by l^{MT}. Image adapted from Rajagopal et al. (2016) with permission from IEEE.

The total force produced by a muscle is the sum of the active CE force and PE force (Robertson et al., 2013). The active isometric force produced by a muscle is a function of its activation (expressed as a percentage of its maximal isometric force), and is also based on normalised force-length and force-length-velocity curves (Rajagopal et al., 2016). These two curves are scaled by experimentally determined factors (maximum isometric force, optimal fibre length, maximum fibre shortening velocity) (Figure 2.9) (Rajagopal et al., 2016). The PE component represents the passive force produced by a muscle when it stretches to resist an external force applied to it. The passive response of a muscle is a function of its normalised fibre length only, with the force produced increasing as the muscle lengthens and stretches (Rajagopal et al., 2016, Robertson et al., 2013). The tendon is modelled as an elastic passive element in series with the muscle (Rajagopal et al., 2016). The force it generates is described as a function of tendon strain, based on the muscle-specific tendon slack length determined experimentally (Figure 2.9).

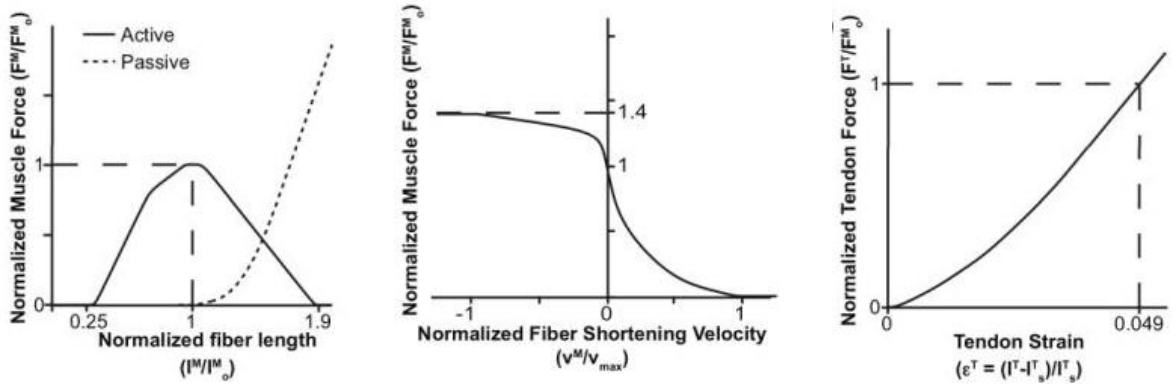

Figure 2.9 A) Active and Passive forces are scaled based on the generic curve for fibre-length force properties (l^M/l^Mo), where the fibre length (l^M) is normalized to the optimal fibre length (l^Mo); B) Active isometric force is scaled based on fibre velocity (v^M) normalized by maximum shortening velocity (v_{max}); C)Tendon force scaled based on the tendon strain (ε^T). Image adapted from Rajagopal et al. (2016) with permission from IEEE.

Trunk muscles are typically modelled as multiple component fascicles (Table 2.1) to provide a more accurate anatomical representation of the muscles' moment generating capacity (line of action, moment arms based attachment points, path of the muscles, and physiological cross-sectional area). The anatomical definitions of the lumbar muscles described in Section 2.1.1 are used extensively by model developers. Although gathering the anatomical information for each muscle from several dissection studies is not ideal (Arnold et al., 2010), it is often necessary due to the limited experimental information available. Models of the lumbar spine generally include all of the muscles described in Section 2.1.1, with a varying number of fascicles per muscle. The only exceptions are the intersegmental muscles and transverse abdominus, which are rarely represented in models due to the small moment they impart about lumbar joints (Adams et al., 2006).

2.2.4 Modelling approach: Optimisation vs EMG-Driven

Musculoskeletal models of the lumbar spine have to contend with the mechanical indeterminacy caused by the large number of structures that can counteract the moments about a joint (Cholewicki et al., 1995). This indeterminacy is faced when partitioning the total moment acting about a joint into the individual contributions made by anatomical structures such as ligaments, muscles, intervertebral discs, and vertebral bodies (van Dieen and Kingma, 2005). The two approaches to determine these unknowns are forward and inverse dynamics. Due to the complexity of the lumbar spine, the inverse dynamics

method (for which the inputs include measured motions and external loads acting on the body) is more widely used to predict muscle forces and joint reactions in the spine. Optimisation (Schultz et al., 1982a, Raabe and Chaudhari, 2016, Bassani et al., 2017) or EMG-based (Cholewicki and McGill, 1996, Granata and Marras, 1995a) models are the two main modelling approaches used to overcome the issue of muscle indeterminacy (Brown and Potvin, 2005). However, there is controversy over which of these methods is most appropriate to predict muscle recruitment patterns (Brown and Potvin, 2005, Staudenmann et al., 2007, McGill and Norman, 1986, Cholewicki et al., 1995, van Dieen and Kingma, 2005, El-Rich et al., 2004, Arjmand et al., 2009, Arjmand and Shirazi-Adl, 2006c, Hughes et al., 1994).

2.2.4.1 Optimisation models

The optimisation method is based on a performance criteria presumed to be in accordance with the strategy of the central nervous system for controlling muscle activation recruitment (de Zee et al., 2007). The performance criteria is represented by one or many mathematical cost (objective) function(s) that can be minimised or maximised while attempting to satisfy equilibrium at the intervertebral joint(s) (Arjmand et al., 2009). Constraint equations are also used in optimisation problems to set lower and upper boundaries for muscle forces, stability (Brown and Potvin, 2005), or other desired restrictions (Arjmand et al., 2009). Numerous objective functions (both linear and non-linear) have been used in the past for different models, with the most common including: 1) minimising the sum of squared muscle stress (Crowninshield and Brand, 1981); 2) minimising compression forces at a particular intervertebral level (Schultz et al., 1982b); 3) minimising the sum of the cubed muscle forces (Hughes et al., 1994); and, 4) minimising maximum muscle stress (An et al., 1984). Non-linear cost functions based on known physiological principles predict muscle force patterns with the highest agreement with recorded electromyographic (EMG) data (Crowninshield and Brand, 1981, Hughes et al., 1994).

Optimisation is a pure mathematical problem that does not use any physiological signals as inputs. As a result, this type of model is often criticised for the subjective choice of objective function and the inability to account for any individual variability in muscle recruitment patterns. In addition, optimisation penalises antagonist co-contraction (Ait-Haddou et al., 2000), which has been demonstrated in a variety of postures (Cholewicki et al., 1995, Martelli et al., 2015, Brown and Potvin,

2005), thus possibly resulting in underestimation of spinal loads (Granata and Marras, 1995b). However, one of the main advantages of optimisation models is that they do not require experimentally measured muscle activity in their formulation, and they can therefore be more easily used and adapted to different tasks.

2.2.4.2 EMG-Driven models

In an attempt to adequately represent co-contraction of trunk muscles, EMG-driven models were developed on the principle that the estimated muscle force patterns follow the recorded muscle activity (McGill and Norman, 1986, Granata and Marras, 1995a, Cholewicki et al., 1995, Staudenmann et al., 2007). In this approach, the tensile force generated by each muscle is based on the EMG signals measured on a limited number of trunk muscles. EMG-driven models are thought to provide more physiologically accurate levels of activations than optimisation models (Cholewicki et al., 1995, Lloyd and Besier, 2003), especially under conditions of no external moment (upright static standing with axial compression, e.g. holding buckets). The muscle forces for EMG-driven models are generally determined by:

$$S_z = Force_j = G\frac{EMG_j(t)}{EMG_{maxj}}A_j f(V_j) f(L_j) \qquad (2.1)$$

where G is the muscle force per unit area, $\frac{EMG_j(t)}{EMG_{maxj}}$ the normalised EMG signals, A_j the muscle cross-sectional area, and $f(V_j)$, $f(L_j)$ are the modulation factors describing EMG and force behaviour as a function of muscle velocity and length, respectively (McGill and Norman, 1986, Marras and Sommerich, 1991, Granata and Marras, 1995a).

Due to the ability of EMG-driven models to account for muscle co-contractions, they are often considered superior to optimisation models for accurately predicting lumbar joint loading, as optimisation models underestimate joint forces (Cholewicki et al., 1995). However, van Dieen and Kingma (2005) obtained similar joint loads for both modelling approaches in a wide range of work

tasks, demonstrating the validity of both approaches to estimate joint loading, and the importance of selecting an appropriate objective function for optimisation models.

Although EMG-based models provide an advantage over optimisation models by allowing the application of individual differences in muscle activation patterns, including antagonist muscle activity (Staudenmann et al., 2007), they also have limitations. Experimental limitations include electrical cross-talk between muscles and difficulty in measuring EMG activities of deep muscles (McGill and Norman, 1986, McGill, 1992). In addition, simplifying and grouping assumptions for the muscles must be made to implement the EMG signals into the model (McGill and Norman, 1986, Granata and Marras, 1995a, McGill and Norman, 1987a, Cholewicki et al., 1995). The EMG signals also need to be normalised to maximum voluntary contraction (MVC) trials, which can be problematic as these trials do not always produce maximum activation of the muscles, especially in participants with LBP where apprehension or pain may lead to underestimation of MVC (Lariviere et al., 2003). EMG-driven models also often produce solutions violating static equilibrium, where the summed contributions of the active and passive structures in the trunk for all three axes about a joint do not correspond to the total moment (Brown and Potvin, 2005, Arjmand and Shirazi-Adl, 2006a, Arjmand et al., 2007, Gagnon et al., 2011), thus leading to the development of hybrid models.

2.2.4.3 Hybrid models

Hybrid models have been created to combine the advantage of both EMG-driven and optimisation methods to estimate muscles forces by correcting the estimated EMG-assisted muscle force, while also balancing moment equations at the intervertebral joints (Cholewicki and McGill, 1994). Hybrid models predict similar muscle recruitment patterns to those predicted by the EMG-driven approach (Cholewicki et al., 1995).

In this approach, the recruitment patterns of agonist and antagonist muscles in the model are based on EMG measurements. These initial estimates of muscle forces are then adjusted by applying the least possible adjustment to individual muscles adjustment to individual muscle forces to balance all three

moments acting about a joint (Cholewicki and McGill, 1994). Mathematically, this method minimises the objective function:

$$\sum_{i=1}^{n} M_i(1-g_i)^2 = min, \tag{2.2}$$

where $$M_i = \sqrt{M_{x_i}^2 + M_{y_i}^2 + M_{z_i}^2} \tag{2.3}$$

With the constraints,

$$\sum_{i=1}^{n} g_i M_{x_i} = M_x \tag{2.4}$$

$$\sum_{i=1}^{n} g_i M_{y_i} = M_y \tag{2.5}$$

$$\sum_{i=1}^{n} g_i M_{z_i} = M_z \tag{2.6}$$

$$g_i \geq 0, i = 1,2,\dots,n$$

where n is the number of muscle fascicles crossing a given joint; g_i the individual muscle gains; M_i (Nm) the estimated moment which the i^{th} muscle produces about the joint centre of rotation estimated from EMG; $M_{x_i}, M_{y_i}, M_{z_i}$(Nm) the muscle moments estimated from EMG, about the X, Y and Z joint axes; and, M_x, M_y, M_z (Nm) the total muscle moment necessary to balance moments acting on the joint about X, Y, and Z axes.

2.2.5 Musculoskeletal Lifting Models

Several biomechanical musculoskeletal models of the lumbar spine have been developed over the last 35 years, typically increasing in complexity (Christophy et al., 2012, Bogduk et al., 1992a, de Zee et al., 2007, El-Rich et al., 2004, Lambrecht et al., 2009, McGill and Norman, 1987a, Shirazi-Adl, 1991, Stokes and Gardner-Morse, 1995). Some of these models represent the spine only, while others represent the full body (with upper and lower limbs).

This section provides an overview of several models in the literature. It begins with a more extensive discussion of lumbar spine models developed in two software (Anybody and OpenSim), both specifically aimed at musculoskeletal modelling. The musculoskeletal models developed on proprietary software by McGill & colleagues, and Kingma, Van Dieen & colleagues are then discussed as these models have significantly contributed to lumbar spine biomechanics literature, both from a modelling point of view and the application of the model to real-life situations. Finally, the models developed by Arjmand, Shirazi-Adl & colleagues are briefly reviewed. Although these models are not strictly musculoskeletal models, due to the use of finite element modelling, they have been used extensively in the biomechanical literature to evaluate lifting tasks. A summary of the lumbar spine musculature and ligaments included in the models reviewed in this section is included in Table 2.2.

Model validation is essential to verify accuracy and suitability to represent the simulated activity or task with the recruited population (Hicks et al., 2015). Model validation is an important step to support the model and prevent erroneous conclusions (Hicks et al., 2015). Consequently, a focus is placed on model validation throughout this section.

Table 2.2 Total number of muscle fascicles and ligaments included in the models reviewed in this section. Muscles are described as reported by the different authors. The type of modelling approach (Optimisation [OPT] or EMG-Driven [EMG] or Hybrid [HYB]) is specified. *indicates that the definition of thoracic and lumbar fascicle was not provided; **indicates the muscle fascicle definition did not equal the total number of fascicles; TA: Transverse Abdominus.

MODEL	Year	# Back Fascicle	LTpT	LTpL	ILpT	ILpL	MF	LD	RA	IO	EO	PS	QL	Other Muscles	Ligament	TYPE
McGill & Norman	1986 & 1992	48	2		2*		2	2	2	4	4	8	2	Sacrospinalis (8)	7	EMG
Cholewicki & Mcgill	1996	90	2	10	2*		24	12	2	4	4	10	10	Pars Lumborum (10)	7	HYB
Van Dieen et al. (A)	1997	114	22*		24*		34		2	4	4	22		TA(2)	-	EMG
Van Dieen et al. (B)	1997	114	12	10	16	8	34		2	4	4	22		TA (2)	-	EMG
Van Dieen et al. **	2004	88	22*		24*		34		2	4	4				-	EMG & OPT
Arjmand et al.	2004	56	2	10	2	8	10		2	2	2	10	8		-	
De Zee et al.**	2007	154	58*				38		1	12	12	22	10		-	OPT
Han et al.	2012	258	34*		24*		62	10	1	6	6	22	10	TA (5) Intersegmental (78)	7	OPT
Bassani et al.	2017	203	58*				62		1	12	12	22	10	TA (5) Intersegmental (21)	-	OPT
Ignasiak et al.	2016	381	58*				38		1	12	12	22	10	Thoracic (227)	-	OPT
Christophy et al.	2012	238	42	10	16	8	50	28	2	12	12	22	36		-	OPT
Senteler et al.	2015	238	42	10	16	8	50	28	2	12	12	22	36		-	OPT
Bruno et al.	2015	414	42	10	16	8	88	28	2	12	16	22	36	TA (10), Neck (52) Thoracic (172) Shoulders(52)		OPT
Raabe & Chaudhari	2016	238	42	10	16	8	74	28	2	12	12	22	36	Lower limbs (86)	-	OPT
Kim & Zhang	2017	Not provided														
Actis et al.	2018	212	42	10	16	8	50	28	2	12	12	22	36	Lower limbs (82)	-	OPT

2.2.5.1 AnyBody Modeling System

The AnyBody Modeling System (AnyBody Technology A/S, Aalborg, Denmark) is a commercial program used for the development and analysis of musculoskeletal systems (Damsgaard et al., 2006). It uses general multibody system dynamics, where each segment is modelled as a rigid body with its own coordinate system (Damsgaard et al., 2006). Existing models developed on AnyBody Modeling System software can be shared between users.

A lumbar spine model without limbs, comprising seven rigid body segments (pelvis/sacrum, five lumbar vertebrae, and a rigid thorax) connected by six 3-DOF spherical joints and 154 trunk muscle fascicles was developed in 2007 (de Zee et al., 2007). Joint centres of rotation were based on work by Pearcy and Bogduk (1988), and muscles were represented by the Hill model, but did not include the force-length and force-velocity relationships. Muscle paths were modelled either as straight lines (also using via points) or curved following wrapping surfaces. Ligaments and other passive components were not included in this base spine model. The validation of the model was limited to comparison with reported *in vivo* L4/L5 intradiscal pressure measurements for one specific task (holding a weight of 20 kg at 60 cm from the chest) (Wilke et al., 2001).

This lumbar spine model was later incorporated in three other models: the full-body musculoskeletal model (Bassani et al., 2017), the enhanced spine model (Han et al., 2012), and the thoracic spine model (Ignasiak et al., 2016a) (Figure 2.10).

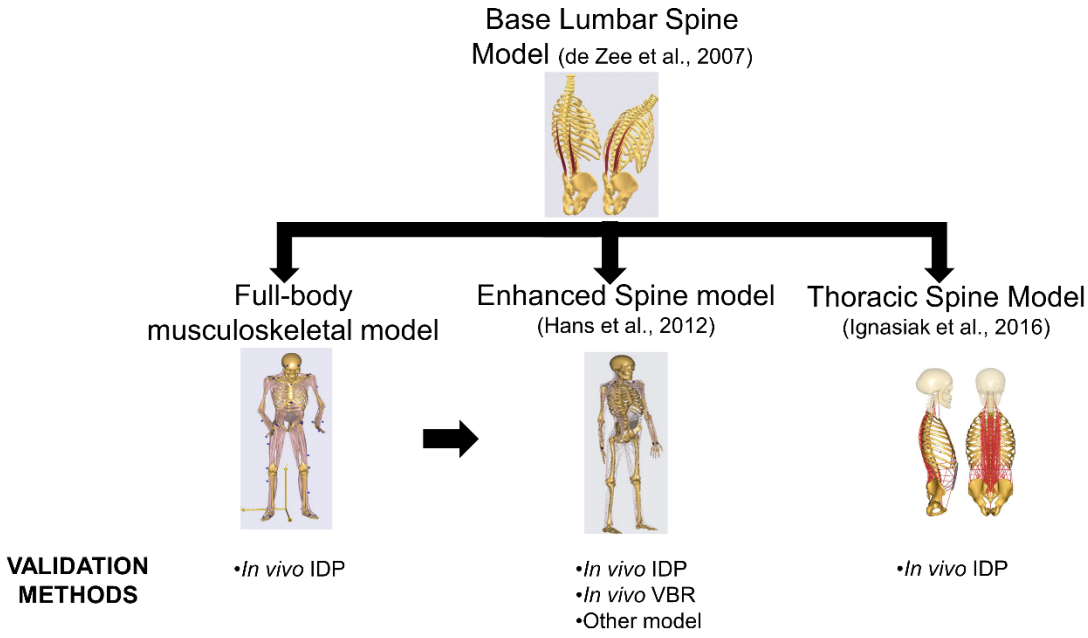

Figure 2.10 Musculoskeletal models on the AnyBody platform that contain a detailed lumbar spine model. Images adapted from (de Zee et al., 2007), (Bassani et al., 2017), (Han et al., 2012), and (Ignasiak et al., 2016a) with permission from Copyright Elsevier.

Full-body musculoskeletal model

The base lumbar spine model was incorporated into a full-body model available on the Anybody Managed Model Repository. This model was developed by collaboration between researchers across academic institutions and is increasingly used by researchers worldwide, with more than 50 publications referenced on the AnyBody Technology website for 2016 alone (Galbusera and Wilke, 2018). However, despite being widely used, it had not been validated specifically for the prediction of L4/L5 lumbar loads in dynamic activities before 2017 (Bassani et al., 2017). Model validation for lumbar loads consisted of replicating in the laboratory 12 specific tasks where L4/L5 *in vivo* intradiscal pressures (IDP) had been measured previously by Wilke et al. (2001) and comparing the corresponding L4/L5 spinal loads estimated by the model to the measurements (Bassani et al., 2017). The L4/L5 compressive forces were converted to IDP by first calculating the average pressure, using a disc area of 18 cm^2 (Wilke et al., 2001), and then adjusting the resulting average pressure using two methods to: 1) a constant correction factor (1.54) (Nachemson, 1960); and 2) a quadratic equation taking into account the relationship between IDP

and flexion angles (Ghezelbash et al., 2016). This adjustment was necessary to model behaviour of the disc under compression loading (Brinckmann and Grootenboer, 1991).

The results showed that the AnyBody full-body model was suitable to describe the IDP for flexion-extension, axial rotation, and lateral bending for angles below ±15° (Figure 2.11). Both methods for estimating IDP had very strong correlations with the *in vivo* measurements (r>0.9). A limitation of this study is that only one subject and one repetition of the tasks were evaluated.

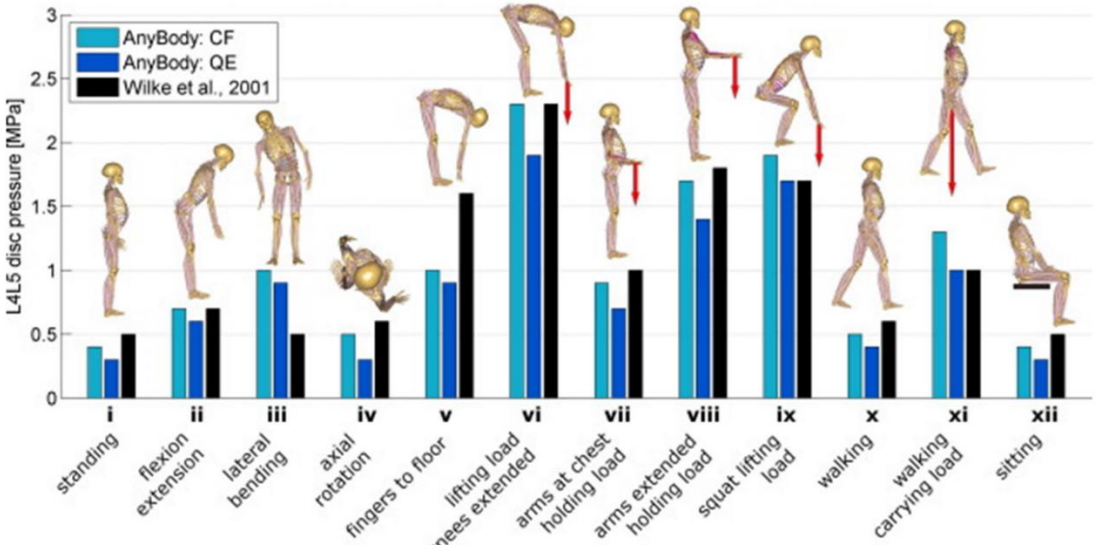

Figure 2.11 Comparisons between *in vivo* IDP measurements and model estimates by the AnyBody full-body model (Bassani et al., 2017). The two AnyBody model estimates corresponds to pressure estimates using a correction factor (CF) and quadratic equation (QE). Image adapted from Bassani et al. (2017) with permission from Copyright Elsevier.

Enhanced spine model

The Anybody full-body model incorporating the base lumbar spine model was also enhanced to include long muscles (4 fascicles), short segmental muscles (56 fascicles), seven ligaments, disc rotational stiffness, and intra-abdominal pressure (IAP) (Han et al., 2012) (Figure 2.10). This model was compared against previously reported *in vivo* IDP measurements (Wilke et al., 2001) (Figure 2.12, top), VBR measurements (Rohlmann et al., 2008, Wilke et al., 1999) (Figure 2.12, bottom), and muscle forces (Schultz et al., 1982a) for a range of static positions. The predictions of the enhanced model were also compared to those predicted by the AnyBody full-body model

(non-enhanced model) for the same activities (Figure 2.12, top and bottom). For the comparisons with IDP and VBR measurements, the variables were normalised to standing position.

Limited information on the validation methods used in this study were provided in the manuscript. Specifically, the approach used to convert the L4/L5 compression forces to IDP was not described, nor were the details for the intervertebral level where the VBR measurements were obtained. Moreover, model inputs for the validation of this model did not include experimental data; kinematics and kinetics data were artificially created by the authors to replicate the activities performed by Schultz et al. (1982a). The muscle forces predicted by both models were compared to each other, without discussing how the muscles were modelled, and the subsequent implications for the comparisons. This is a major limitation of this study as it lacks transparency over the methods and assumptions made when simulating the static positions. Consequently, it is difficult to relate the results from the validation of the enhanced model (Han et al., 2012) to those obtained for the validation study by Bassani et al. (2017) on the AnyBody full-body model. The results were also not expressed identically, and different activities were selected. The estimates for the base model (corresponding to the AnyBody full-body model) in the Han et al. (2012) study do not correspond to those obtained by Bassani et al. (2017), for the same activity, when both are expressed as a percentage of standing posture.

Overall, the enhanced model predicted generally lower values than those of the AnyBody full-body model for the static positions evaluated for all three comparisons, thus yielding values closer to those reported in the literature. However, given the limited information provided on the validation methods and the lack of experimental data for some of the components incorporated in the enhanced model (IAP pressure, ligaments, discs), it is difficult to fully understand the benefits of the enhanced model over the AnyBody full-body model.

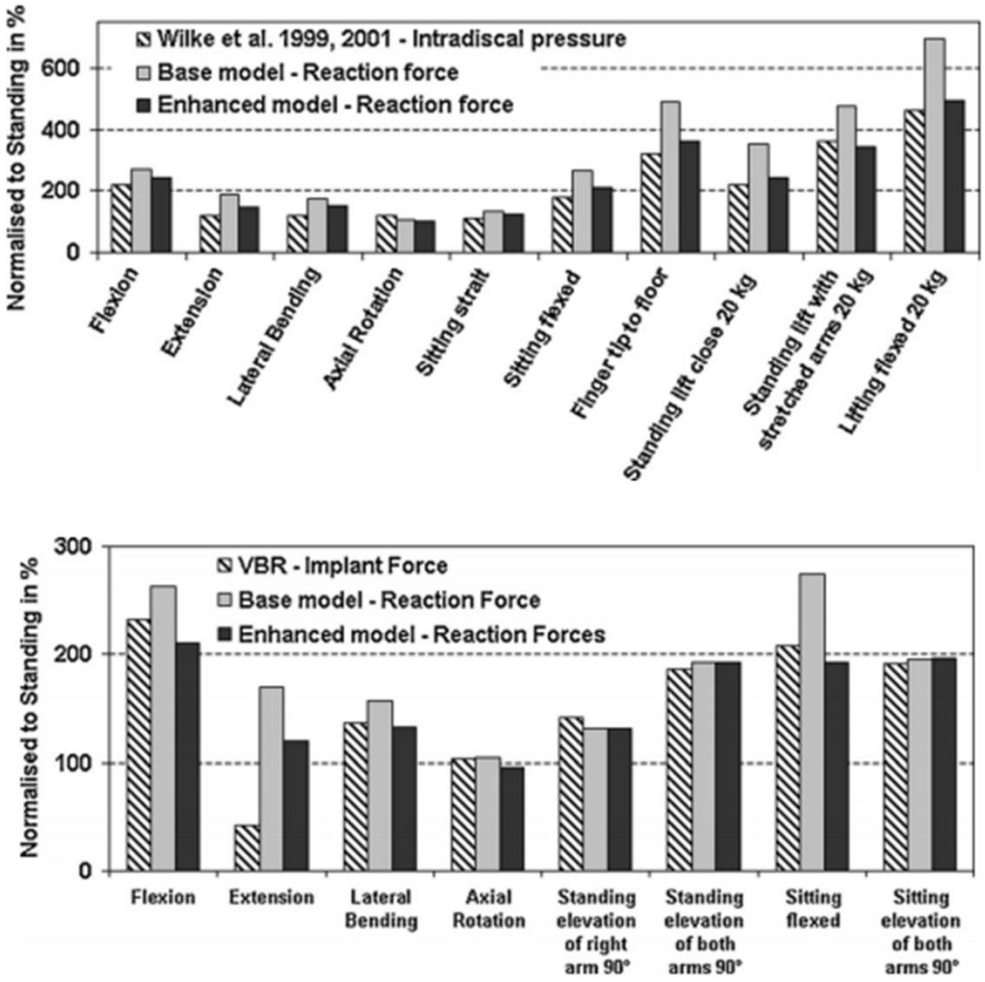

Figure 2.12 Comparisons between *in vivo* IDP measurements and model estimates for the enhanced model and the base model (AnyBody full-body model). Images adapted from Han et al. (2012) with permission from Copyright Elsevier.

Thoracic spine model

The thoracic spine model was developed using the base lumbar spine model (de Zee et al., 2007), adding rigid bodies for the thoracic region and an articulated ribcage to estimate spinal loading during dynamic tasks (Ignasiak et al., 2016a). Similar to the enhanced model validation (Han et al., 2012), the kinematics of the spine were created artificially to replicate tasks for which IDP had been measured *in vivo (Polga et al., 2004)*. The IDP predicted by the model were strongly associated with the reported *in vivo* IDP (R^2=0.89). However, this model is limited to theoretical simulations, where motion to the spine is prescribed instead of using experimental data collected in the laboratory. Nonetheless, these simulations indicated that the rigid thorax assumption is suitable for lowermost spinal levels (L4/L5, L5/S1).

2.2.5.2 OpenSim Modelling software

The OpenSim (SimTK, Stanford, CA) is a freely available open-source modelling software that has been developed to accelerate the development and sharing of simulation technology for musculoskeletal modelling (Delp et al., 2007). Many models developed by other users for the analysis of a wide range of movements are publicly available on the repository.

A detailed lumbar spine model comprising five intervertebral lumbar joints and 238 muscle fascicles was published and shared on the OpenSim platform in 2012 (Christophy et al., 2012). Although the model geometry was based on reported cadaveric (muscle origin and insertion points) or *in vivo* measurements (joint kinematics), it was not validated for the evaluation of lumbar spine loading.

The detailed lumbar spine developed by Christophy et al. (2012), has been incorporated into several other OpenSim models developed for various uses (Figure 2.13): the enhanced model (Senteler et al., 2015), the thoracolumbar model (Bruno et al., 2015), the full-body lumbar spine (FBLS) model (Raabe and Chaudhari, 2016), the whole-body model (Kim and Zhang, 2017), and a model to evaluate individuals with transtibial amputations (TTA) (Actis et al., 2018) (Figure 2.13).

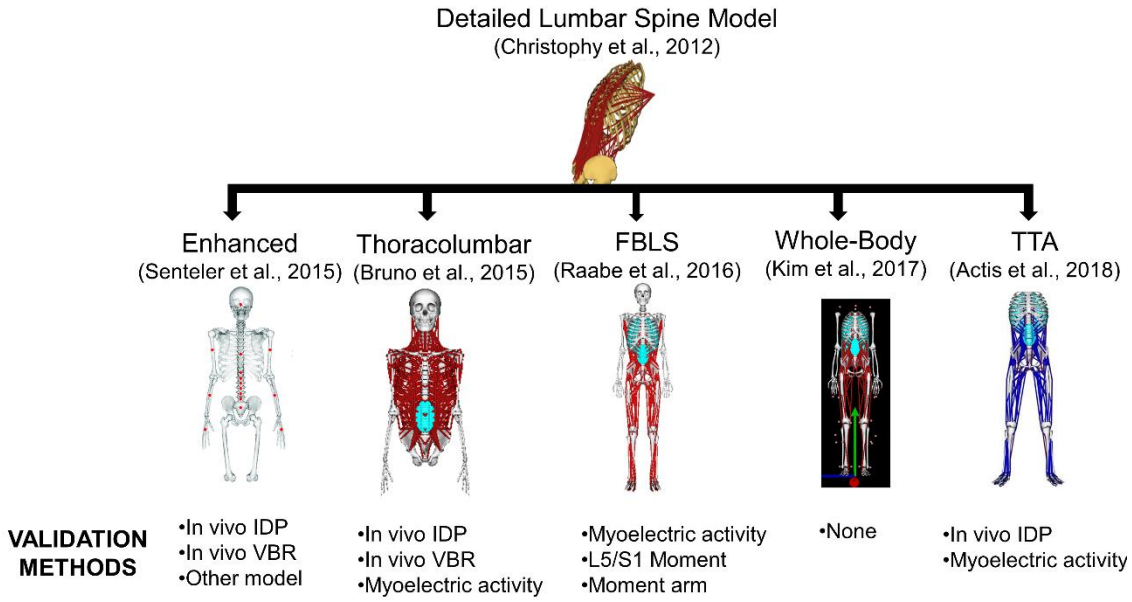

Figure 2.13 Musculoskeletal models on the OpenSim platform that contain the detailed lumbar spine model developed by Christophy et al. (2012): the enhanced model, the thoracolumbar model, the full-body lumbar spine (FBLS) model, the whole-body model and the model to evaluate individuals with transtibial amputations (TTA). Images adapted from Christophy et al. (2012) (Open access, no permission required), Senteler et al. (2015) with permission from Taylor & Francis, Kim and Zhang (2017) with permission from Taylor & Francis, Actis et al. (2018) with permission from Copyright Elsevier.

Enhanced Model

The enhanced model combined the detailed lumbar spine model (Christophy et al., 2012), the neck model (Vasavada et al., 1998), and the upper extremities (Holzbaur et al., 2005) and was published to the OpenSim model library (https://simtk.org/projects/intervertebr_jr). Linear 6-DOF bushing elements were introduced at each intervertebral level to capture the passive stiffness from the passive tissues (discs, ligaments, and capsules; facet joints were neglected), thus allowing for motion in 6-DOF at each level, resulting in a 30-DOF system for the lumbar spine. The matrix representing the bushing elements neglected coupled motion, and therefore remained symmetric. Translational and rotational stiffness values for the bushing elements were determined based on experimental load-displacement data (Heuer et al., 2007). The spinal loads estimated by the resulting model were validated against predicted joint L3/L4 compression forces by another model (Schultz et al., 1982a) (Figure 2.14a), VBR measurements (Rohlmann et al., 2008) (Figure 2.14b), and *in vivo* IDP measurements (Sato et al., 1999, Wilke et al., 2001) (Figure 2.14c), during

static and dynamic forward flexion and lifting. Kinematic and kinetic data were created artificially by the authors to replicate the reported various activities; no experimental data were collected for this validation. The results showed that the model compared well with the reported experimental data for forward bending and light lifting tasks (<8 kg) only, as the model estimates were within 10% of the values reported by the experimental studies. However, the model over-estimated spinal loads when compared to VBR and IDP for extension and heavy lifting tasks (20 kg), respectively.

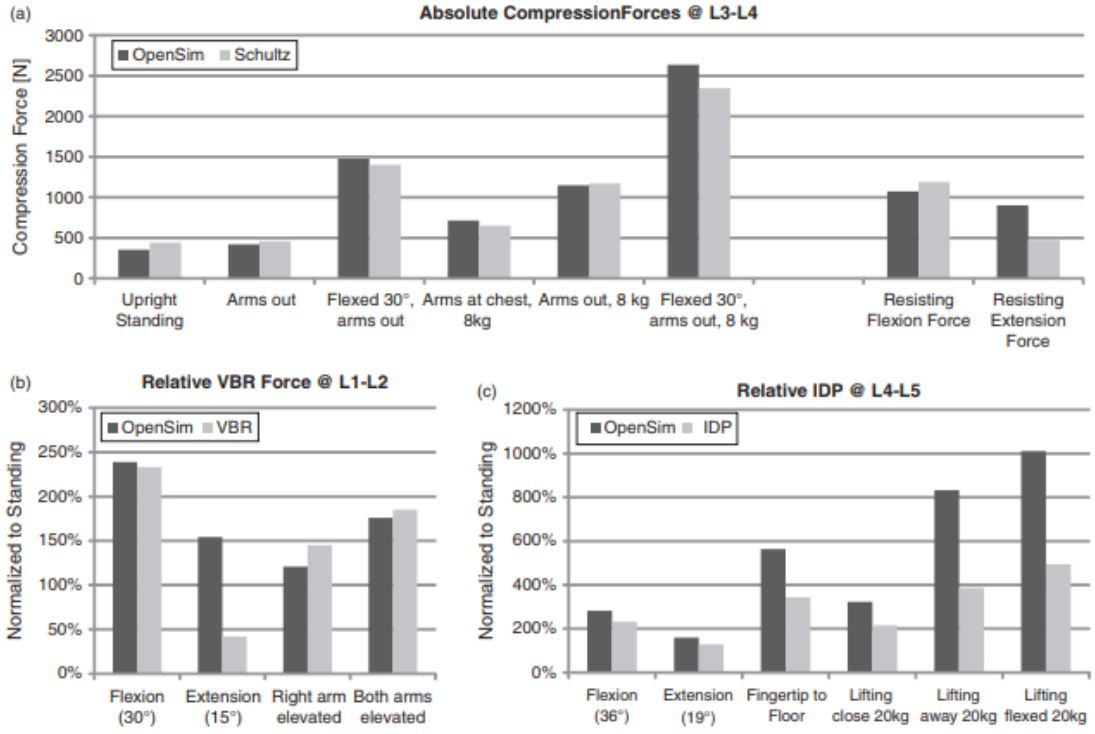

Figure 2.14 Comparisons between a) compression forces, b) *in vivo* VBR forces, and c) *in vivo* IDP measurements and model estimates for the enhanced model. Images adapted from Senteler et al. (2015) with permission from Copyright Tayler & Francis.

A major limitation of this model was that although 6-DOF bushings were introduced at each lumbar level, only 1-DOF about the sagittal plane (flexion-extension) was enabled for the simulations. This was due to a lack of experimental data to describe the sub-millimeter intervertebral translations, and difficulties in solving the under-constrained systems that contains 30-DOF in the lumbar spine (6-DOF at each of the five lumbar joints). Although the model was enhanced to represent the contributions of some of the passive tissues of the lumbar spine during

forward bending and lifting tasks, its practical use appears limited as only the primary movement (flexion-extension) can be used. In addition, its application to ergonomics studies where experimental data is collected in the laboratory is unclear as it has not been assessed; the model did not include lower legs for the application of ground reaction forces.

Thoracolumbar Model

A fully articulated model of the thoracolumbar spine reported by Bruno et al. (2015) was developed and validated for lifting tasks. Similar to the enhanced lumbar spine model (Senteler et al., 2015), this model combined previous models for the lumbar spine (Christophy et al., 2012), the neck (Vasavada et al., 1998), and the upper extremities (Holzbaur et al., 2005). Trunk muscle cross-sectional areas and positions were adjusted to accurately represent *in vivo* muscles using data obtained from computed tomography scans. The model was validated against *in vivo* IDP measurements (Wilke et al., 2001, Sato et al., 1999, Takahashi et al., 2006, Schultz et al., 1982a) and VBR measurements (Rohlmann et al., 2008). Measured myoelectric activity for the erector spinae was also correlated with the erector spinae tension predicted by the model (Schultz et al., 1982a). Again, similar to the enhanced lumbar spine model (Senteler et al., 2015), the motions and forces for the simulations were created artificially as no experimental data were included in the simulations. The methodology for the model validation contained extensive details, providing for a thorough understanding. The compressive forces estimated by the model were converted to IDP by first calculating the average pressure, using disc area of 18 cm^2 (Wilke et al., 2001) and then adjusting the resulting average using a constant correction factor characterising the compression-IDP relationship (Dreischarf et al., 2013). Model predictions of compression forces and trunk muscle tension were highly correlated (R=0.88-0.91) to previous *in vivo* measurements (Figure 2.15).

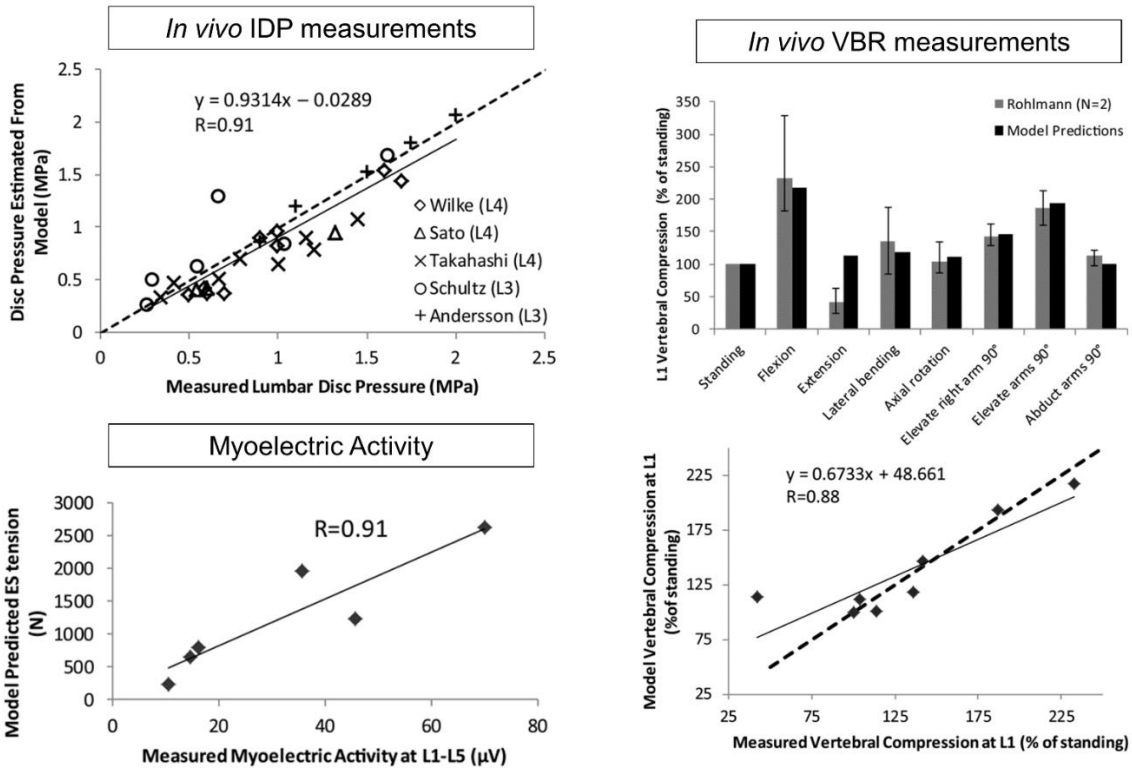

Figure 2.15 Validation results for the thoracolumbar model. Images adapted from Bruno et al. (2015) (Copyright restrictions).

This model has been thoroughly validated but it did not include lower limbs to locate and apply the ground reaction forces to the model. Most importantly, it cannot currently be used with kinematic data collected in the laboratory due to the large number of DOFs in the spine and the lack of coupling constraints to determine the motion at each intervertebral level. As a result, this model cannot be used for studies where experimental data are collected in the laboratory.

Full-Body Lumbar Spine Model

The Full-body lumbar spine model (FBLS) (Raabe and Chaudhari, 2016) was developed by combining a full-body model (Hamner et al., 2010), the detailed lumbar spine model (Christophy et al., 2012), and a model of the patella (Arnold et al., 2010). The resulting model comprised upper and lower limbs, but only the lower limbs and trunk contained muscles. The FBLS model was validated to study jogging activities by qualitatively comparing the maximum isometric joint moments about all three axes at L5/S1 (axial rotation, lateral bending, and flexion-extension) produced by the model to experimental data collected in this study (Raabe and Chaudhari, 2016),

and from previous studies (Kumar et al., 1995b, Kumar et al., 1995a, Khalaf et al., 1997, Keller and Roy, 2002). In addition, experimentally measured surface EMG on participants were directly compared to muscle activations predicted by the model over a gait cycle.

The experimental maximum isometric moments measured on participants did not correspond exactly to those estimated by the model for the same participants. These discrepancies were attributed to differences in muscle properties between the model and participants, and to participants potentially not maximally activating all of their trunk muscles during the trial. However, although there were differences between the model and experimental data, the general behaviour was comparable.

The lower extremity muscle activations predicted by the model generally compared well to those measured by EMG, on the same participants. However, there was more variability for the trunk muscles, with predicted muscle activations generally poorly matching with experimental measurements (Figure 2.16). The poor agreement between the EMG measurements and model predictions was attributed to the use of static optimisation to determine muscle activations in the model, as it cannot predict anticipatory actions during running (Raabe and Chaudhari, 2016).

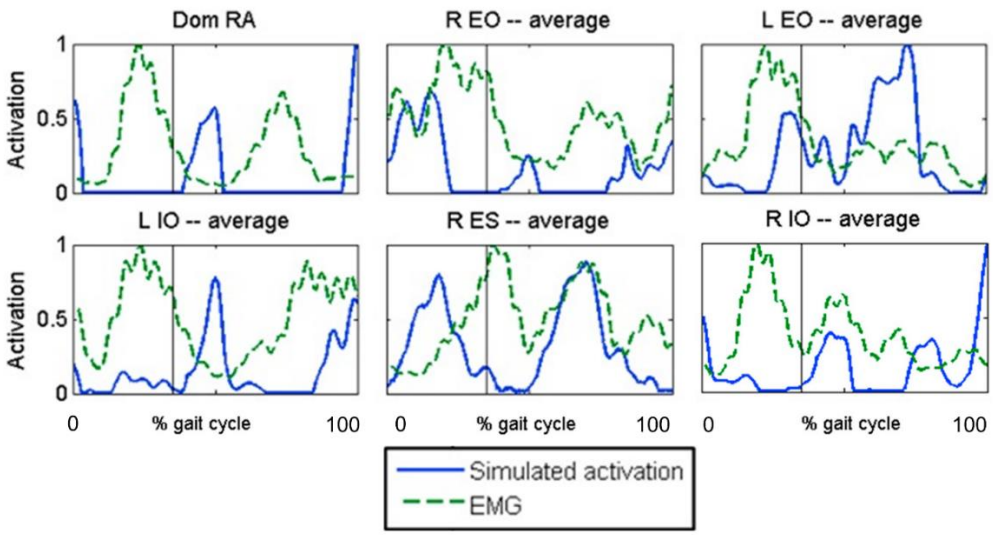

Figure 2.16 Results of the direct comparison between the experimental EMG and the simulated activation by the model for the back muscles during a gait cycle, for the rectus abdominus on the dominant side (Dom RA), right external oblique (R EO), left external oblique (L EO), left internal oblique (L IO), right erector spinae (R ES), and right inter oblique. Image adopted from Raabe and Chaudhari (2016) with permission from Copyright Elsevier.

Although the trunk muscle and isometric moment validations were not convincing, this study demonstrated that the model can be used for simulations of experimental data collected in the laboratory, which is not case for the enhanced spine model (Senteler et al., 2015) and the fully articulated thoracolumbar spine model (Bruno et al., 2015).

Whole-Body Model

Kim et al. (2017) incorporated the detailed lumbar spine model into a whole-body model with legs and arms to estimate lumbar spinal loading and trunk muscle forces during asymmetric lifting tasks. However, this whole-body model is not available on the public database and most importantly, its validation for the lifting tasks has not been documented (Kim and Zhang, 2017). This is a limitation of this model as validation is fundamental to prevent erroneous conclusions (Hicks et al., 2015).

Transtibial Amputation Model

The transtibial amputation (TTA) model was developed to study lumbar loads in a patient population with TTA (Actis et al., 2018). The model included a lower body model and the detailed lumbar spine model (Christophy et al., 2012), but did not include upper extremities. The lumbar loads predicted by the model were validated by comparing them to previously reported IDP measurements for various trunk movements (Sato et al., 1999, Wilke et al., 2001, Nachemson, 1965); the compressive forces estimated by the model were converted to IDP using an equation relating disc pressure to trunk angles (Ghezelbash et al., 2016) and then normalised to standing position. The comparison of the IDP values was evaluated by t-tests. The model IDP estimates for standing, flexion, axial rotation, and lateral bending motions were similar to those reported in the literature (Wilke et al., 2001, Sato et al., 1999), but extension produced significantly larger IDP estimates for the model compared to *in vivo* measurements (Figure 2.17), which may be explained by the substantial forces transferred to posterior elements in that motion (Pollintine et al., 2004).

Experimental EMG signals measured on participants were also compared to those estimated by the model for the trunk muscles, with both values normalised to peak activation for each trial and each participant. Agreement between the two signals was quantified as the percentage of each trial during which both signals (EMG activity and model muscle activations) were either above or below a 0.5 threshold at the same time. Model and EMG agreement for the lumbar and thoracic erector spinae muscle was above 70% for flexion movements, but other motions (extension, axial rotation, and lateral bending) did not produce consistent agreement across participants.

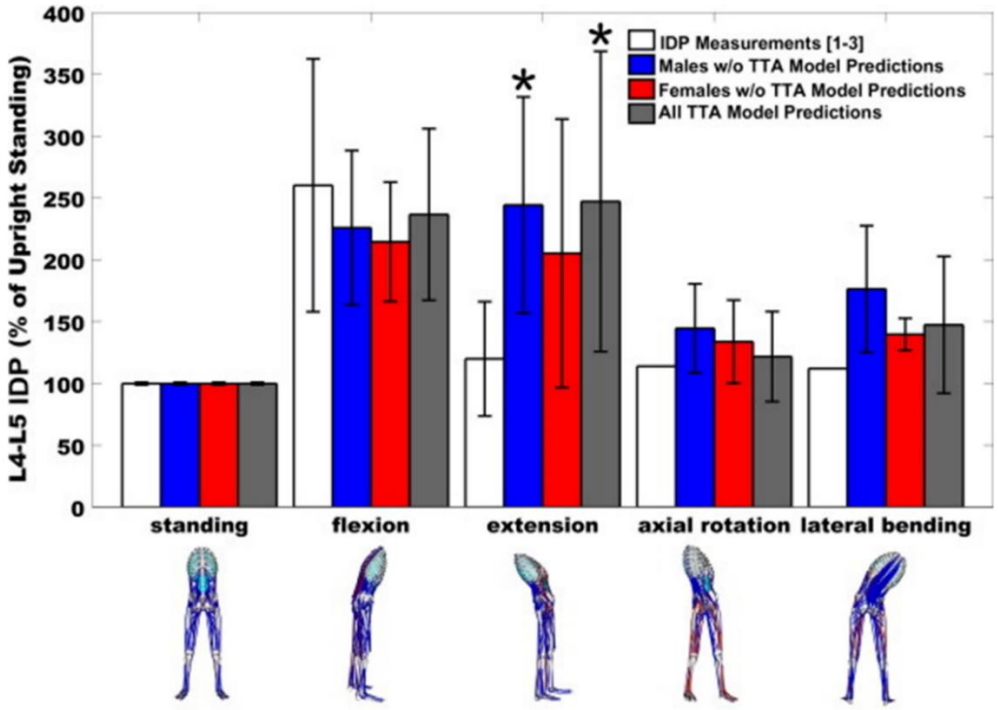

Figure 2.17 Comparisons between *in vivo* IDP measurements and model estimates for the TTA model (Actis et al., 2018) with permission from Copyright Elsevier.

Although the comparisons between the model estimates and the experimental data were mostly satisfactory for the trunk movements evaluated, it was not evaluated for lifting tasks. The decision to use a threshold (0.5, with signals normalised to peak activation) to evaluate agreement between EMG signals and model estimates of muscle activations was not explained. It is preferable to compare both the shape and timing of the EMG signal and model estimate curves, rather than to use a threshold. Nonetheless, the validation study demonstrated that this model can be used for simulations of experimental data collected in the laboratory. However, this model did not include upper limbs, which precludes its application to lifting tasks where external loads are applied to the hand(s).

Summary

The detailed lumbar spine model (Christophy et al., 2012) has been incorporated into several other models, for various uses. Despite these validation studies of the detailed lumbar spine model

in different adaptions of the model, there is currently no full-body model with a detailed lumbar spine that has been validated for lifting tasks on the OpenSim platform.

Several models were validated using comparisons to reported *in vivo* IDP measurements. However, it is difficult to relate the results between the studies, as few details were generally provided on the trunk angle at which the comparison was conducted.

2.2.5.3 McGill & colleagues

McGill & colleagues are pioneers of the lumbar EMG-driven model. Their lumbar spine model evolved over the years, with numerous iterations improving the anatomical and functional representation of the lumbar spine (McGill, 1992, McGill and Norman, 1986, Cholewicki and McGill, 1996). The current model comprised six lumbar joints each with 3-DOF, 90 muscles representing the trunk musculature, and passive tissue forces (disc, 7 ligaments, and other tissues) (Figure 2.18). This model was composed of two parts; the first part was a dynamic linked-segment model of the body estimating three-dimensional (3D) L4/L5 reaction moments using an inverse dynamics Newtonian mechanics approach starting at the hands, while the second part of the model partitioned the reaction moments obtained from the linked-model to the components of the lumbar spine as follows:

$$M_{r_{L4/L5}} = \sum M_m + \sum M_{passive\ components} \qquad (2.7)$$

where $M_{r_{L4/L5}}$ (Nm) is the reaction moment at L4/L5, M_m (Nm) is the moment contribution from the 90 muscles, and $M_{passive\ components}$ (Nm) is the contribution of the passive tissues (discs, 7 ligaments) (Cholewicki and McGill, 1996).

The passive tissue forces were first predicted by assuming stress-strain or load deformation relationships for the individual passive tissues. The remaining moment was then partitioned between the muscle fascicles based on their EMG activations and their physiological cross-sectional area, taking into account force-velocity muscle properties (Cholewicki and McGill, 1996, McGill, 2007).

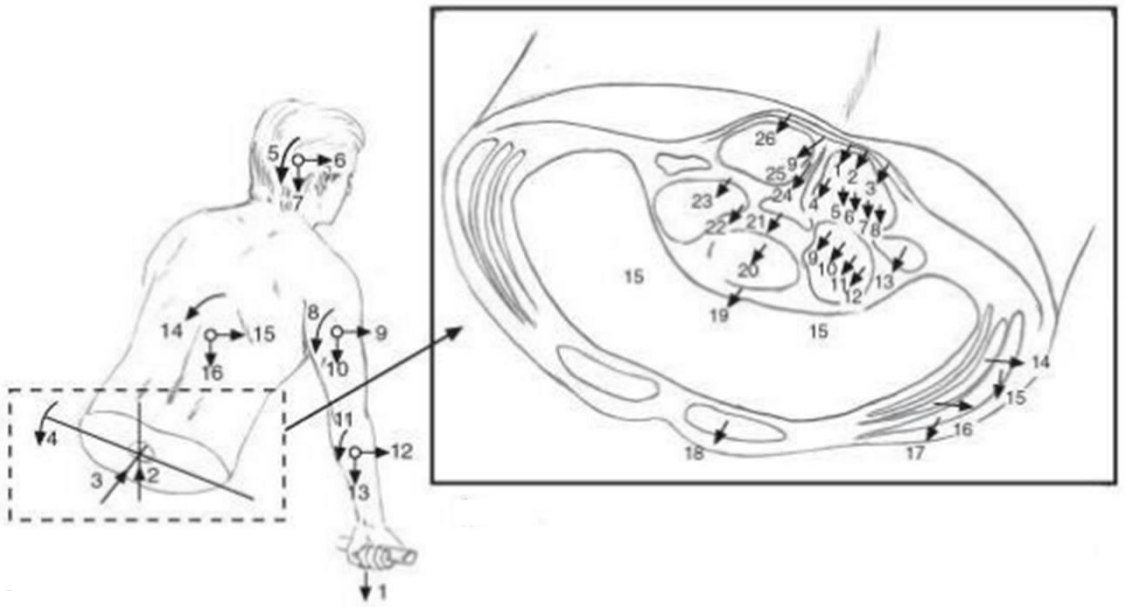

Figure 2.18 The models developed by McGill & colleagues partitioned the moments into tissue forces (muscles forces 1-18; ligaments 19-26; and disc). Image adapted from McGill (2007) (Copyright restrictions).

The first versions of this model were exclusively EMG-driven models (McGill and Norman, 1986, McGill, 1992), but its latest version incorporated an EMG-assisted optimisation hybrid method (Cholewicki and McGill, 1994, Cholewicki et al., 1995) to address the equilibrium violation limitation associated with EMG-driven models. In this approach, the force estimated for each muscle with the EMG signal was adjusted with an optimisation algorithm to satisfy the external moment requirements (Cholewicki and McGill, 1994).

This model was validated through a process consisting of component validation, internal validity checks, such as comparing the reaction moments to the sum of individual tissue moments predicted by the model, sensitivity analysis, and judgemental evaluation by comparing joint compression forces to other models simulating similar tasks (Granata and Marras, 1995a). The model was not compared to *in vivo* IDP measurements (Sato et al., 1999, Takahashi et al., 2006, Wilke et al., 2001) or VBR measurements (Rohlmann et al., 2014a, Dreischarf et al., 2015) as it was developed before these data were available.

This validated model has been used in a wide range of lifting studies, to estimate L4/L5 joint forces and also to evaluate spine stability to determine an individual's motor patterns (McGill,

1991a, McGill, 1992, McGill et al., 2003, McGill and Norman, 1986, Potvin and Tousignant, 1996).

2.2.5.4 Kingma & colleagues

Kingma and colleagues (Kingma et al., 1996, van Dieen, 1997, van Dieen and Kingma, 2005) used an approach similar to that of McGill and colleagues (McGill and Norman, 1986, McGill, 1992), but estimated forces and moments at L5/S1 instead of L4/L5. In this approach, a 3D link-segment model (Kingma et al., 1996) also estimated the reaction moments at L5/S1 before distributing the moment to the muscles included in the model, using EMG signals as inputs to determine muscle forces. Different versions of the model included between 88 (van Dieen and Kingma, 2005) and 114 (van Dieen, 1997) muscle fascicles crossing the L5/S1 joint, depending on the inclusion of transversus abdominus, psoas major muscle, and latissimus dorsi muscle. The discussion of the validation of this model is limited in the literature (van Dieen and Kingma, 2005, van Dieen, 1997), but muscle predictions agreed well with surface EMG data for corresponding muscles.

This model has been used extensively over the last 30 years to study spinal loads in a wide range of lifting tasks (Kingma et al., 1998, van Dieen et al., 1998, Kingma and van Dieen, 2004, Kingma et al., 2006, Faber et al., 2011, Kingma et al., 2016), using kinetic and kinematic data collected in the laboratory.

2.2.5.5 Arjmand model

In contrast to previously described optimisation and EMG-driven models, Arjmand and colleagues developed a kinematics-driven nonlinear finite element approach (El-Rich et al., 2004, Shirazi-Adl et al., 2005, Shirazi-Adl et al., 2002, Arjmand and Shirazi-Adl, 2006a) to solve the redundant active-passive system.

The musculoskeletal model of the trunk developed by Arjmand & Shirazi-Adl has been used in static (Arjmand and Shirazi-Adl, 2006a, El-Rich et al., 2004) and dynamic (Shahvarpour et al., 2015b) applications, as well as for stability analyses (Bazrgari and Shirazi-Adl, 2007,

Shahvarpour et al., 2015a). Their thoracolumbar finite element model is a sagittally symmetric T1-S1 beam-rigid body model comprising six deformable beams to represent the discs from T12-S1 and seven rigid elements to represent T1-T12 (single body) and lumbosacral vertebrae (L1-S1). The beams model the overall nonlinear stiffness of the T12-S1 motion segments (vertebrae, disc, facets, and ligaments).

The model comprises 46 local muscle fascicles (attached to lumbar vertebrae) and 10 global muscle fascicles (attached to thoracic cage). Muscle forces are estimated using a kinematics-based algorithm. In this approach, two modules are used: 1) a finite element module to solve the nonlinear ligamentous response of muscle/external forces and prescribed kinematics; and 2) a module to calculate muscle forces based on instantaneous configuration, equilibrium considerations, and optimisation algorithm. The iterative interactions between these two modules yield the converged solution of deformation, internal loads, muscle forces, and stability at each time step.

The model has been modified and improved over the years to take into account nonlinear passive properties of spine muscles and ligaments, and muscle wrapping (Arjmand and Shirazi-Adl, 2006a) and the stiffening role of compressive forces on passive responses of intervertebral segment motions (Arjmand and Shirazi-Adl, 2006a). More recently, all translational DOFs of the spine segments were introduced in the model (Ghezelbash et al., 2015). An advantage of this model is that equilibrium conditions at all lumbar and thoracolumbar joints are satisfied (Arjmand et al., 2007).

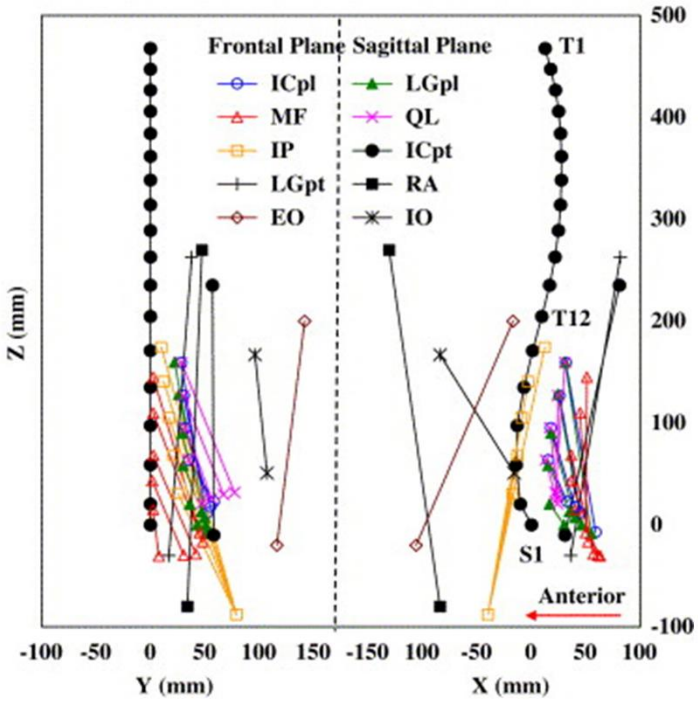

Figure 2.19 Frontal and sagittal planes for the finite element model with 46 local and 10 global muscle fascicles: ICpl: Iliocostalis Lumborum pars lumborum, ICpt: Iliocostalis Lumborum pars thoracic, IP: iliopsoas, LGpl: Longissimus Thoracis pars lumborum, LBpt: Longissimus Thoracis pars thoracic, MF: Multifidus, QL: Quadratus Lumborum, IO: Internal Oblique, EO: External Oblique, and RA: Rectus Abdominus Only one fascicles per side is shown. Image adapted from Arjmand et al. (2006) with permission from Copyright Elsevier.

Although the model has a high biomechanical fidelity, it renders analysis too complex and time-consuming for practical application to substantial participant cohorts. It is also not a full-body model, it only contains the trunk, and therefore cannot as easily take into account external forces from experimental data.

2.2.6 Limitations of computational modelling

Although the value and benefits associated with dynamic simulations of human movement are widely recognised (Fernandez and Pandy, 2006, Buchanan et al., 2004, Pandy, 2001, Thelen et al., 2006, Delp et al., 2007), estimates of joint loading and muscle forces predicted by the model cannot be easily directly compared to *in vivo* measurements to check their validity (Cholewicki et al., 1995). Instead, indirect methods consisting of component validation, internal validity checks, and sensitivity analyses must be used to evaluate model outputs (Cholewicki and McGill,

1996). The models reviewed in this section were validated using several methods, including comparisons with *in vivo* IDP and VBR, comparison with EMG experimental signals, comparison with other models, and internal validity checks. However, the methods used to compare the model estimates to *in vivo* measurements were not always clearly described. This made it challenging to relate the validation results between models. These limitations in the validation of models highlight the fact that they are currently best suited to evaluate relative changes in spinal loading, rather than absolute magnitudes.

Several models reviewed in this section are not suitable for studies of clinical problems studies involving kinematic and kinetic data collection on participants, thus limiting their use to only theoretical questions. For these models, the kinematics and kinetics data used for the simulations were created artificially. This is a drawback because such models cannot be used to evaluate real-life situations.

It is also challenging to review and compare these models as they incorporate different numbers of muscles, use different sources for PCSA values for muscles (or use CSA), group muscles differently, and use different maximum muscle stress values. This is a limitation of models (McGill, Kingma, and Arjmand groups) developed using local software or proprietary software that is not accessible to other researchers, thus also limiting their use and replication of results. This is an advantage of the AnyBody and OpenSim modelling software which allow model-sharing amongst users. However, AnyBody requires an expensive licence, thus limiting access to the models and software. On the other hand, OpenSim is freely accessible to researchers worldwide, which is an advantage over other non-open source models used in previous lifting studies. In addition, OpenSim provides a graphical user interface showing the simulations. Other models, with the exception of AnyBody, do not provide visual feedback of the simulations, making it hard to detect errors in the input data and results.

2.3 Biomechanical evaluation of lifting and ADL

Activities involving bending, lifting, carrying, and pulling, have been associated with an increased risk for the development of back pain (Ferguson et al., 2002, Waters et al., 1993, Norman et al., 1998, Heneweer et al., 2011). Due to the high prevalence of back injuries in occupations involving lifting, and the associated high costs, lifting has received considerable attention in the biomechanics literature. Many ADLs, such as gardening, cleaning, sit-to-stand, and other domestic chores, share the same characteristics as material manual handling occupational tasks, i.e. frequent forward bending and repetitive lifting of light-to-moderate objects. However, due to the challenges associated with capturing kinematics and kinetics data in the field, few non-occupational activities have been investigated with dynamic musculoskeletal models to estimate 3D spinal loads and thereby understand their associated risk for injuries and subsequent LBP. Instead, video-based (Azar et al., 2010) and static model approaches and self-reported questionnaires (Azar et al., 2005) have been used to evaluate spinal loads for tasks such as sweeping, carrying an infant, and gardening. However, a full dynamic analysis is preferred because static models underestimate spinal loads (McGill and Norman, 1985). Bed making and car egress are two of the only tasks that have been simulated in the laboratory and analysed dynamically.

A search of the literature was performed to identify studies that investigated the biomechanics of lifting and other ADLs that have involve motions that are risk factors for LBP. The following tasks were identified in the literature: lifting, more specifically one-handed lifting, car egress, and bed making. A brief review of the findings of these studies is presented in this section.

2.3.1 Lifting

Symmetrical two-handed lifting of heavy loads (20 kg) has been the main research focus in the biomechanics literature, for the purpose of establishing safety guidelines on lumbar loads in industrial settings (van Dieën et al., 1999). The spinal loads estimated by models have been used to develop guidelines for LBP prevention during lifting (van Dieen and Kingma, 2005). A lifting equation was developed and updated by the National Institute for Occupational Safety and Health

(NIOSH) to assist safety and health practitioners evaluate lifting demands in the sagittal plane (NIOSH, 1981, Waters et al., 1993). This lifting equation is based on three criteria (biomechanical, physiological, and psychophysical) and provides an empirical method for computing a weight limit for manual lifting. The biomechanical criteria are based on the original horizontal (Gill et al., 2007, Schipplein et al., 1995) and vertical (Davis et al., 1998) distances of the load with respect to L5/S1, the distance to lift, the frequency of lifting, the handles available on the load to lift, dimensions of the load lifted (Waters et al., 1993, van Dieën et al., 1999) and the sagittal symmetry of load relative to the individual at pick-up.

The most commonly advised lifting technique, especially for heavy loads, is the squat lift (Figure 1.1), in which the knees are flexed and the back is kept as straight as possible. However, squatting is associated with a higher energetic cost and higher perceived exertion than stooping (Krismer et al., 2007, Croft et al., 1998, Airaksinen et al., 2006), in which the legs are kept straight and the torso is bent forward and downward at the hips (Figure 1.1). The high physiological cost of the squat probably explains why individuals often shift from the squat to the stoop technique when repetitively performing a task (van Dieen et al., 1998). The biomechanical rationale for promoting the squat technique over the stoop remains controversial (Kingma et al., 2006, van Dieën et al., 1999, Bazrgari et al., 2007), likely due to various factors that affect back loading during lifting.

Despite the common use of one-handed lifting techniques in industry and for ADLs, they have only been evaluated in a limited number of studies (Marras and Davis, 1998, Cook et al., 1990, Wilson et al., 1997, Kingma and van Dieen, 2004, Ferguson et al., 2002, Kingma et al., 2016). This might be because the NIOSH lifting guidelines penalises for asymmetry, which is typically associated with one-handed lifts (Waters et al., 1993, Marras and Davis, 1998, Arjmand et al., 2012). Although symmetric lifting is preferred over asymmetric tasks (including lifting) as they have been associated with an increased risk of low back injuries (Marras et al., 1995), one-handed lifts produce lower spine compression loads than two-handed lifts for sagittally symmetric positioned objects (Marras and Davis, 1998, Kingma and van Dieen, 2004). In addition, an advantage of one-handed lifting is that the free hand can be used to support the trunk.

Previous studies of one-handed supported lifting have focused on industrial settings, where workers are required to lift material from deep bins (Kingma and van Dieen, 2004, Ferguson et al., 2002, Cook et al., 1990, Wilson et al., 1997). Using the outside of the bin to support the trunk (via the hand) while retrieving a load of 14 kg resulted in lower muscle activation of the erector spinae muscle than the two-handed stoop (Cook et al., 1990). The "golfer's lift", studied by Wilson et al. (1997), uses one arm to stabilise the body on an object, while the other hand performs the lift and the contralateral back leg is lifted as a counterweight (Figure 2.20). This technique reduced peak lumbar spine extension moments compared to two-handed stooping. In addition, self-reported levels of low back pain were lower for the golfer's lift than for the two-handed stoop (Wilson et al., 1997), probably because the peak L4/L5 net external moments were lower, thus relieving demand on back extensors. Similarly, Ferguson et al. (2002) found that supporting the body weight on the side of the bin with one hand reduced spinal loading by at least 15%, compared to two-handed stooping (Figure 1.1).

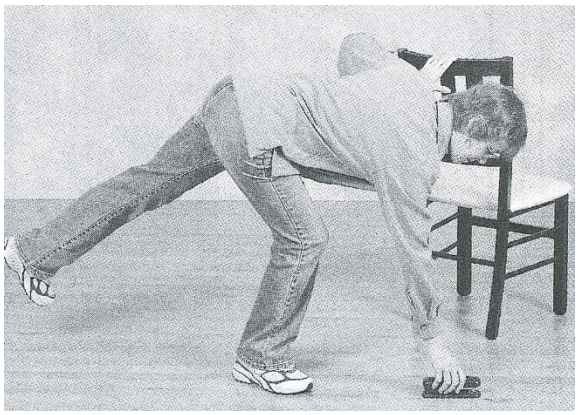

Figure 2.20 Golfers' lift. Image adapted from McGill (2007) (Copyright restrictions).

Kingma and van Dieen (2004) evaluated spine loading resulting from variations of the one-hand lifting technique: unsupported, supported, and supported with leg backward ("golfer's lift") with respect to two-handed lifting. Their results agreed with previous findings (Cook et al., 1990, Wilson et al., 1997, Ferguson et al., 2002), with reduction in lumbar moments and compression forces (5-10%) for unsupported one-handed lifts, and more substantial (15-30%) reductions when

the free hand was used to support the upper body on an external object (Kingma and van Dieen, 2004).

Although one-handed supported lifting reduces spinal loading (Kingma and van Dieen, 2004, Ferguson et al., 2002, Wilson et al., 1997), external objects are not always available to support the upper body. In such situations, the free hand (or forearm) can be placed on the ipsilateral thigh to brace the trunk. A single study in the scientific literature has investigated this braced arm-to-thigh lifting technique, in young healthy males. Ten healthy young males performed four lifting techniques (self-selected, squat, stoop, and weight lifters techniques) using the hand and the elbow support on the thigh, to lift a pencil and a beer crate (20 kg) (Kingma et al., 2016) (Figure 2.21). The weight lifters technique is characterised by a wide foot stance, moderately bent knees, and flexed hips with a straight back (Figure 2.21, C and D).

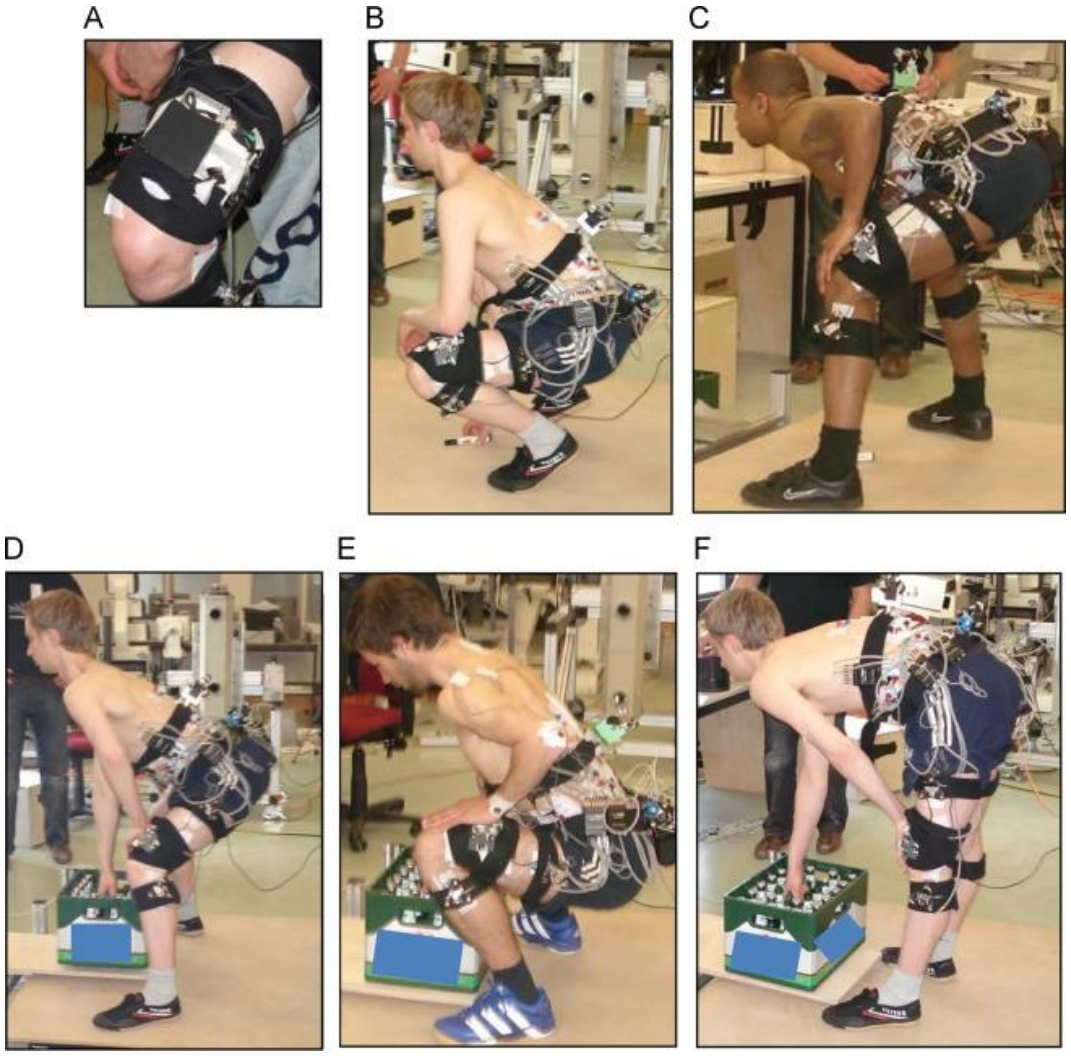

Figure 2.21 A) Support surface on the thigh to measure support from hand or elbow; B) Squat lifting technique to lift a pencil using the elbow support method; C) Weight Lifters technique to lift a pencil using the hand support method; D) Weight Lifters technique to lift a 20kg crate using the hand support method; E) Squat lifting technique to lift a 20kg crate using the hand support method; F) Stoop lifting technique to lift a 20kg using the hand support method. Image adapted from Kingma et al. (2016) with permission from Copyright Elsevier.

Supported lifts reduced extension moments, compression and AP shear forces at L5/S1, compared to unsupported lifting methods (Kingma et al., 2016), for both the crate and pencil lifting. One drawback of the hand support on the thigh was that it increased asymmetric trunk motion and moments at L5/S1. Nonetheless, hand support on the thigh is beneficial for spine loading when objects can be lifted with one hand (Kingma et al., 2016). This braced arm-to-thigh technique (BATT) can be used to lift light-to-moderate loads, or other ADLs, and may be especially useful for individuals suffering from LBP. These individuals are thought to have impaired neuromuscular control affecting their ability to successfully recruit muscles to stabilise the spine

(Lariviere et al., 2002, Hodges and Moseley, 2003, Hodges and Richardson, 1996, Hodges and Richardson, 1999). However, this braced technique has not been biomechanically studied in this specific population.

2.3.2 Car egress

Driving is one of the only common ADLs to receive some attention in the biomechanics literature. Although trivial for most individuals, car ingress and egress involve complex movements that are challenging for older and disabled individuals (Jung et al., 2015, Chateauroux and Wang, 2010, Cherednichenko et al., 2006). Most studies have focused on car egress motions as they are more problematic than car ingress (Chateauroux and Wang, 2010). The majority of the population uses *one-leg first* technique, where individuals move one leg out of the car while rotating the trunk, stand up, and then bring the second leg out of the vehicle (Figure 2.22A) (Chateauroux and Wang, 2010). However, older individuals or individuals with a disability use a *two-legs out* egress movement, where both legs are brought out of the car while swivelling on the seat, before rising out of the vehicle (Figure 2.22B) (Chateauroux and Wang, 2010). The rising phase resembles a sit-to-stand motion, but is complicated by the interaction with the internal vehicle environment. The *two-legs out* method is considered more stable than the one-leg first technique as both feet are in contact with the ground during car egress (Chateauroux and Wang, 2010). Individuals with a disability, and older individuals, also frequently use hand supports on the seat, steering wheel, or thigh, during car egress, but the effect of this hand support on spinal joint loading has not been assessed (Chateauroux and Wang, 2010).

A)

B)

Figure 2.22 Car egress methods: A) *one-leg first* technique; B) *two-legs out* egress movement. Images adapted from (Chateauroux et al., 2007) (Copyright restrictions).

Studies evaluating car egress have mainly focused on the kinematics (Chateauroux and Wang, 2010, El Menceur et al., 2008, Causse et al., 2012), with only one pilot study examining the feasibility of measuring the interaction of the participant with the vehicle to understand the egress motion quantitatively (Causse et al., 2009).

2.3.3 Bed making

Bed making is a common ADL (and occupational task) that involves frequent forward bending and loading (mattress). In addition, the position of the bed relative to the body limits the movements. This task was simulated in the laboratory to investigate the effect of the bed size and height on spinal loads (Milburn and Barrett, 1999). Two-dimensional kinematics in the sagittal plane were measured using retroreflective markers and the spinal loads at L5/S1 were estimated with a dynamic two-dimensional model (LiftTrack version 2.1, Motion Analysis Corporation, Santa Rosa, CA). Peak L5/S1 compression forces were above 6000 N for some of the tasks, while peak shear forces were all below 400 N. A limitation of this study is that it only evaluated the motions in the sagittal plane. In addition, the loads acting at the hands were only measured for one participant and assumed to be the same across participants. Nonetheless, this study quantified spine loads during bed making, demonstrating that this task is physically demanding and produces compression forces similar to those experienced during heavy lifting tasks (20 kg).

2.4 Injury thresholds

In vivo studies use musculoskeletal models described in Section 2.2.5 to estimate the forces acting on the spine during various activities. *Ex vivo* studies measure the damage caused by the application of forces to human tissues. The combination of these two types of studies represent the mechanical basis for LBP research (Hsiang et al., 1997).

External moments, with compression and shear loads, applied at the lumbar intervertebral joints can lead to tissue failures of the anatomical structures of the spine, thus resulting in subsequent back injuries. Due to the orientation of the L4 and L5 vertebral bodies (approximately 45° with the horizontal in the sagittal plane), the facet joints, ligaments, and discs at L4/L5 and L5/S1 experience large shear forces to resist the tendency of the superior vertebra to slide anteriorly, especially when loads are held in the hands. In addition, these two joints experience the largest compression loads in the lumbar spine. For these reasons, the L4/L5 and L5/S1 joints are more prone to injuries in the lumbar spine. The L4/L5 joint is more susceptible to injury than L5/S1, as the latter is partially protected from torsional strain because it is deep-set in the pelvis and anchored by the iliolumbar ligaments (Bogduk, 2005).

Spinal compression is more frequently studied than shear and torsion (Adams et al., 2006, Gallagher and Marras, 2012). High compression forces can result in vertebral endplate fracture (Perey, 1957) and prolapse of the intervertebral disc (Brinckmann et al., 1989). However, this type of loading is more likely to affect the endplates of the vertebral body than the disc because the disc can usually resist higher compressive forces than the adjacent vertebrae (Adams et al., 2006). Brinckmann et al. (1988) measured maximum compressive strength values for adult lumbar vertebral segments ranging from 2100 N to 9600 N, with variations due to bone material properties and dimensions. Based on these cadaveric results, the NIOSH published guidelines for spine loading, with a maximum compressive force of 3400 N at the L5/S1 joint (NIOSH, 1981, Waters et al., 1993). This threshold has been used widely in industry to design safe lifting tasks. Repetitive motion can also lead to tissue fatigue, thus increasing the risk of back disorders (McGill, 2007, Marras et al., 1995, Norman et al., 1998). Repetitive loading can reduce the

compression strength limit at which failure occurs by up to 50% when 5000 cycles are applied in *ex vivo* specimens (Adams et al., 2006, Hansson et al., 1987, Brinckmann et al., 1988). Most of the compression forces experienced at the vertebral levels during everyday life are generated by tension in the trunk muscles, with bending and lifting creating larger forces in the lumbar spine (Adams et al., 2006), and thus demonstrating the importance of including the contribution of muscles in biomechanical models.

The lumbar spine can experience large shear forces during occupational tasks involving forward bending due to gravity acting on the upper body. AP shear forces can cause damage to the vertebrae, leading to failure of the facet joints (van Dieën et al., 1999) and pedicles. The lumbar facets and neural arch can withstand approximately 2000 N of shear load (Cripton, 1995), but a generally accepted maximum limit of 1000 N shear has been established for single exertions (McGill et al., 1998). A modified shear load limit of 700 N has recently been suggested for frequent loading (up to 1000 loading cycles per day) that can lead to fatigue failure (Gallagher and Marras, 2012). Although the maximum limits associated with shear are lower than those for compression, the spinal structures loaded in shear are also weaker and may be similarly vulnerable to injury given large or repetitive loading (Gallagher and Marras, 2012).

Extension moments can cause damage to the posterior spinal ligaments, posterior intervertebral discs, and muscles, during forward bending and lifting movements (Adams and Hutton, 1982, van Dieën et al., 1999, Adams et al., 1994) The combined action of forward bending and compression is thought to be more damaging to the intervertebral discs and ligaments than compressive forces alone (Dolan et al., 1994a). Cadaveric tests on lumbar segments indicated that injuries start to occur at moments between 50-80 Nm (Adams and Dolan, 1991, Adams et al., 1994, Adams et al., 2006, Adams et al., 1980), with the interspinous and supraspinous ligaments being the first components to sustain damage (Adams et al., 1980). Biomechanically, loading of these tissues can be reduced during lifting by placing the load held in the hands as close as possible to the body to decrease the moment arm, and therefore lower the tissue loads necessary to support the reaction moments (McGill, 1997).

2.5 Summary

This chapter demonstrated that although several musculoskeletal models of the lumbar spine exist across different modelling platforms, there is currently no validated freely available full-body model with a detailed lumbar spine suitable to evaluate lumbar spine loads during lifting tasks. In addition, although the BATT technique has been evaluated in young healthy males, it has not been evaluated in individuals with LBP, either for lifting tasks or other ADLs identified as risk factors for LBP.

Chapter 3 Methodology

Chapter 3 provides additional details on the methodology for the experiments described in Chapters 4, 5, and 6 as they were presented as independent manuscripts, with only brief description of their corresponding methods. The literature on lifting studies and spine modelling in OpenSim is limited, thus requiring the development of new methods for each of the studies in this thesis. Several iterations were often required to obtain the final methodology presented in Chapters 4 to 6. Therefore, this additional information is provided to aid understanding of the decision-making rationale for the studies presented in Chapters 4 to 6. This section is also intended for researchers that wish to use OpenSim to study lifting tasks or other ADLs, either building on the work presented in this thesis or conducting their own experiments, to avoid the need to develop and test similar methods.

This chapter is divided into three main sections: 1) Participant recruitment; 2) Experimental approach and instrumentation; and, 3) OpenSim simulations. The first section focuses on the recruitment of participants with LBP (Chapter 5), as it was challenging to recruit participants with LBP. The second section presents the new experimental methods and apparatus developed for this thesis. Finally, the third section discusses the challenges faced when using OpenSim to simulate lifting tasks. This chapter frequently refers to the following chapters, where the method or topic discussed was used.

3.1 Participant recruitment

For the study presented in Chapter 5, participants with non-specific and persistent LBP were recruited. Individuals suffering from *known* spinal disorders such as scoliosis, degenerative spondylolisthesis, cauda equina syndrome, spinal tumours, or any previous spine surgery, were excluded from the study. Individuals with a pain catastrophising score above 30 were also excluded because of their tendency to negatively exaggerate painful stimuli, such as lifting tasks (Sullivan et al., 1995). A limit of 30 on the body mass index (BMI) was used in an attempt to reduce skin artefact errors associated with reflective surface markers and reduce errors associated with landmark palpation, particularly pelvis and torso. These exclusion criteria (Table 5.1) were

determined by reviewing several studies that involved LBP participants (Krismer et al., 2007, Lariviere et al., 2002).

The spinal clinic at the Royal Adelaide Hospital was initially targeted as the main site for recruitment, with the support of spine surgeons. However, most patients from this source did not meet BMI or pain catastrophising criteria. Recruitment sites were expanded to local physiotherapy clinics, general practices, chiropractors, gyms, and posting boards at the University of Adelaide. Despite this expansion, recruiting eligible individuals was challenging, spanning over approximately 1.5 years.

After completing a screening questionnaire (Appendix A), each eligible participant was assessed during a brief phone interview. Participants with LBP were asked the following questions to determine if they were suitable for the LBP category:

1. Did they have an episode of LBP in the past 2 weeks? If not, when was their last episode?
2. How did their LBP affect their ADLs?
3. Did they experience pain lifting groceries, vacuuming, or other ADLs?
4. What seemed to aggravate the LBP?
5. How did they rate pain experienced in the lower back (0 to 10) on a daily basis?
6. Were they currently consulting a health professional (doctor, physiotherapist, chiropractor, etc.) for their LBP?

These questions were formulated based on discussion with other researchers experienced in recruiting participants with LBP. Participants had to demonstrate a clear behaviour where LBP affected their daily life to be included in the study.

Healthy participants were asked if they had experienced back pain in the last year and if they had difficulties performing any tasks due to pain experienced in the back. This was to confirm that they fulfilled the inclusion criteria for the healthy group.

For the studies in Chapters 4 and 6, only young healthy male participants were recruited, as is typical of many similar biomechanical task evaluations.

3.2 Experimental approach and instrumentation

This section provides additional details on the methods used for data collection used in the studies presented in Chapters 4 to 6: the marker set used for data collection in Chapters 4 to 6; surface EMG electrodes used in Chapters 4 and 5; the instrumentation used to measure the bracing force on the thigh in Chapters 4 to 6; the design of the box used for lifting tasks in Chapters 4 and 5; the instrumentation developed for the evaluation of ADLs in Chapter 6.

3.2.1 Marker Set

For the studies in Chapters 4 to 6, full-body kinematics were collected using 88 reflective markers, including both anatomical and tracking markers (Figure 3.1). This full-body marker set was similar to those used in previous lifting studies (Kingma et al., 1996, Kim and Zhang, 2017, Bassani et al., 2017), but it contained more tracking markers, i.e. markers not used to define anatomical coordinate systems but used to track the motion of a body segment, for the trunk and limbs. Previous studies have typically tracked the trunk only using markers placed at the proximal and distal ends of trunk [C7 and anterior superior iliac spine (ASIS)], occasionally with a marker (or cluster of markers) placed at T10 or T12 (Kingma et al., 1996, Kim and Zhang, 2017, Bassani et al., 2017). In this thesis, the lumbar and thorax regions were tracked separately using four skin-mounted markers; pilot tests showed that using anatomical markers only at the proximal and distal ends of the trunk resulted in angles above the reported physiological range of motions (Pearcy et al., 1984), specifically for trunk flexion and axial rotation. Additional markers for the upper and lower limbs were also included in the marker set developed for this thesis to improve tracking of these limbs, especially given the possible obstruction of these markers during lifting tasks and the ADLs.

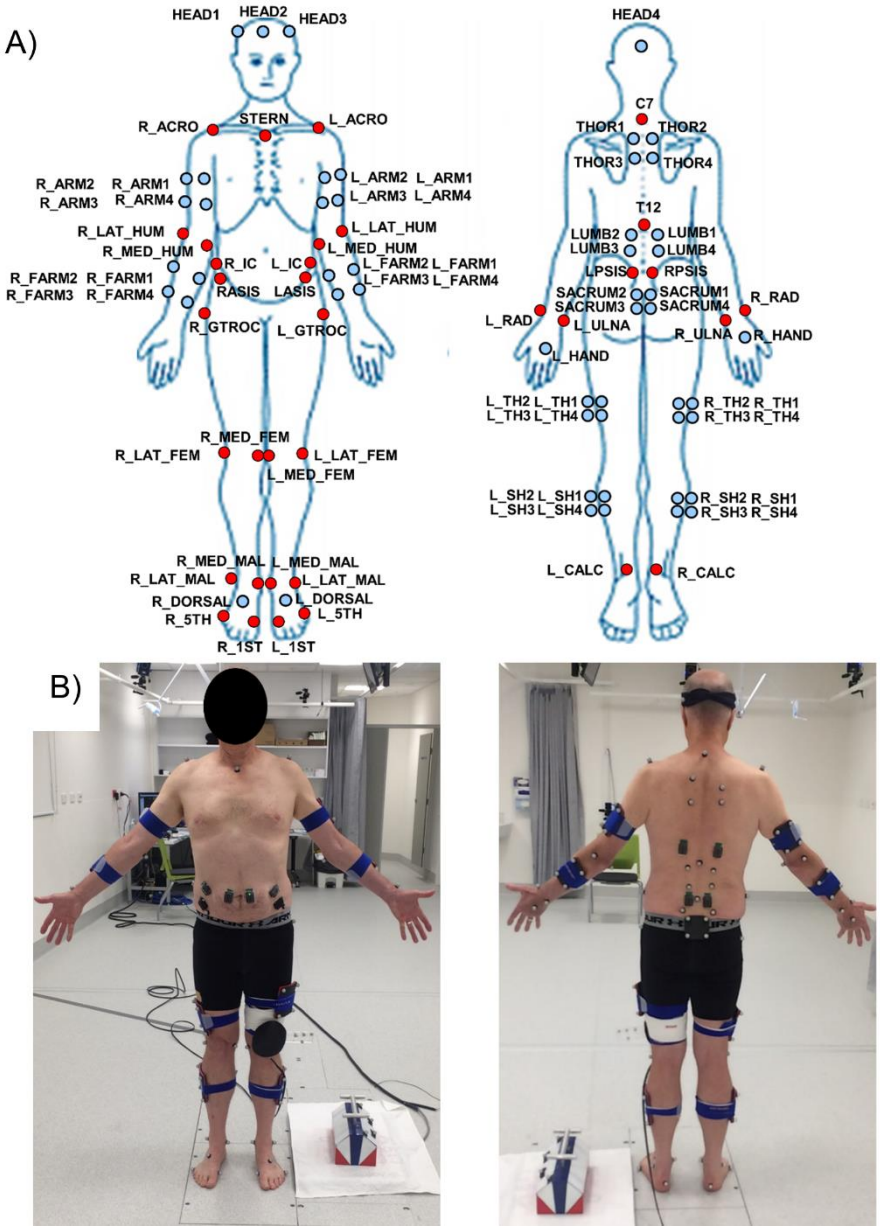

Figure 3.1 A) Full-body marker set used for data collection: anatomical markers are represented by red dots while tracking markers are represented by blue dots. B) Exemplar of a participant with the full-body marker set used in Chapters 4 to 6. Tracking clusters are secured to the participant using Fabrifoam (Exton, PA, USA) wraps. Individual tracking and anatomical markers were adhered to the skin using double-sided tape.

Rigid 3D printed plastic plates were used to form the clusters of four markers that were used to track the pelvis/sacrum body, as well as the upper and lower limbs. This method was chosen over individually skin-mounted markers because it prevents independent movement of each marker tracking the same rigid body (Fukaya et al., 2012). In addition, rigid clusters reduce soft tissue movement (when used with wide elastic bands as performed in Chapters 4 to 6) and provide for easier mounting on participants (Cappozzo et al., 1995, Cappello et al., 1997).

The pelvis/sacrum cluster design was a U-shaped plastic plate adhered to the skin overlying the sacrum with double-sided tape, and further secured by the elastic band of the compression shorts worn by the participants (Figure 3.2, also shown in Figure 3.1 B and Figure 3.17, for an exemplar participant). This rigid cluster was used because individual markers placed on the right and left anterior superior iliac spine (ASIS) were obstructed during the forward bending motions studied in Chapters 4 to 6. Since at least three non-collinear reflective markers are required on each segment to define its orientation in space, this rigid cluster allowed for adequate tracking of the pelvis/sacrum (tracked as one rigid body) over the entire trial. Individually skin-mounted markers placed on the iliac crests were also trialled, but they produced higher marker errors compared to the rigid cluster placed on the sacrum, likely due to the higher skin motion artefact at this anatomical location.

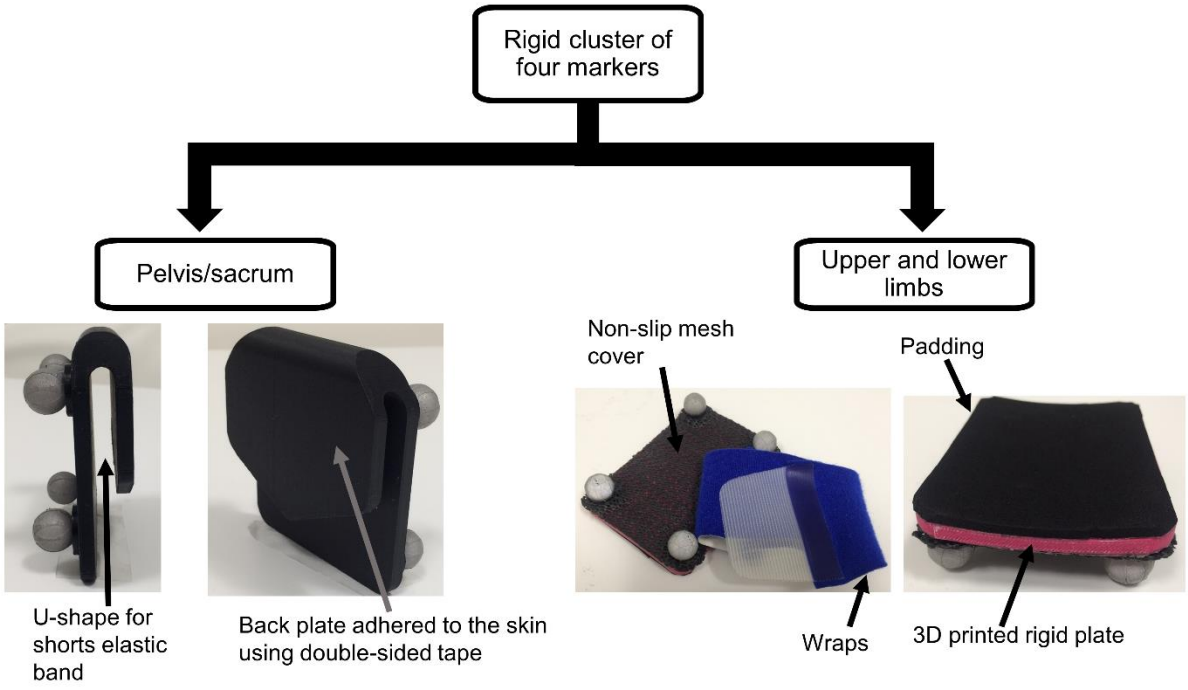

Figure 3.2 Pelvis/sacrum: a rigid cluster of four markers fixed to the corners. The back plate was placed inside the compression shorts worn by the participants and adhered to the skin using double-sided tape. The elastic band of the compression shorts was placed between the front and back plate of the pelvis cluster. Upper and lower limbs:Top side of the cluster with non-slip mesh cover. Underside of the cluster with high density foam padding. Wraps were used to attach the cluster to the upper and lower limbs.

Rigid clusters of four markers were also used to track lower and upper limbs (Figure 3.2, also shown in Figure 3.1B and Figure 3.17 for an exemplar participant). The interface of the cluster

with the skin was padded to conform to the shape of the limbs and minimise sliding of the rigid cluster on the skin. These clusters were secured to the arms and legs using wide Fabrifoam wraps (Exton, PA, USA). A non-slip textured mesh covered the top side of the rigid cluster interfacing with the wraps, also to minimise slipping of the cluster during motion.

Rigid plastic clusters were trialled for tracking the motion of the thorax and lumbar spine bodies. However, rigid plates were difficult to secure using double-sided tape and wraps at these locations. In addition, they interfered with the location of the EMG electrodes in the lumbar region for studies in Chapters 4 and 5. Consequently, individually skin-mounted markers were used (Figure 3.1). Great care was taken to place markers consistently on these regions; thorax markers were placed on the inside of the scapula to minimise attribution of shoulder movements to thorax motion.

3.2.2 EMG Surface Electrodes

EMG measurements of trunk muscles were collected for the studies in Chapters 4 and 5. Muscle selection and location of electrodes was based on a procedure developed for an EMG-driven model for the trunk reported in the literature (McGill, 1991b, McGill, 1992); eight surface electrodes (Delsys Inc, Boston, MA, USA, electrode material: 99% Ag-AgCl, common mode rejection ratio: >80 dB, Interelectrode distance: 10mm, signal latency: 48 ms; sampling frequency: 2000 Hz; signal condition: bandpass filter 10-450 Hz) were placed (Figure 3.3) on participants to collect muscle activity from four muscles (Table 3.1**)**. The electrodes were secured using double-sided tape and over-taped (Fixomull transparent, BSN Medical, Hamburg, Germany) to avoid dislodgement during the experiment.

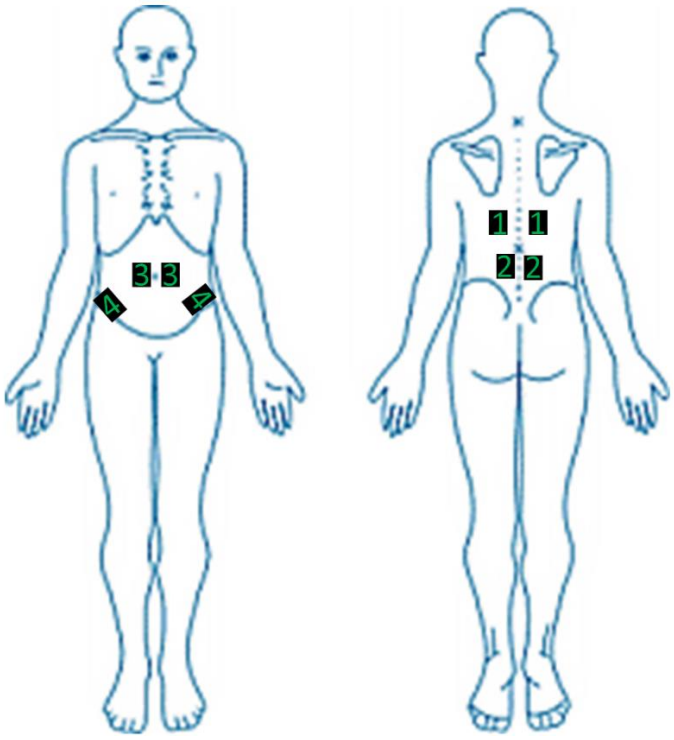

Figure 3.3 Bilateral EMG placement for four trunk muscles: 1) Thoracic Erector Spinae, 2) Lumbar Erector Spinae, 3) Rectus Abdominis, 4) External Obliques.

Table 3.1 EMG electrode placement on the trunk based on McGill (1992).

Electrode #	Muscle	Electrode Placement
1	Thoracic Erector Spinae	Place electrode 5 cm lateral to T9 spinous process
2	Lumbar Erector Spinae	Place electrode 3 cm lateral to L3 spinous process
3	Rectus Abdominis	Place electrode 3 cm lateral to umbilicus
4	External Obliques	Place electrode approximately 15 cm lateral to umbilicus, along muscle fibres

Maximum voluntary contraction trials were collected for these four muscles on all participants. Back musculature was recruited by placing the participants on their stomach on a physiotherapy bed, with their torso hanging over the edge of the bed and their legs restrained to the bed with straps. They performed back extensions against manual resistance applied at the shoulders. Abdominal muscles were recruited by placing participants in a seated position on a physiotherapy table with their knees bent and their feet restrained to the bed with a strap. Sit-up motions were performed against manual resistance applied at the shoulders. EMG was only collected for the studies presented in Chapters 4 and 5.

3.2.3 Thigh Bracing measurement

The bracing force applied to the thigh by the hand was measured and incorporated into the simulations. A three-axis load cell (Type 9327C, Kistler, SUI) was selected due to its small size (42 x 42 x 42 mm), allowing it to be attached to the thigh, while also minimising the offset between the hand and the thigh. Its low mass (380 g) did not add significant weight to the leg of the participants that could have limited their movements. The load cell measured vertical forces in the 0-8 kN range, while it was rated to 1 kN for both shear forces. Measurement of thigh bracing by the hand has only been reported in one other study in the literature (Kingma et al., 2016). The load cell used in their study had a similar top surface area to the Kistler load cell used in this thesis, but had a lower height and weight (ATI, mini45, SI-580-20; 17.5 mm height, 45 mm diameter, 99.8 g). However, at the time of purchase in 2014, the Kistler load cell selected for this project had a substantially lower profile than other 3-to-6 axis load cells available on the market. In addition, it could be integrated into the existing signal conditioner and charge amplifier in the study laboratory.

The load cell was incorporated into an assembly that allowed for interface with the hand and attachment to the thigh (Figure 3.4). This assembly was composed of four parts and was designed for a previous pilot project in the study laboratory which also measured thigh bracing forces (Appendix B).

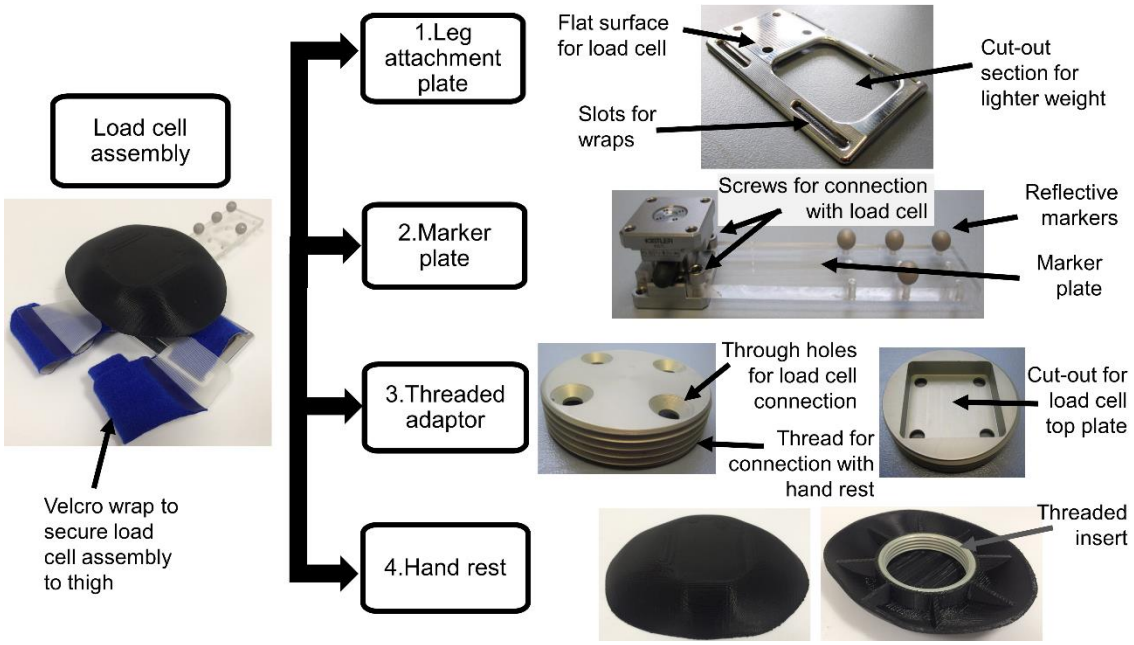

Figure 3.4 The load cell assembly comprised four custom designs: 1) Leg attachment plate: a curved aluminium plate was attached to the thigh using Velcro wraps. The load cell was connected to the flat section of the leg attachment; 2) Marker plate: an acrylic plate with four markers rigidly attached to it to track its orientation and location; 3) Threaded adaptor: an aluminium threaded part that connected the load cell to the hand rest; 4) Hand rest: a rigid three-dimensional printed plate for the hand interface.

The leg attachment was an aluminium plate secured to the thigh using Velcro Fabrifoam wraps (Exton, PA, USA) through slots on its side (Figure 3.4). The top section of the plate was flat to secure the load cell, via four countersunk through holes, while the bottom section was curved to provide a better interface with the thigh. The dimensions of the leg attachment plate were larger than those of the load cell to reduce possible motion between the attachment plate and the thigh. This leg attachment plate also comprised a cut-out section to reduce its weight.

The acrylic marker plate was connected to the load cell with two screws. Four markers were glued to the marker plate to track the location and orientation of the load cell during the trials (Figure 3.4). The markers were placed into holes spaced 30 mm part lengthwise and 16 mm apart across the width of the plate.

The threaded adaptor was a male threaded aluminium circular part comprising four countersunk through holes, connecting the hand rest to the load cell (Figure 3.4). It was connected to the load cell with four screws.

The hand rest was a 3D printed plastic ellipsoid part with a rounded top to facilitate interaction with the hand (Figure 1.1Figure 3.4). An aluminium female threaded insert was press fit to the underside of the hand rest for connection with the threaded adapter.

3.2.4 Box for lifting tasks

Participants lifted a custom box (30.5 x 19 x 15.5 cm) from the ground for the studies presented in Chapters 4 and 5 (Figure 3.5). Its mass could be varied by changing the amount of lead shot placed in it. Motion of the box was tracked using four reflective markers fixed to its surface. The handle of the box was designed to allow for one-handed (centre of handle) and two-handed (handles on each side) lifting techniques, while maintaining the same height. This box had similar dimensions to those used in other lifting studies (typically wooden boxes resembling a beer crate) (Ferguson et al., 2002, Kingma et al., 2016). However, the width of this handle was smaller than the width of wooden boxes used in those studies focusing on heavy lifting (Ferguson et al., 2002, Kingma et al., 2016), as the box design was based on the size of objects commonly lifted in ADLs.

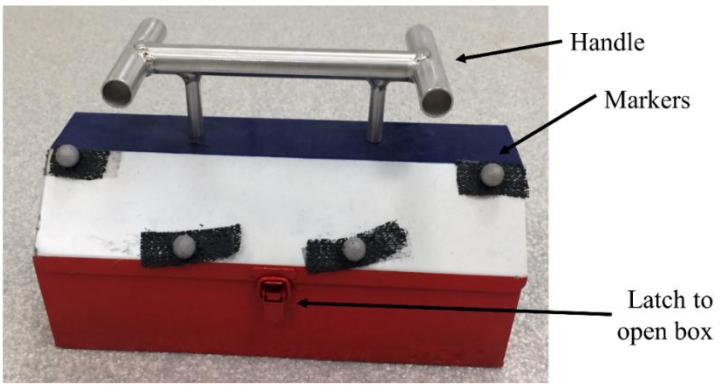

Figure 3.5 Box used for lifting tasks with a handle allowing for one-handed and two-handed lifting tasks. The mass of the box could be changed by modifying the mass of lead shot placed in the box. Its motion was tracked by markers glued on it.

3.2.5 Activities of daily living

Three activities of daily living were simulated in the laboratory in order to investigate the effect of bracing on spinal loading in Chapter 6. These three tasks were weeding in a standing position (gardening), reaching for an object in a low cupboard, and car egress. The selection process, including the selection criteria, and the apparatus designed and constructed for the simulations for these tasks are discussed in Chapter 6.

The apparatus used for these three tasks are described briefly in this section and more detailed images of the instrumentation are provided. For the weeding task, the pulling action during weeding was replicated using a magnet placed on a magnetic steel plate (Figure 3.6A) and the pulling force was measured using a load cell (MC3A-1000, AMTI, USA), rigidly attached to the metallic plate. For the cupboard tasks, a steel frame with a wooden shelf was used to simulate the task of reaching for objects in low cupboards (Figure 3.6B). The dimensions of the steel structure replicate those of a standard kitchen bottom cabinet (Appendix C).

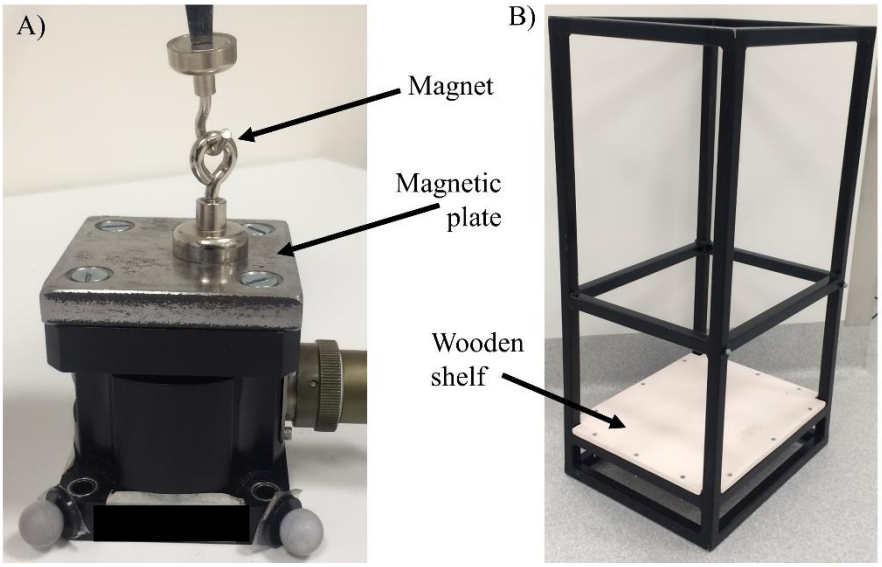

Figure 3.6 A) Magnet placed on steel magnetic plate rigidly attached to the AMTI load cell (MC3A-1000, AMTI, USA) to measure pulling force. B) Cupboard frame design to simulate the task of reaching for objects in low cupboards.

For car egress, two steel structures (main body and door) were used to replicate the dimensions of a standard average Australian car (e.g. Ford Monroe) (Figure 3.7, Appendix D). Previous studies investigating car egress motions in the laboratory typically used stripped vehicles, retaining the components around the driver's seat such as the door, the steering wheel, and the complete driver's seat (seat and back rest) (Chateauroux and Wang, 2010, El Menceur et al., 2008). However, due to marker visibility constraints in this study, a design constructed from steel square sections representing the driver's compartment was preferred. A load cell (MC3A-1000, AMTI, USA) was rigidly attached to the car frame, either on the door frame (Figure 3.7) or the

dashboard (Figure 3.8), to measure hand support with these two contact points during car egress. The load cell was covered by a rigid plastic 3D printed hand rest (Figure 3.8) to provide an interface between the load cell and the hand.

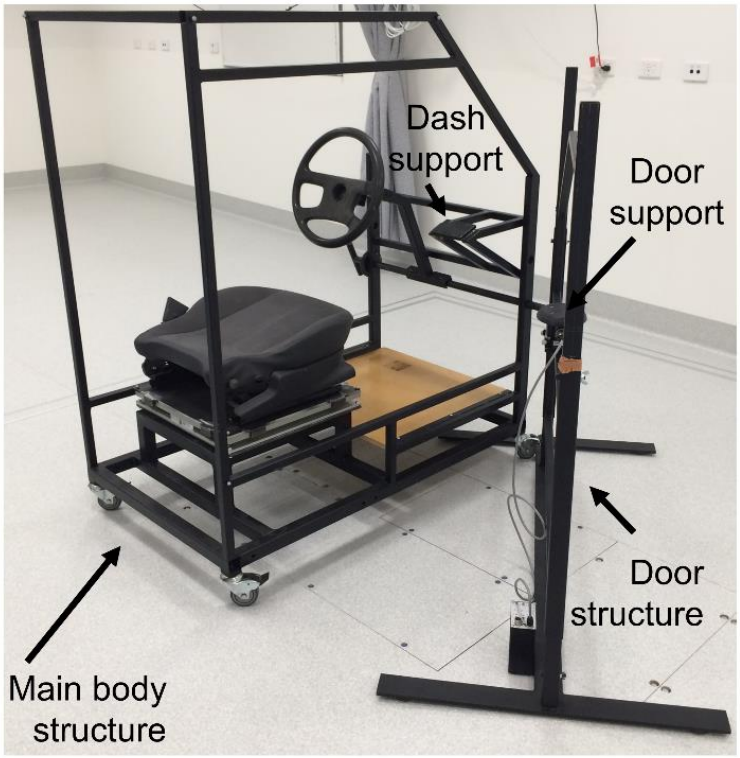

Figure 3.7 The car design comprising a main body and a door structure to simulate car egress in the laboratory. A three-axis load cell (MC3A-1000, AMTI, USA) was secured to the door structure or the dash on the main body structure to measure hand support at these contact points.

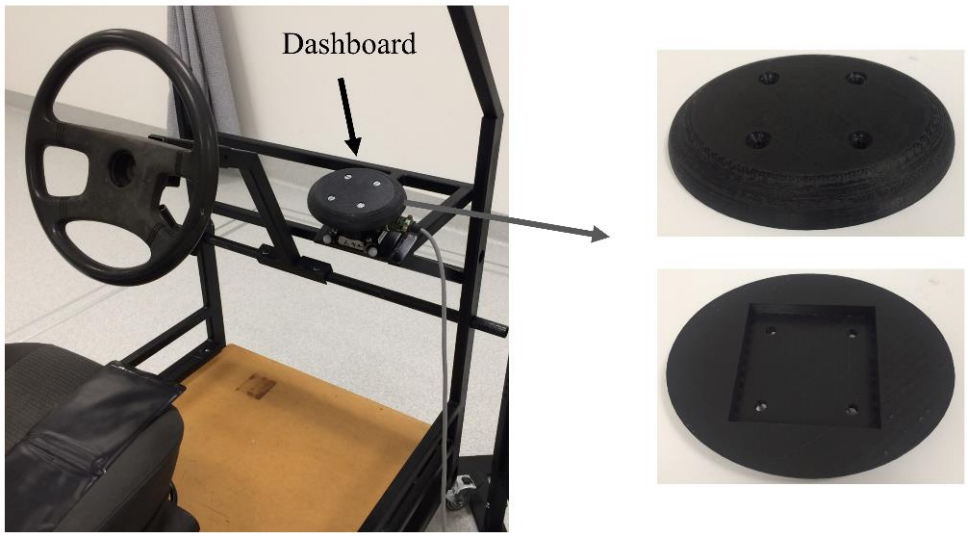

Figure 3.8 Closer view of the dashboard on the main body structure, instrumented with an AMTI load cell (MC3A-1000, AMTI, USA). A rigid plastic three-dimensional printed hand rest covered the load cell.

3.3 OpenSim Simulations

Dynamic simulations were created for each participant for the lifting and ADL tasks studied in Chapters 4 to 6, using the modelling software OpenSim (version 3.3) (Delp et al., 2007). Before importing the data into OpenSim, the experimental kinetic and kinematic data collected for these studies (Chapters 4 to 6) required several pre-processing steps, such as filtering, transforming the coordinate systems between the acquisition devices and OpenSim, and structuring the experimental data into the file format for OpenSim (TRC and STO files for kinematics and kinetics, respectively). The original MOtoNMS MATLAB toolbox developed by Mantoan et al. (2015) was modified considerably, as it was tailored to gait analysis, rather than lifting or other ADL tasks. The ensuing workflow for each simulation contained the analyses required to estimate joint forces, using static optimisation to estimate muscle forces (Figure 3.9). However, OpenSim is predominantly used to analyse gait and running motions. Consequently, several challenges were faced throughout the workflow when analysing lifting and other ADLs. One previous study evaluated lumbar spinal loading during lifting tasks, but details on their simulation methodology was not provided (Kim and Zhang, 2017). This section presents the challenges for the different steps of the workflow and describes their solutions, along with the iterations often required to resolve the issues.

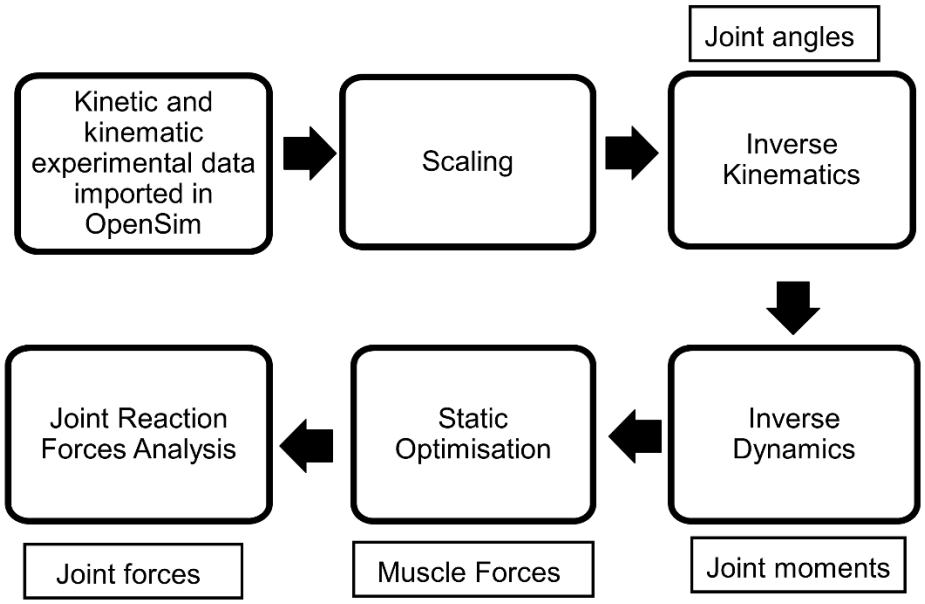

Figure 3.9 OpenSim workflow used for the studies presented in this thesis (Chapters 4 to 6). After the experimental data was imported into OpenSim, the generic model was scaled to the dimensions of each participant, before performing inverse kinematics to obtain joint angles, inverse dynamics to obtain joint moments, static optimisation to obtain muscle force estimates, and finally joint reaction force analysis to obtain the joint force estimates.

A custom MATLAB (version 2017b, Mathworks, Nattick, MA, USA) program utilising the OpenSim application program interface (API) was developed to assist with data analysis in OpenSim. This program saved a considerable amount of time by automatically generating the required setup files for each participant and running the analyses in the OpenSim workflow (Figure 3.9), especially given the large number of participants recruited for the studies in this thesis (total of 51 participants). In addition, some of the workload was transferred to the Phoenix high performing computer at the University of Adelaide to reduce the computing time associated for lengthy analyses, such as static optimisation. Despite using this batch processing approach, it is important to note that the results of each analysis for each trial and participant were carefully reviewed to ensure their validity.

A brief description of the program is provided here. Once launched, this program prompted the user to identify which participant to select and which analysis to perform, via a graphical user interface (GUI) (Figure 3.10). Multiple participants and analyses could be selected simultaneously, allowing for batch processing of the data. This program was used for the lifting

tasks analysed in Chapters 4 and 5, as well as the ADLs simulated in Chapter 6 (Study 3 as shown in the GUI).

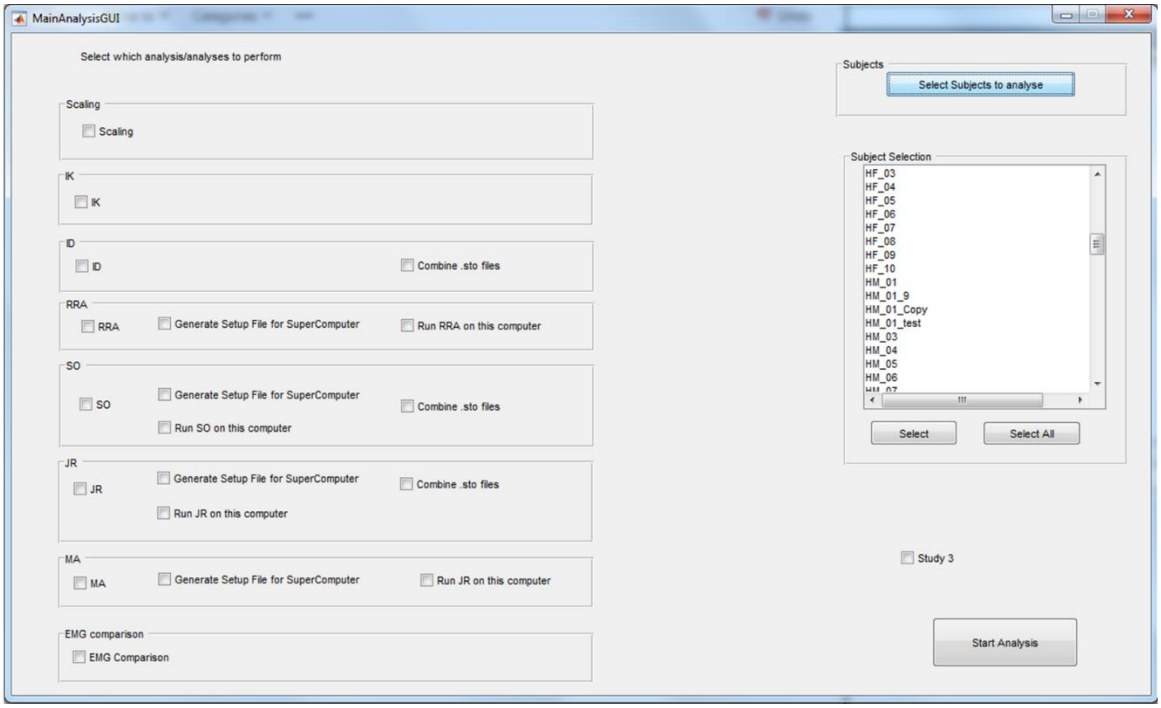

Figure 3.10 Graphical user interface (GUI) prompting the user to select participant and analysis to perform, once the MATLAB program has been launched.

After selection of the participant(s) and analysis/es, the user was prompted to select which trial(s) to analyse, for the corresponding participant and analysis (Figure 3.11). The results of the analyses were then automatically saved in each participant's folder.

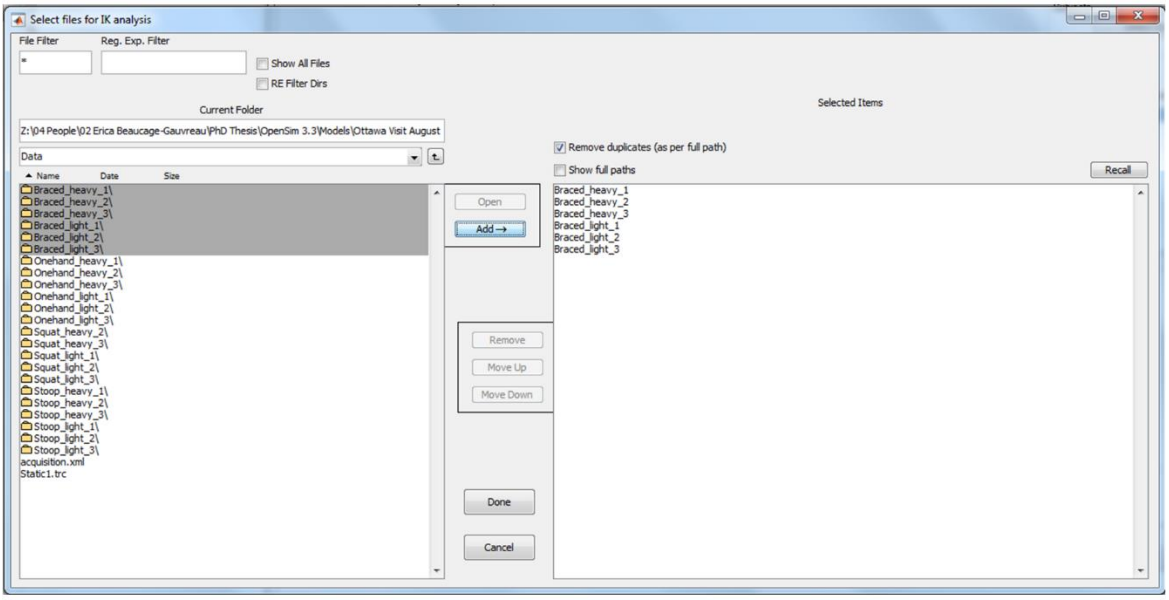

Figure 3.11 Graphical user interface (GUI) prompting the user to select participant and analysis to run, once the MATLAB program has been launched.

3.3.1 Model

A full-body OpenSim model was used to analyse the activities evaluated in this thesis (Figure 3.12), using the workflow described above (Figure 3.9). The model and its validation are described in detail in Chapter 4 (Beaucage-Gauvreau et al., 2019). However, this section provides additional information on the considerations and modelling decisions for the lower limb and trunk musculature included in the final model presented in Chapter 4. A brief explanation of how muscles are modelled in OpenSim is first presented in this section, to provide context for those not familiar with OpenSim.

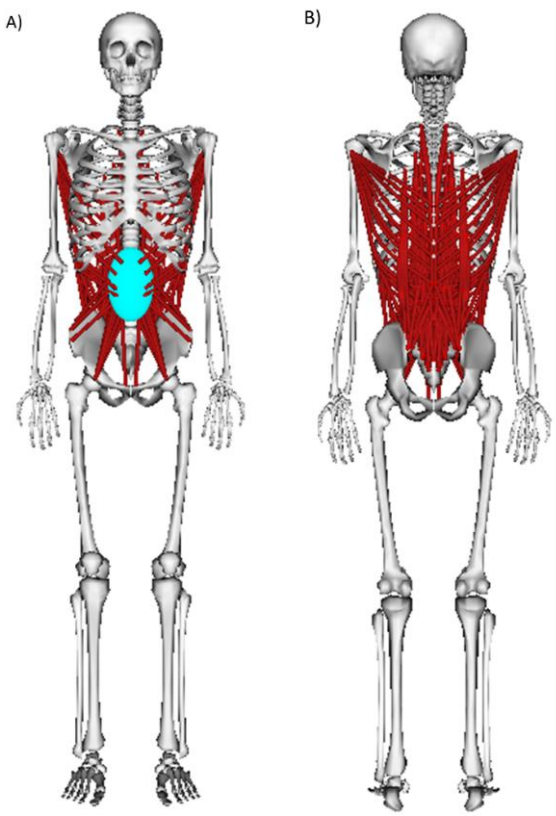

Figure 3.12 Front (A) and rear (B) views of the generic model used in this thesis, with 238 muscle fascicles for the lumbar region and a total of 29 degrees-of-freedom.

Muscles in the model are divided into several fascicles to mimic the diverse mechanical function of the real muscle. The path of each muscle fascicle is defined by the points at which it attaches to the rigid bodies of the model. The three main types of attachment points in OpenSim are: 1) Fixed point; 2) Via point; and, 3) Wrap point (using wrapping surfaces). A fixed point represents the path of the muscle by a set of straight lines connecting each pair of adjacent points. A via point is also fixed to a body, but is only active for a specified range of motion of the joint. A wrap point is more computationally demanding because an algorithm in OpenSim automatically calculates the path of a muscle so that it wraps over a wrap object (sphere, ellipsoid, cylinder, or torus), resulting in a curved path that follows the surface of the object.

3.3.1.1 Lower limb muscles

The full-body model developed for this thesis originally included lower limb musculature (86 muscle fascicles) and was validated for running motions (Hamner et al., 2010). However, the forward bending motions and lifting tasks studied in Chapters 4 to 6 produce larger hip flexion

angles than running. Due to these large flexion angles, combined with hip adduction and rotation, the psoas and iliacus muscle fascicles included in the lower limb musculature, had moment arm discontinuities (Figure 3.13). The squat and the BATT lifting techniques, studied in Chapters 4 and 5, include this combination of hip movements, thus resulting in moment arm errors for these two muscles during the simulations.

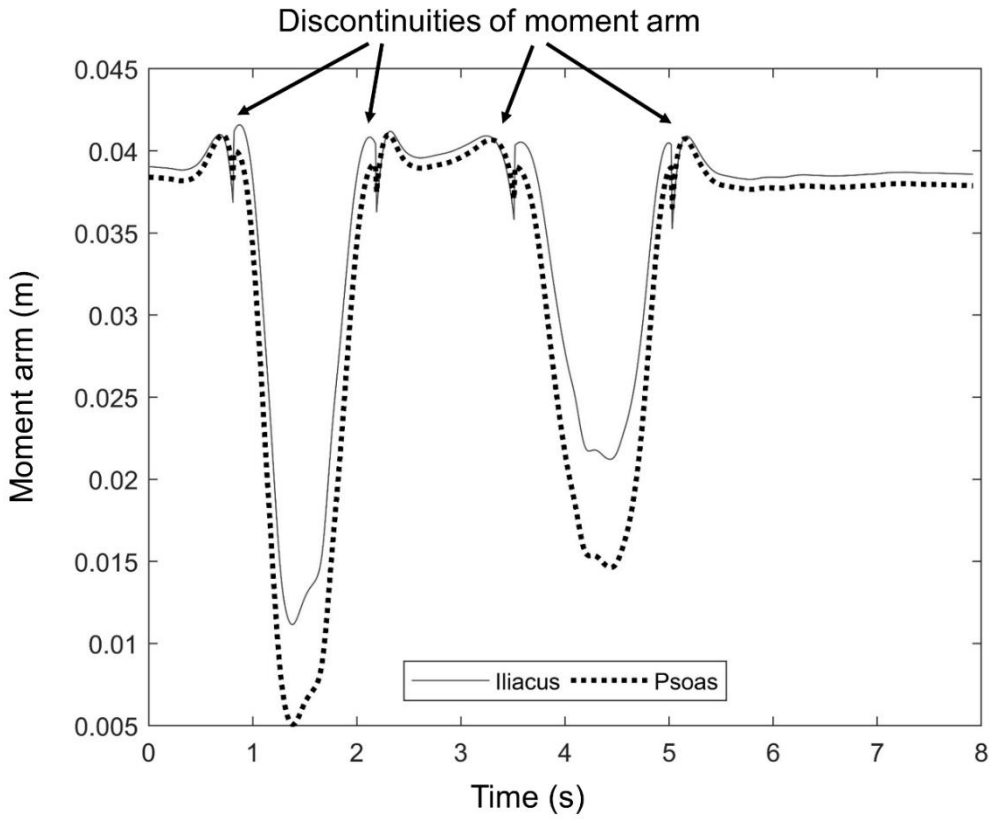

Figure 3.13 Discontinuities in the moment arms of the iliacus and psoas muscle throughout a lifting trial caused by the via point of the muscle path.

The psoas and iliacus muscle fascicles were attached to the femur and pelvis rigid bodies, and crossed the hip joint with a combination of fixed and via points. They were active between 90° of hip extension and 45° of hip flexion (Figure 3.14). The moment arm discontinuities were caused by the via point of these two muscles not lying on the muscle path between the fixed points, at large flexion angles. In order to eliminate these discontinuities in the moment arms, the via points were removed and replaced by wrapping objects in an attempt to produce more physiological moment arms for the iliacus and psoas muscles.

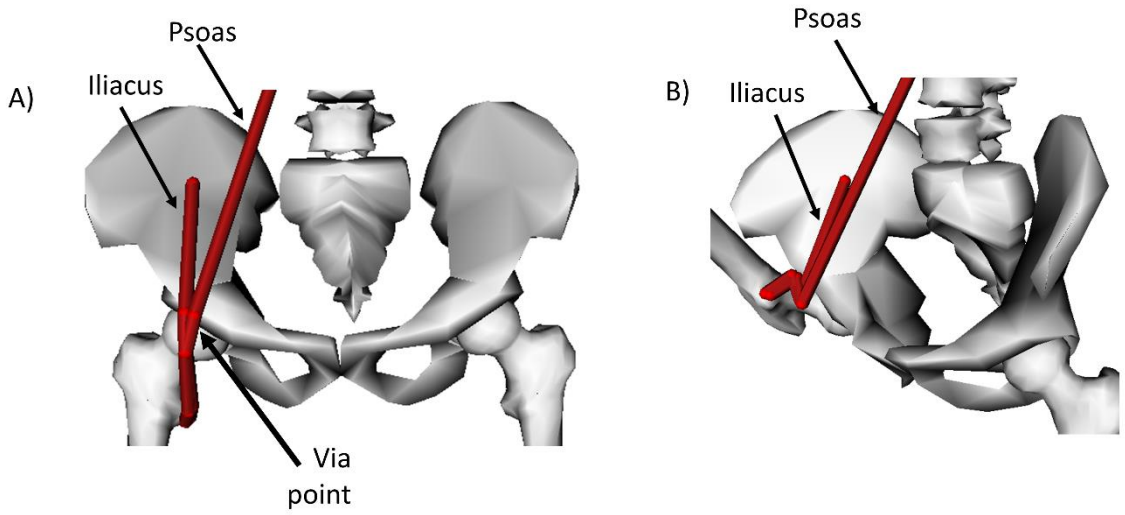

Figure 3.14 A) Muscle path of the iliacus and psoas crossing the hip joint in neutral position (0° for flexion, adduction, and rotation), including the via point. B) Muscle path of the iliacus and psoas at 50° of flexion. The via point is inactive for hip flexion angles larger than 45°.

The selection criteria for the wrapping surface were that it had to produce a continuous physiological moment arm throughout the hip ranges of motion and that it had to preserve the path of the psoas muscle fascicles in the transverse plane as these fascicles also cross the lumbar spine. Based on experimental data, the hip flexion moment arms for the psoas and illiacus needed to be between 3-3.5 cm (Arnold et al., 2000) and 3-5 cm (Blemker and Delp, 2005), respectively, at hip flexion angles above 80°. The moment arm for the psoas needed to increase continuously with increasing flexion angles (Arnold et al., 2000), while the moment arm for the illiacus needed to decrease slightly as flexion angles increased, for angles above 90° (Blemker and Delp, 2005). In addition, the wrapping object could not change the moment arm of the psoas with respect to the L4/L5 joint (Bogduk et al., 1992b), as it could affect spinal loading estimated by the model at this joint.

Various combinations of wrapping surface(s) were tested (Figure 3.15); however, they still resulted in moment arm discontinuities because the muscle disengaged from the wrapping object(s) within certain ranges of hip flexion angles. It is worthy to note that wrapping objects can be difficult to implement, especially at large angles, because the OpenSim algorithm

automatically calculates the muscle path, not necessarily wrapping around the surface as intended. Consequently, wrapping surfaces were discarded as an option to produce physiologically accurate moments for the psoas and iliacus.

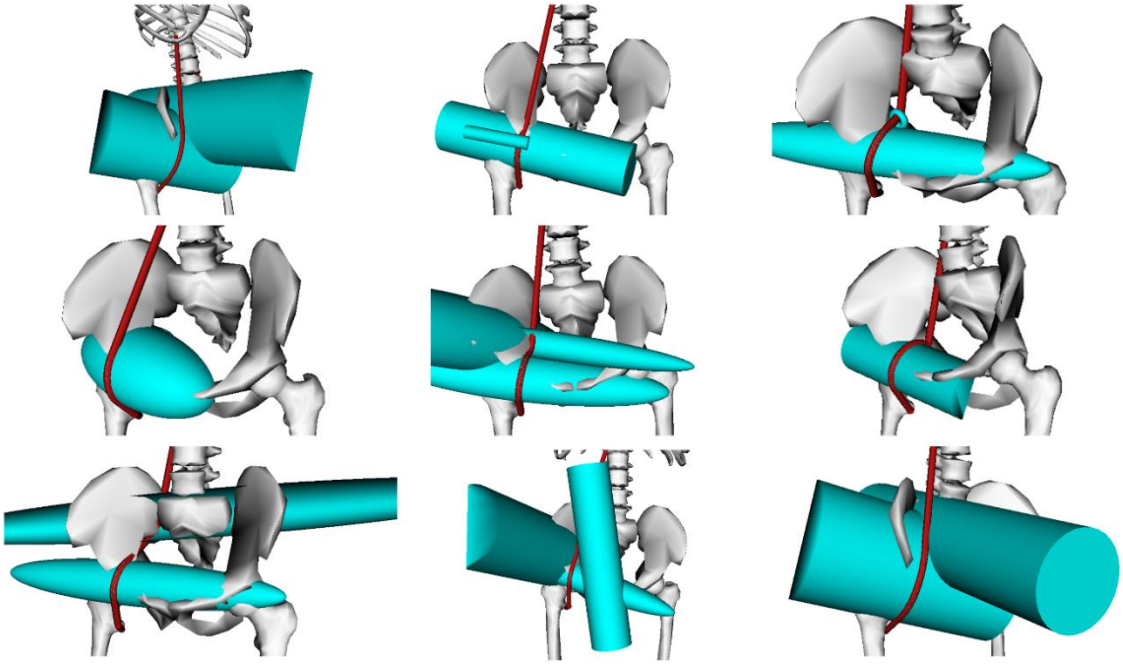

Figure 3.15 A sample of the various wrapping object(s) tested on the model to produce physiological moment arms without discontinuities for the iliacus and psoas muscle fascicles.

Forward bending produces extension reaction moments at the hips (Figure 3.16). Consequently, hip flexors, including the iliacus and psoas muscles, are not highly recruited during this motion, as confirmed by the small activations predicted by the model.

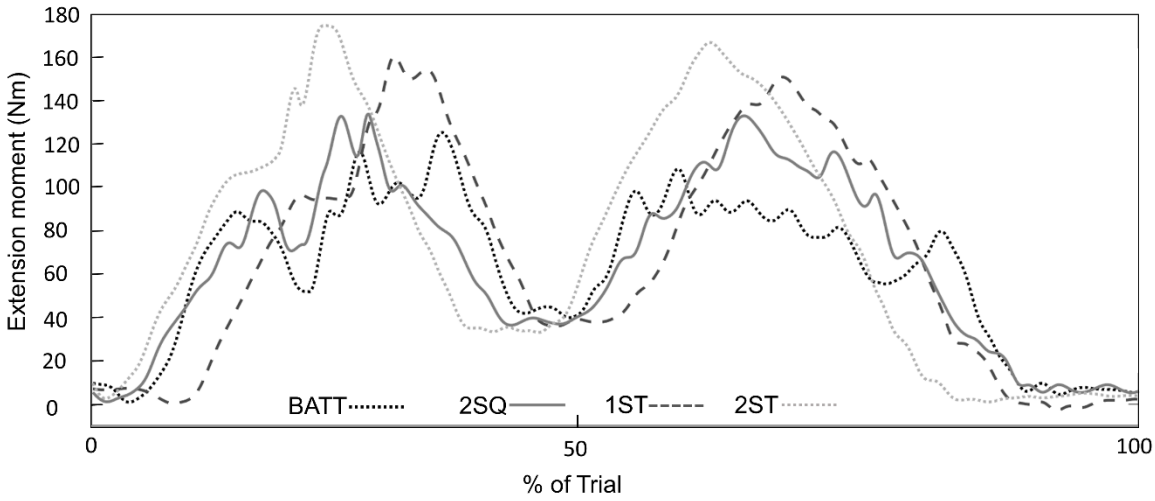

Figure 3.16 Hip extension moments for the four lifting techniques evaluated in Chapters 4 and 5. These lifting techniques are the braced arm-to-thigh technique (BATT), two-handed squat (2SQ), one-handed stoop (1ST), and two-handed stoop (2ST).

Given the difficulty in obtaining physiological moment arms at high hip flexion and the low muscle activations estimated by the model for these muscles during forward bending, lower limb muscles were completely removed from the model and replaced by reserve actuators to activate the ankle, knee, and hip joints during the simulations. Inaccurate moment arms and discontinuities are a potential source of error in simulations because they can lead to incorrect muscle activation predictions, and thus incorrect joint force estimates. This is particularly important for the psoas fascicles, as they also cross the lumbar spine joints which are of interest in this thesis. The attachment points for the psoas crossing the hip joint were removed, but those crossing the lumbar spine remained. Removing the lower limb muscles had a minimal effect on spinal joint loads (Figure 4.5).

3.3.1.2 Trunk muscles

The resulting full-body model comprised 238 musculotendon actuators (Figure 3.12), only representing the trunk musculature. Muscle properties of the base model (Raabe and Chaudhari, 2016) were modified to satisfy equilibrium for all lifting tasks. The validation process for the modification muscle properties is discussed in detail in Chapter 4. The updated muscle properties are presented in Table 2.1, as they are not included in Chapter 4.

Table 3.2 Muscle names and the abbreviations of its fascicles, with corresponding maximum isometric force, optimal fibre length (OFL), and tendon slack length (TSL). Only the fascicles on the right side are included in this table, but an equal number of fascicles existed on the left side of the model.

Muscle	Abbreviation	Maximum Isometric Force (N)	OFL (cm)	TSL (cm)
Rectus Abdominus	rect_abd_r	662.00	8.25	30.34
Psoas major	Ps_L1_VB_r	267.41	5.75	19.36
	Ps_L1_TP_r	77.19	5.66	19.07
	Ps_L1_L2_IVD_r	147.15	5.3	17.83
	Ps_L2_TP_r	258.58	4.93	16.58
	Ps_L2_L3_IVD_r	150.54	4.55	15.31
	Ps_L3_TP_r	127.77	4.25	14.31
	Ps_L3_L4_IVD_r	45.36	3.82	12.85
	Ps_L4_TP_r	202.69	3.64	12.25
	Ps_L4_L5_IVD_r	85.10	3.11	10.47
	Ps_L5_TP_r	186.36	3.07	10.34
	Ps_L5_VB_r	232.89	2.68	9.03
Quadratus Lumborum	QL_post_I_1_L3_r	75.59	3.71	4.42
	QL_post_I_2_L4_r	156.41	2.13	2.53
	QL_post_I_2_L3_r	58.56	3.33	3.96
	QL_post_I_2_L2_r	36.55	4.8	5.71
	QL_post_I_3_L1_r	77.19	6.51	7.75
	QL_post_I_3_L2_r	56.49	4.74	5.65
	QL_post_I_3_L3_r	96.36	3.35	3.99
	QL_mid_L3_12_3_r	41.93	3.2	6.16
	QL_mid_L3_12_2_r	47.72	3.45	6.65
	QL_mid_L3_12_1_r	79.53	3.54	6.82
	QL_mid_L2_12_1_r	156.09	2.41	4.64
	QL_mid_L4_12_3_r	42.10	4	7.71
	QL_ant_I_2_T12_r	45.39	5.98	11.52
	QL_ant_I_3_T12_r	85.28	5.89	11.34
	QL_ant_I_2_12_1_r	28.08	5.55	10.69
	QL_ant_I_3_12_1_r	53.17	5.48	10.55
	QL_ant_I_3_12_2_r	35.25	5.23	10.07
	QL_ant_I_3_12_3_r	40.63	4.54	8.74
Multifidus	MF_m1s_r	81.20	2.22	5.34
	MF_m1t_1_r	71.96	2.63	8.77
	MF_m1t_2_r	59.73	3.24	10.8
	MF_m1t_3_r	99.76	3.54	11.8
	MF_m2s_r	54.48	2.13	5.5
	MF_m2t_1_r	57.47	2.27	7.46
	MF_m2t_2_r	145.89	2.84	9.34
	MF_m2t_3_r	161.19	3.18	10.44
	MF_m3s_r	83.72	1.96	4.71
	MF_m3t_1_r	90.98	3.75	11.28
	MF_m3t_2_r	90.98	3.16	9.49
	MF_m3t_3_r	90.98	3.16	9.49
	MF_m4s_r	101.07	2.71	4.29
	MF_m4t_1_r	90.12	2.49	6.15
	MF_m4t_2_r	90.12	3.25	8.02
	MF_m4t_3_r	90.12	3.71	9.17
	MF_m5s_r	34.88	0.93	1.47
	MF_m5t_1_r	34.88	3.07	7.6
	MF_m5t_2_r	34.88	2.3	5.68
	MF_m5t_3_r	34.88	1.65	4.07

	MF_m1_laminar_r	39.05	1.4	3.69
	MF_m2_laminar_r	30.97	1.18	3.11
	MF_m3_laminar_r	35.78	1.26	3.31
	MF_m4_laminar_r	25.95	1.33	3.49
	MF_m5_laminar_r	55.94	0.97	2.56
Iliocostalis Lumborum	IL_L1_r	147.44	12.92	5.7
	IL_L2_r	183.22	9.19	4.05
	IL_L3_r	216.76	6.11	2.69
	IL_L4_r	414.91	4.24	1.87
	IL_R5_r	57.32	25.79	18.42
	IL_R6_r	72.69	21.61	17.89
	IL_R7_r	87.66	18.44	17.55
	IL_R8_r	77.92	16.29	16.13
	IL_R9_r	95.91	10.95	18.61
	IL_R10_r	191.84	9.57	16.26
	IL_R11_r	235.18	6.82	13.62
	IL_R12_r	206.17	5.04	10.07
Longissimus Thoracis	LTpT_T1_r	325.89	26.1	11.02
	LTpT_T2_r	240.66	27.74	11.54
	LTpT_T3_r	172.50	28.14	11.7
	LTpT_T4_r	60.58	28.19	11.72
	LTpT_T5_r	57.01	26.35	10.96
	LTpT_T6_r	81.41	26.19	11.46
	LTpT_T7_r	79.71	24.67	13.04
	LTpT_T8_r	79.71	21.97	13.91
	LTpT_T9_r	139.43	23.18	13.68
	LTpT_T10_r	120.51	21.31	12.57
	LTpT_T11_r	115.08	18.5	10.92
	LTpT_T12_r	94.29	14.62	8.63
	LTpT_R4_r	60.50	25.64	15.13
	LTpT_R5_r	56.96	24.11	14.22
	LTpT_R6_r	81.41	23.39	15.27
	LTpT_R7_r	79.71	24.23	14.49
	LTpT_R8_r	130.02	24.66	12.09
	LTpT_R9_r	110.68	25.92	10.61
	LTpT_R10_r	120.42	21.62	12.58
	LTpT_R11_r	115.39	16.75	11.76
	LTpT_R12_r	94.33	14.31	7.36
	LTpL_L5_r	157.80	0.1	5.15
	LTpL_L4_r	151.84	4.71	4.37
	LTpL_L3_r	121.28	6.43	5.92
	LTpL_L2_r	108.38	8.33	7.57
	LTpL_L1_r	106.16	10.53	9.04
External Obliques	EO1_r	111.74	5.70	3.59
	EO2_r	132.35	5.52	3.79
	EO3_r	138.90	4.66	3.84
	EO4_r	134.09	4.48	3.93
	EO5_r	155.94	5.15	4.71
	EO6_r	226.96	5.71	5.65
Internal Obliques	IO1_r	123.98	1.12	10.1
	IO2_r	150.07	1.17	10.49
	IO3_r	151.21	1.38	12.42
	IO4_r	179.05	1.16	10.46
	IO5_r	157.08	1.19	10.67
	IO6_r	138.61	1.11	10.03
Latissimus Dorsi	LD_L1_r	90.40	7.25	33.19
	LD_L2_r	84.54	7.8	35.71
	LD_L3_r	104.52	8.25	37.8

LD_L4_r	100.73	8.62	39.49
LD_L5_r	101.69	8.57	41.73
LD_T12_r	53.71	6.49	31.59
LD_T11_r	62.92	6.06	29.51
LD_T10_r	64.48	4.56	29.13
LD_T9_r	40.62	3.99	25.49
LD_T8_r	40.79	4.86	23.68
LD_T7_r	37.07	4.58	22.3
LD_R12_r	42.90	5.62	27.37
LD_R11_r	63.33	4.91	23.9
LD_Il_r	65.37	2.01	46.5

3.3.1.3 Lumbar joints

Kinematic coupling ratios were required to determine the intervertebral motion of the six lumbar joints in the model. The need for kinematic coupling ratios is fairly unique to the spine as the intervertebral motions cannot be accurately measured *in vivo* due to the small size of the vertebral bodies and the inaccuracies caused by skin motion artefact. Consequently, the motion of the entire trunk is measured using skin markers placed at its proximal and distal ends and then distributed over the intervertebral joints during modelling. The ratios for the motion distribution were based on *in vivo* data [Flexion: Arjmand and Shirazi-Adl (2006a), Lateral bending: Dvorak et al. (1991), Axial rotation: Fujii et al. (2007)]. For this model, the L5/S1 joint was defined as the independent coordinate. The linear coefficient for each rotational DOF of this joint (flexion-extension, lateral bending, axial rotation) was set to 1 so that the results from inverse dynamics would report these moments directly. The linear coefficients for the kinematic couplings for the other intervertebral joints were normalised to the L5/S1 ratio value (Table 4.3), in order to correspond to the motion ratios for the lumbar spine reported in the literature. The values for these kinematic couplings are shown in Chapter 4 (Table 4.2).

3.3.2 Scaling

The rigid body segments of the full-body model were scaled linearly and uniformly to the anthropometry of each participant, using joint centres and anatomical markers (Table 3.3). This scaling procedure is similar to that typically used in musculoskeletal modelling studies. Each scaled model was visually inspected to ensure that the body segments were anatomically proportionate (e.g. no large pelvis and small femur). In this model, the trunk was composed of

multiple rigid bodies (thorax and lumbar vertebral bodies) that were all scaled using the same scaling factor. This differs slightly from models used in gait and running studies where the trunk is modelled as one rigid body.

During the calibration trials, participants were instructed to hold a static pose with the box in hands to better represent the arm range of motion experienced during lifting tasks. Pilot tests demonstrated that adopting this pose improved motion tracking of the arms (Figure 3.17), compared to the standard "T"-pose.

Table 3.3 Definition of the rigid body segments of the full-body model, using the anatomical markers placed on participants. ** The talus, calcaneus, and toe bodies formed one rigid body for the foot; the subtalar (inversion-eversion) and metatarsal-phalangeal joints were locked in the neutral position, as motions of these joints are not measured well with skin reflective markers, subsequently increasing computational errors. * Hands were not scaled. Wrist flexion and deviation joints, were locked in the neutral position.**

Body Segment	Proximal End	Distal End
Feet (talus, calcaneus, toes)**	Mid-point between medial and lateral malleolus	Mid-point between 1st and 5th metatarsal
Shank (tibia)	Functional knee joint centre	Mid-point between medial and lateral malleolus
Thigh (femur)	Functional hip joint centre	Functional knee joint centre
Pelvis (including sacrum)	Hip joint centres	
Trunk (thorax & lumbar vertebral bodies)	ASIS-PSIS	C7
Arm (humerus)	Acromion process	Mid-point between medial and lateral humerus epicondyle
Forearm (ulna & radius)	Mid-point between medial and lateral humerus epicondyle	Mid-point between ulna head and radius styloid process
Hand***	N/A	

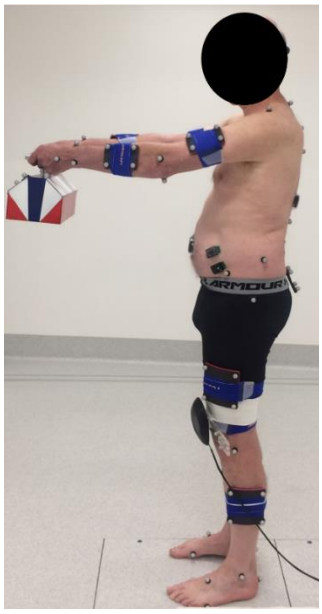

Figure 3.17 Static pose held by participants during calibration trials, to represent the positions of the arms during lifting.

3.3.3 Inverse Kinematics Analysis

Inverse kinematics was solved using a weighted least-squares equation to minimise the difference between the locations of the experimental markers and their corresponding virtual markers placed on the model (equation (3.1)).

$$min\left[\sum_{i\in markers} w_i\left\|x_i^{exp} - x_i(q)\right\|^2\right] \qquad (3.1)$$

where, q is the vector of generalised coordinates being solved, x_i^{exp} is the experiment location of the marker i, and $x_i(q)$ is the position of the corresponding virtual model marker. The relative marker weights (w_i) are specified by the user. For the experiments performed in this thesis, the largest tracking weights were placed on the trunk and pelvis markers because the lumbar joints were of interest. Several combinations of marker weights were tested and those shown in Table 3.4 generated the best solutions (i.e. the smallest root mean square (RMS) marker error).

The RMS error values obtained for the studies in chapters 4 to 6 were higher than the threshold (2 cm) recommended by OpenSim (https://opensim.stanford.edu/). However, this limit is based

on gait motions, which involve smaller ranges of motion for the trunk and limbs. Full body tracking with large trunk motions inevitably results in larger RMS errors, as reported by a study on sit-to-stand motions with a comparable model full-body model that used a RMS threshold of 3.5 cm (Caruthers et al., 2016). Each trial for the studies in Chapters 4 to 6 was reviewed individually to ensure that the model followed closely the experimental markers. During this inspection, two main tracking issues were observed: one for squat lifts and one for car egress motion.

Table 3.4 Marker weights used for the different markers for inverse kinematics. Marker weights are relative to each other. Consequently, the absolute values are essentially irrelevant. W1 represents the weights given to the markers for lifting, cupboard, and weeding tasks, while W2 corresponds to the weights for the car egress tasks.

Body Segment	Marker name				W1	W2
Right/Left Foot	R/L_CALC				15	0
	R/L_1ST		R/L_5TH		15	5
	R/L_DORSAL				0	5
Right/Left Shank	R/L_SH1	R/L_SH2	R/L_SH3	R/L_SH4	10	10
Right/Left Thigh	R/L_TH1	R/L_TH2	R/L_TH3	R/L_TH4	10	10
Right/Left Arm	R/L_ARM1	R/L_ARM2	R/L_ARM3	R/L_ARM4	10	0
	L_LAT_HUM		L_MED_HUM		0	5
Right/Left Forearm	R/L_FARM1	R/L_FARM2	R/L_FARM3	R/L_FARM4	10	0
	R/L ULNA				15	5
	R/L_HAND				15	2
	R/L RAD				0	5
Sacrum/ pelvis	SACRUM1	SACRUM2	SACRUM3	SACRUM4	20	20
Lumbar spine	LUMB1	LUMB2	LUMB3	LUMB4	20	20
Torso	THOR1	THOR2	THOR3	THOR4	20	15
	C7				15	0

Participants were instructed to keep their heels in contact with the ground (force platforms) for all activities, because the feet are modelled as rigid bodies. However, some participants lifted their heels, especially for squat lifts (Figure 3.18). The inverse kinematics RMS errors for these trials were unacceptable because the rigid body assumption for the foot was violated; the model was over-constrained due to this violation, combined with full-body tracking, large trunk, leg and arm motions, and soft tissue artefact, thus resulting in poor inverse kinematics solutions. As a

result these trials had to be discarded. This is typically not an issue for simulations with smaller ranges of motions (i.e. gait).

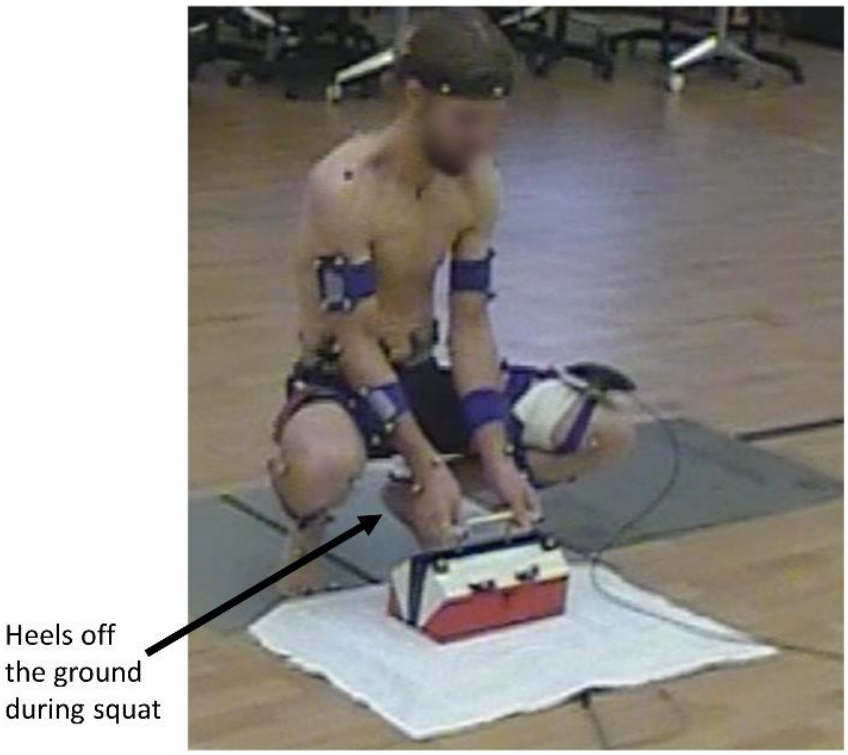

Figure 3.18 Squat lifting trial where the participant lifted his heels from the ground. This figure was obtained from a video capture during motion, thus decreasing its quality.

The second tracking issue was associated with car egress using hand support on the dashboard and the one-leg first method (Figure 3.19). These car egress trials were particularly affected by large shoulder motions and large trunk axial rotation. As a result, the kinematics could not be tracked properly by the current model, generating solutions with large RMS errors. These trials were not further analysed as they reached trunk angles that were outside the range of motion for which the model was validated (Chapter 4). Ideally, any future analysis of this manner of car egress should be accompanied by modification of the model to improve tracking of the shoulder motion, possibly by adding more DOFs to the joint.

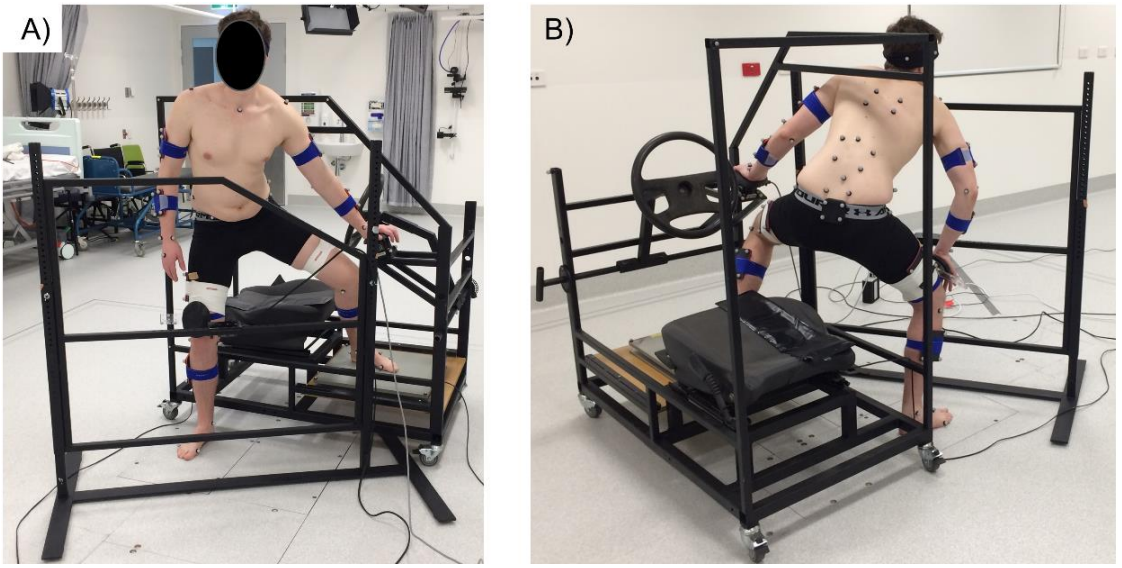

Figure 3.19 Participant performing car egress task with *one-leg first* technique, with support for the dash. A) Participant using the dash support only, with the left hand. Ground reaction forces for the left foot are measured using a force platform placed on the foot well, while the ground reaction forces for the right foot are measured using a force platform incorporated in the ground; B) Car egress with *one-leg first* similar to A), but thigh bracing is also used.

3.3.4 Inverse Dynamics Analysis

Inverse dynamics determines the generalised forces (net forces and net torques) at each joint for a given movement (equation *(3.2)*).

$$M(q)\ddot{q} + C(q,\dot{q}) + G(q) = \tau \qquad (3.2)$$

where $q, \dot{q}, \ddot{q}$ are the vectors of generalised positions, velocities, and accelerations, respectively; $M(q)$ is the system mass matrix; $C(q,\dot{q})$is the vectors of Coriolis and centrifugal forces; $G(q)$is the vector of gravitational forces; and τ is the vector of generalised forces.

All external forces acting on the participant need to be incorporated into the simulations with this OpenSim model. The ground reaction forces for all lifting trials were measured by two 6-DOF force platforms (one under each foot). The measured forces were applied to the calcaneus body of each foot, based on the centres of pressure determined by the force platforms (Figure 3.20).

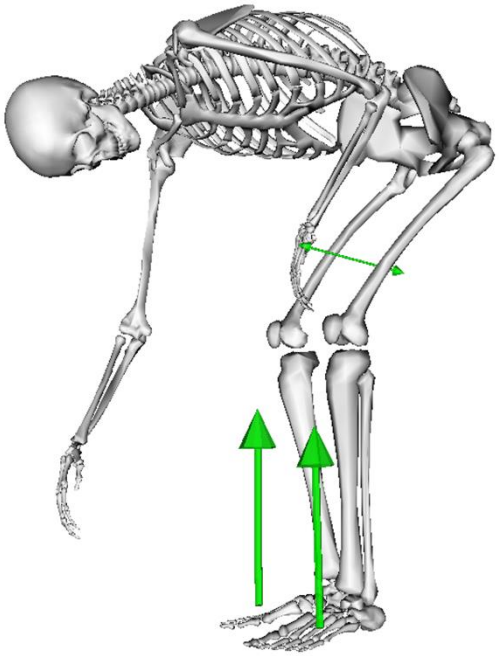

Figure 3.20 Ground reaction forces applied at the feet and the bracing force applied to the thigh, with an equal and opposite force applied to the ipsilateral hand.

The bracing force measured by the load cell for the braced techniques was applied to the thigh body, with an equal and opposite force applied to the ipsilateral hand body (Figure 3.20). The force measured by the load cell was transformed into the global coordinate system of the OpenSim software, using a local right hand orthogonal coordinate system created with the load cell markers, corresponding to the axes of the load cell (Figure 3.21). The global point of application of the force on the thigh (and corresponding hand) in OpenSim was determined by transforming the location of the origin of the local coordinate system, based on its position relative to the load cell origin and the measured offset of 23 mm with respect to the thigh skin surface (Figure 3.21).

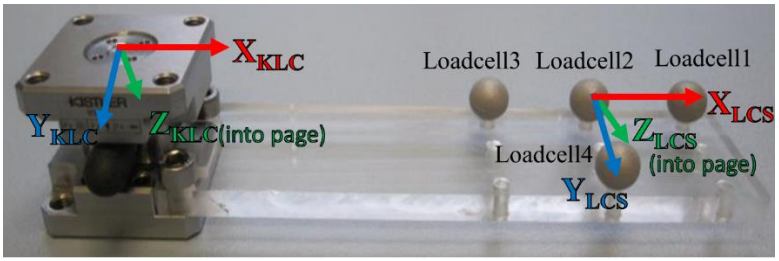

Figure 3.21 Local coordinate system (X_{LCS},Y_{LCS}, Z_{LCS}) created by the markers rigidly attached to the load cell assembly to match the Kistler load cell coordinate system (X_{KLC},Y_{KLC}, Z_{KLC}) to transform the forces measured by the load cell to the OpenSim global coordinates system and apply to the thigh of the model.

3.3.4.1 Lifting tasks

The main difficulty associated with simulating lifting tasks in OpenSim is that the box needs to connect to model, essentially acting as an additional rigid body attached to the hand(s), but only for a finite time period during the trial. Differing from ground reaction forces and the bracing force, the forces created by the box acting at the hand do not simply correspond to a signal measured by a sensor (force platform or load cell). The methodology to include the external forces created by the box held in the hand(s) during lifting is not clearly defined in the OpenSim documentation or used in other models. Two-handed lifts pose an additional challenge because a "child" body in OpenSim cannot be connected to two "parent" bodies and form a closed loop. Specifically for two-handed lifts, a box body cannot be connected to both hands, thus closing the loop between the trunk and arms. This section describes the different methods explored to incorporate the forces created by the box on the hand(s) in the OpenSim simulations.

3.3.4.1.1 Detecting when box is off the ground

The lifting tasks studied in Chapters 4 and 5 involved box pick-up and put-down from ground level. For each of these lifting trials, participants started empty-handed in the upright standing position, before lifting a box from the ground to upright standing, then returning the box to the ground, and ending the trial in upright standing, empty-handed (Figure 3.22). Consequently, the time period when the box was off the ground had to be determined to appropriately model the resulting forces acting at the hands. Two methods were tested to detect when the box was off the ground: an electrical switch and a force platform (Figure 3.23).

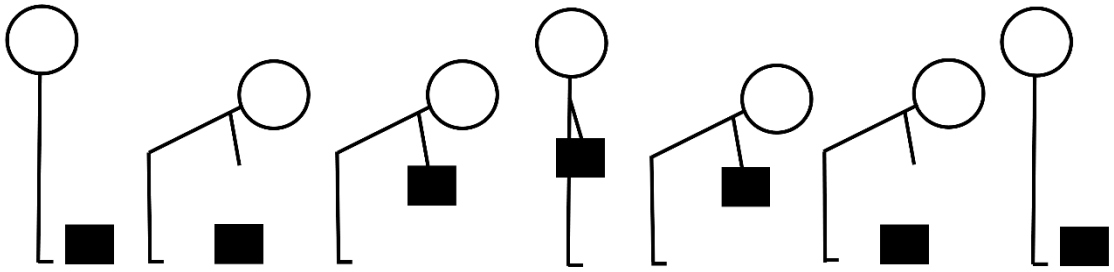

Figure 3.22 Lifting tasks studied in Chapters 4 and 5 started and ended in the upright standing position, with the box on the ground. For each lift, participants picked up the box, returned to the upright standing positions, and put the box back on the ground.

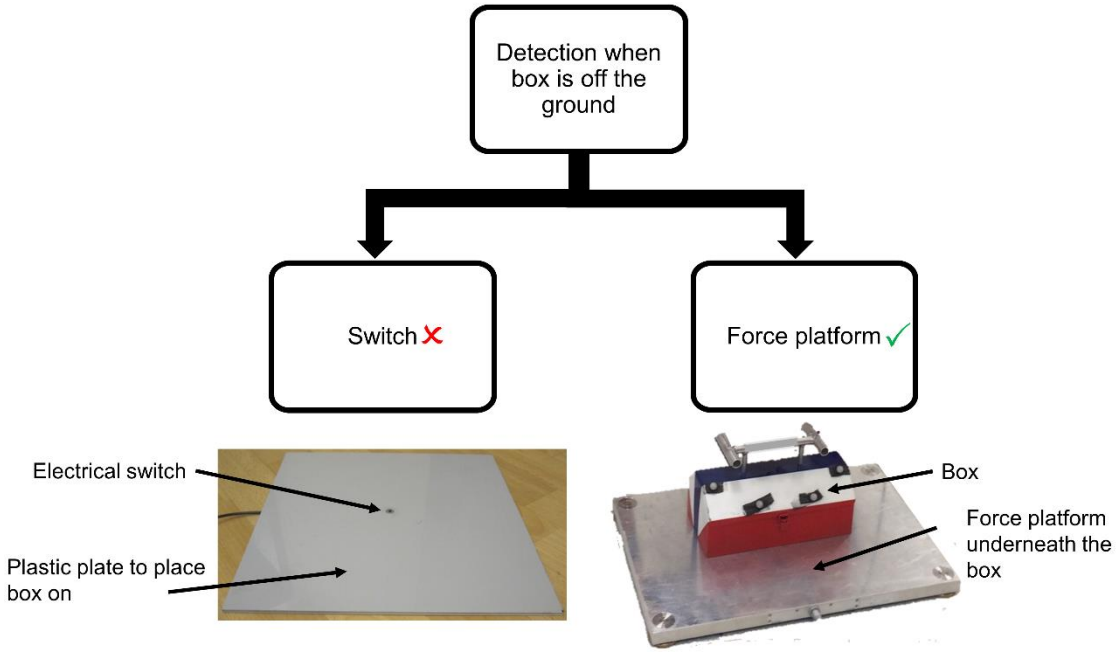

Figure 3.23 The two methods trialled to detect when the box was off the ground: a switch and a force platform.

A simple switch placed underneath the box was initially used to detect when the box was off the ground (Figure 3.23). For this method, a 0 to 1.25 V rising edge signal, synchronised through Vicon Nexus, was produced by the electrical switch when the box was picked up and replaced. This method was not optimal because participants did not always follow the instructions to replace the box on the electrical switch, thus making it difficult to clearly determine the instant the box contacted the ground. In addition, this approach assumed an instantaneous ground-to-hand box transfer, whereas in reality this transition lasted approximately 0.1 seconds.

Due to these limitations associated with the switch, it was replaced by a force platform (Model 9286BA, Kistler, SUI) placed underneath the box (Figure 3.23). This method quantified the duration of the transition phase when the box was picked-up or put-down, as well as the weight distribution between the hands and the ground for that period. The force platform also revealed that participants often leaned *onto* the box during these transition phases, either immediately before picking it up or putting it down, thus increasing modelling complexity.

3.3.4.1.2 Box forces applied at hand(s)

Several iterations were required to correctly integrate the forces created by the box at the hand(s) in the lifting task simulations of Chapters 4 and 5. This section describes the three methods that were tested: external forces applied at the hands, a box body incorporated in the model, and the integration of the mass properties of the box to those of the hands (Figure 3.24).

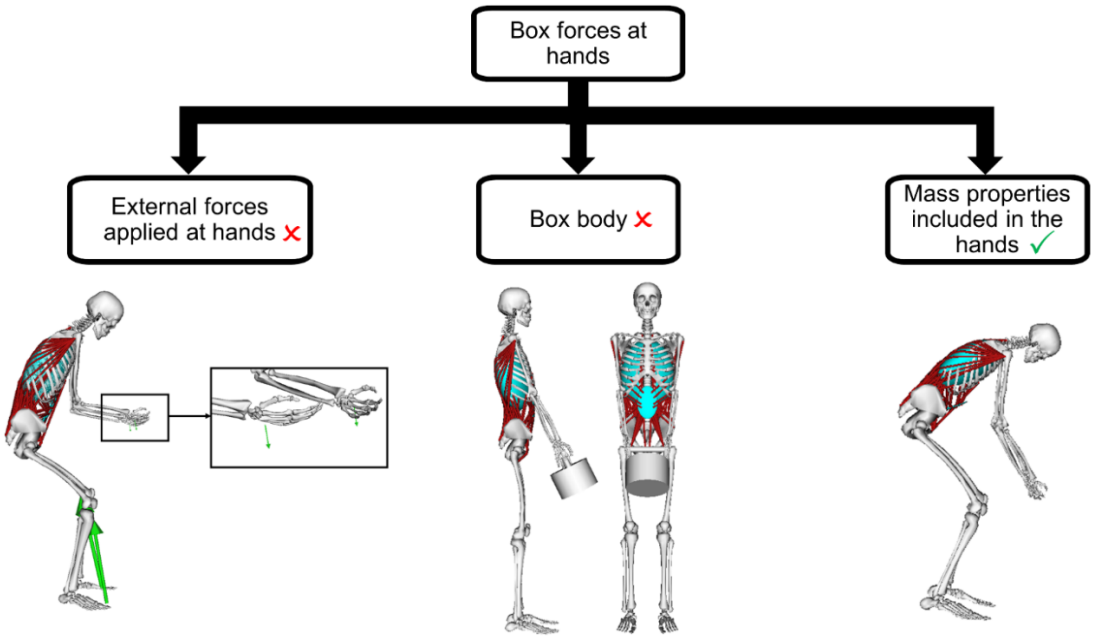

Figure 3.24 Three methods to integrate the forces created by the box at the hands were trialled: external forces (green arrows) applied at the centre of mass of the hands of the model during a lifting simulation for a two-handed lift; a rigid body representing the box attached to both hands, and incorporating the mass properties of the box to the hands.

External forces applied at the hands

First, the box held in the hands was modelled as an external force acting at the centre of mass of the hand(s) (Figure 3.24). This external force comprised the weight (due to gravity) of the box, and its accelerations. The linear accelerations were determined by differentiation of the position data of four markers placed on the box, but the rotational accelerations were not included. This method was tested with both methods of detecting box-ground interactions (switch and force platform). For the switch, the external force was applied to the hands when the box was detected to be off the ground. For the force platform, the signal measured by the force platform was applied for the entire duration of the trial. In this instance, the force platform was balanced (zeroed) with the box placed on it such that the weight of the box would be acting at the hands when it was raised, combined with the forces created by the linear accelerations of the box. This method also modelled the changing forces acting at the hands when the box was picked up or put down. The pelvis residuals for the simulations with the switch were larger than those with the force platform during the transition phases, because the former could not model the weight distribution between the hands and the ground, thus further highlighting the need to use a force platform instead of a switch, to quantify the transition phase (Figure 3.25).

The "external forces applied at the hands" method produced acceptable results but did not include the rotational accelerations of the box.

Box Body

In order to include the rotational accelerations of the box in the simulations, an additional rigid body connected at the hand(s) was added to the model to represent the box (Figure 3.24). Its motion was tracked using the four markers on the box (Section 3.2.4). This method has been used previously to study shoulder muscle co-activation during one-handed lifts (Blache et al., 2015a, Blache et al., 2015b). For two-handed lifts, the box was modelled as two identical rigid bodies (mass and inertial properties), connected by a 0 DOF weld connection to satisfy the closed-loop

constraint in OpenSim. The inertial properties of the box were determined assuming a simple rectangular shape with its mass uniformly distributed.

The box rigid body was only included in the model when the box was off the ground (connected to the hand(s)), and an identical model but without the box rigid body was used of the remainder of the trial.

This method increased modelling complexity because the joint (as defined by the number of DOFs, position, and orientation) connecting the hand(s) to the box was challenging to model, as the box was not held consistently during the trials or across participants. In addition, the model could not track the subtle wrist motions during the lifting trials as wrist motion was not measured during data collection. Several types of joints were tested (0-DOF, 1-DOF, 3-DOF), but ultimately the model was over-constrained and could not produce adequate solutions for inverse dynamics or static optimisation. Consultation with Dr Ajay Seth from the OpenSim team during a workshop confirmed that this method was not currently feasible due to current internal constraints of OpenSim.

Mass properties included in the hands

An alternative to including a "box" rigid body in the model was to combine the mass properties of the box with those of the hand(s), when the box was off the ground. This method is similar to the external forces applied at the hands, but includes both linear and rotational accelerations of the box. To achieve this, each lifting trial was segmented into four phases: 1) unloaded reach down from upright standing; 2) load pick-up to upright standing; 3) upright standing to load put-down; 4) unloaded stand up to upright standing (Figure 5.2). The transitions between unloaded (phases 1 and 4) and loaded (phases 2 and 3) portions of the trial were not modelled for inverse dynamics, static optimisation, and joint reaction analyses because a new model with different hand mass properties would have been required at each frame to correctly model the distribution of the mass of the box between the ground and hands for that time period. This resulted in two short gaps (approximately 0.1 s duration) in the analysis. This method was selected for the lifting

studies in Chapters 4 and 5, as it produced the best results with regards to kinematics tracking and residuals at the pelvis (Figure 3.25).

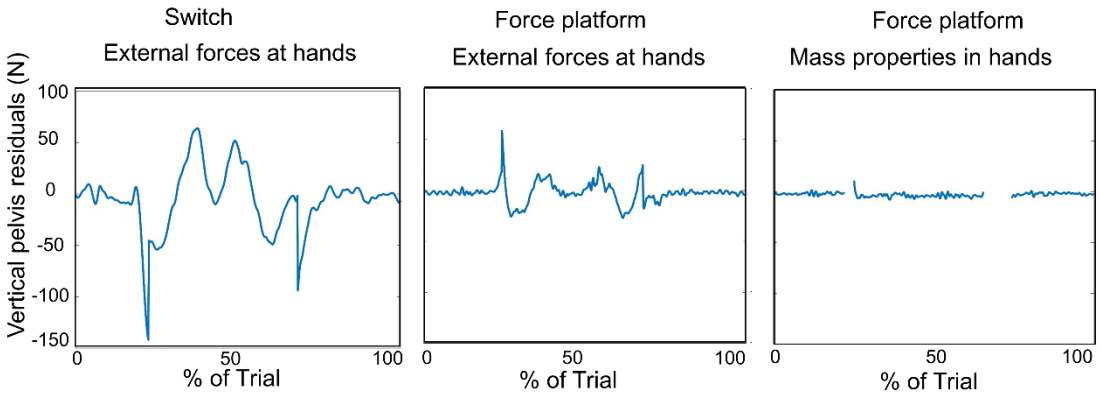

Figure 3.25 Pelvis residuals in the vertical direction for the three different methods to integrate the forces created by the box at the hands: external forces at the hands combined with switch, external forces combined with force platforms, and mass properties incorporated to those of the hands combined with force platform. The small gaps correspond to the transition periods between unloaded & loaded phases.

3.3.4.2 Activities of daily living

The forces measured by the load cell for the pulling action during weeding and the hand support on the car frame during car egress were applied as external forces applied on the hand body of the model during the simulations (Figure 3.26), in a similar manner to ground reaction forces.

Similarly to the transformation of the bracing force, the forces measured by the load cell for pulling action during the weeding task and the door frame support for the car egress task were transformed to the global coordinates of the OpenSim software (Section 3.3.4), using a local right hand orthogonal coordinate system created with markers placed on the AMTI load cell markers corresponding to the axes of the load cell (Figure 3.27).

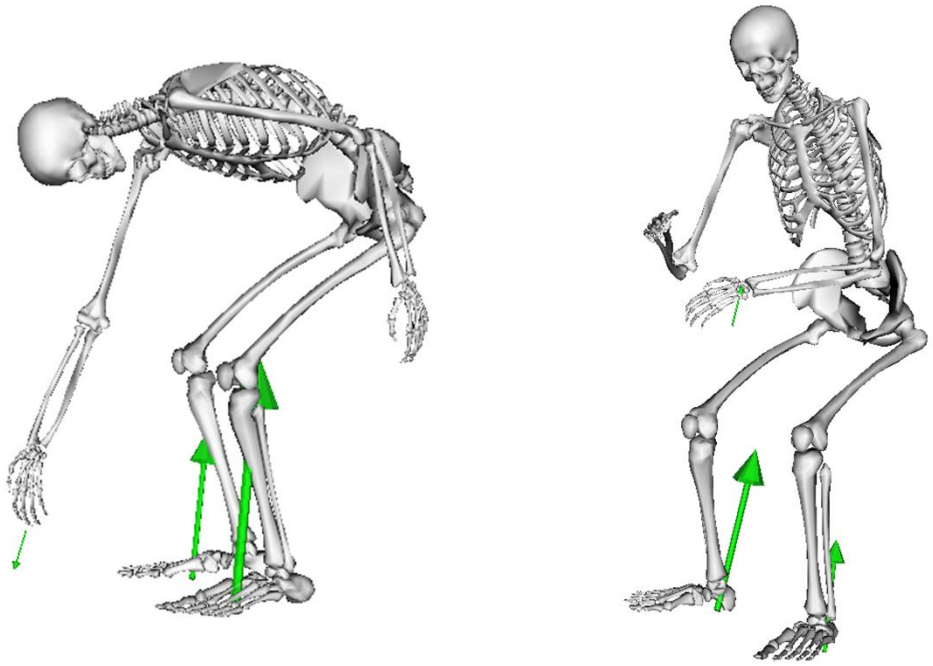

Figure 3.26 A) Ground reaction forces applied at the feet and the pulling force created by the magnet for the Weeding activity. B) Ground reaction forces applied at the feet and the force applied at the hand by support from the door frame.

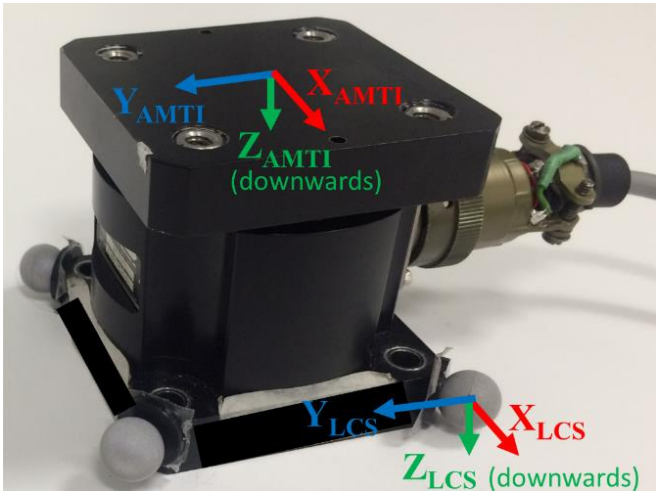

Figure 3.27 Local coordinate system (X_{LCS},Y_{LCS}, Z_{LCS}) created by the markers rigidly attached to the AMTI load cell assembly to match the AMTI load cell coordinate system (X_{AMTI},Y_{AMTI}, Z_{AMTI}) to transform the forces measured by the load cell to the OpenSim global coordinates system and apply on the hand body of the model.

3.3.5 Static Optimisation Analysis

Static optimisation was used to resolve the net joint moments into individual muscle forces at each frame for the studies in Chapters 4 to 6. Muscle forces were determined by minimising the

sum of squared muscle activations (a_m) (equation (3.3)), while taking into account the force-length-velocity properties of the muscles in the model.

$$J = \sum_{m=1}^{n} (a_m)^2 \qquad (3.3)$$

Reserve actuators were also added at each joint that did not have muscles crossing over it, and at the L5/S1 intervertebral joint. These reserve actuators augmented the force provided by the musculotendon actuators, when the muscles could not produce the force required at a given point in the simulation. Forces produced by these reserve actuators should be low [< 5% of peak joint torque (Hicks et al., 2015)] when muscles are present at the joint such that muscle recruitment is prioritised over reserve actuator recruitment. Recruitment of these forces was penalised in the static optimisation by setting low optimal forces for the L5/S1 joint (1 N). The torque applied by reserve actuators at L5/S1 was below the recommended threshold for the simulations in this thesis (Hicks et al., 2015). Although L5/S1 is the independent coordinate, equilibrium was achieved at all intervertebral joints during static optimisation.

3.3.6 Joint Reaction Analysis

The joint reaction analysis calculates the joint forces and moments between two consecutive bodies (parent and child bodies) as a result of all forces acting on the model. Trunk flexion is the primary rotation, occurring about the mediolateral axis, Z_{L5}. Lateral bending is the secondary rotation that occurs about an intermediate floating axis mutually perpendicular to Z_{L5} and Y_{L5}. Axial rotation is the final rotation, occurring about the Y_{L4}-axis, fixed to the L4 rigid body. Throughout this thesis, the reaction forces at L4/L5 are reported as applied to the L5 parent body, and expressed in the L5 parent body coordinate system. For example, this means that flexion angles (about Z_{L5}), flexion moments (about Z_{L5}), and medio-lateral forces towards the left are all negative.

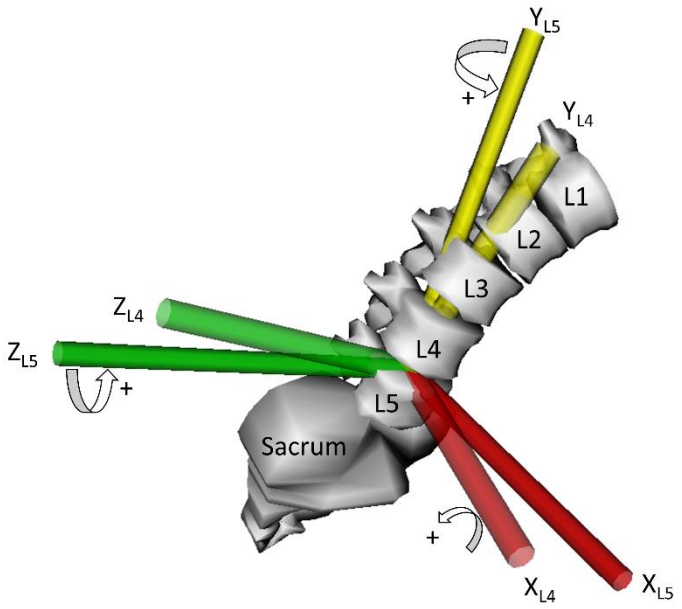

Figure 3.28 The L4/L5 joint is represented by a three degree-of-freedom "custom joint" (spherical joint), with a body-fixed ZXY Euler rotation sequence. L4 is the child body, while L5 is the parent body in this joint.

Statement of Authorship – Chapter 4

Title of Paper	Quantitative evaluation of facet deflection, stiffness, strain and failure load during simulated cervical spine trauma
Publication Status	☑ Published ☐ Accepted for Publication ☐ Submitted for Publication ☐ Unpublished and Unsubmitted work written in manuscript style
Publication Details	Beaucage-Gauvreau, E., Robertson, W.S.P., Brandon, S.C.E., Fraser, R, Freeman, B. J.C., Graham, R.B., Thewlis, D., Jones C.F., 2019. Validation of an OpenSim full-body model with detailed lumbar spine for estimating lower lumbar spine loads during symmetric and asymmetric lifting tasks. Computer Methods in Biomechanics and Biomedical Engineering, in press.

Principal Author

Name of Principal Author (Candidate)	Erica Beaucage-Gauvreau		
Contribution to the Paper	Developed testing methods and model validation, performed testing with all participants, performed all data analysis, interpreted data, wrote manuscript and acted as corresponding author.		
Overall percentage (%)	75%		
Certification:	This journal article reports on original research I conducted during the period of my Higher Degree by Research candidature and is not subject to any obligations or contractual agreements with a third party that would constrain its inclusion in this thesis. I am the primary author of this paper.		
Signature		Date	08/02/2019

Co-Author Contributions

By signing the Statement of Authorship, each author certifies that:

i. the candidate's stated contribution to the publication is accurate (as detailed above);

ii. permission is granted for the candidate in include the publication in the thesis; and

iii. the sum of all co-author contributions is equal to 100% less the candidate's stated contribution.

Name of Co-Author	William S.P. Robertson		
Contribution to the Paper	Assisted with development of methods, and reviewed manuscript.		
Signature		Date	18/02/2019

Name of Co-Author	Scott C. E. Brandon		
Contribution to the Paper	Assisted with development of model and its validation, data analysis, and data interpretation, and also reviewed manuscript.		
Signature		Date	19/02/2019

Name of Co-Author	Robert Fraser		
Contribution to the Paper	Reviewed manuscript.		
Signature		Date	22/02/2019

Name of Co-Author	Brian J. C. Freeman		
Contribution to the Paper	Supervised development of work, and reviewed manuscript.		
Signature		Date	19/02/2019

Name of Co-Author	Ryan B. Graham		
Contribution to the Paper	Assisted with development of methods, data analysis and data interpretation, and reviewed manuscript.		
Signature		Date	19/02/2019

Name of Co-Author	Dominic Thewlis		
Contribution to the Paper	Supervised development of work, assisted with data collection and interpretation, and reviewed manuscript.		
Signature		Date	14/02/2019

Name of Co-Author	Claire Jones		
Contribution to the Paper	Supervised study design and development of work, assisted with data analysis and interpretation, and reviewed manuscript.		
Signature		Date	15/02/2019

Chapter 4 Validation of an OpenSim full-body model with detailed lumbar spine for estimating lower lumbar spine loads during symmetric and asymmetric lifting tasks

4.1 Introduction

Low back pain (LBP) is a widespread problem with a lifetime prevalence of 58-84% in western countries (Woolf and Pfleger, 2003). Although mainly considered idiopathic, lifting has been identified as an independent risk factor for the development of LBP (Ferguson and Marras, 1997) because the high loads experienced in the spine may cause injury to the spinal structures (Norman et al., 1998). Direct measurement of *in vivo* spinal loads is challenging, as it requires invasive measurements of intradiscal pressure (IDP) (Wilke et al., 2001, Sato et al., 1999, Takahashi et al., 2006) or invasive surgery to implant an instrumented vertebral body replacement (VBR) in patients affected by spinal disorders. Alternatively, musculoskeletal models simulating the complexities of the spinal architecture and vertebral joint geometries have been developed to understand the internal spinal loading conditions during lifting tasks; examples include finite element models (Bazrgari et al., 2007, Bazrgari and Shirazi-Adl, 2007), static (Arjmand et al., 2006, Arjmand and Shirazi-Adl, 2005) and dynamic (de Zee et al., 2007, Cholewicki et al., 1995, Granata and Marras, 1995a, McGill and Norman, 1986, Kingma et al., 1996) models. However, these models are not open source and it is difficult to use these techniques as the software that implements them is generally unavailable (Delp et al., 2007).

OpenSim (SimTK, Stanford, CA) (Delp et al., 2007) is an emerging open source modelling and simulation platform with a growing library of musculoskeletal models. Despite this large database, there is currently no validated full-body lifting model publicly available on the OpenSim modelling platform (Table 4.1). Lifting tasks have previously been studied using OpenSim (Kim and Zhang, 2017), but the model used was not publicly released, nor was it validated specifically for lifting. A fully articulated model of the thoracolumbar spine by Bruno et al. (Bruno et al., 2015) was validated for lifting tasks, but it did not include lower limbs to locate and apply the ground reaction forces to the model, and most importantly, it cannot currently

be used with kinematic data collected in the laboratory. Another model of the lower limbs and trunk with a detailed lumbar spine was developed to examine trunk motion (Actis et al., 2018). However, this model did not include upper limbs, which precludes application to lifting tasks where external loads are often applied to the hand(s). Only one publicly available full-body model with a detailed lumbar region, which was developed and validated for walking and jogging, exists on the OpenSim modelling platform (Raabe and Chaudhari, 2016). The musculoskeletal geometry and joint definitions of this Full-Body Lumbar Spine (FBLS) model were not tailored to lifting tasks. Appropriate model validation is essential to answer specific research questions and prevent erroneous conclusions (Hicks et al., 2015). Therefore, the aims of this study were to adapt the trunk musculature and movements of the existing FBLS model (Raabe and Chaudhari, 2016) to match lifting analysis requirements, and to validate the resulting model for the evaluation of lumbar spine loading during symmetrical and asymmetrical lifting tasks.

Table 4.1. Comparison of the different OpenSim model studies that have been published and that contain a detailed lumbar region.

OpenSim Model	Validation	Limitations	#DOF	#Segment	#Muscles
Actis et al. (2018)	Trunk movements in three rotational DOFs	• No upper limbs to track load and apply corresponding external forces to model	19	18	294
Kim et al. (2016)	None	• Model not available in database • Model not validated for lifting tasks	49	23	258
Raabe et al. (2016)	Walking and Jogging	• Only validated for walking and jogging	29	21	324
Bruno et al. (2015)	Symmetrical lifting	• No lower limbs • Model cannot perform Inverse Kinematics	96	68	552
Christophy et al. (2012)	None	• No upper or lower limbs • Model not validated for lifting tasks	5	14	238

4.2 Methods

4.2.1 Model Modification

The lifting full-body (LFB) model was developed by modifying the FBLS model (Raabe and Chaudhari, 2016) to suit the analysis of lifting tasks (Figure 4.1, Table 4.2). The resulting LFB model comprised 30 segments, 29 degrees-of-freedom (DOFs), and 238 Hill-type musculotendon actuators (trunk musculature only) (Figure 4.1). The existing 1-DOF T12/L1 intervertebral joint in axial rotation (AR) was replaced by a spherical joint (3-DOF) with the centre of rotation based on the geometric trends reported by Pearcy and Bogduk (1988). The trunk comprised eight rigid body segments (welded pelvis-sacrum, L5, L4, L3, L2, L1, and torso [lumped thoracic and cervical vertebrae, ribcage, scapulae, and head]) and six spherical joints located at the six intervertebral joints (T12/L1, L1/L2, L2/L3, L3/L4, L4/L5, L5/S1). Linear kinematic coordinate coupling constraints were used to distribute net trunk motion across the six intervertebral joints using ratios reported in literature (Flexion-extension (FE) (Arjmand and Shirazi-Adl, 2006a), Lateral Bending (LB) (Dvorak et al., 1991), and axial rotation (Fujii et al., 2007)) (Table 4.3); similar methods have been used to determine kinematics in cervical spine models (Vasavada et al., 1998, Cazzola et al., 2017). Consequently, trunk motion was reduced to three DOFs (FE, LB, AR) as the linear kinematic constraints related the generalised coordinates of the L5/S1 joint (independent coordinate) to the other intervertebral levels (dependent coordinates). Altering these ratios corrected lumbar segmental motion to more physiological angles (Hansen et al., 2006) during lifting motions, especially for the T12/L1 joint. Limits on the range of motion (ROM) of the shoulder (Brown et al., 1988), elbow (Brown et al., 1988), knee (Signorile et al., 1995), hip (Pua et al., 2008, Hemmerich et al., 2006) and lumbar spine (Pearcy and Tibrewal, 1984, Pearcy et al., 1984) joints were increased to better represent motions at these joints during lifting, within physiologically reasonable limits.

Table 4.2. Summary of the modifications to the FBLS model. [A]The lower back wrapping surface (LBwrap body) and [B]leg muscles were removed as they created physically inaccurate moment arms for the hips, knees, and back. [C]Lumbar coupling constraint coefficients and [C]limits on range of motion for flexion-extension (FE), lateral bending (LB), axial rotation (AR) were altered to better represent lifting motions. [D]All maximum isometric muscle forces were increased, with a maximum muscle stress of 100 N/cm^2 to satisfy equilibrium for lifting tasks evaluated in this study. [E]Two DOFs were added to the abdomen body to resolve physically inaccurate moment arms of the EO and IO.

Property			FBLS Model	LFB Model
Number of Segments			31	30[A]
Total Degrees-of-freedom			29	29
Musculotendon actuators			324	238[B]
Range of motion[C]	Hip	FE	-120° to 120°	-140° to 120°
		LB	-120° to 120°	-120° to 120°
		AR	-120° to 120°	-120° to 120°
	Lumbar	FE	-70° to 26°	-80° to 26°[D]
		LB	-25° to 25°	-25° to 25°
		AR	-56° to 56°	-56° to 56°
	Knee	FE	-120° to 10°	-135° to 10°
		LB	-	-
		AR	-	-
	Elbow	FE	0° to 150°	-10° to 160°
		PRO-SUP	0° to 90°	-90° to 120°
	Arm	FE	-90° to 90°	-90° to 180°
		ABD-ADD	-120° to 90°	-180° to 90°
		AR	-90° to 90°	-140° to 100°
Muscle maximum isometric force[D]			-	increased
FE coefficient[C]	T12/L1		-	0.5714
	L1/L2		3.3081	0.9286
	L2/L3		2.7733	1.1429
	L3/L4		2.3024	1.6429
	L4/L5		1.6193	1.8571
	L5/S1		1	1
LB coefficient[C]	T12/L1		-	1.549
	L1/L2		1.3869	2.0392
	L2/L3		1.8458	2.4314
	L3/L4		1.8104	2.4314
	L4/L5		1.3363	1.8627
	L5/S1		1	1
AR coefficient[C]	T12/L1		7.2140	0.75
	L1/L2		1.0129	0.8125
	L2/L3		1.1688	0.875
	L3/L4		1.4804	1.0625
	L4/L5		1.4804	1.0625
	L5/S1		1	1
Abdomen coefficient[E]	FE		0.6429	7.1429
	LB		-	5.5617
	AR		-	11.3122

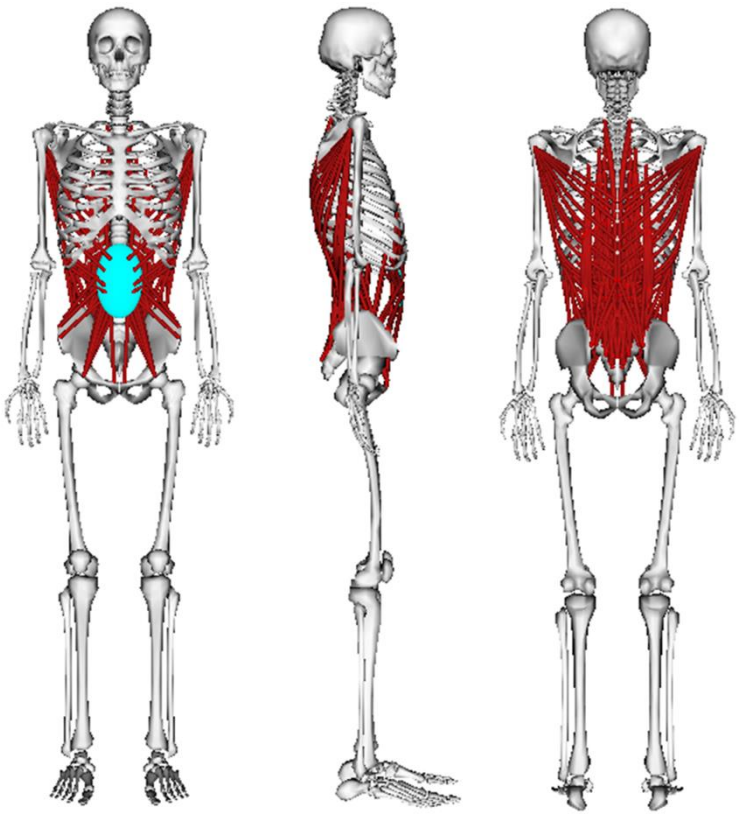

Figure 4.1 The Lifting Full-Body (LFB) model with 238 musculotendon actuators for the trunk musculature.

Lower limb muscles were removed from the model as the existing muscle geometry, and resulting moment arms, were physically inaccurate for the upper end of the hip ROM experienced during lifting tasks (Arnold et al., 2000, Delp et al., 1990, Blemker and Delp, 2005) (Figure 4.2). As a result, the upper and lower limbs did not include muscles and their joints were activated by ideal torque actuators. Trunk musculature was modelled by eight major muscle groups: the erector spinae (ES), rectus abdominis (RA), external obliques (EO), internal obliques (IO), multifidus (MF), quadratus lumborum (QL), psoas major (PS), and latissimus dorsi (LD) (Christophy et al., 2012). The attachment points and muscle paths for the muscle fascicles of these groups were based on cadaveric studies [ES: Bogduk (2005), Macintosh and Bogduk (1987), Bogduk et al. (1992a); RA: Stokes and Gardner-Morse (1999); EO and IO: Stokes and Gardner-Morse (1999),Wilkenfeld et al. (2006); MF: Macintosh and Bogduk (1986); QL: Phillips et al. (2008); PS: Bogduk et al. (1992b), Santaguida and McGill (1995); LD: Bogduk et al. (1998)]. The muscle

fascicles for the erector spinae follow the shape of the trunk using multiple fixed points attaching at the ribs. These multiple fixed points along the spine prevent the muscles from passing through the body in flexion. Based on personal communication with Dr Dennis Anderson (December 1st, 2016), the lower back wrapping surface (LBwrap body) in the original FBLS model was removed as it introduced discontinuities in the moment arms of several muscle fascicles of the ES (Figure 4.3), while the Cylinder wrapping surface from the original model was maintained. The attachment points of the other muscle fascicles remained unchanged, with the exception of the PS; the attachment points not spanning the lumbar joints were removed, thus retaining only the sections of the fascicle that crossed the lumbar region. Lateral bending and axial rotation DOFs were added to the existing FE DOF of the abdomen body using linear kinematic coupling constraints to resolve physically inaccurate moment arms of the EO and IO.

Table 4.3 Percentage of lumbar motion at each intervertebral joint based on the total trunk motion, as implemented in the LFB model.

JOINT	FE % Trunk ROM	LB % Trunk ROM	AR % Trunk ROM
T12/L1	8	14	13
L1/L2	13	18	15
L2/L3	16	21	16
L3/L4	23	21	19
L4/L5	26	16	19
L5/S1	14	9	18

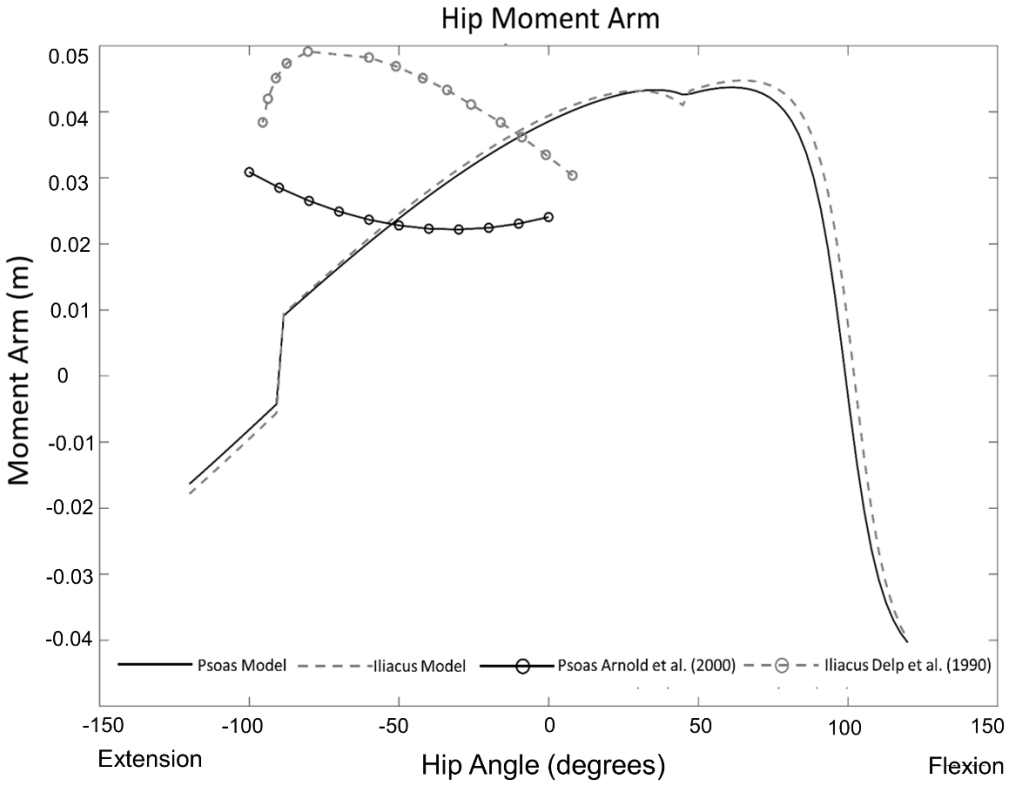

Figure 4.2 Psoas and iliacus moment arms for the hip in the FBLS model over a range of hip flexion and extension angles, compared to the physiological moment arms for the psoas and iliacus measured by Arnold et al. (2000) and Delp et al. (1990), respectively. Illustrates non-physiological moment arms and discontinuities produced in the FBLS model.

All maximum isometric muscle forces were increased, with a maximum muscle stress (MMS) of 100 MPa (Bruno et al., 2015, Maganaris et al., 2001, O'Brien et al., 2010), to ensure the model could satisfy equilibrium for all lifting activities evaluated in this study. This MMS value is in the upper range of values typically used in modelling (46-140 MPa) (Bogduk et al., 1992a, Holzbaur et al., 2005). However, the corresponding maximum isometric extensor moments for the LFB model (165-275 Nm for trunk flexion angles between 0° and 60°) were within the reported ranges for males (171-480 Nm) and females (87-299 Nm) (Hansen et al., 2006) (Figure 4.4). Notably, the flexion angle-moment relationship was not linear as would be expected (Raschke and Chaffin, 1996); this is discussed in more detail in Chapter 7, section 7.6.1. Importantly, increasing MMS to 100 MPa enabled the LFB model to satisfy equilibrium for all lifting activities evaluated in this study, including those with masses above 14 kg, which was not the case for the original FBLS model. Compressive forces at L4/L5 were computed for various MMS values (46 MPa; 60 MPa; 80 MPa; 100 MPa) to evaluate the sensitivity of the LFB model

to the MMS assumption. For all lifting simulations that satisfied equilibrium, the changes in compressive forces at L4/L5 were small (≤3%, compared to 100 MPa) across the range of MMS values (Table 4.4). Thus, increasing MMS did not significantly affect the lumbar loads predicted by the LFB model.

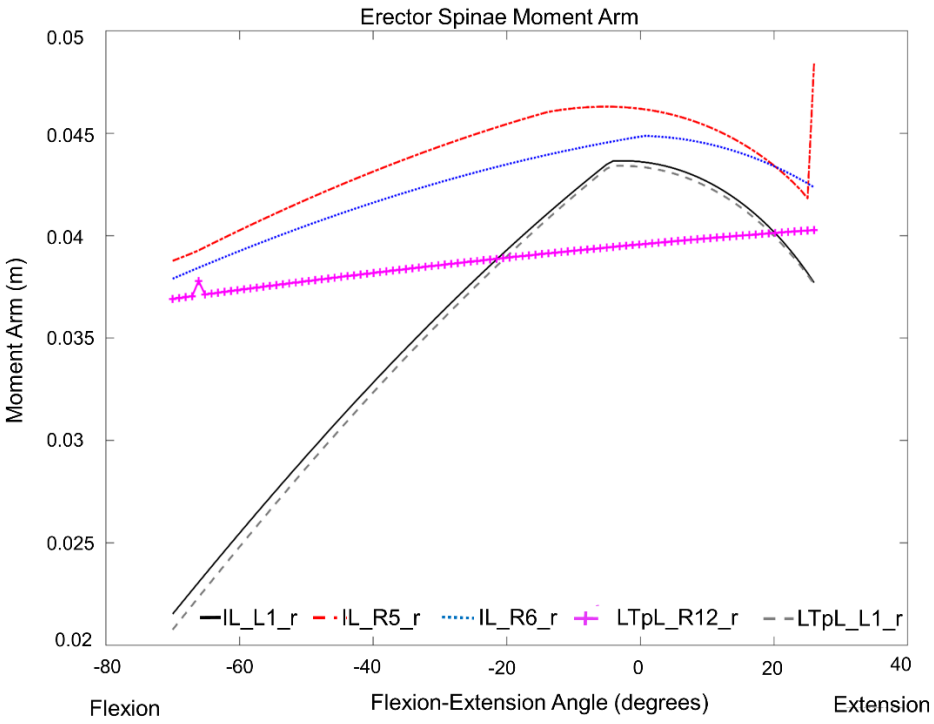

Figure 4.3 Discontinuities associated with the moment arms of five fascicles (IL_L1, IL_R5, IL_R6, LTpL_L1, LTpT_R12) of the ES muscle over a range of trunk flexion and extension angles for the original FBLS with the presence of the LBwrap body. The LBwrap body was removed from the LFB as it also did not allow for three-dimensional scaling of the welded sacrum-pelvis (parent body).

Reserve actuators were used at the independent intervertebral joint (L5/S1) to supplement the muscles. Their applied torques were less than 1% of the peak torque from inverse dynamics, well below the recommended threshold of 5% (Hicks et al., 2015).

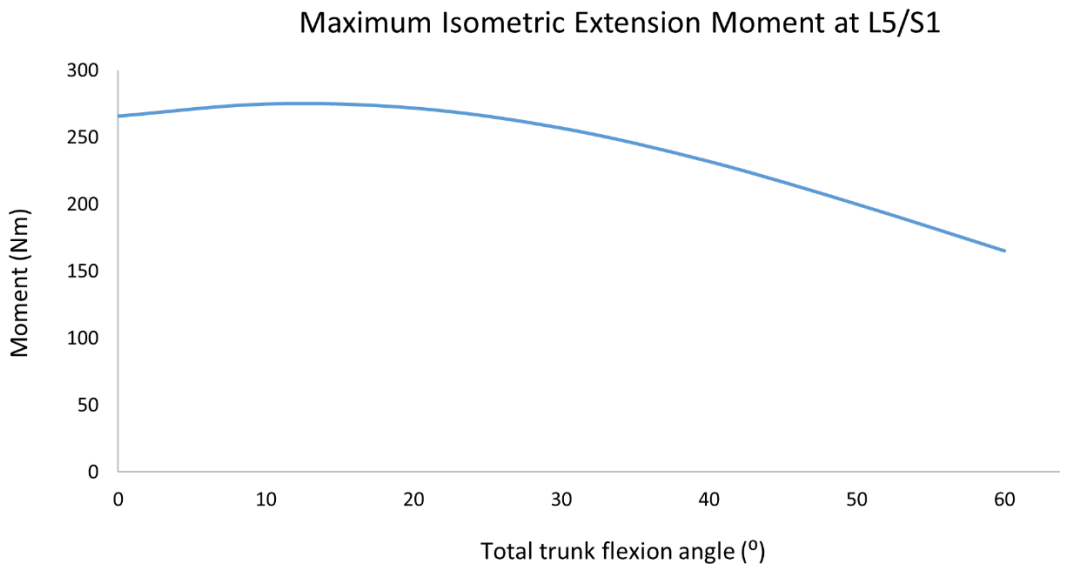

Figure 4.4 Maximum Isometric Extension Moment for the ES for trunk flexion angles between 0° and 60°. These values were obtained via a series of forward dynamics simulations with the model locked (motionless) at various trunk flexion angles and with maximum activation of all the muscle fascicles for the ES muscle group (MF, LTpT, and IL muscle fascicles). These maximum isometrics were measured at L5/S1 to match reported experimentally measured maximum isometric moments. These isometric moments are within the range of reported experimented in the literature (Hansen et al., 2006).

These modifications to the original FBLS model were necessary to prevent the model from failing during lifting tasks and to correct T12/L1 intervertebral motion and erroneous muscle moment arms for the trunk and leg for the ROM experienced during lifting tasks. The effect of the modifications on spinal loading are illustrated in Figure 4.5.

Table 4.4 Percentage difference in L4/L5 compressive load corresponding to different maximum muscle stress (MMS) values, with respect to the final LFB model that has an MMS value of 100 MPa. An "X" indicates that the model was not able to satisfy equilibrium for the lifting task [braced arm-to-thigh technique (BATT), one-handed stoop (1ST), two-handed squat (2SQ) and two-handed stoop (2ST)] and corresponding MMS.

Lifting Task	Maximum Muscle Stress		
	46 MPa	60 MPa	80 MPa
BATT (15kg)	X	3%	2%
BATT (0 kg)	X	<1 %	<1 %
1ST (15 kg)	X	X	<1 %
1ST (0 kg)	X	X	<1 %
2SQ (6 kg)	X	<1 %	<1 %
2SQ (10 kg)	X	X	<1 %
2SQ (14 kg)	X	X	<1 %
2SQ (15 kg)	X	X	<1 %
2ST (6 kg)	X	<1 %	<1 %
2ST (10 kg)	X	X	X
2ST (14 kg)	X	X	X
2ST (15 kg)	X	X	X

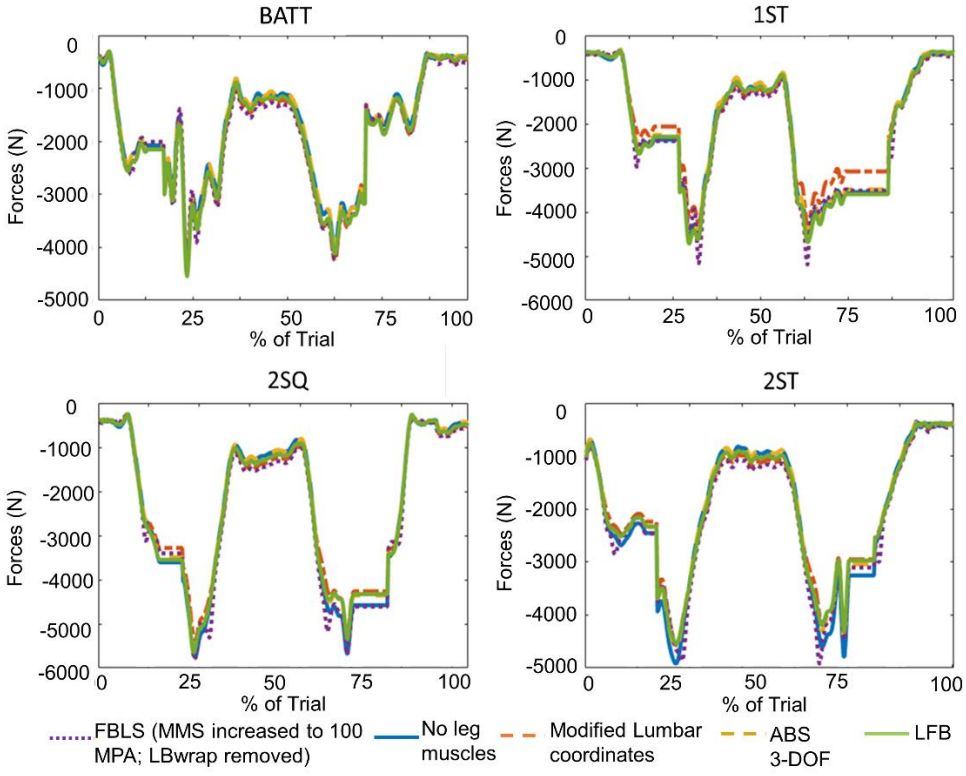

Figure 4.5 L4/L5 intervertebral joint compression forces for exemplar braced arm-to-thigh technique (BATT), one-handed stoop (1ST), two-handed squat (2SQ) and two-handed stoop (2ST) lifts for one participant, for the original model (FBLS), with each modification to the original model (no leg muscles, modified lumbar coordinates, and addition of 2 DOF to the abdomen body (ABS 3-DOF) and the LFB model (all modifications combined). The original FBLS had to be modified (increased maximum muscle stress to 100 MPa and removed LBwrap) to satisfy equilibrium for the lifting tasks. The resultant changes in compressive force were not substantial.

4.2.2 Experimental Data Collection

The study protocol was approved by the institution's human research ethics committee (R20170816). Written informed consent was obtained from three healthy male participants (22.6 ± 2.3 years old, 81.6 ± 3.8 kg, 184.1 ± 5.5 cm).

Participants first performed functional calibration movements to determine the locations of the hip and knee joint centres; a Star Arc straight-leg motion (Camomilla et al., 2006) and cycles of unloaded knee FE motion, respectively. The subsequent tasks performed by the participants were chosen to replicate activities for which prior studies had acquired *in vivo* IDP measurements (Wilke et al., 2001) and VBR loads (https://orthoload.com), or to replicate lifting tasks evaluated by other, proprietary dynamic lifting models (Kingma et al., 1996, Cholewicki et al., 1995). Participants completed three repetitions of each of the activities illustrated in Table 4.5.

Lifting tasks (Table 4.5, Tasks 1-4) involved lifting and replacing a box of varying mass (0-15kg) that rested mid-sagittally in front of the participant on top of a force platform (Model 9286BA, Kistler, SUI) on the ground. The force platform (3 cm height) was used to determine the instant the participant applied an upward force to the box. The handle of the box allowed for two-handed and one-handed pick up, at a height of 21.5 cm from the floor. The mass of the box was adjusted to replicate the loading condition for the matching lifting activity with one of the four lifting techniques: two-handed stoop (2ST), two-handed squat (2SQ), one-handed stoop (1ST), and braced arm-to-thigh technique (BATT). The BATT is a one-handed lifting method in which the dominant hand picks up the object, while the free hand supports the trunk by applying a bracing force on the corresponding thigh.

Static tasks (Table 4.5, Tasks 5-8) consisted of unloaded and loaded (5 kg mass in each hand) standing with straight legs and holding trunk flexion angles of 0°, 10°, 20°, and 30°.

Kinematic and kinetic data were collected with a 12-camera motion analysis system (model MXF-20, Vicon, Oxford Metric, UK) and two force platforms (BP400600, AMTI, USA). Reflective markers were placed on the feet, shanks, thighs, pelvis, sacrum, trunk, arms, forearms,

Table 4.5 The eight tasks performed by the participants to replicate those evaluated by [A]Potvin et al. (1991), [B]Kingma et al. (2015), [C] Wilke et al. (2001), [D] Sato et al. (1999), [E]Takahashi et al. (2006), and [F]OrthoLoad. The mass in the conditions indicated the loads lifted by the participants. The 10 kg loading condition was compared to reported in vivo VBR measurements (bold), while the other loading conditions were compared to results from other proprietary models.

TASK #	TASKS		CONDITIONS					COMPARISON
1	2ST	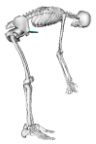	0 kg (pen)[A]	15 kg[A]	6 kg[B]	14 kg[B]	**10 kg[F]**	Other Lifting Model **VBR**
2	2SQ	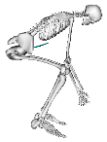	0 kg (pen)[A]	15 kg[A]	6 kg[B]	14 kg[B]	**10 kg[F]**	Other Lifting Model **VBR**
3	1ST		0 kg (pen)[A]			15 kg[A]		Other Lifting Model
4	BATT		0 kg (pen)[A]			15 kg[A]		Other Lifting Model
5	Upward static standing		0 kg in hands[C,D,E]			5 kg in each hand[E]		IDP
6	Static forward bending at 10° flexion		0 kg in hands[C,E]			5 kg in each hand[E]		IDP
7	Static forward bending at 20° flexion		0 kg in hands[C,E]			5 kg in each hand[E]		IDP
8	Static forward bending at 30° flexion		0 kg in hands[E]					IDP

and hands, allowing for full-body tracking (Figure 3.1). A three-axis load cell (Type 9327C, Kistler, SUI), with custom hand rest and thigh interface, was used to measure the bracing force applied by the hand to the thigh directly above the knee for the braced lifting technique (Figure 4.6). Four reflective markers were rigidly fixed to the load cell assembly to determine the location

and orientation of the bracing force applied to the thigh (Figure 4.6). Surface EMG data were recorded using eight electrodes (Trigno, Delsys, USA) placed bilaterally over the RA, EO, lumbar ES and thoracic ES muscles (Figure 3.3) (McGill, 1991a). Analog (Force platforms, load cell, EMG signals) and kinematic signals were collected synchronously through Vicon Nexus (Vicon, Oxford Metric, UK) at 2000 Hz and 100 Hz, respectively.

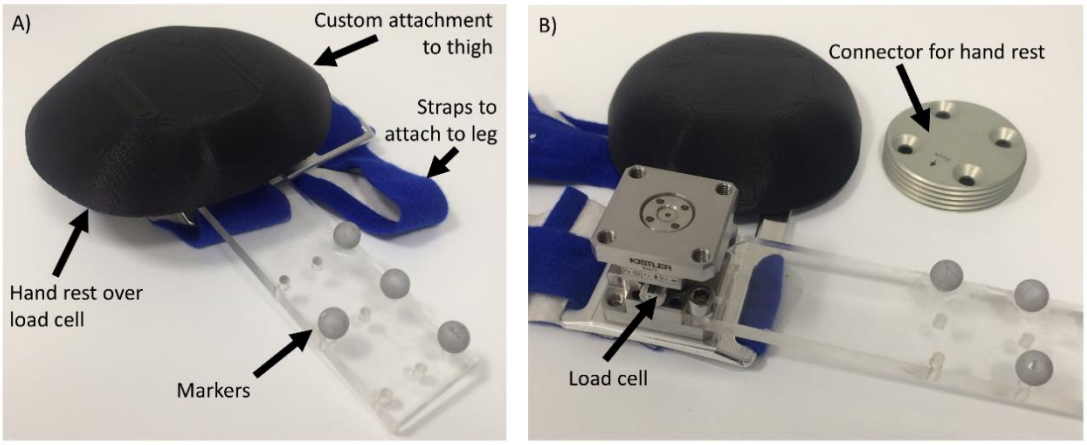

Figure 4.6 A) Load cell attached to the participant's thigh to measure the bracing force applied by the participant's hand on the thigh, via the custom hand rest, during braced arm-to-thigh technique lifts. The markers rigidly attached to the load cell were used to track its position and orientation. B) View of load cell placed under hand rest.

4.2.3 Data processing

Kinematic and kinetic data were low-pass filtered using a bi-directional 2nd order Butterworth filter, cut-off frequency 6 Hz. EMG signals were 20–450 Hz band-pass filtered, rectified, low-pass filtered at 2.5 Hz, and normalised to the peak activation of each lifting cycle.

The generic LFB musculoskeletal model was scaled to the anthropometry of each participant, using joint centres, while preserving their body weight. The hip and knee joint centres were estimated using the SCoRE (Camomilla et al., 2006) and SARA (Ehrig et al., 2007) algorithms, respectively. Other joint centres were calculated as the mid-point between lateral and medial bony landmarks at the proximal and distal ends of body segments (Table 3.3). Muscle properties, including optimal fibre length and tendon slack length, were scaled by the algorithm. Inverse kinematics, inverse dynamics, static optimisation, and joint reaction analyses were performed in OpenSim via custom MATLAB (version 2017b, Mathworks, Nattick, MA, USA) scripts to

estimate muscle activations and joint reaction forces in the lumbar spine (Delp et al., 2007). The criterion used to estimate the muscle forces via the static optimisation analysis was minimisation of the sum of squared muscle activations (Crowninshield and Brand, 1981). Joint reaction forces and moments were obtained for each lumbar spine level (applying and expressing forces in the parent body reference frame).

The force(s) created by the mass of the box held in the hand(s) was modelled by increasing the mass properties of the hand(s) according to the condition of the corresponding lifting task, at the instant indicated by the force platform. For two-handed lifts, the mass of the box was divided equally between both hands, while for one-handed lifts the total mass was added to the hand that lifted the load.

4.2.4 Model Validation

Model simulations were validated by direct comparison between synchronised estimated muscle activations and experimentally measured electromyography (EMG) muscle activity from the participants in this study (Raabe and Chaudhari, 2016). Model validation was also performed by indirect comparison with reported *in vivo* IDP (Wilke et al., 2001, Takahashi et al., 2006, Sato et al., 1999) and reported *in vivo* vertebral loading recorded by VBR implants (Rohlmann et al., 2014a, Dreischarf et al., 2015) previously measured on different participants.

4.2.4.1 Direct comparison: Muscle activation & experimental EMG signals

The experimental EMG activity recorded for the trunk muscles was compared to the muscle activation estimated by the model (van den Bogert et al., 2008). To compare the experimental measurements to the multiple fascicles represented in the model, the activation of the model's muscle fascicles located below the corresponding experimental electrodes were summed and normalised to the peak activation over the lifting cycle (Bruno et al., 2015, Actis et al., 2018) (Figure 4.7). The two curves were compared using a cross-correlation analysis (*xcorr* function in MATLAB version 2017b, Mathworks, Nattick, MA, USA) (Nelson-Wong et al., 2009); the mean peak cross-correlation coefficient and the mean time lag between peak normalised muscle

activation estimated by the LFB model and peak normalised measured EMG excitation for each lifting technique (2ST, 2SQ, 1ST, BATT) were obtained by averaging these values across three trials of each condition within a task, across all participants to obtain one value for each lifting task (Table 4.5, Tasks 1-4).

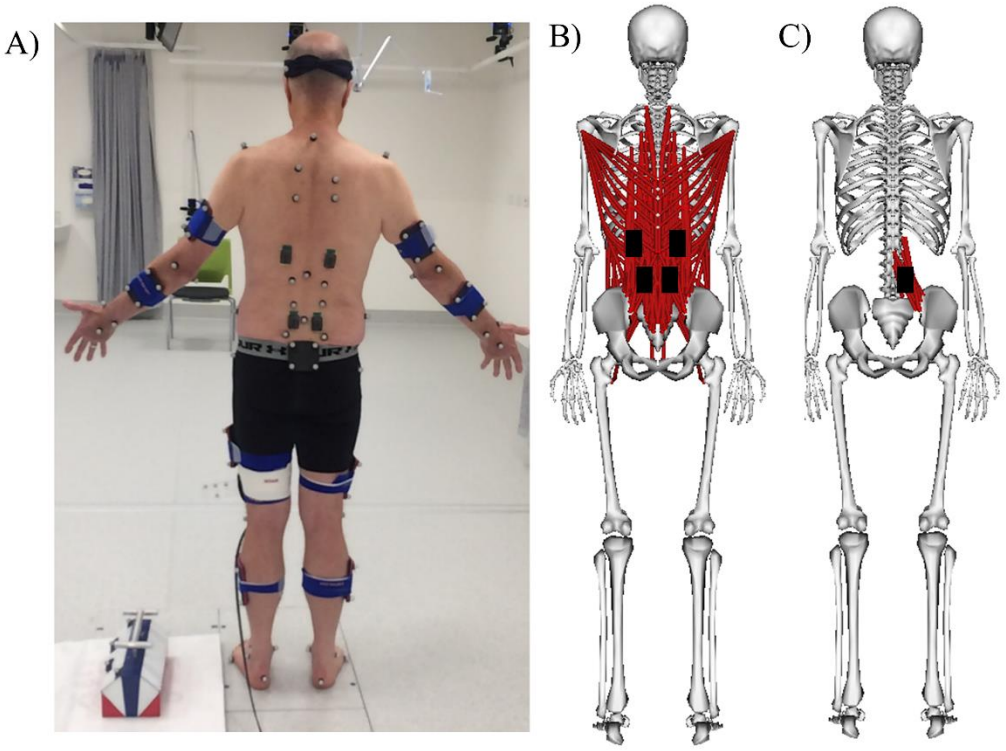

Figure 4.7 A) Surface electrodes for the right and left thoracic erector spinae (top electrodes) and lumbar erector spinae (bottom electrodes) on a participant. B) These electrodes were placed on the model using the same anatomical landmarks and guidelines. C) The activations of the muscle fascicles located below an electrode were summed to correspond to the activation measured by the electrode. For example, the activations of the muscle fascicles placed under the electrode for the lumbar erector spinae were added to compare with the muscle activity measured by the EMG electrode.

4.2.4.2 Indirect Comparisons

4.2.4.2.1 Comparison with *in vivo* IDP measurements

In vivo IDP measurements are correlated with compressive loading at the intervertebral joints. The L4/L5 compression forces estimated by the model were converted to IDP using the mean disc cross-sectional areas (CSA) reported by the corresponding studies (Sato et al., 1999, Takahashi et al., 2006, Wilke et al., 2001) in equation (1) (Ghezelbash et al., 2016):

$$IDP(P,\theta) = -1.556 \times 10^{-2} + 1.255P + 1.243 \times 10^{-2}\theta + 3.988 \times 10^{-2}P^2 - 1.212 \times 10^{-2}P\theta + 1.669 \times 10^{-3}\theta^2 \quad (4.1)$$

where P (MPa) is the nominal pressure (compressive force/CSA) and θ(°) is the L4/L5 intersegmental flexion angle.

The resulting converted IDPs were compared to *in vivo* IDP measurements previously reported for unloaded and loaded static standing tasks for a range of trunk forward bending angles (Takahashi et al., 2006, Sato et al., 1999, Wilke et al., 2001) (Table 4.5, Tasks 5-8).

4.2.4.2.2 Comparison with *in vivo* VBR measurements

The intervertebral compression forces estimated by the model were compared to those recorded by VBR implants during similar lifting tasks (Table 4.5, Tasks 1-2 with load condition of 10 kg) for four male patients (66.0 ± 3.91 years old, 65.25 ± 5.12 kg) (https://orthoload.com). The implants covered multiple intervertebral joints and spanned different levels in the patients. The compressive intervertebral joint force estimated by the model corresponding to the most caudal implanted level was selected for comparison. The intervertebral compression forces measured by the implants and estimated by the model were both normalised to the intervertebral load during neutral, unloaded, standing to allow for comparison and in accordance with previous validation studies (Bruno et al., 2015, Han et al., 2012). The normalised compressive loads at three points during the lifting cycle were chosen for the comparison: 1) upright unloaded standing (start), 2) maximum compressive load, 3) upright standing loaded with a mass of 10 kg. These values were obtained by averaging the measured and estimated lumbar compressive loads across all trials of each condition within a task, across all participants (Table 4.5, Tasks 1-2 with load condition of 10 kg).

4.3 Results

Mean peak compressive estimates (normalised to body mass in kg) ranged from 30.9 N/kg to 63.5 N/kg (2523 N to 5183 N), while the shear forces ranged from 7.9 N/kg to 19.6 N/kg (650 N to 1600 N), for the lifting tasks (Table 4.5, Tasks 1-4). The model estimates increased as the mass lifted increased from 0 kg to 15 kg for each of the four lifting techniques (Figure 4.8). The trends in these results are in agreement with those reported by Potvin et al. (1991) and Kingma et al. (2016), at L4/L5 and L5/S1, respectively, for the same tasks and with similar participants. The magnitude of the model estimates for shear forces were higher than those obtained by Potvin et al. (1991) but similar to those found by Kingma et al. (2016). Compressive forces calculated with the University of Michigan's 3D Static Strength Prediction Program (University of Michigan, Ann Arbor, v.7.0.4) (3DSSPP^{TM}) for peak trunk angle postures were also similar to values obtained with the LFB model for 2SQ, 2ST, and 1ST (55 N/kg, 62 N/kg, 60 N/kg) but lower than those obtained for the BATT lifts (38 N/kg).

4.3.1 Direct comparison

4.3.1.1 Muscle activation & experimental EMG signals

The average experimental EMG signals collected on the back and abdominal muscles and their respective estimated muscle activations by the model for three repetitions of the four lifting techniques (2ST, 2SQ, 1ST, BATT) with a mass of 15 kg for one representative participant are shown in Figure 4.9 and Figure 4.10, respectively. The LFB model's predictions for muscle activation were similar to the recorded experimental EMG signals for the lumbar and thoracic ES. Qualitatively, the curve for estimated activation by the model followed the curve for the experimental EMG signals, both in the timing and pattern of the signals, with the exception of the RA abdominal muscles.

The peak cross correlation values for the back muscles were all above 0.82, and reached values as high as 0.93 (Figure 4.11). The 2SQ task showed the highest peak cross-correlation values for the back muscles (r=0.84-0.92). The symmetrical (2SQ, 2ST) and asymmetrical (1ST, BATT)

lifting tasks showed similar results. The peak muscle force estimated by the model preceded the corresponding peak EMG signal by an average of 0.05 ± 0.47 s.

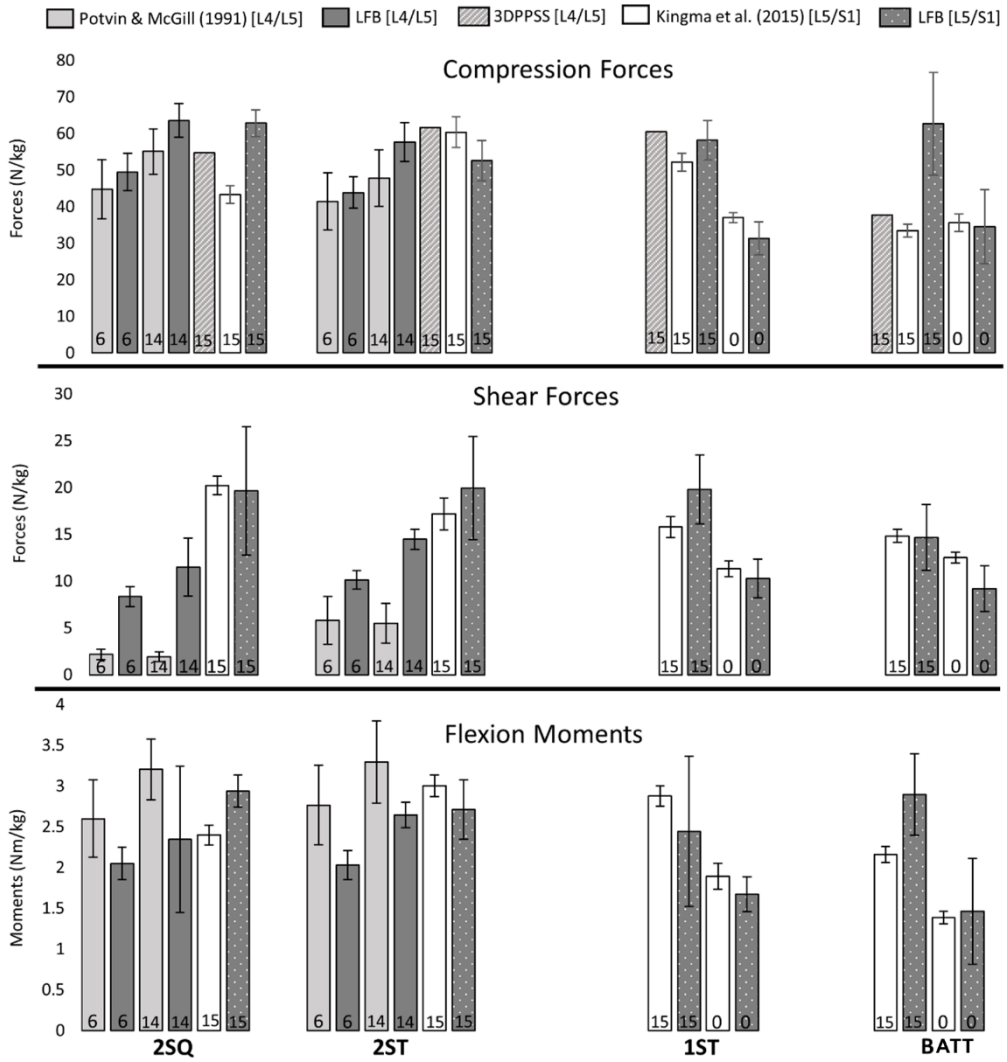

Figure 4.8 Magnitudes of compression and shear forces, and moments, obtained by the model for different lifting tasks (Table 4.5, Tasks 1-4). Estimates obtained by Potvin & McGill (1991), Kingma et al. (2016), and 3DPPSS for similar tasks are also shown. The number in the bar graph corresponds to the mass lifted by the participants.

4.3.2 Indirect Comparisons

4.3.2.1 IDP measurements

The mean vertebral loading estimated by the model for unloaded upright standing were 0.423, 0.451, and 0.519 MPa, similar to the 0.340, 0.5, and 0.539 MPa measured by three different studies (Wilke et al., 2001, Takahashi et al., 2006, Sato et al., 1999, Bassani et al., 2017), respectively. The correlation between IDP measurements and model estimates was strong

(R^2=0.868) (Figure 4.12). The model generally overestimated vertebral loading when compared to the measurements, but followed the same trend of increasing pressures with increasing flexion angles.

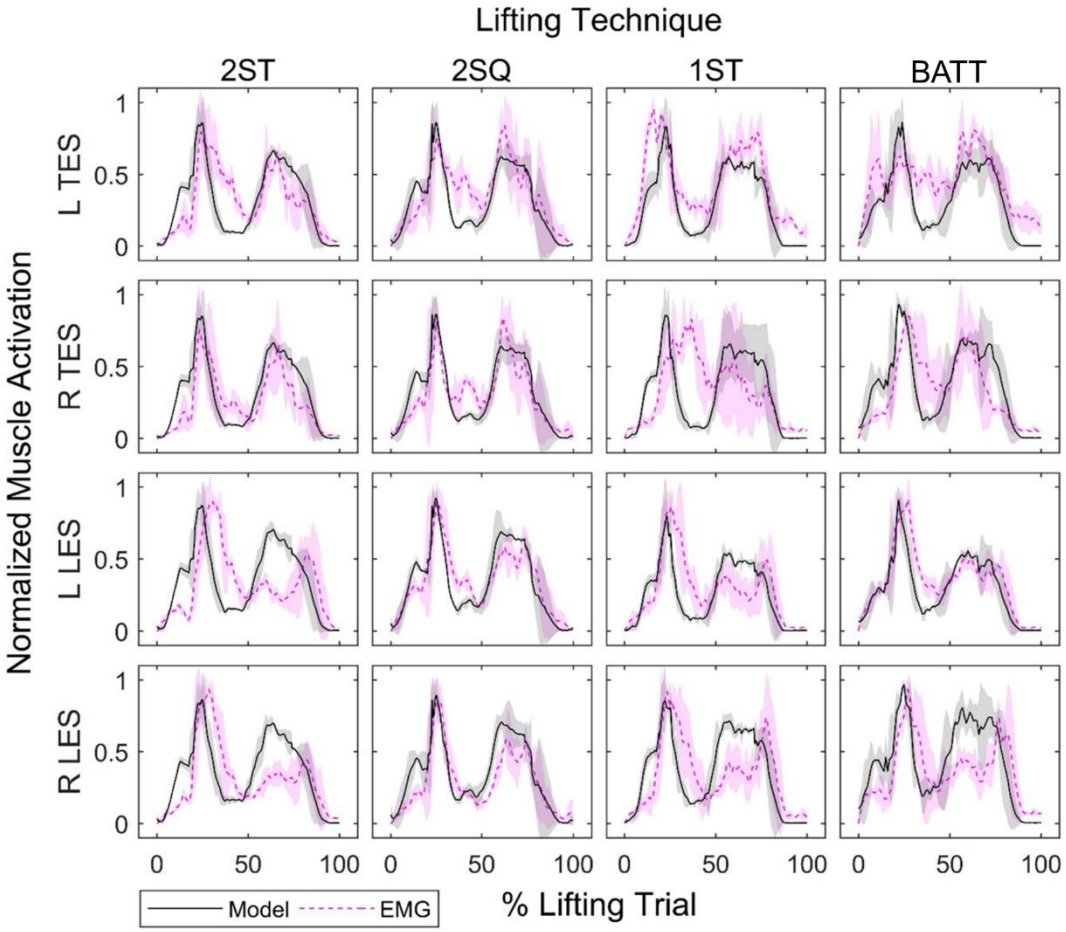

Figure 4.9 Normalised EMG signals for the left thoracic erector spinae (ES) (L TES), right thoracic ES (R TES), left lumbar ES (L LES), right lumbar ES (R LES) (purple dotted lines), and model estimates for the corresponding muscles (solid black lines), for four different lifting techniques. The shaded area around each curve represents ± 1 standard deviation.

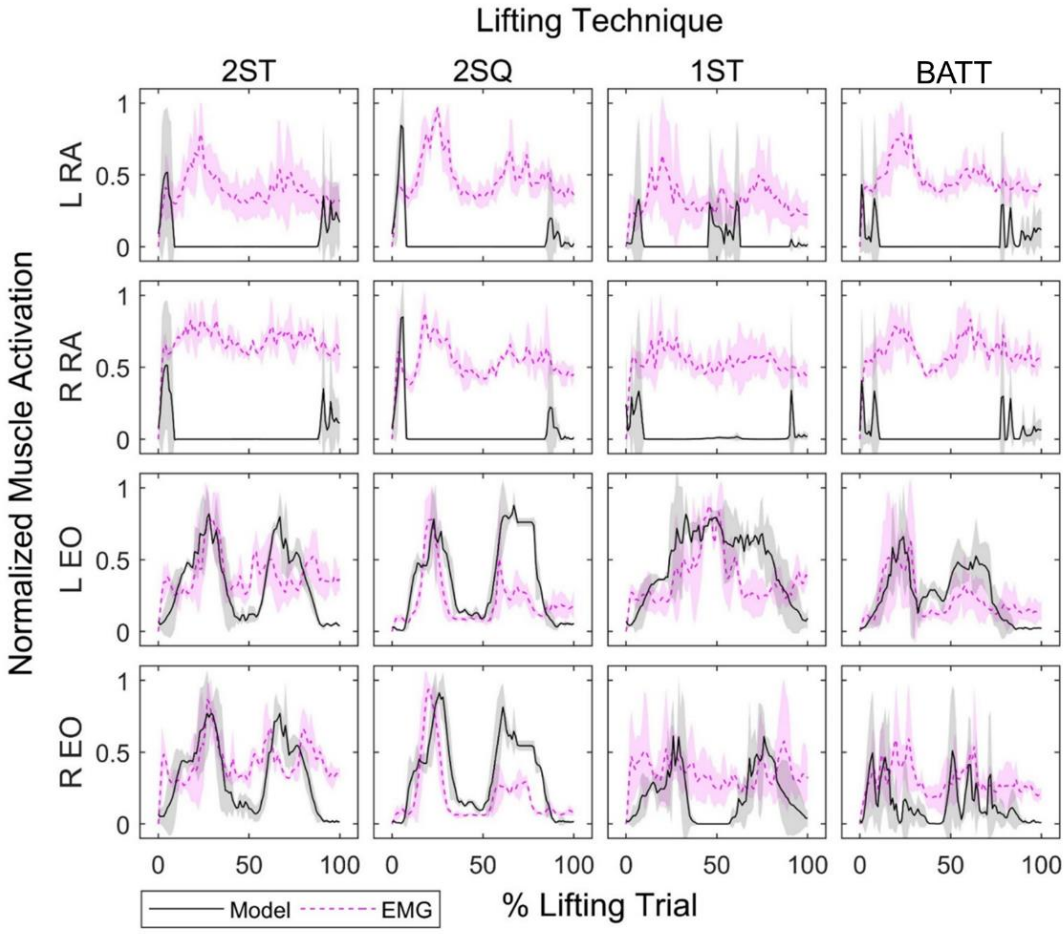

Figure 4.10 Normalised EMG signals for the left rectus abdominus (RA) (L RA), right RA (R RA), left external obliques (EO) (L EO), right EO (R EO) (purple dotted lines), and model estimates for the corresponding muscles (solid black lines), for four different lifting techniques. The shaded area around each curve represents ± 1 standard deviation.

4.3.2.2 VBR measurements

The normalised joint reaction forces estimated by the model were higher than those acting on the VBR at lumbar level L1/L2 and L2/L3, but smaller than those measured at L3/L4 for 2ST and 2SQ lifts (Figure 4.13). The VBR measurements for the maximum compressive load within the same subject showed large variation at L3/L4 for 2ST (1319% to 3008% of standing weight) and 2SQ (764% to 3058% of standing weight). The VBR measurements and model estimates for upright standing with load in hands was between 178%-577% and 174%-373% of unloaded standing weight, respectively (Figure 4.13). Curves of the full lifting trials are illustrated in Figure 4.14.

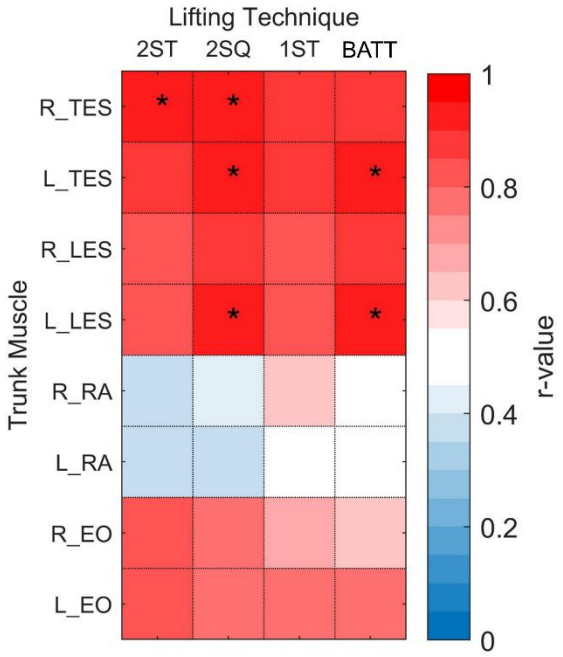

Figure 4.11 Mean peak cross-correlation r-values between the model estimates and the experimental EMG for the four different lifting techniques for the back (R_TES, L_TES, R_LES, L_LES) and abdominal (R_RA, L_RA, R_EO, L_EO) muscles. * indicates r-values higher than 0.9.

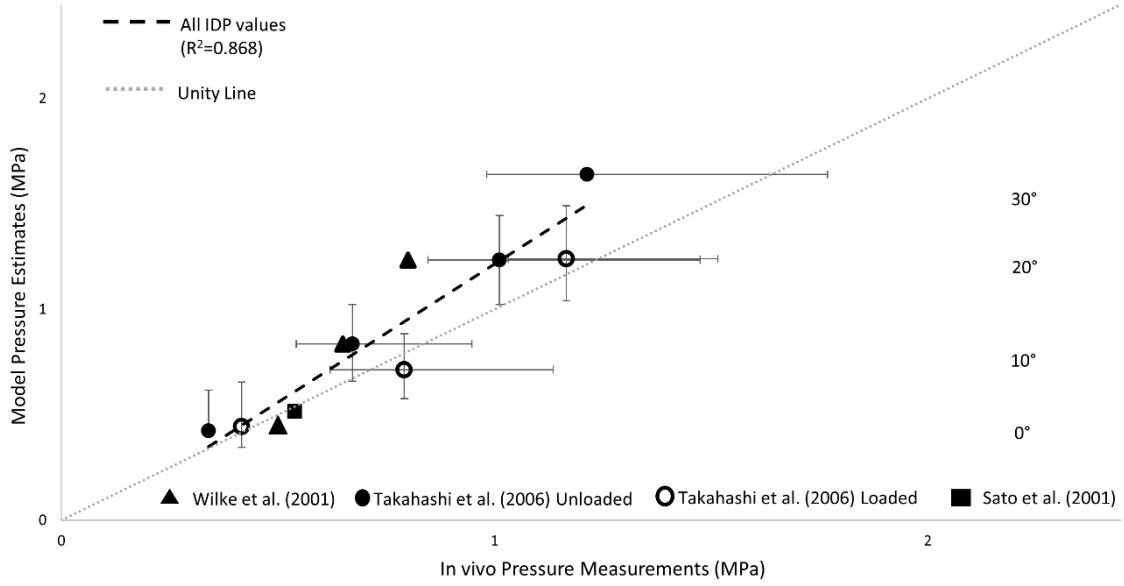

Figure 4.12 IDP estimated by the model and normalised to standing posture IDP were correlated to reported IDP measurements also normalized to standing posture IDP. The dotted line represents unity. The error bars correspond to the range for the IDP measurements and IDP estimates. Triangle and circle points represent the IDP measurements reported by Wilke et al. (2001) and Takahashi et al. (2006), respectively. Filled dots represent unloaded tasks, while empty dots represent loaded tasks with a mass of 5 kg in each hand.

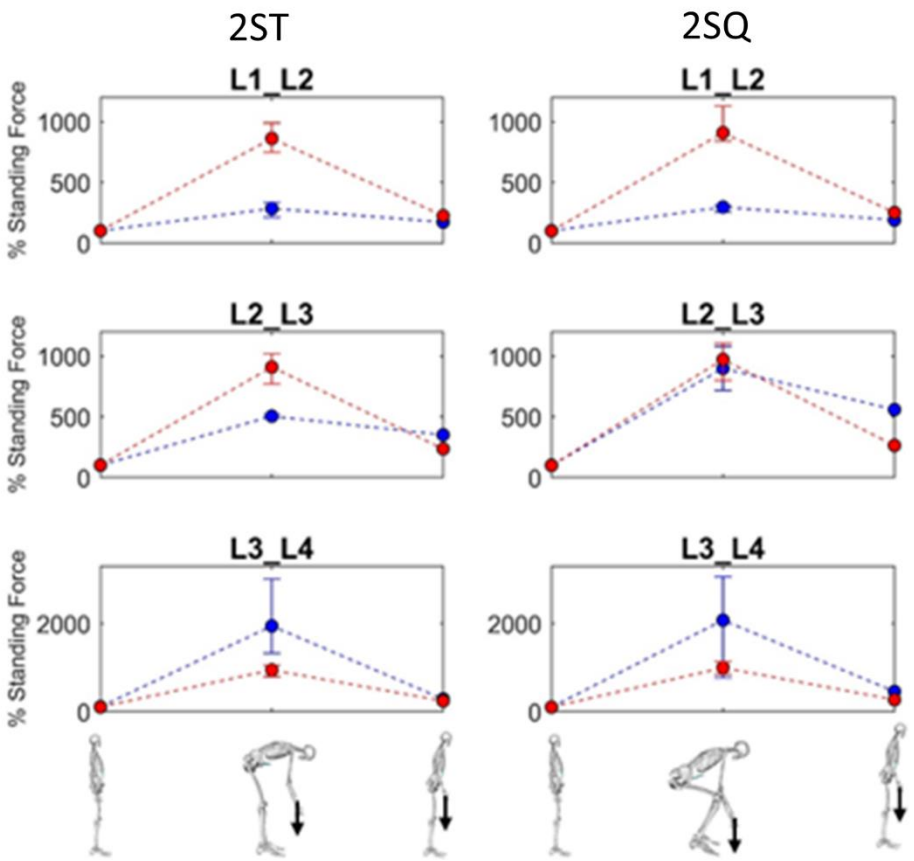

Figure 4.13 VBR measurements (blue) and model estimates (red) normalized to standing posture spinal load at three lumbar levels for two-handed stoop (2ST) and two-handed squat (2SQ) lifts with a mass of 10kg at three points of the lifting cycle: 1) unloaded upright standing, 2) maximum loading when picking up the mass, and 3) loaded upright standing. The error bars indicate the range of values obtained for the maximum vertebral loading.

4.4 Discussion

Task specific validation of musculoskeletal models is important to prevent erroneous conclusions and ensure meaningful simulation results (Hicks et al., 2015); this study validated a modified full-body OpenSim model for lifting tasks (LFB model) specifically to allow an understanding of the internal lumbar vertebral loading for symmetrical and asymmetrical lifting tasks.

The LFB model estimated compressive forces within the ranges reported in the literature by other non-open source models for the same lifting tasks (Potvin et al., 1991, Kingma et al., 2016) and the ergonomic tool 3DSSPP™. However, 3DSSPP™ only allows the evaluation of static postures and consequently, compressive forces were only calculated for peak trunk angle postures for the four lifting techniques with a mass of 15 kg. The difference in shear forces values should be

treated cautiously, as estimates are sensitive to modelling postural parameters (Kingma et al., 2016).

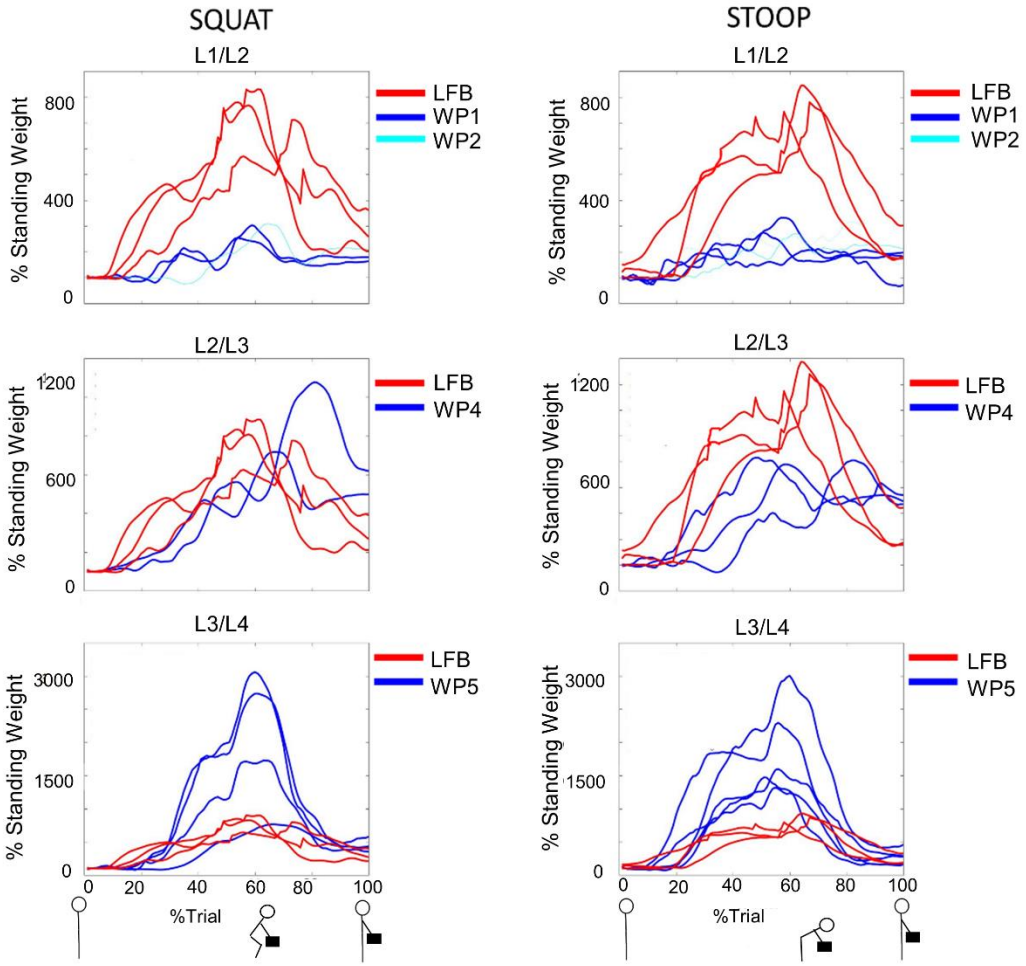

Figure 4.14 VBR load, normalised to the upright standing position, for four patients at three intersegmental levels. Model force estimates, normalised to the upright standing position, for three participants for the corresponding intersegmental levels.

4.4.1 Direct comparison

Muscle activations predicted by the model compared well with measured EMG signals for the back muscles, both in activity levels and timing, for all lifting techniques. The shapes of the curves were similar for the model and the experimental EMG signals; both exhibited a clear double peak pattern characterising the instants when the load was picked up and put down, when the greatest external moments are applied to the back. The mean time difference between peak muscle force and peak EMG magnitude was of the same order of magnitude as the electro-

mechanical delay (EMD) (between peak force and peak EMG of the ES) reported by van Dieen et al. (1991) (0.137 ± 0.29 s) and Marras (1987) (0.2 s).

The best agreement occurred for the 2SQ lift, while both stoop lifts (2ST, 1ST) showed a slightly lower agreement (Figure 4.11). Ligaments contribute approximately 16% of the total trunk flexion moment during stoop lifts, compared to 2% for squats (regardless of the load lifted) (Potvin et al., 1991), but are not included in the LFB model. Consequently, the slightly lower agreement in stoop lifts is likely due to elevated recruitment of muscles to compensate for missing passive structures.

The poor results for the RA muscles were expected because static optimisation (used in this analysis) penalises antagonist co-contraction (Ait-Haddou et al., 2000). Since the prime-mover muscles during lifting are the trunk extensors (Cresswell and Thorstensson, 1994), the effect of the abdominal contractions on the net forces and moments is minimal (Cholewicki et al., 1999a). Activation of the antagonist abdominal muscles, and the resulting intra-abdominal pressure (IAP), results in unloading of the lumbar spine during lifting tasks (Stokes et al., 2010); however, the contribution of IAP to increased lumbar spine stiffness and stability is thought to be more significant than its effects on vertebral loading (Cholewicki et al., 1999a). The LFB model is not suitable to evaluate the effect of abdominal muscle activity on spine loading, and future work should consider the contributions of RA activations to IAP, and therefore to the loading, stiffness and stability of the lumbar spine.

4.4.2 Indirect comparisons

Direct validation of absolute joint reaction forces is currently not possible due the difficulty in obtaining *in vivo* experimental data; therefore indirect comparison was undertaken using IDP and forces normalised to upright standing values measured in different individuals. Since the *in vivo* studies did not report full-body kinematics and kinetics, equivalent analyses (scaling, inverse kinematics, inverse dynamics, static optimisation, joint reaction) could not be undertaken to facilitate direct comparison.

The large IDP ranges reported in the *in vivo* IDP studies for the same tasks illustrates the difficulty in obtaining *in vivo* spinal loading data. Nevertheless, the estimated IDP values agreed strongly with the *in vivo* measurements (R^2=0.868). In addition, vertebral loading estimates increased as the mass lifted and forward bending also increased during dynamic lifting tasks, indicating the model can appropriately estimate changes in spinal loading during loaded and unloaded dynamic trunk movements.

Although the agreement between the normalised VBR measurements and the model estimates was low, the same trends were observed: increasing intervertebral forces with forward bending and higher intervertebral forces when the load was held in hands compared to when participants were empty-handed. Despite the valuable information provided by these *in vivo* VBR implants, the resulting measurements must be treated cautiously as their accuracy and reliability are limited due to 1) load sharing between the VBR, the internal fixation device, the remaining bone, and the added bone material (Rohlmann et al., 2014b); 2) variation in surgical procedures and spinal implant level; 3) small patient cohort; 4) variation in kinematics due to spinal fusion; and 5) variation in patient anthropometry. These limitations are further illustrated by the large within-patient variation in the spinal load measured.

The model in this study has several limitations: it may not be suitable to evaluate lifting techniques with larger trunk motions (FE >65° of flexion, AR>35°, LB>25°) or with large hip and knee flexions (>135°), such as deep squats. The model has currently only been tested with static optimisation, and as result, may not predict co-contraction accurately, especially in static tasks. Future work should seek to incorporate an EMG-informed model where the estimated muscle activations would be based on the experimental activation (Kingma et al., 2016, Cholewicki et al., 1995) and to include the action of the intra-abdominal pressure on the stability of the lumbar spine and spinal loading. The rigid thorax assumption is limiting for predictions of upper lumbar spine loading, but is suitable for lifting studies targeting lowermost spinal levels (L4/L5, L5/S1) (Ignasiak et al., 2016b). In addition, the use of linear kinematic coupling constraints could result in underestimation of spine loading, but were required to determine

intersegmental vertebral body motion in inverse kinematics. Non-linear responses of passive structures (ligaments, facet joints, intervertebral discs) are not included in the current model and incorporating these may improve the estimation of spinal loads (Ghezelbash et al., 2018, Shirazi-Adl, 2006, Arjmand et al., 2006).

Despite these limitations, and the inherent complexity associated with tracking trunk motion, the validation results indicate that the LFB model developed in this study is an appropriate tool to non-invasively evaluate changes in lumbar loading during symmetrical and asymmetrical lifting tasks. The difference between the absolute values of the IDP estimates and measurements indicates that the LFB model is validated for relative evaluations of spine loading during lifting tasks, rather than the prediction of absolute values. The inclusion of upper and lower limbs facilitates the application of external forces to the model, such as the ground reaction forces, the mass lifted, and the bracing force applied to the thigh to provide support to the trunk during BATT lifts. The advantage of the LFB model over more simplistic static models, such as the 3DSSPP™, is that it allows modification of individual muscle properties, in addition to incorporating the dynamic properties of the lifting tasks, as these are known to significantly influence spinal loads (McGill and Norman, 1985). With further development, the LFB could be used to investigate the role of muscles in stabilising the spine and the effect of muscle fatigue during repetitive lifting tasks. Finally, the open-source nature of the model makes it available to researchers worldwide, which is an advantage over other non-open source models used in previous lifting studies.

Statement of Authorship – Chapter 5

Title of Paper	A braced arm-to-thigh (BATT) lifting technique reduces lumbar spine loads in healthy and low back pain participants
Publication Status	☐ Published ☐ Accepted for Publication ☑ Submitted for Publication ☐ Unpublished and Unsubmitted work written in manuscript style
Publication Details	Currently under review

Principal Author

Name of Principal Author (Candidate)	Erica Beaucage-Gauvreau		
Contribution to the Paper	Developed study design and testing methods, performed testing with all participants, performed all data analysis, interpreted data, wrote manuscript and acting as corresponding author.		
Overall percentage (%)	75%		
Certification:	This journal article reports on original research I conducted during the period of my Higher Degree by Research candidature and is not subject to any obligations or contractual agreements with a third party that would constrain its inclusion in this thesis. I am the primary author of this paper.		
Signature		Date	08/02/2019

Co-Author Contributions

By signing the Statement of Authorship, each author certifies that:

i. the candidate's stated contribution to the publication is accurate (as detailed above);

ii. permission is granted for the candidate in include the publication in the thesis; and

iii. the sum of all co-author contributions is equal to 100% less the candidate's stated contribution.

Name of Co-Author	Scott C. E. Brandon		
Contribution to the Paper	Assisted with data analysis and data interpretation, and also reviewed manuscript.		
Signature		Date	19/02/2019

Name of Co-Author	William S.P. Robertson		
Contribution to the Paper	Assisted with development of methods, and reviewed manuscript.		
Signature		Date	17/02/2019

Name of Co-Author	Robert Fraser		
Contribution to the Paper	Assisted with study design and reviewed manuscript.		
Signature		Date	22/02/2019

Name of Co-Author	Brian J. C. Freeman		
Contribution to the Paper	Supervised development of work, and reviewed manuscript.		
Signature		Date	19/02/2019

Name of Co-Author	Ryan B. Graham		
Contribution to the Paper	Assisted with data interpretation and reviewed manuscript.		
Signature		Date	19/02/2019

Name of Co-Author	Dominic Thewlis		
Contribution to the Paper	Supervised development of work, assisted with data collection and interpretation, and reviewed manuscript.		
Signature		Date	14/02/2019

Name of Co-Author	Claire Jones		
Contribution to the Paper	Supervised and assisted with study design and development of work, assisted with data collection, analysis, and interpretation, and reviewed manuscript.		
Signature		Date	15/02/2019

Chapter 5 A braced arm-to-thigh (BATT) lifting technique reduces lumbar spine loads in healthy and low back pain participants

5.1 Introduction

Activities of daily living (ADLs) frequently involve one-handed lifting; however, optimal techniques for one-handed lifts have received little attention in the biomechanics literature, especially compared to two-handed lifting techniques (Kingma et al., 2006, Kingma et al., 2010, Kingma and van Dieen, 2004, Lariviere et al., 2002, van Dieën et al., 1999). One-handed lifting techniques produce lower lumbar extension moments and compression forces than two-handed lifting techniques, for objects lifted symmetrically in the sagittal plane. (Kingma and van Dieen, 2004, Marras and Davis, 1998, Cook et al., 1990). In addition, one-handed lifting techniques enable the free hand to support the upper body on external objects to further reduce spinal loading, compared to two-handed lifts (Ferguson et al., 2002, Kingma and van Dieen, 2004, Cook et al., 1990, Wilson et al., 1997). However, external objects are not always available for support during lifting tasks. Instead, the free hand can be placed on the ipsilateral thigh to brace the trunk. The effect of such hand support on the thigh has only been investigated in one study with a small cohort of 10 young healthy males, lifting a pencil and a 20 kg crate from the floor using four lifting techniques (Kingma et al., 2016). Hand support on the thigh reduced peak moments in the lower back by 13-26%, depending on the lifting technique and object lifted (Kingma et al., 2016). Compression and AP shear forces at L5/S1 were also reduced up to 28% with the hand-thigh support compared to unsupported lifts.

A braced arm-to-thigh technique (BATT) can be used to perform various ADLs that involve lifting light-to-moderate loads, especially by individuals suffering from low back pain (LBP) or older individuals. However, the BATT has not been evaluated from a biomechanical perspective in these specific populations. The aim of this study was to compare spinal loading (moments and forces) at L4/L5, and trunk kinematics, for BATT versus unsupported one-handed and two-handed lifting techniques in participants with LBP and healthy participants. It was hypothesised that the BATT would reduce spinal loading compared to unsupported lifting techniques in both

participant groups. The secondary aims, which were exploratory in their nature, were to compare the magnitude of the bracing force applied by the LBP and healthy groups, and to investigate the relationship between bracing force and spinal loads.

5.2 Methods

This study used a prospective case-control design. The study protocol was approved by the institution's human research ethics committee (Protocol 140307). Written informed consent was obtained from all participants prior to study enrolment. Participants with LBP had been suffering from persistent LBP for at least three months prior to enrolling in the study, while control participants had been LBP-free for at least one year. Exclusion criteria are listed in Table 5.1 Exclusion criteria for participant recruitment.

All participants completed the Oswestry Disability Index (ODI) (Fairbank and Pynsent, 2000) and the Roland-Morris Questionnaire (RMQ) (Stratford et al., 1996) to measure functional disability. The two components of the Fear-Avoidance Beliefs Questionnaire (work subscale, FABQw, and physical activity subscale, FABQpa) (Waddell et al., 1993), were used to measure participants' fear avoidance beliefs and how these may affect their LBP.

Table 5.1 Exclusion criteria for participant recruitment.

Exclusion criteria
• BMI >30 • Degenerative spondylolisthesis (diagnosed) • Previous spine surgery • Spinal tumors • Cauda Equina Syndrome • Muscle or nerve diseases • Balance disorders • Previous surgery in the trunk area (including abdominal) • Pregnancy • Pending or ongoing workers compensation claim • Pain Catastrophising score >30 • Age <30 years old or Age > 70 years old.

5.2.1 Experimental Data Collection

Participants completed three repetitions of four lifting techniques, with two loading conditions (2 kg and 10 kg) (24 trials total): 1) two-handed stoop (2ST), i.e. lifting box with both hands while

bending trunk at the hips and keeping legs straight; 2) two-handed squat (2SQ), i.e. lifting box with both hands, with knees flexed and trunk as upright as possible; 3) one-handed stoop (1ST), i.e. lifting box with dominant hand while bending trunk at the hips and keeping legs straight; and 4) BATT, i.e. lifting box with dominant hand while using the free hand to apply a bracing force to the ipsilateral thigh to support the trunk, with a straight back and bent knees (Figure 5.1). The BATT closely corresponded to the weight lifters technique (WLT) evaluated by Kingma et al. (2016). Participants performed the 2 kg loading condition first, but the order of lifts within each loading condition was randomised. Participants began each trial in upright standing, then lifted a box from the floor to upright standing, returned the box to the floor, and then returned to upright standing. Participants rated pain and discomfort in their lower back after each trial using a Visual Analog Scale (VAS) between 0 and 10. VAS was an outcome variable.

Prior to testing, participants were trained and given time to practice each technique until they felt comfortable. For all techniques, participants were instructed to maintain heel-to-ground contact for the duration of the trial, due to the rigid body assumption for foot modelling. Participants were free to adopt a staggered or aligned feet stance. For the BATT, participants placed the palm of the bracing hand on a three-axis load cell (Type 9327C, Kistler, SUI), secured to the distal anterior thigh (just above the knee) using a custom thigh interface and comfortable hand rest surface (Figure 4.6, Figure 5.1). Four reflective markers were rigidly fixed to the load cell to determine the position and orientation of the bracing force applied to the thigh (Figure 4.6, Figure 5.1). A force platform (Model 9286BA, Kistler, SUI) was used to determine the period the box was off the ground (Figure 5.1).

Full-body kinematics were collected with a motion capture system (100 Hz, 10 x Vantage V5 or 12 x MXF-20 cameras, Vicon Motion Systems, UK) and 88 reflective markers (Figure 3.1). Two force platforms (2000 Hz, BP400600, AMTI, USA) synchronously measured ground reaction forces under each foot.

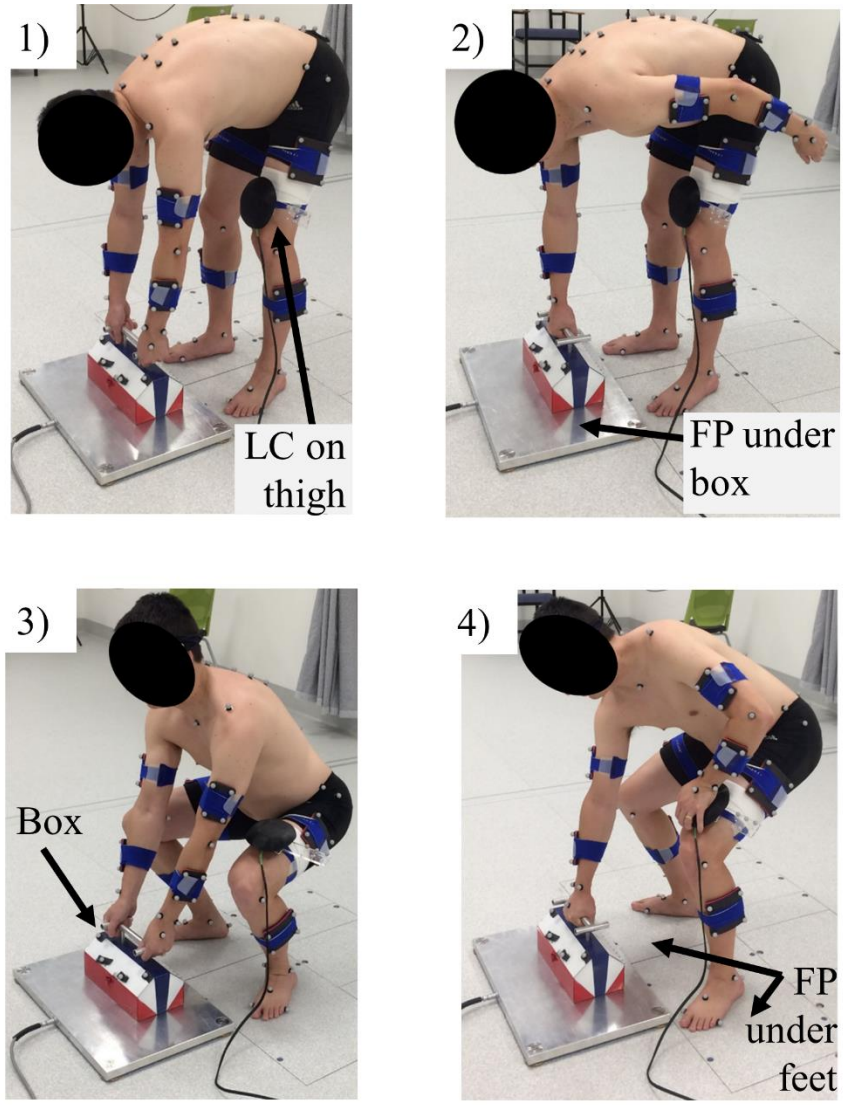

Figure 5.1 The four lifting tasks performed by the participants: 1) two-handed stoop (2ST); 2) one-handed stoop (1ST); 3) two-handed squat (2SQ); 4) Braced-arm-to-thigh (BATT). A load cell (LC) was secured to the thigh to measure the bracing forces. A force plate (FP), 3 cm in height, was placed under the box to determine the instant the participant lifted the box from the ground and put it back down. The handle of the box allowed for two-handed (one hand on each side, see 1)&3) and one-handed pick up (one hand at top centre, see 2)&4), from a height of 21.5 cm from the floor. Two FP, one under each foot, measured the ground reaction forces.

5.2.2 Simulations

Kinematic and kinetic data were low-pass filtered using a bi-directional 2nd order Butterworth filter, cut-off frequency 6 Hz in MATLAB (version 2017b, Mathworks, Nattick, MA, USA). The generic Lifting Full-Body (LFB) OpenSim model, which has been validated to evaluate lumbar loads for lifting tasks (Beaucage-Gauvreau et al., 2019), was linearly scaled to the anthropometry of each participant. The only modification to the model was to change the muscle properties for the Latissimus Dorsi, External Obliques, Internal Obliques, and Rectus Abdominus muscle

fascicles from the Thelen class (Thelen, 2003) to the Millard class (Millard et al., 2013) to resolve discontinuities and minimum length issues. Inverse kinematics, inverse dynamics, static optimisation, and joint reaction analyses were performed in OpenSim (version 3.3), via custom MATLAB (version 2017b, Mathworks, Nattick, MA, USA) scripts, to estimate moments and rigid-body joint reaction forces at the L4/L5 intervertebral joint (Delp et al., 2007). Joint reaction forces, applied to the L5 body, were expressed in the L5 body reference frame.

5.2.3 Data Analysis

Each lifting trial simulation was divided into four phases: 1) unloaded reach down from upright standing; 2) load pick-up to upright standing; 3) upright standing to load put-down; 4) unloaded stand up to upright standing (Figure 5.2). The mass of the box was added to the hands(s), according to the lifting task (Beaucage-Gauvreau et al., 2019). The brief (~0.1s) transitions between the unloaded and loaded phases were not modelled.

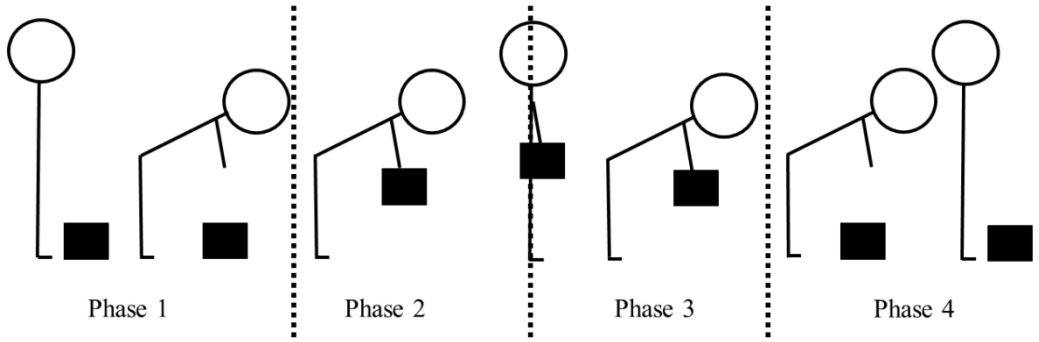

Figure 5.2 Lifting trials were divided into four phases. In phase 1, participants started in an upright position and bent down to pick up the box. In phase 2, participants picked up the box and returned to the upright position, with the box in hand(s). In Phase 3, participants bent down to put the box back on the force platform located on the ground. Finally, in phase 4, participants returned to the upright position, empty-handed. Phases 2 and 3 were loaded phases where the mass properties of the hand(s) of the model were adjusted to include the box, while phases 1 and 4 were unloaded.

For the primary aim, outcome variables were trunk lateral bending angle, trunk axial rotation angle, and 3D moments and forces at L4/L5 at the instant of peak trunk flexion angle during phases 3 and 4. The peak loaded value (i.e. maximum value across phases 2 and 3) for each parameter was also determined. The peak values for all outcome variables over the entire trial were also determined.

For the secondary aim, the peak resultant bracing force over each entire BATT trial was determined. In addition, peak compression forces at L4/L5 in phases 2 and 3 were categorised as occurring either A) during bracing (hand in contact with thigh), or B) outside bracing (hand not in contact with thigh) for all BATT trials, to evaluate participants' ability to use the bracing force (Figure 5.3).

Lateral bending and axial rotation angles and moments, and medio-lateral shear forces for left-handed participants were inverted to consistently describe results with respect to the bracing and lifting hands.

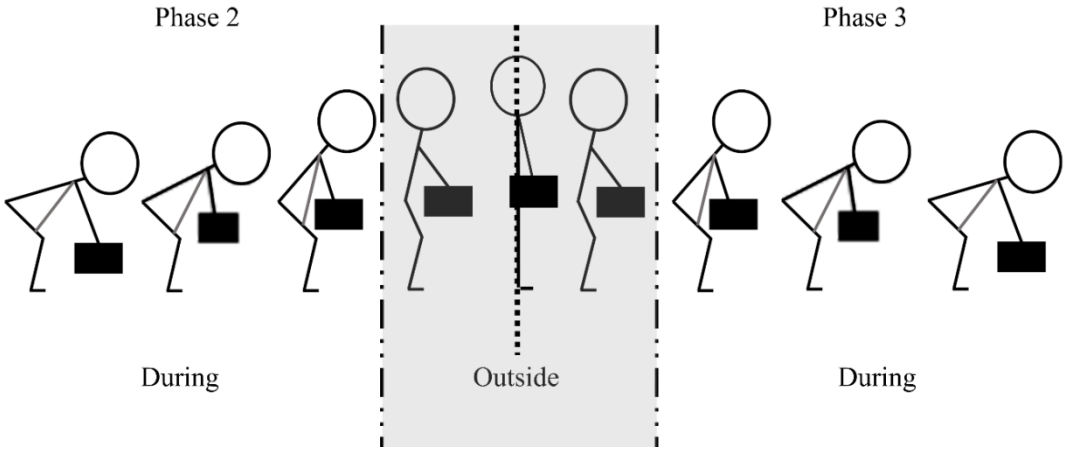

Figure 5.3 Illustration of the bracing categories (during vs outside) for phases 2 and 3 for braced arm-to-thigh technique (BATT) lifts. In the during category, trunk flexion angles are larger and contact between the hand and the thigh produces the bracing force during box pick-up or put-down. In the outside category, the bracing action is completed as participants have smaller trunk flexion angles. The left arm is shown in grey, while the right arm is in black.

5.2.4 Statistical Analyses

Statistical analyses were performed using SPSS v25 (IBM, Illinois, USA). Independent t-tests were used to compare age, mass, height, and ODI, RMQ, and FABQ scores between LBP and healthy groups.

Linear mixed-effects models were developed to identify associations between lifting techniques (the *a priori* variable) and the outcome measures (3D trunk angles, 3D moments and forces at L4/L5, and VAS). The normality and homogeneity of variance of each outcome variable were assessed to ensure the assumptions of linear mixed model were met. For each model, participant

was included as a random effect. The following potential cofounders were included as fixed effects: participant group (LBP or healthy), lifting technique×participant group, mass lifted (2 kg or 10 kg), sex, age, ODI score, and repetition number of each lifting technique (1, 2, or 3). A manual backward step-wise approach was used to refine each model until only significant predictors remained (α=0.05). The lifting technique reference variable was BATT because only comparison with BATT was of interest. If the interaction term was significant, least squares difference post hoc comparisons were completed to investigate individual comparisons with respect to BATT only.

The effect size of lifting technique on these outcome variables was calculated using Cohen's f^2 (Selya et al., 2012), where f^2 = 0.02, 0.15, and 0.35, correspond to small, medium, and large effect size, respectively (Cohen, 1988).

For the secondary aim, three additional linear mixed-effects model were developed for BATT lifts only, using a similar methodology, excluding the interaction term. One model identified if the participant group (LBP or healthy) was associated with the peak bracing force, while the other two models identified if the bracing category (during or outside) was significantly associated with the peak thigh bracing force or the magnitude of the L4/L5 compression force at peak flexion angle in phases 2 and 3.

5.3 Results

Lifting technique was significantly associated with the majority of kinematic and kinetic outcome measures, while participant group was only significantly associated with asymmetric moments and forces, for the peak loaded values. The mass lifted was also significantly associated with the majority of kinetic outcome measures (Table 5.2).

Table 5.2 Summary of the linear mixed-effects models (*p* values) for the outcome variables: compression, antero-posterior (AP), and medio-lateral (ML) forces at L4/L5; flexion-extension (FE), lateral bending (LB), and axial rotation (AR) moments at L4/L5; FE, LB, and AR trunk angles.

Outcome Variables	Fixed Effects							
	Lifting technique	Participant group	Mass Lifted	Lifting Type × Participant Group	Age	Rep#	ODI	Sex
Compression force at L4/L5	<0.001	-	<0.001	-	-	-	-	<0.001
AP shear force at L4/L5	**	**	<0.001	0.006	-	-	-	-
ML shear force at L4/L5	<0.001	0.023	<0.001	-	-	-	-	-
FE moment at L4/L5	<0.001	-	<0.001	-	-	-	-	<0.001
LB moment at L4/L5	<0.001	0.015	<0.001	-	0.003	-	-	<0.001
AR moment at L4/L5	**	**	-	0.033	-	-	-	-
FE angle	<0.001	-	-	-	0.002	-	-	0.045
LB angle	<0.001	-	-	-	-	-	-	0.021
AR angle	<0.001	-	-	-	-	-	-	-
VAS	***	***	<0.001	<0.001	-	0.006	0.045	-

5.3.1 Participants

Twenty healthy participants were matched in age and gender to 18 participants with LBP (Table 5.3, $p>0.05$ for age, mass, and height). Participants with LBP had higher ODI and higher Roland-Morris scores than the healthy participants ($p<0.001$ for both). Participants with LBP also had higher scores for the work subscale (FABQw) and the physical activity subscale (FABQpa) of the FABQ ($p<0.001$ for both).

A total of 912 trials were recorded (38 participants×4 lifting techniques×2 masses lifted×3 repetitions) for this study. Sixteen trials were discarded during post-processing due to marker occlusion or data acquisition issues; this did not affect more than one trial per participant. All 2SQ trials (6 trials) for one LBP participant were removed because heel-to-floor contact was not maintained. Unlike repeated measures ANOVA and similar statistical tests, linear mixed-effects models produce unbiased statistical results despite missing values. Consequently, linear mixed-effect models were the appropriate statistical analysis for this dataset.

Table 5.3 Demographics and questionnaire (Oswestry Disability index (ODI), Roland-Morris, and Fear-Avoidance Behaviour (FABQ)) scores for the study participants. The FABQ has two components: work (FABQw) and physical activity (FABQpa). Measures in bold indicate significant difference between low back pain (LBP) and healthy participants (p<0.05).

		LBP	Healthy
N (F)		18 (9F)	20 (10F)
Age (years)		48.1 ± 11.5	47.9 ± 11.4
Mass (kg)		70.0 ± 10.4	73.6 ± 14.5
Height (cm)		168.8 ± 7.9	171.6 ± 8.8
ODI score (%)		14.0 ± 6.2	0.7 ± 0.2.3
Roland-Morris score (%)		16.4 ± 11.0	1.5 ± 4.6
FABQ	**FABQw**	11.1 ± 9.2	0.9 ± 2.4
	FABQpa	10.3 ± 5.3	2.1 ± 5.6

5.3.2 Trunk angles

There was a significant association between trunk kinematics and lifting technique (p<0.001), but not with participant groups (Figure 5.4). Trunk flexion angle (f^2=0.15) was lower for the BATT than the 1ST and 2ST (p<0.001), but higher than the 2SQ (p<0.001). The 2SQ and 2ST techniques were mainly symmetrical in the sagittal plane, with small trunk axial rotation and lateral bending angles. Compared to all other techniques, the BATT had greater peak lateral bending angles towards the lifting hand (p<0.001, f^2<0.02), and greater peak axial rotation angles towards the bracing hand (p<0.001 with 2SQ and 2ST, p=0.002 for 1ST, f^2<0.02 for all lifting techniques).

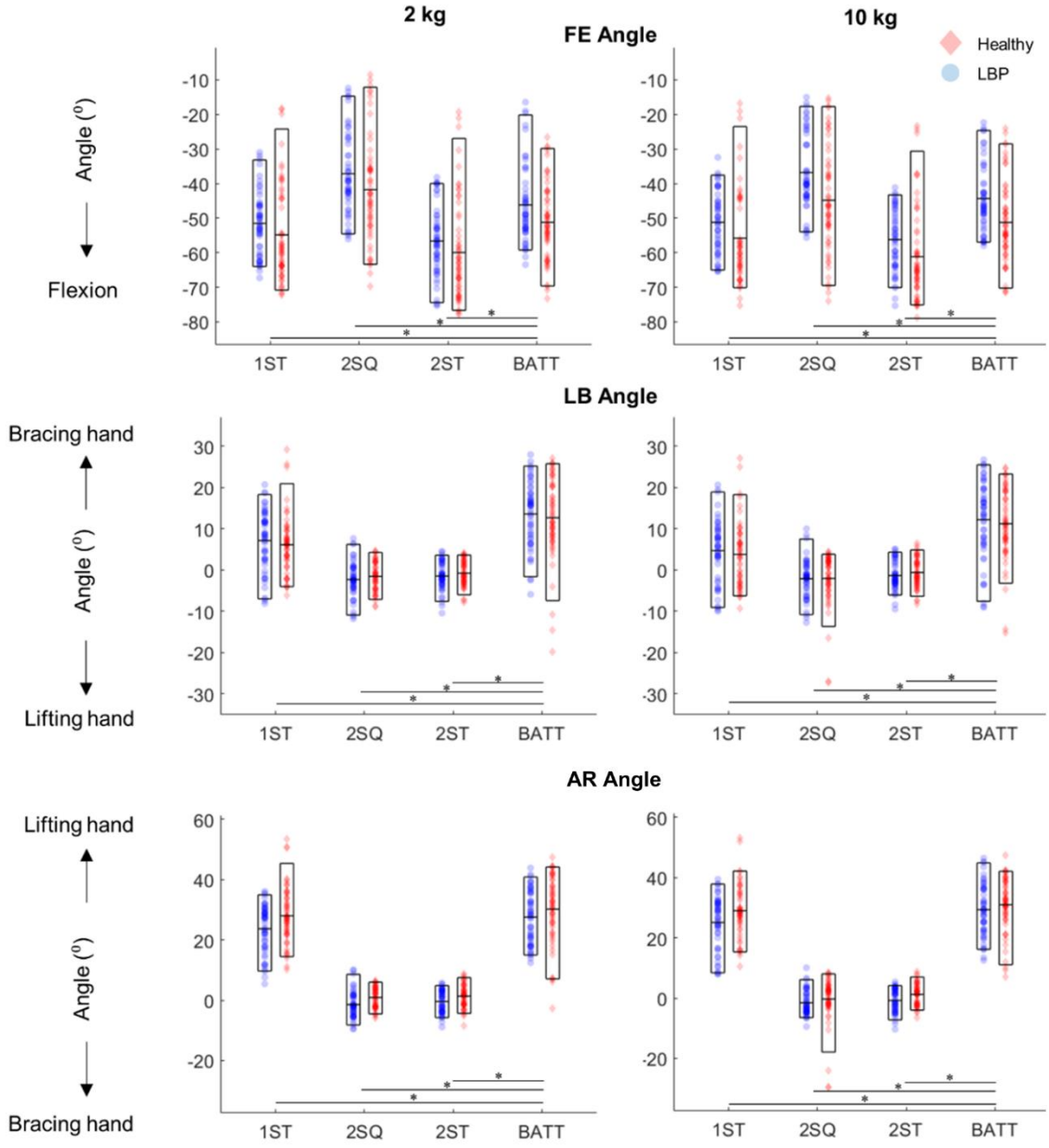

Figure 5.4 Peak trunk flexion-extension (FE) angle, and lateral bending (LB) and axial rotation (AR) trunk angles at peak trunk flexion angle, in the loaded portion of the trial for the four lifting techniques (one-handed stoop [1ST], two-handed squat [2SQ], two-handed stoop [2ST], braced arm-to-thigh [BATT]) for the 2 kg and 10 kg masses. The angles for all trials for low back pain (LBP) and healthy participants are represented as blue circles and red diamonds, respectively. The top and bottom horizontal bars of the boxes represent the 5th and 95th percentile values, while the mean value is shown by the horizontal bar in the box.

5.3.3 Moments at L4/L5

There was a significant association between L4/L5 moments and lifting technique and mass lifted, with greater moments for the 10 kg mass (Figure 5.5) ($p<0.001$). The BATT reduced extension moments compared to 1ST, 2SQ and 2ST lifts ($p<0.001$, $f^2=0.13$), and increased asymmetric moments (axial rotation and lateral bending) compared to the other techniques ($p<0.001$, $f^2<0.02$).

Lateral bending moments were higher for healthy participants for all lifting techniques ($p<0.001$), thus resulting in lower spinal loading, but the results were mixed for axial rotation moments (Figure 5.5). The mean axial rotation moments for unsupported techniques (1ST, 2ST, 2SQ) were close to zero, while the mean for the BATT showed a larger reaction moment towards the lifting hand, as well as greater variability across participants, for both masses lifted.

5.3.4 Forces at L4/L5

The L4/L5 forces generated with the 10 kg mass were significantly greater than those with the 2 kg mass, for all lifting techniques ($p<0.001$). The BATT significantly reduced compression and AP shear compared to the other three techniques ($p<0.001$, $f^2=0.14$ for compression, $f^2<0.02$ for AP shear) (Figure 5.6). Conversely, medio-lateral shear forces were significantly higher for the BATT compared to 2SQ and 2ST techniques ($p<0.001$, $f^2<0.02$), but comparable to 1ST ($p=0.611$). For the BATT, participants with LBP had significantly lower AP ($p=0.004$) and medio-lateral ($p=0.023$) shear forces than healthy participants, but similar compression forces between both groups.

Final linear mixed-effects models for peak loaded values are presented in Appendix E. The same general trends for significant predictors were observed for the outcome measures obtained individually in phase 3 (Appendix F), phase 4 (Appendix G), and the peak value over the entire trial (Appendix H).

5.3.5 Bracing Force

Peak bracing forces were higher for the 10 kg mass than the 2 kg mass ($p<0.001$), but similar between healthy and LBP groups ($p=0.305$), with large variations between participants (Figure 5.7). Peak thigh bracing forces were significantly higher when peak L4/L5 compression forces occurred outside bracing ($p<0.001$), and L4/L5 compression forces at peak flexion angle were significantly lower for this bracing category ($p<0.001$). Final multi-variable linear mixed-effects models for BATT trials are presented in Appendix I.

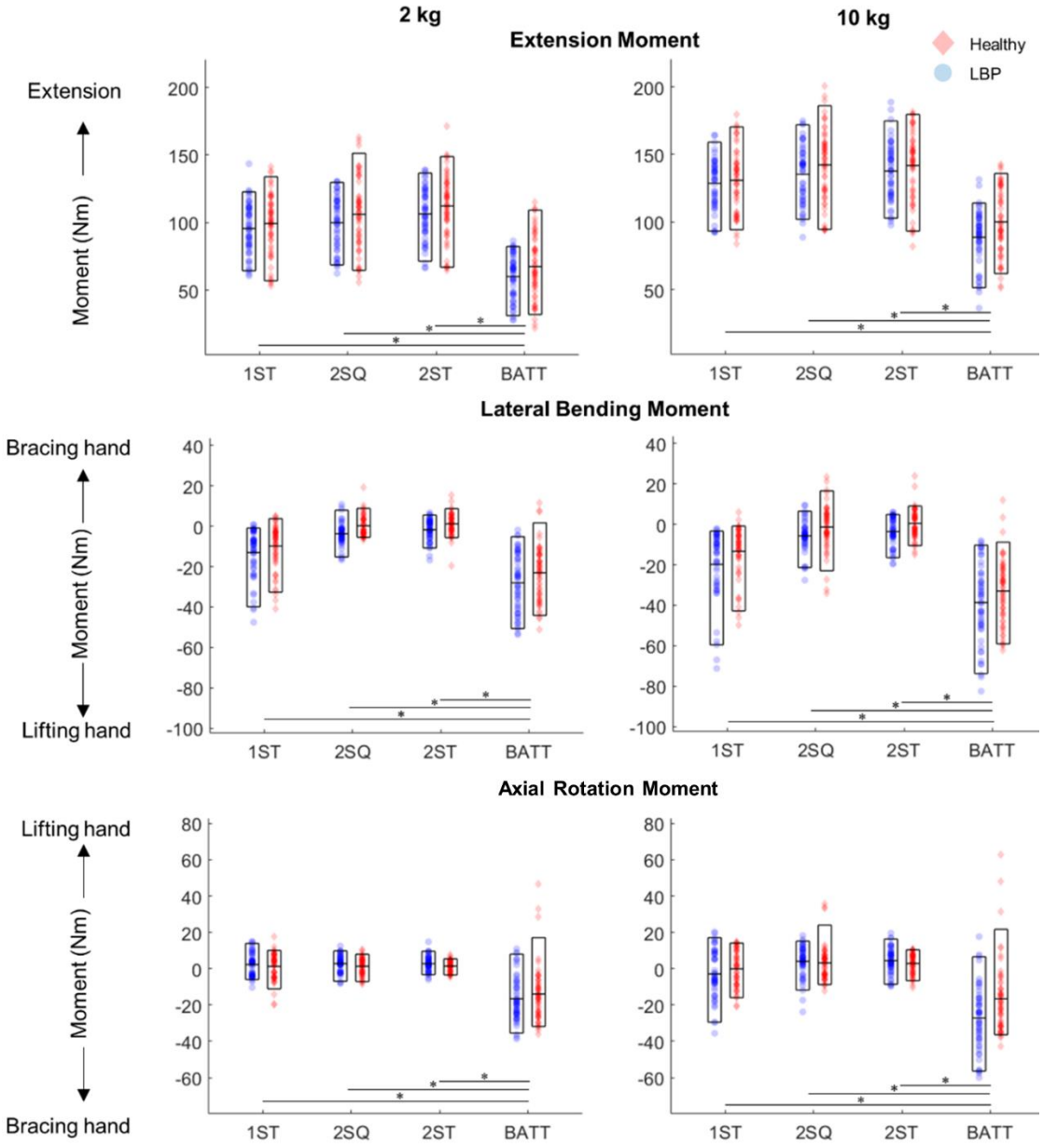

Figure 5.5 Extension, lateral bending, and axial moments at L4/L5 corresponding to peak trunk flexion angle in the loaded portion of the trial for all four lifting techniques (one-handed stoop [1ST], two-handed squat [2SQ], two-handed stoop [2ST], braced arm-to-thigh [BATT]) for the 2 kg and 10 kg masses. The moments for all trials for low back pain (LBP) and healthy participants are represented as blue circles and red diamonds, respectively. The top and bottom horizontal bars of the boxes represent the 5th and 95th percentile values, while the mean value is shown by the horizontal bar in the box.

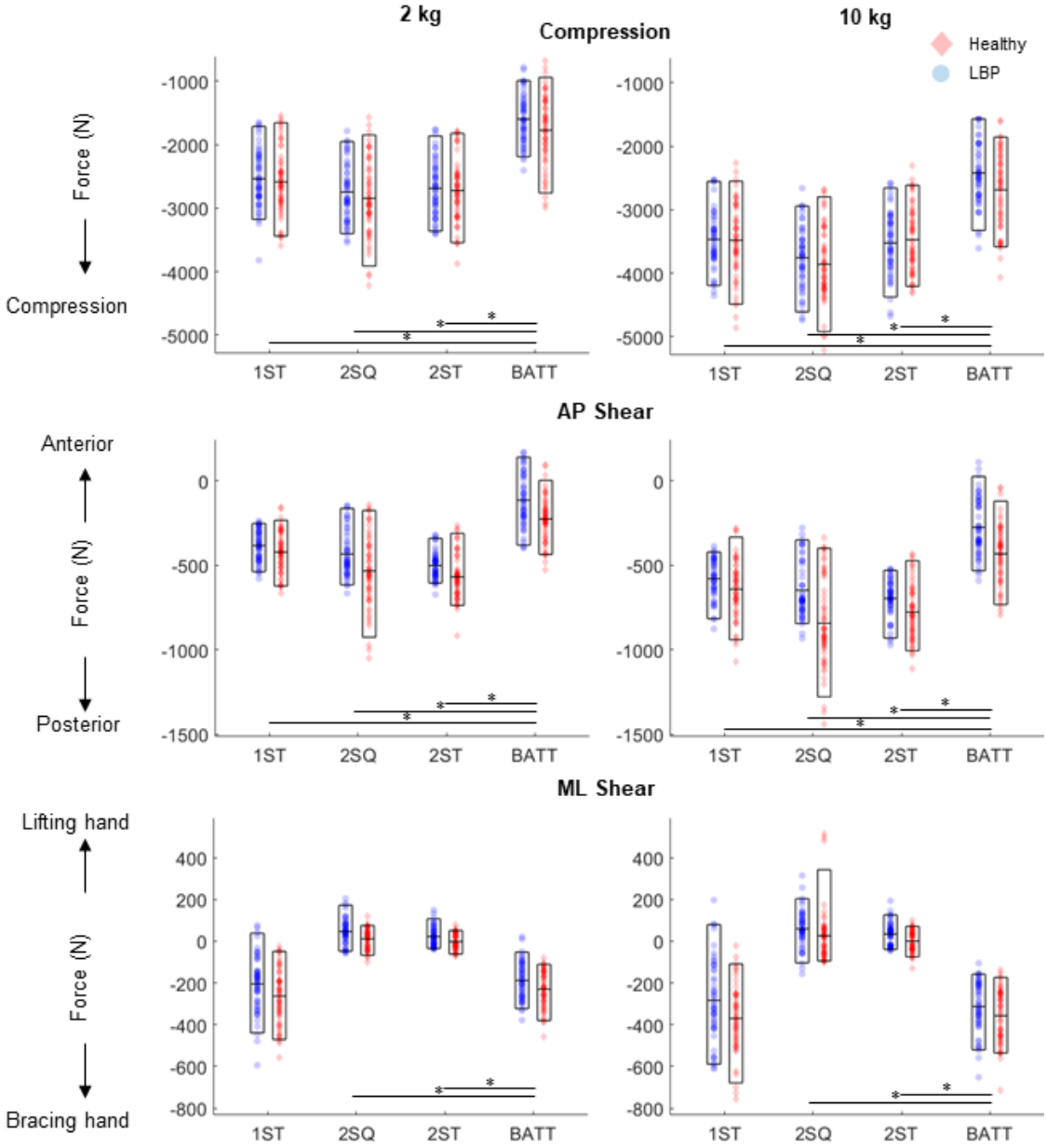

Figure 5.6 Compression, Anterior-Posterior (AP), and Medio-Lateral (ML) reaction forces at L4/L5 at peak trunk flexion angle in the loaded portion of the trial for all four lifting techniques (one-handed stoop [1ST], two-handed squat [2SQ], two-handed stoop [2ST], braced arm-to-thigh [BATT]) for the 2 kg and 10 kg masses. The forces for all trials for low back pain (LBP) and healthy participants are represented as blue circles and red diamonds, respectively. The top and bottom horizontal bars of the boxes represent the 5th and 95th percentile values, while the mean value is shown by the horizontal bar in the box.

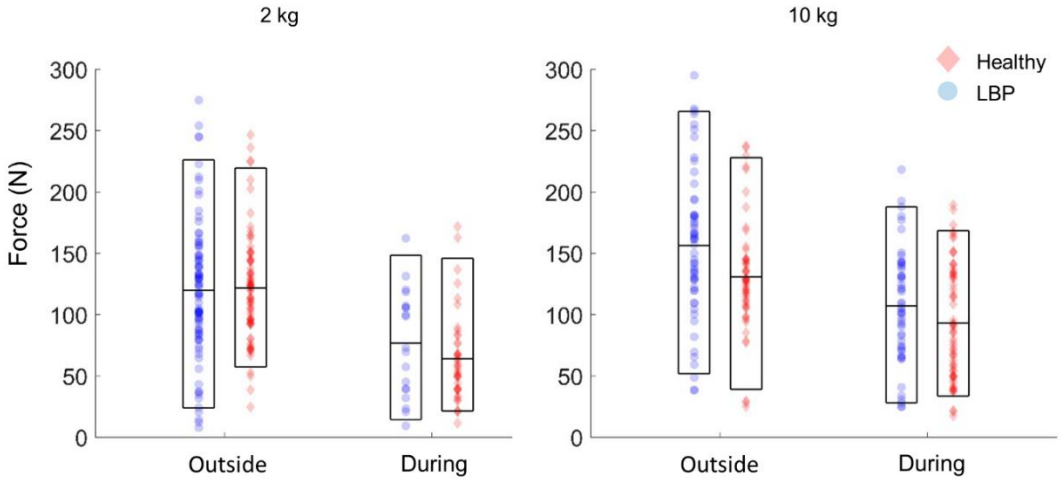

Figure 5.7 Peak resultant bracing force for all BATT trials for all participants for the 2 kg and 10 kg masses. The top and bottom horizontal bars of the boxes represent the 5th and 95th percentile values, while the mean value is shown by the horizontal bars in the box. In the outside category, peak L4/L5 compression forces did not coincide with the bracing period, and for the during category peak L4/L5 compression forces coincided with the bracing period.

5.3.6 VAS

Overall, both participant groups reported low VAS for each lifting technique, with mean scores below 1. VAS was significantly lower for the BATT than the 1ST and 2ST techniques, but only for participants with LBP (p<0.001).

5.4 Discussion

The aim of this study was to investigate the effect of the BATT on spine loading and trunk kinematics, in LBP and healthy populations. BATT significantly reduced L4/L5 flexion moments, and both compression and AP shear forces at L4/L5, compared to unsupported lifting techniques. However, BATT led to asymmetrical motion, producing larger lateral bending and axial rotation trunk angles and moments than the other three techniques. Reflecting this postural asymmetry, medio-lateral shear forces were higher for the BATT than for the two-handed symmetrical lifts (2ST and 2SQ). Trunk asymmetry during lifting has been identified as a risk factor for back injuries (Hoogendoorn et al., 2000); however, the effect of asymmetry on injury risk while using a support (external object or the thigh) has not been assessed in the literature.

The compression force and extension moment reductions observed in this study (25%-45% and 37%-48% reduction, respectively, across lifting techniques and mass lifted) were higher than the 15-30% compression force and 30% extension moment reductions previously reported when supported by a hand on an external object (Ferguson et al., 2002, Kingma and van Dieen, 2004). AP shear force reductions at L4/L5 (25%-45% across lifting techniques and mass lifted) agreed with the results of Kingma et al. (2016) at L5/S1. In addition to differences in modelling and loads lifted with these studies, the higher reductions for the BATT could be explained by the larger trunk flexion angles typically required when using an external bracing object rather than the thigh.

All lifting tasks evaluated were below injury thresholds associated with heavy lifting [3400 N for compression forces (Brinckmann et al., 1989) and 700-1000 N for AP shear forces (Gallagher and Marras, 2012)], likely due to the relatively low masses (2 kg and 10 kg) used in this study to simulate loads lifted in common ADLs. However, comparisons with injury thresholds must be interpreted with caution, as musculoskeletal models are currently most useful for evaluating relative changes rather than absolute magnitudes. In addition, although evidence that mechanical tissue overload from a single event is linked to injury, back injury from cumulative trauma from repetitive sub-failure loading during occupational tasks is more common (Bogduk, 2005, McGill, 2007, Brinckmann et al., 1988, Coenen et al., 2014). Irritated tissues can also produce pain at loading levels well below the cadaverically-determined tolerance during repeated and prolonged tasks (McGill, 2007). The BATT reduced loading of the lower back compared to unsupported lifting techniques and can therefore potentially reduce LBP injury risk linked to biomechanical factors.

Peak thigh bracing forces were similar to the range (102-218 N) reported by Kingma et al. (2016), for four different lifting techniques (self-selected, one-handed squat, one-handed stoop, WLT), lifting a pencil and a 20 kg crate. The large variance in peak bracing forces between participants (Figure 5.7) suggests differences in participants' willingness and ability to effectively use the hand support. It appears that peak L4/L5 compression force did not coincide with bracing for

some participants because their bracing was so effective. For those participants, peak compression force occurred at smaller trunk flexion angles where there was no contact between the hand and thigh/load cell (i.e. bracing action was completed or small) (Figure 5.8). Real-time feedback on the bracing force during task training and/or during data collection may help elucidate bracing timing and magnitude that most effectively reduces spinal loads. A time series analysis relating the moments at L4/L5 resulting from the hand support on the thigh, to those due to inertial forces, could also provide additional insight on the effect of the bracing force on spinal loading.

Peak L4/L5 compression force for *unsupported* lifting techniques (1ST, 2SQ, 2ST) generally occurred at, or near, peak trunk flexion in the loaded portion of the lifting trial because L4/L5 moments counteract both the weight of the flexed trunk and of the box held in the hand(s). Consequently, the point of peak trunk flexion during the loaded portion of the lifting trial was chosen for comparison between all lifting techniques to address the temporal shift in peak L4/L5 compression force observed in many participants during BATT trials (Figure 5.8).

The majority of participants with LBP recruited for this study were classified in the "minimal disability" category according to the ODI, indicating that they can cope with most ADLs (Fairbank and Pynsent, 2000). FABQ scores were also below thresholds, indicating fear avoidance behaviour or concerns regarding return to work were not relevant to this cohort (Fritz and George, 2002). Despite the significant difference in VAS scores for participants with LBP for the BATT compared to stoop lifts (1ST and 2ST), participants reported very low pain and discomfort scores across all techniques and it is doubtful that these differences were clinically significant. Recruitment of participants with LBP with high ODI scores was limited and might explain the minimal differences in spinal loading and trunk kinematics observed across participant groups. Participant group was only a significant predictor for lateral bending moments and ML shear forces. Participants with LBP had lower lateral bending moments but higher ML shear forces. This inverse relationship observed between these two outcomes can likely be explained by multiple dependent factors such as muscle lines of actions, participant kinematics,

and external forces. Nevertheless, these differences between groups were small and might not be clinically relevant. Future cohorts should include individuals with higher ODI to better evaluate the clinical relevance of the BATT on LBP, as measured by the VAS.

There are some limitations associated with the OpenSim model used in this study. The trunk angles estimated by the model for some participants were on the upper end of the physiological range of motion. This is because the rigid thorax assumption and the inherent complexity associated with tracking trunk motion meant that some motion that actually occurred at the hips and/or shoulders was attributed to the trunk. However, trunk angles were within the validated range of motion for the LFB model (Beaucage-Gauvreau et al., 2019). Static optimisation was used to estimate muscle forces; this approach fails to predict abdominal muscle co-activation (Beaucage-Gauvreau et al., 2019) and to apply participant-specific muscle activation patterns, which may be altered for LBP participants (MacDonald et al., 2009). A model integrating electromyography could help to identify muscle recruitment pattern differences between LBP and healthy groups for the different lifting techniques (Marras et al., 2001). The L4/L5 intervertebral loads estimated for the BATT could not be validated against *in vivo* measurements because this task was not specifically undertaken in previous tasks measuring *in vivo* IDP (Wilke et al., 2001, Takahashi et al., 2006, Sato et al., 1999). These modelling limitations in measuring trunk kinematics and predicting muscles activations likely affected the L4/L5 loads estimated by the model. However, the conclusions from this study are unaffected because within-subject comparisons for the different lifting techniques were performed.

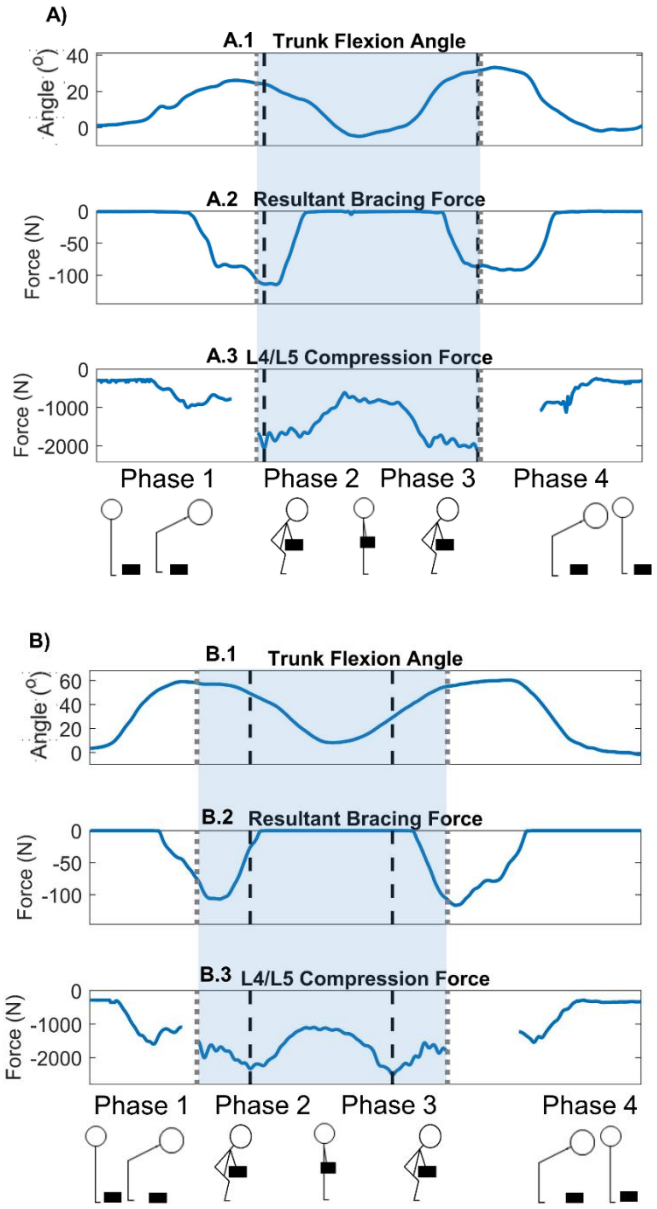

Figure 5.8 Exemplar of one participant for trunk flexion angle, resultant bracing force and L4/L5 compression force over two braced arm-to-thigh technique (BATT) lifts. The shaded blue area corresponds to the loaded portion (phases 2 and 3 with box in hands) of the trial, while phases 1 and 4 are unloaded periods before and after the lift. Vertical black dashed lines indicate the instant of peak L4/L5 compression force in phases 2 and 3, while grey vertical dotted lines indicate the instant of peak trunk flexion in phases 2 and 3. A) The peak L4/L5 compression forces (A.3) occur almost at the instant of peak trunk flexion angle in phases 2 and 3 (A.1). The peak L4/L5 compression force coincide with the bracing action on the thigh (A.2). B) The peak L4/L5 compression forces (B.3) do not coincide with the bracing action on the thigh (B.2), and occur at small trunk flexion angle in phases 2 and 3 (B.1).

The transitions between unloaded and loaded phases of the lifting trials were not modelled due to limitations associated with modelling the distribution of the mass of the box between the ground and hands for each data point. This assumption likely did not affect the results as peak spinal loading generally occurred during the loaded portion of the lifting tasks. Finally, the load

cell assembly caused a 6 cm offset between the hand and thigh, which may have subtly affected arm and shoulder kinematics compared to bracing directly on the thigh. In addition, small moments due to off-centre placement of the hand on the resting surface were not accounted for in the analysis as the load cell placed on the thigh only had three DOFs. To minimise the impact of these factors on the results, the protocol incorporated training and practice prior to data collection, and participants adjusted the location of the load cell on the thigh to the most comfortable position for bracing (which was usually as close to the knee as possible).

In conclusion, lumbar spinal loads were substantially reduced by the BATT, compared to unsupported lifts for both healthy and LBP groups. The BATT is promising for healthy individuals and those with LBP to perform lifting tasks with low-to-moderate loads.

Statement of Authorship – Chapter 6

Title of Paper	Lumbar spine loads are reduced for activities of daily living when using a braced arm-to-thigh technique
Publication Status	☐ Published ☐ Accepted for Publication ☐ Submitted for Publication ☑ Unpublished and Unsubmitted work written in manuscript style
Publication Details	

Principal Author

Name of Principal Author (Candidate)	Erica Beaucage-Gauvreau		
Contribution to the Paper	Developed study protocol and designed testing apparatus, performed testing with all participants, performed all data analysis, interpreted data, and wrote manuscript.		
Overall percentage (%)	75%		
Certification:	This journal article reports on original research I conducted during the period of my Higher Degree by Research candidature and is not subject to any obligations or contractual agreements with a third party that would constrain its inclusion in this thesis. I am the primary author of this paper.		
Signature		Date	08/02/2019

Co-Author Contributions

By signing the Statement of Authorship, each author certifies that:

i. the candidate's stated contribution to the publication is accurate (as detailed above);

ii. permission is granted for the candidate in include the publication in the thesis; and

iii. the sum of all co-author contributions is equal to 100% less the candidate's stated contribution.

Name of Co-Author	Scott C. E. Brandon		
Contribution to the Paper	Assisted with data analysis and data interpretation, and also reviewed manuscript.		
Signature		Date	19/02/2019

Name of Co-Author	William S.P. Robertson		
Contribution to the Paper	Assisted with development of study design and methods.		
Signature		Date	17/02/2019

Name of Co-Author	Robert Fraser		
Contribution to the Paper	Assisted with study design and methods, and also reviewed manuscript.		
Signature		Date	22/02/2019

Name of Co-Author	Brian J. C. Freeman		
Contribution to the Paper	Assisted with study design and methods, and also reviewed manuscript.		
Signature		Date	19/02/2019

Name of Co-Author	Ryan B. Graham		
Contribution to the Paper	Assisted with data interpretation and reviewed manuscript.		
Signature		Date	19/02/2019

Name of Co-Author	Dominic Thewlis		
Contribution to the Paper	Supervised development of work, assisted with data collection and interpretation, and reviewed manuscript.		
Signature		Date	14/02/2019

Name of Co-Author	Claire Jones		
Contribution to the Paper	Supervised and assisted with study design and development of work, assisted with data analysis, and interpretation, and reviewed manuscript.		
Signature		Date	15/02/2019

Chapter 6 Lumbar spine loads are reduced for activities of daily living when using a braced arm-to-thigh technique

6.1 Introduction

Many ADLs such as gardening, cleaning, and other domestic tasks require frequent forward bending, which has been associated with an increased risk of back pain (Heneweer et al., 2011). Many of these tasks can be performed with one hand, therefore allowing the trunk to be supported by resting the free hand on an external object or the ipsilateral thigh. The braced arm-to-thigh technique (BATT) reduces extension moments and compression loading in the lower back compared to unsupported techniques for lifting tasks (Kingma et al., 2016) (Chapter 5). However, it has never been evaluated biomechanically in the context of other common activities of daily living (ADLs). Moreover, evaluation of spinal loads during ADLs are generally underrepresented in the biomechanical literature, regardless of the technique employed.

Three tasks were chosen for this study: weeding (gardening, in a standing posture), reaching into low cupboards, and car egress. These one-handed tasks were selected because they involve movements beyond those required for lifting and also include a biomechanical risk factor associated with the development of low back pain. In addition, these tasks could be simulated in the laboratory, thus allowing trunk kinematics to be measured and spinal loads to be estimated.

Given the paucity of literature on the investigation of spinal loads for ADLs, weeding and reaching for objects in low cupboards have not been studied previously. Car ingress/egress is one of the only common ADLs that has been studied previously. Car ingress/egress motion involves complex movements that can be challenging for the elderly and individuals with a disability, potentially leading them to stop driving (Jung et al., 2015, Cherednichenko et al., 2006, El Menceur et al., 2008, Cappelaere et al., 1991). Existing studies of car egress have predominantly focused on movement analysis, to understand the strategies and techniques used by individuals to exit a car. Individuals with a disability often adopt a *two-legs out* technique, where individuals swivel on the seat and bring both legs out of the car before rising out of the vehicle (Chateauroux

and Wang, 2010). These individuals also often place their hand on the seat, door, or thigh, to provide support during egress (Chateauroux and Wang, 2010). However, kinematic studies of car accessibility are not sufficient to provide an understanding of how the spinal loads experienced during car egress are affected by hand support (Causse et al., 2009, Chateauroux and Wang, 2010, El Menceur et al., 2008). Spinal loads during car egress, with or without hand support, have not been reported.

The primary aim of this study was to compare trunk kinematics, moments and forces at L4/L5, for self-selected and BATT techniques, during three common ADLs simulated in the laboratory. The secondary aim was to investigate the effect of the bracing force magnitude on spinal loading.

6.2 Methods

This study used a prospective observational design to investigate the effect of thigh bracing on spinal loading in three common ADLs. The study protocol was approved by the Royal Adelaide Hospital's human research ethics committee (Protocol R20170816). Written informed consent was obtained from ten healthy male participants (77.2 ± 4.6 kg, 178.7 ± 5.9 cm, 25.6 ± 2.8 years old) recruited for this study.

6.2.1 Apparatus

Custom apparatus were designed and built to simulate in the laboratory the three ADLs selected for this study.

For the weeding task, the pulling action was replicated in the laboratory using a magnet (22 kg pull force, PMYP-F25, Frenergy Magnets, AU) placed on a ferromagnetic plate. The magnet comprised an M5 eyelet, into which a small hook (D20 mm x 37 mm M4 thread, PMYP-E20, Frenergy Magnets, AU) was placed during the pulling action (Figure 3.6A). The ferromagnetic plate was rigidly attached to a three-axis load cell (MC3A-1000, AMTI, USA) to measure the pulling force. In turn, the load cell was secured to a heavy steel plate on the floor to ensure it would not move during the trials (Figure 6.1 A,B). The magnet was 9.4 cm from the ground.

For the cupboard task, a steel structure replicating the dimensions of a bottom kitchen cabinet was used to simulate the task of reaching for an object into a low cupboard (Figure 3.6B). This structure was constructed from steel square sections to minimise marker obstruction during trials, with a wooden shelf 11.5 cm from the floor.

For the car egress task, a standard medium-sized Australian car (e.g. Ford Mondeo) was replicated in the laboratory by two steel structures; one for the main car body and one for the door. Both were constructed from steel square sections to minimise marker obstruction (Figure 3.7, Figure 6.1 E,F). The main body structure reproduced the dimensions of the driver's compartment and included a steering wheel and a car seat (Figure 6.2). The distance between these two components could be adjusted. The car seat backrest was removed to maximise marker visibility during data collection. The door was replicated by a separate structure, placed to the right of the main body because drivers are seated on the right in Australian cars. The door armrest was replicated by a steel square section, located 65 cm from the ground (Figure 6.3). The door was instrumented with a 3-axis load cell (MC3A-1000, AMTI, USA) secured to the "armrest" and covered by a custom hand resting surface (Figure 6.1 E,F).

6.2.2 Experimental Data Collection

Full-body kinematics were collected with a 10-camera motion analysis system (100 Hz, model MXF-20, Vicon, Oxford Metric, UK) using 88 reflective markers (Figure 3.1). Two force platforms (2000 Hz, BP400600, AMTI, USA) synchronously measured ground reaction forces under each foot. During the experiment, participants completed three trials of the following simulated tasks: 1) Weeding (gardening); 2) Reaching into a low cupboard; and 3) Car egress.

For the weeding task, participants started in the upright standing position magnet on the magnetic plate. Participants placed the hook in the magnet eyelet and exerted an upward force until the magnet released from the magnetic plate (Figure 3.6; Figure 6.1 A, B). The trial stopped once the participant had returned to the upright standing position, with the magnet in hand.

For the cupboard task, participants started in the upright standing position before bending forward to reach for the shelf on the cupboard structure, with their dominant hand (Figure 6.1 C, D). Participants were instructed to lightly tap the edge of the wooden shelf, before returning to the upright standing position.

For the car egress task, participants started in the driving position, before swivelling to their right, and egressing the car using the *two-legs out* method (Figure 6.1 E, F). Participants were instructed to use the door for support during *all* car egress motions, using their left hand. The load cell was always placed on participants' right thigh because drivers are seated on the right in Australian cars.

Participants first completed three trials of each task in a self-selected manner (without thigh support), although for car egress participants were constrained to using the *two-legs out* method and the door armrest support with the left hand. Participants were then instructed in and completed three trials using thigh support (BATT). In the case of car egress, participants also used the door armrest support. For the BATT, participants were instructed to place the palm of the bracing hand (non-dominant for weeding and cupboard tasks, and right for car egress task) on a three-axis load cell (Type 9327C, Kistler, SUI), secured to the distal anterior ipsilateral thigh, using a custom thigh interface and hand rest surface (Figure 4.6). Four reflective markers were rigidly fixed to the load cell assembly to determine the location and orientation of the bracing force applied to the thigh (Figure 3.4). Participants were allowed to practice each task until they felt comfortable, prior to data collection.

A total of 180 trials were recorded (10 participants × 3 tasks × 2 conditions × 3 repetitions) for this study.

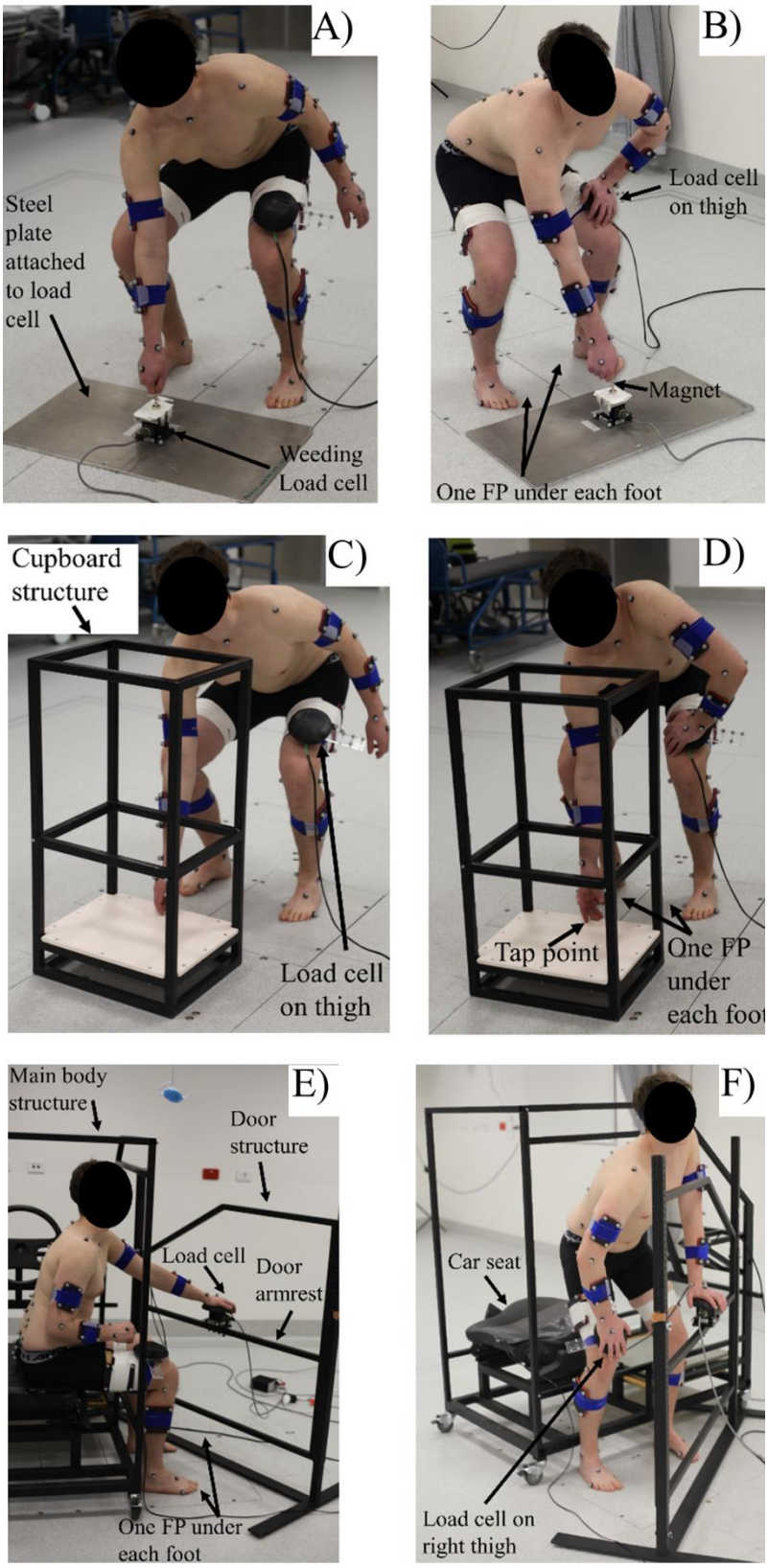

Figure 6.1 Three simulated tasks in the laboratory in two conditions: A) Weeding using a self-selected technique; B) Weeding using the BATT; C) Reaching for objects in low cupboard using a self-selected technique; D) Reaching for objects in low cupboard using the BATT; E) Car egress using door support only; F) Car egress using door support and BATT.

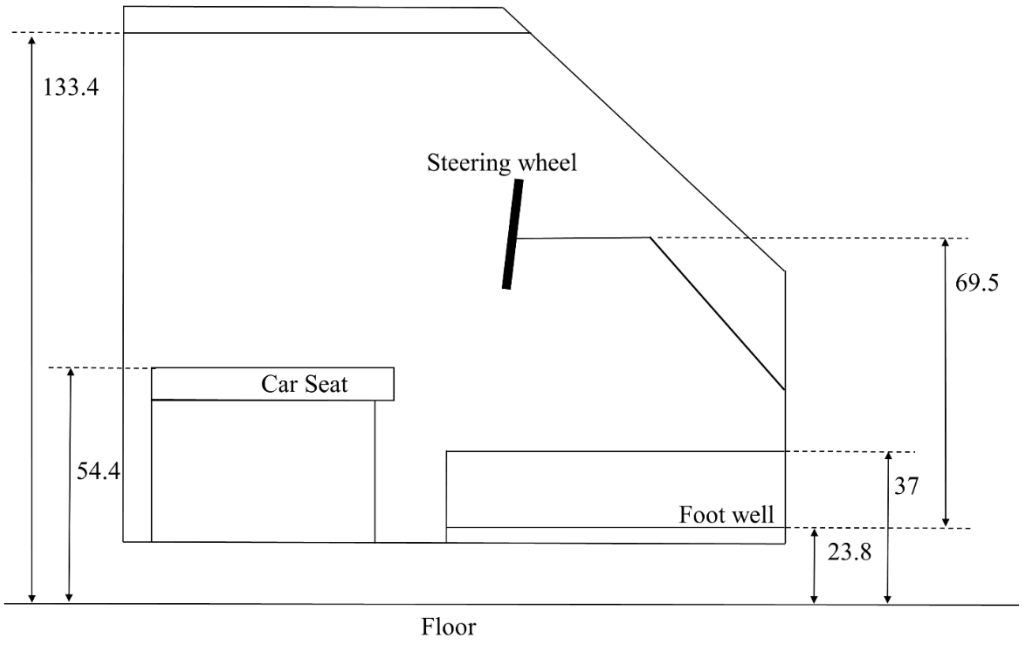

Figure 6.2 Measurements for the main body structure replicating an average-sized Australian car. All measurements are in cm.

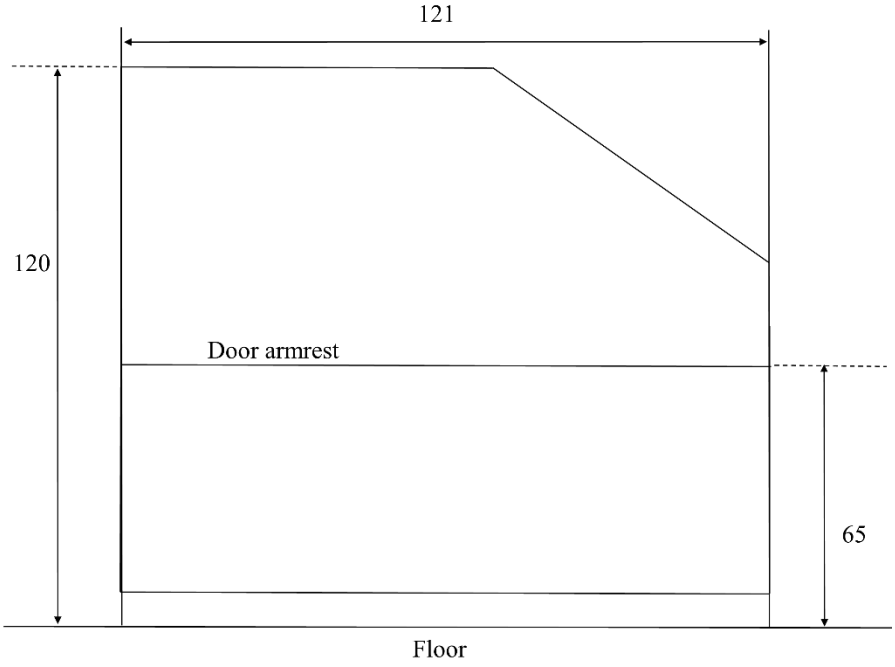

Figure 6.3 Measurements for the door structure replicating an average-sized Australian car. All measurements are in cm.

6.2.3 Musculoskeletal Modelling Simulation

The generic LFB OpenSim musculoskeletal model was linearly scaled to the anthropometry of each participant (Beaucage-Gauvreau et al., 2019) (Chapter 4). The LFB model was modified slightly, changing the muscle properties for the Latissimus Dorsi, External Obliques, Internal

Obliques, and Rectus Abdominus muscle fascicles from the Thelen class (Thelen, 2003) to the Millard class (Millard et al., 2013) to resolve discontinuities and minimum length issues. Inverse kinematics, inverse dynamics, static optimisation, and joint reaction analyses were performed in OpenSim (version 3.3), via custom MATLAB (version 2017b, Mathworks, Nattick, MA, USA) scripts, to estimate moments and joint reaction forces at the L4/L5 intervertebral joint (Delp et al., 2007).

6.2.4 Data processing

Kinematic and kinetic data were filtered using a low-pass bi-directional 2nd order Butterworth filter, cut-off frequency 6 Hz, in MATLAB (version 2017b, Mathworks, Nattick, MA, USA). For the car egress, analyses started when participants had completed swivelling and were sitting on the edge of the seat, with one foot placed on each force platform on the ground.

Outcome variables for each trial were: peak trunk angles, peak L4/L5 moments, and peak L4/L5 forces, for all three planes of motion, and peak resultant bracing force (for BATT trials only). The relationship between spinal loads and thigh bracing force during BATT was investigated by comparing trunk flexion angles at peak L4/L5 compression force between self-selected techniques and BATT for the three ADLs. Therefore, trunk flexion angle at peak L4/L5 compression was also an outcome variable for each trial. These outcome variables were averaged for each condition (self-selected or BATT) and each task, for each participant.

Lateral bending and axial rotation angles and moments, and medio-lateral shear forces, for one left-handed participant were inverted such that results were consistently described with respect to right and left hands.

6.2.5 Statistical Analyses

Paired t-tests were used to compare trunk kinematics, spine loads, and trunk flexion angles at peak L4/L5 compression force for the self-selected technique (no thigh bracing) to the BATT (SPSS v25, IBM, Illinois, USA) (α=0.05). The effect size of the technique on these outcome variables was calculated using Cohen's d, where d = 0.20-0.49, 0.50-0.79, and >0.80,

correspond to small, medium, and large effect size, respectively (Cohen, 1988). The peak bracing force was evaluated using descriptive statistics only.

6.3 Results

Twenty-three trials were discarded during post-processing (15 of 60 for the cupboard task; 0 for the weeding task; 8 for the car egress task). Two participants had to be discarded for the cupboard task only (12 trials total), due to marker visibility or data acquisition issues. Other discarded trials did not affect more than one trial per participant. The values for trunk angles, moments, and compression and AP shear forces at L4/L5, and resultant bracing force (for BATT trials only) over the trial duration for each task participant were averaged and are illustrated in Figure 6.4 to Figure 6.9.

The mean pulling force created by the magnet on the ferromagnetic plate for the weeding task for all participants was 48.8 ± 18.3 N.

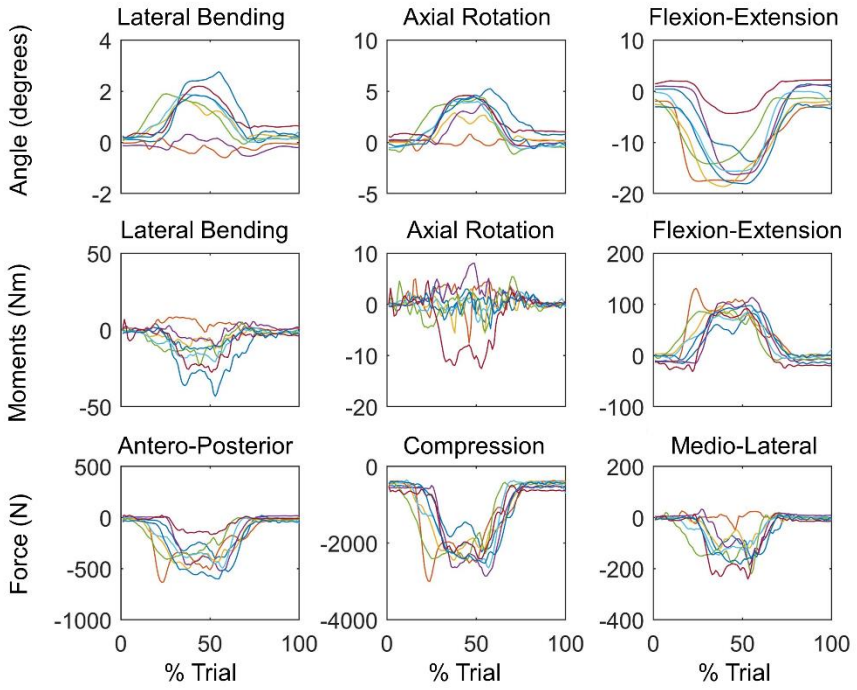

Figure 6.4 Mean three-dimensional angles (top), moments (middle), and forces (bottom) for each participant for the weeding task, using a self-selected technique.

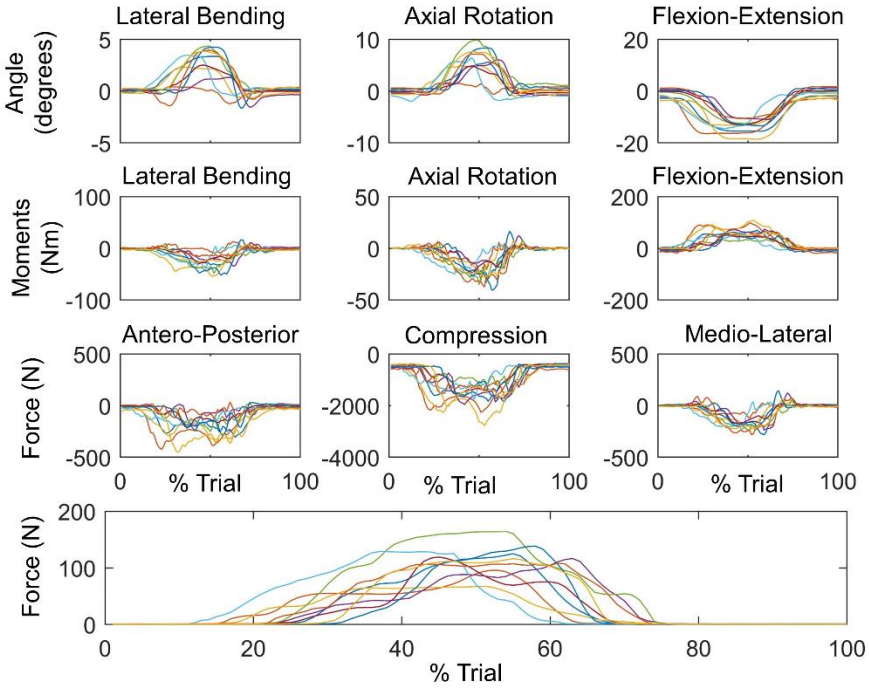

Figure 6.5 Mean three-dimensional angles (top row), moments (2nd row), and forces (3rd row) for each participant for the weeding task, using the BATT technique. The mean resultant bracing force for each participant is shown in the bottom row.

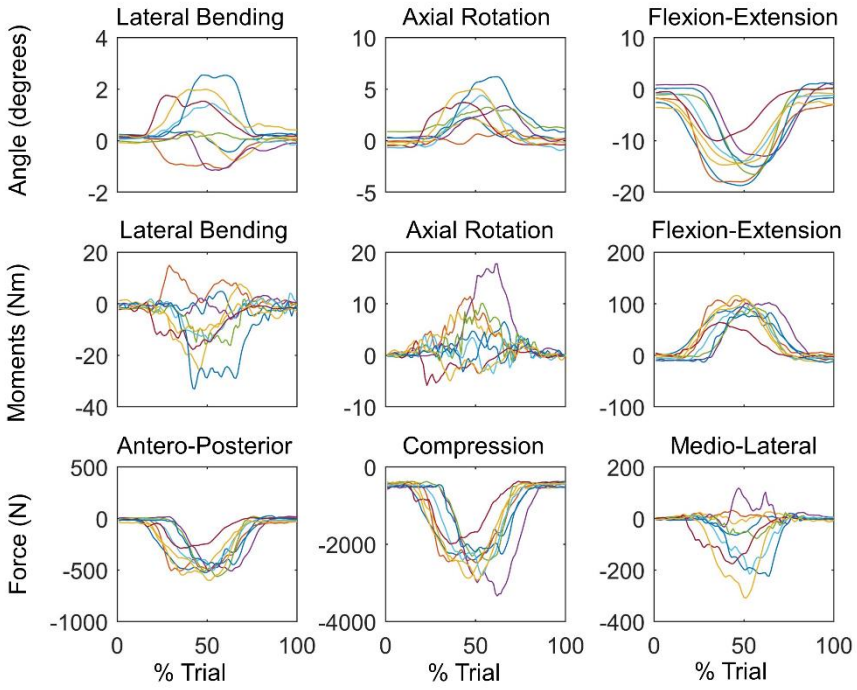

Figure 6.6 Mean three-dimensional angles (top), moments (middle), and forces (bottom) for each participant for the cupboard task, using a self-selected technique.

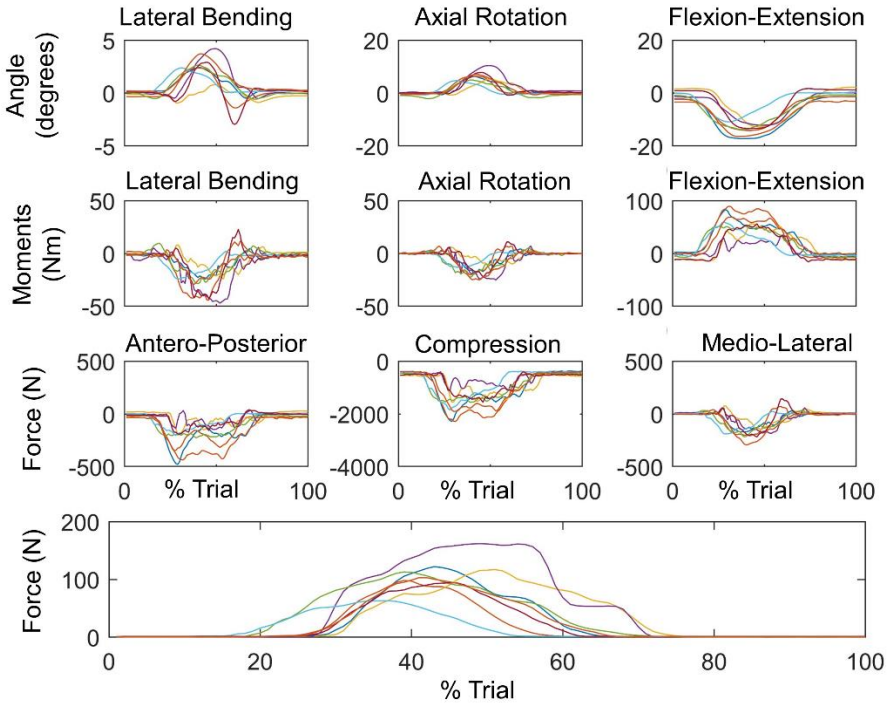

Figure 6.7 Mean three-dimensional angles (top row), moments (2nd row), and forces (3rd row) for each participant for the cupboard task, using the BATT technique. The mean resultant bracing force for each participant is shown in the bottom row.

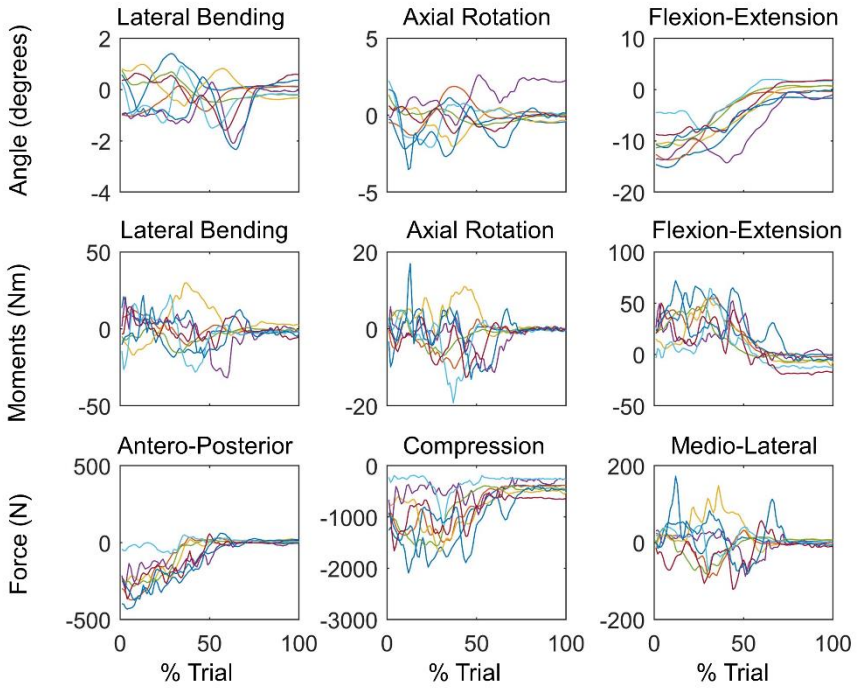

Figure 6.8 Mean three-dimensional angles (top), moments (middle), and forces (bottom) for each participant for the car egress task, using a self-selected technique.

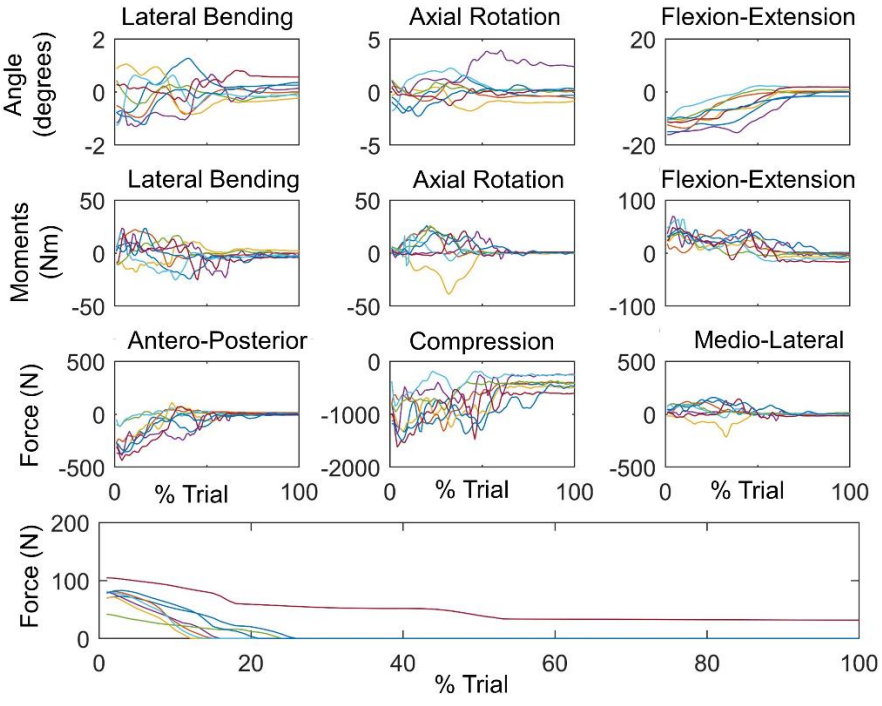

Figure 6.9 Mean three-dimensional angles (top row), moments (2nd row), and forces (3rd row) for each participant for the car egress task, using the BATT technique. The mean resultant bracing force for each participant is shown in the bottom row.

6.3.1 Trunk angles

Peak trunk flexion angles were similar for the self-selected and BATT techniques for all tasks (weeding: p=0.22, d=0.4; cupboard: p=0.22, d=0.4; car egress: p=0.488, d=0.2). The BATT significantly increased lateral bending (LB) and axial rotation (AR) angles towards the bracing leg for the weeding (LB: p<0.001, d=1.4; AR: p<0.001, d=1.0) and cupboard tasks (LB: p=0.03, d=1.1; AR: p=0.002, d=1.5), compared to the self-selected technique (Figure 6.10). The BATT reduced lateral bending towards the left hand (door support) for car egress (p=0.032, d=1.0), but had no significant effect on axial rotation angles.

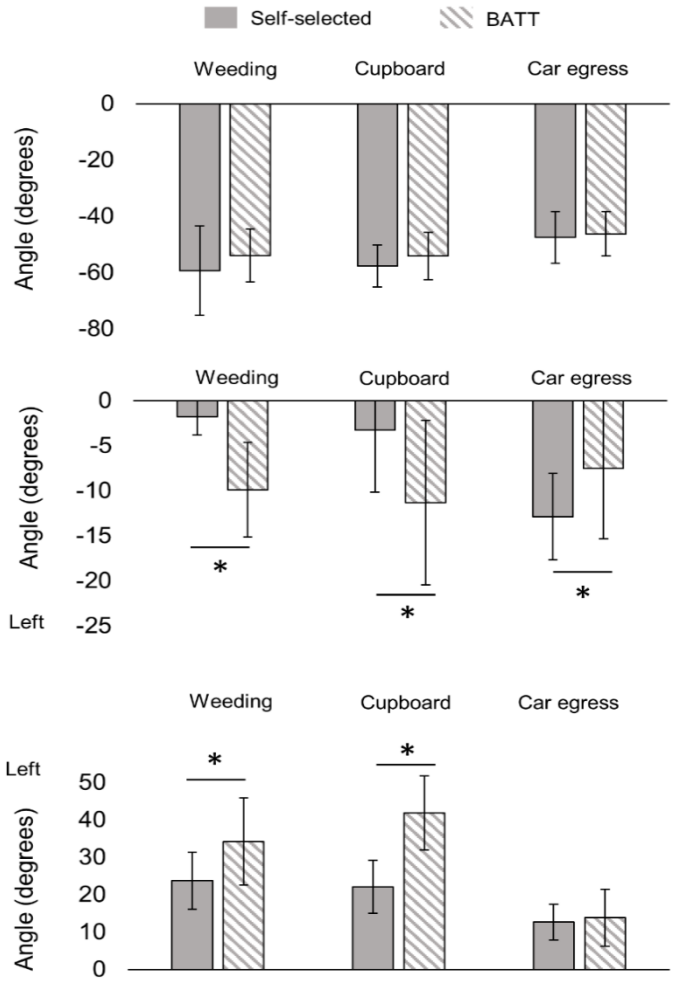

Figure 6.10 Peak trunk angles for flexion (top), lateral bending (middle), and axial rotation (bottom).

6.3.2 Moments at L4/L5

Extension moments were significantly reduced for the BATT for all tasks, compared to self-selected techniques (weeding: $p<0.001$, d=1.4; cupboard: $p<0.001$, d=1.5; car egress: $p=0.002$, d=0.9). The BATT significantly increased lateral bending and axial rotation moments for cupboard (LB: $p<0.001$, d=1.3; AR: $p<0.001$, d=1.7) and car egress (LB: $p=0.023$, d=0.9; AR: $p<0.001$, d=1.1) tasks compared to self-selected techniques, while it only significantly changed axial rotation moments for weeding ($p<0.001$, d=1.7) (Figure 6.11). The BATT changed the direction of the moment in axial rotation for the cupboard and car egress tasks, as well as the direction for the lateral bending moment for the car egress task.

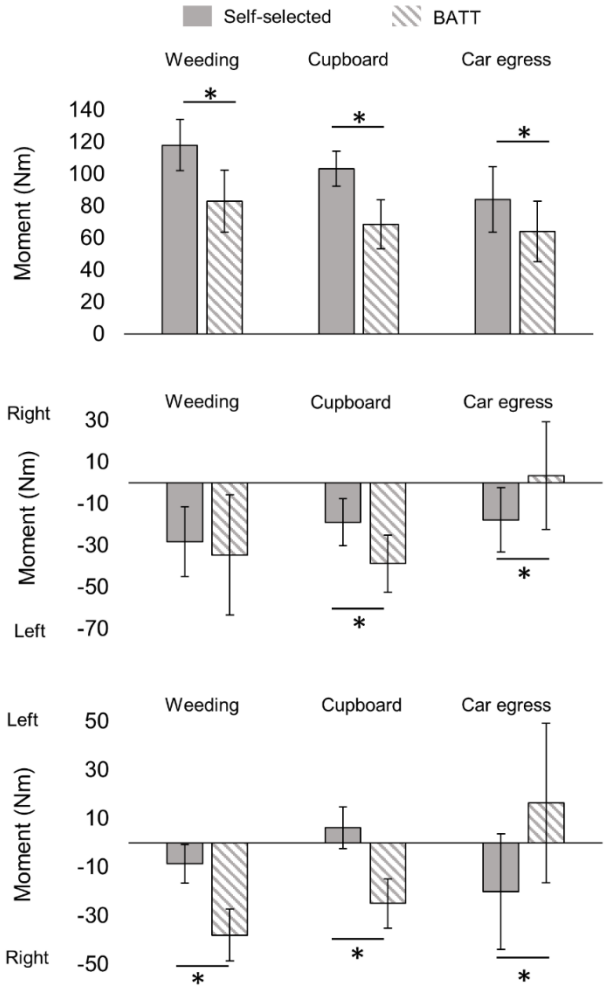

Figure 6.11 Peak L4/L5 moments estimated by the model for extension (top), lateral bending (middle), and axial rotation (bottom).

6.3.3 Forces at L4/L5

The BATT significantly reduced peak compression (weeding: $p<0.001$, d=1.5; cupboard: $p<0.001$, d=1.6; car egress: $p=0.001$, d=1.0) and AP shear forces (weeding: $p<0.001$, d=1.2; cupboard: $p<0.001$, d=1.5; car egress: $p=0.033$, d=0.8) for all tasks, compared to self-selected techniques. However, the medio-lateral shear forces only significantly increased for the BATT for the weeding tasks ($p=0.02$, d=1.1) (Figure 6.12), while it changed direction from left to right for car egress ($p=0.005$, d=1.3).

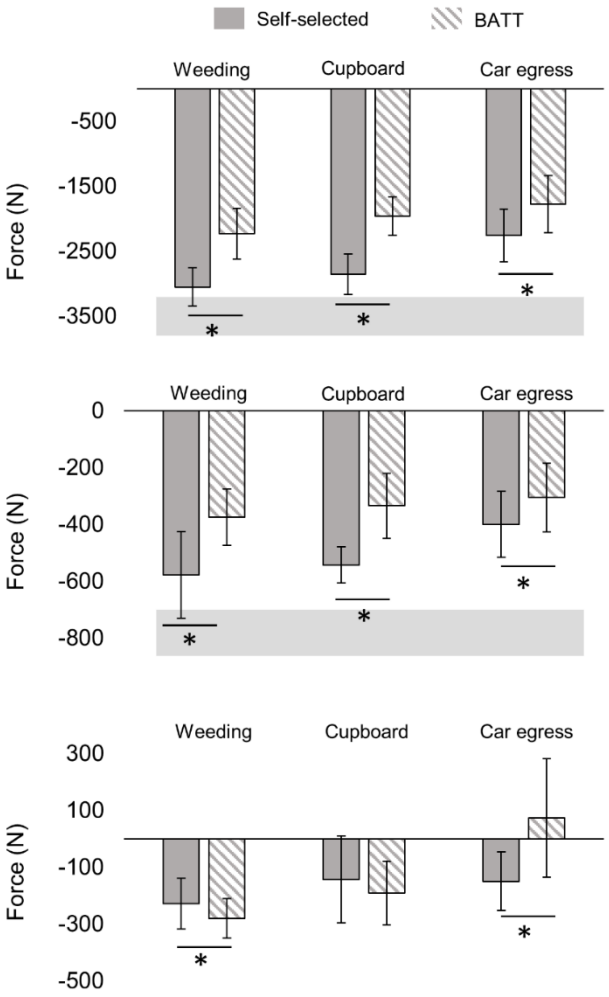

Figure 6.12 Peak model estimates for compression (top), anterio-posterior shear forces (middle), and medio-lateral shear forces (bottom). The shaded areas in the top and middle bar graphs correspond to the injury thresholds for compression (>3400N) and shear (>700N) forces, respectively.

6.3.4 Flexion at peak compression angle

Trunk flexion angles *at peak compression forces* were significantly lower for the BATT compared to a self-selected technique for the cupboard task (p=0.01, d=1.1), but not weeding or car egress (Figure 6.13).

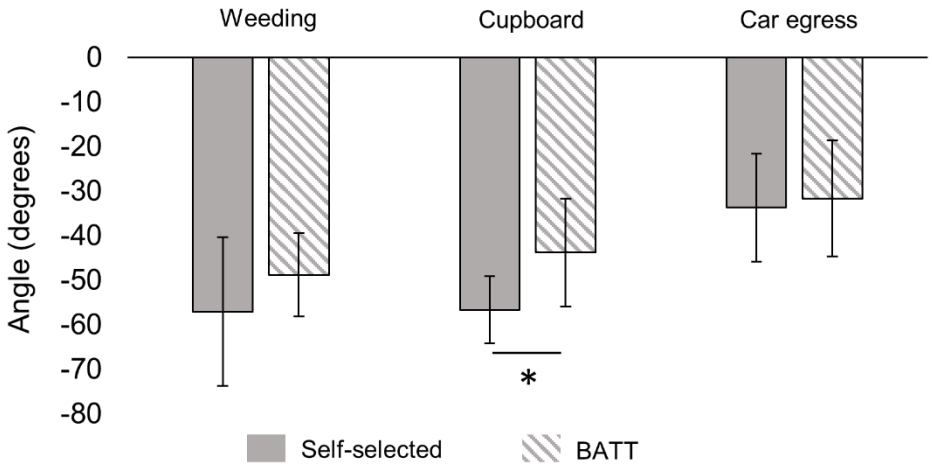

Figure 6.13 Trunk flexion angles at peak L4/L5 compression forces for the three activities of daily living for the self-selected techniques and the BATT.

6.3.5 Bracing Force

Mean peak resultant bracing forces for the three tasks were 125.3 ± 23.6 N for weeding, 119.7 ± 24.4 N for cupboard, and 113.3 ± 14.9 N for car egress (Figure 6.14), with a large variation in bracing force between participants for all tasks.

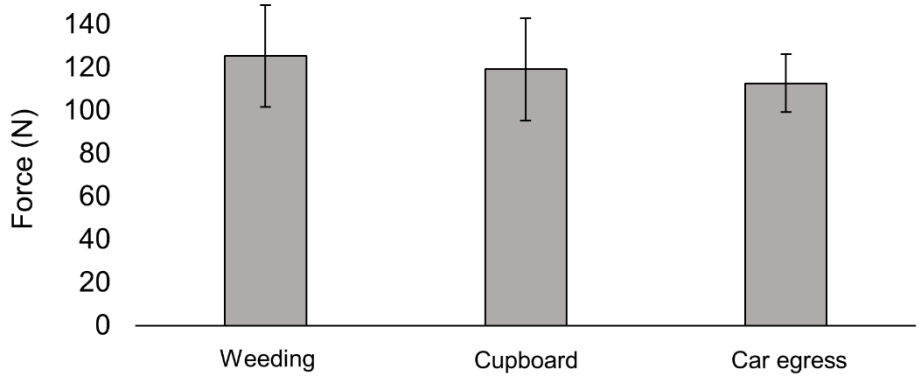

Figure 6.14 Peak resultant bracing force for weeding, cupboard and car egress tasks for the BATT condition.

6.4 Discussion

The aim of this study was to apply the BATT to three common ADLs (reaching for objects in low cupboards, weeding, and car egress) and to evaluate its effect on trunk kinematics and L4/L5 joint loads (moments and forces about three axes of motion) compared to self-selected techniques. The BATT reduced L4/L5 extension moments, and L4/L5 compression and AP shear forces, compared to self-selected methods.

Material handling activities that include flexion, axial rotation, lifting, carrying, and pulling are associated with a higher risk of LBP (Heneweer et al., 2011). In addition, repetitive loading of the lower back can lead to fatigue failure of spinal structures (e.g. facet joints, endplates, intervertebral disc, ligaments) at loads that are substantially lower than the ultimate strength of these structures, and well within the range of forces and repetitions experienced in ADLs (Adams et al., 2006, Brinckmann et al., 1988, Hansson et al., 1987). Spinal loads experienced during various lifting tasks have been studied extensively in the biomechanics literature (Kingma et al., 2016, Kingma et al., 2010, Kingma and van Dieen, 2004, Kingma et al., 1998, Potvin et al., 1991). Numerous studies have also focused on occupations such as nursing and automotive manufacturing, in which workers are exposed to biomechanical risk factors associated with the development of LBP (Smedley et al., 1995, Eriksen et al., 2004, Norman et al., 1998, Frazer et al., 2003). However, several activities of daily living require motions associated with LBP risk factors and they have not been investigated in the biomechanics literature, with respect to quantifying spinal loads.

The three tasks evaluated in this study were chosen because they include some of the biomechanical risk factors for LBP and involve movements beyond lifting which was studied in Chapter 5. All three tasks (weeding, cupboard, and car egress) required large trunk flexion, an important biomechanical risk factor associated with LBP. The weeding task also included the added risk factor associated with pulling and typically involves prolonged forward bending, increasing exposure to these two risk factors. The cupboard task involved reaching for an object in a confined space, thus restricting motion when picking up an object. The selected ADLs also

cover a range of activities that individuals with various functional disabilities could perform; weeding would likely not be performed by individuals with debilitating LBP, while reaching for objects in low cupboards and driving are more integral to everyday living. The trunk range of motion for the cupboard and weeding tasks is similar to many other ADLs that require frequent forward bending, such as making a bed, emptying a dishwasher, and vacuuming. Alternatively, the *two-legs out* car egress technique evaluated in this study resembles the sit-to-stand motion, a biomechanically demanding ADL (Hughes and Schenkman, 1996) known to be problematic for older individuals and those with weakened muscles or diseased joints (Wretenberg and Arborelius, 1994). However, studies on sit-to-stand have mainly focused on lower limbs (Caruthers et al., 2016, Doorenbosch et al., 1994, Goulart and Valls-Solé, 1999, Mak et al., 2003), despite the potentially large spinal loads due the momentum of the torso being used to rise up and forward, while keeping both feet on the ground. Consequently, the findings of this study could be generalised to other ADLs with comparable features. The tasks selected were limited to one-handed tasks so that the BATT could be used. External contact for the non-dominant hand was limited to a single point so that it could be measured with existing instrumentation in the laboratory. In addition, the trunk range of motion for these tasks had to be within the range for which the model had been validated in the study in Chapter 4 (flexion<65°, axial rotation<35°, lateral bending<25°).

The BATT substantially reduced compression (27-45%), AP shear forces (31-62%), and extension moments (31-51%) at L4/L5 for all three tasks, compared to a self-selected technique, therefore reducing overall spine loading. Self-selected techniques typically adopted by participants for the weeding and cupboard tasks corresponded closely either to a one-handed stoop (straight legs with trunk flexion at the hips) or one-handed squat technique (flexed knee and straight back) lifting techniques (Figure 5.1). Similar reductions were obtained for extension moments (53-61%) and compression forces (52-63%), when the BATT was compared to one-handed stoop and squat lifting a 2 kg mass (Chapter 5). However, the reductions obtained in this study were higher than previously observed for lifting a pen using a technique similar to the

BATT, where the hand support on the thigh reduced extension moment and compression forces at L5/S1 by 4-37% and 4-14%, respectively, compared to one-handed stoop and squat lifting (Kingma et al., 2016). The reduction in AP shear force for cupboard and weeding tasks was less that the reduction previously observed for a 2 kg lifting task (87-137%) (Chapter 5) but greater than for pen lifting (2-10%) (Kingma et al., 2016). The smaller reductions for AP shear forces compared to Chapter 5 could be related to the larger trunk flexion angles required for the weeding and cupboard tasks, as the box was 23 cm from ground in Chapter 5, while cupboard and weeding tasks were approximately 10 cm from the ground. It is difficult to fully assess the disparity with the results for pencil lifting (Kingma et al., 2016), but possible factors include modelling differences between the studies (EMG-driven, L5/S1 vs L4/L5), specific task instructions for the lifting tasks, different participants, and different ability to use the thigh bracing force.

The compression and AP shear forces experienced in the spine for the three tasks evaluated in this study were below the injury thresholds for heavy lifting; 3400 N for compression forces (Brinckmann et al., 1989) and 700-100 N for AP shear forces (Gallagher and Marras, 2012) (Figure 6.12). The mean peak compression forces (2850-3047 N) and extension moments (103-117 Nm) experienced during the cupboard and weeding tasks for the self-selected techniques were similar to those experienced during lifting tasks for light objects (pencil: 2405-2495 N, 83-105 Nm (Kingma et al., 2016); 2 kg: 2805-3049 N, 105-112 Nm in Chapter 5), using similar techniques. The mean peak AP shear forces for cupboard and weeding tasks (542-577 N) were also similar to those obtained for 2 kg lifting tasks with the same model (434-582 N), but lower than those found for pen lifting (745-750 N), for similar lifting techniques (Kingma et al., 2016). However, absolute shear force estimates are especially sensitive to modelling parameters, thus limiting comparison with other studies using different models (Kingma et al., 2016).

The BATT increased trunk asymmetry for the cupboard and weeding tasks. These findings were expected as the BATT inherently causes lateral bending towards the bracing leg, while the self-selected technique for these tasks was symmetrical in the sagittal plane, with trunk angles near neutral position. The increased axial rotation toward the bracing leg for these two tasks was also

expected due to the bracing action on the thigh. The large trunk axial rotation in the self-selected techniques for the weeding and cupboard tasks is caused by the dominant hand reaching action. During car egress, lateral bending trunk angle (towards the bracing leg) was lower for the BATT due to the addition of the thigh support with the right hand. Although axial rotation has been identified as a risk factor for LBP (Hoogendoorn et al., 2000), there is no evidence in the literature that the asymmetry resulting from the BATT is linked to injuries when accompanied by support provided by a hand support on the thigh. Further studies are needed to determine if asymmetry in the presence of support still presents a risk factor for LBP injuries.

The relationship between spinal loads and bracing force during BATT was investigated by comparing trunk flexion angles at peak L4/L5 compression force between self-selected techniques and BATT for the three ADLs. This comparison point differs from that selected in Chapter 4, in which the L4/L5 compression force at trunk peak flexion was used. This was because trunk motion followed a predictable profile for the lifting tasks, with two reasonably well defined profiles for L4/5 compression for unsupported and BATT lifting tasks (Chapter 5, Figure 5.8). In contrast, trunk angles did not follow a repeatable profile for unsupported and BATT techniques between participants for the ADLs studied herein; instead, peak L4/L5 compression force was selected as a comparator variable. Based on the results from Chapter 5, it was expected that the trunk flexion angle at peak L4/L5 compression force would be lower for the BATT than for the self-selected technique; however, this was only the case for the cupboard task. The lack of a consistent and significant effect of BATT on trunk flexion in the other two tasks is likely due to the large variability in the self-selected techniques adopted by the participants, ranging from a full squat (pelvis below the flexed knee) to stoop techniques. Conversely, the presence of the cupboard structure in the cupboard task likely provided a more constrained task volume, thus limiting the variability of strategies used to accomplish the task. This may explain why a significant reduction in trunk angle between self-selected and BATT was only observed for the cupboard task. The mean peak bracing forces for the three ADLs were between 113-125 N, similar to the 117-132 N range observed for lifting tasks (2 kg and 10 kg) (Chapter 5). To evaluate

the relationship between the BATT and spine loading in more detail, future studies should prescribe the non-braced technique (rather than allowing self-selected) and provide additional training sessions for BATT.

The residual forces at the pelvis when participants were in contact with the seat (up to 600 N) were larger than the thresholds recommended for gait (residual forces <5% of peak net external forces and residual forces < 1% height of centre of mass × net external force), but were within the acceptable range when participants were standing (Hicks et al., 2015). These residuals are actuators added to the pelvis rigid body (ground body in this model) during simulations to account for discrepancies between the model, measured motions, and forces; in other words, these residuals ensure that Newton's 2nd law is satisfied throughout the analysis. It was hypothesised that the large residuals at the pelvis during the simulations were principally caused by the lack of inputs to represent the pelvis-car seat interactions (these forces and moments were not measured) rather than other potential issues, such as unsuitable kinematics or inertial properties. To determine if including the seat forces in the simulations reduced the residual loads, and most importantly, whether it affected the L4/L5 joint load estimates, a force platform (ACG-O, AMTI, USA) was incorporated into the car structure, underneath the seat (Figure 6.15). The time delay created by the viscoelastic properties of the car seat was measured by placing a load cell (MC3A-1000, AMTI, USA) on the seat and applying a downward force with a hand. The difference in peak force timing on the load cell and force platform was approximately 0.4 s.

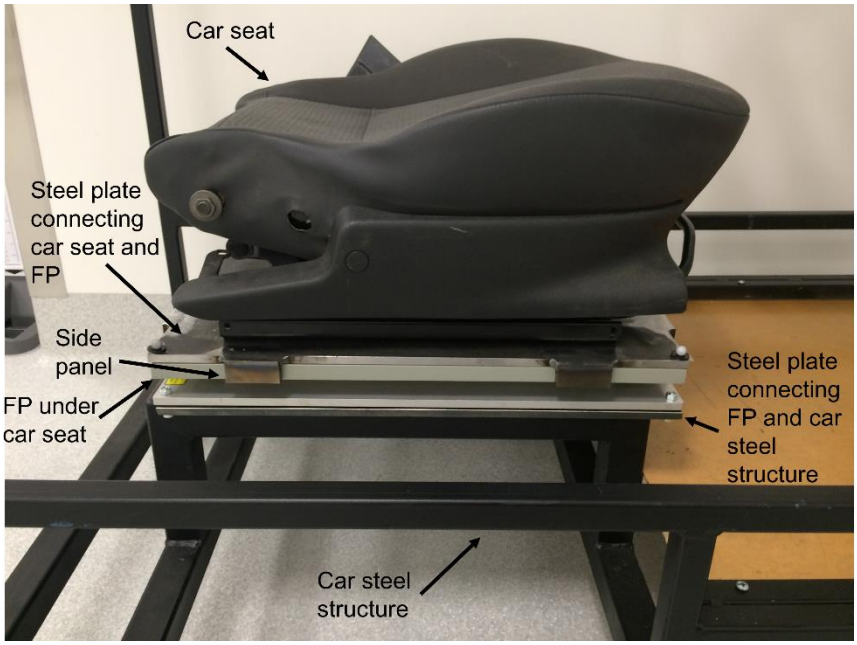

Figure 6.15 Main body structure for the car apparatus with a force platform (FP) placed under the car seat to measure the seat-participant interactions. The FP was rigidly attached to the car steel structure via a steel plate at the bottom. Another steel plate was placed on top of the FP, onto which the car seat was rigidly attached. This steel plate was held in place on top of the FP using small side panels, on all side of the FP.

One participant performed a sit-to-stand motion from the car seat using the same car egress protocol previously described, without bracing on the door frame or thigh. These data were used for three simulations with the following conditions: 1) no seat forces (corresponding to the experimental set-up in this study); 2) seat forces, not including viscoelastic properties of seat; and, 3) seat forces including viscoelastic properties (with time delay of 0.4 s). Condition 1 confirmed that the pelvis residual loads closely matched the seat forces (Figure 6.16, top). The residuals at the pelvis were greatly affected by the conditions of the simulations, with condition 3 substantially reducing them to almost within the recommended thresholds (Figure 6.16, middle). The peak pelvis residuals for condition 3 (approximately 100 N) were still higher than the recommended thresholds, but in line with the results reported by Caruthers et al. (2016), in a study on sit-to stand motion where seat forces were not measured or incorporated in the simulations with a similar OpenSim model. Despite the large variation in the pelvis residuals between the conditions, the L4/L5 load estimates were unaffected (Figure 6.16, bottom) because the magnitudes of the residuals adjusted to achieve dynamic consistency between the motion and

the applied forces for each simulation condition. This confirms the validity of model estimates for the car egress task, even when the seat forces are not measured.

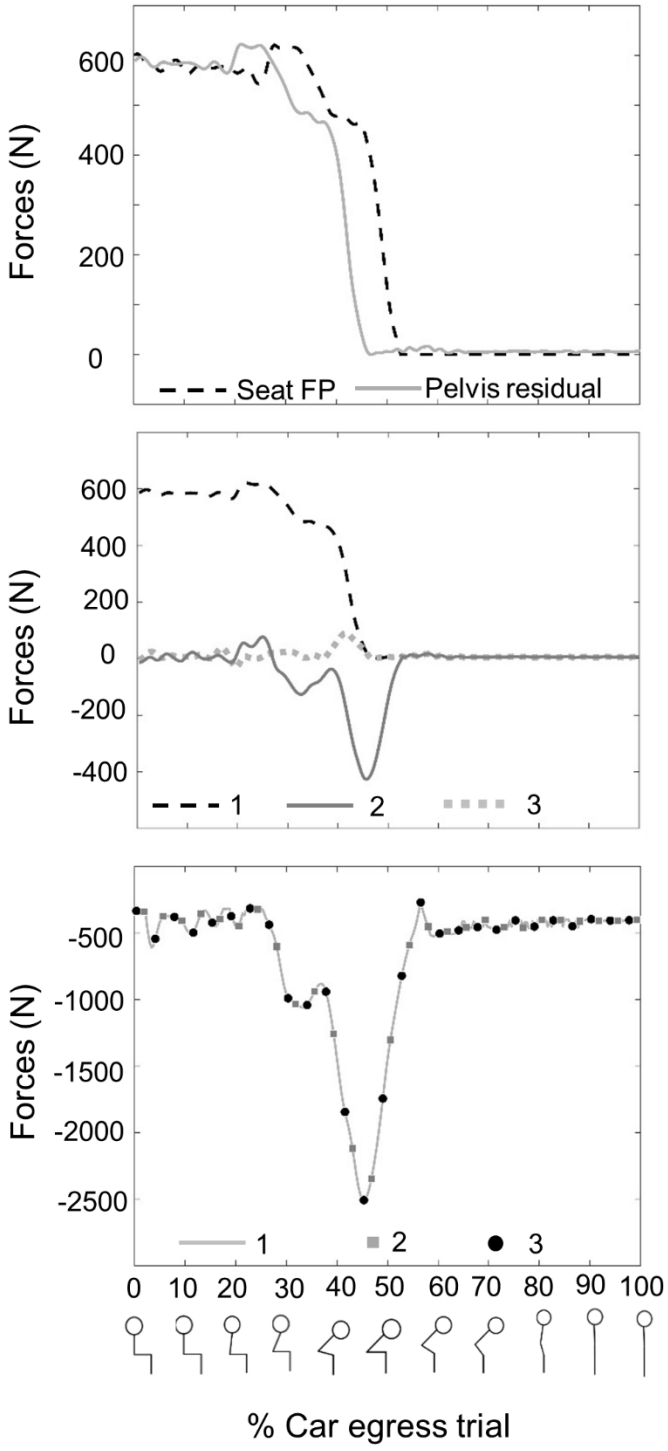

Figure 6.16 Top: Vertical component of the forces measured by the force platform (FP) placed under the car seat and vertical pelvis residual for condition 1; Middle: Vertical pelvis residuals for the conditions 1, 2, and 3; Bottom: L4/L5 compression forces estimated by the model for conditions 1, 2, and 3.

Car egress is a complex movement for motion analysis and simulation as almost all body segments are involved in the motion. For this reason, this study evaluated the *two-legs out* car egress technique despite the *one-leg first* strategy being more often used (Chateauroux and Wang, 2010). The *one-leg first* technique requires greater trunk motion, especially trunk axial rotation, which is challenging to properly measure using motion capture systems. Pilot testing included the *one-leg first* car egress technique with support from the dash (see Section 3.3.3), but the large shoulder motion and trunk axial rotation involved in this movement meant that the current LFB model was not able to simulate this task. In addition, only the hand-door and hand-thigh interactions were measured in this study, thus limiting the car egress motion to these two supports on the car frame. Consequently, the "self-selected" car egress motion simulation may not have been completely natural for some participants. Future work should include additional car egress techniques that are less constrained and allow hand interactions with other components of the car frame (e.g. steering wheel, seat).

There are also limitations associated with the model used in this study. The LFB model is validated for a limited range of lifting tasks (Beaucage-Gauvreau et al., 2019). However, the trunk range of motion for the three ADLs chosen for this study was within the range of motion for which the model has been evaluated. In addition, musculoskeletal models are currently most valuable to evaluate relative changes between conditions rather than absolute magnitudes of spine loading; this study evaluated within-participant changes.

The small cohort of ten young healthy males recruited for this study did not represent the LBP population that may most benefit from the BATT technique to perform common ADLs. Performing a similar study with a larger cohort and participants with LBP may reveal a more obvious effect of the BATT on spine loading. This study also focused on the peak values for each outcome variable, regardless of timing, which is a common method in similar studies. While there was a well-defined peak for compression and AP shear forces, trunk flexion angle, and extension moments during the trials, axial rotation and lateral bending angles and moments typically had series of maxima of similar magnitude throughout the trial, especially for the BATT. A more

comprehensive data analysis evaluating the varying spinal loads with respect to time may provide data appropriate to perform a risk assessment of these tasks (Callaghan and McGill, 2001).

Musculoskeletal models are often used to study gait and lifting, but they are rarely used to evaluate other tasks, despite the high risk of LBP associated with many ADLs due to frequent forward bending and pulling. To the best of the authors' knowledge, this is the first biomechanical study to evaluate spinal loads and trunk kinematics during common ADLs. The BATT was applied to these three tasks, and it substantially reduced L4/L5 extension moments, and L4/L5 compression and AP shear forces, compared to self-selected methods.

Chapter 7 General Discussion

7.1 Overview

Three studies were undertaken to address the aims of this thesis. In study 1, a novel full-body model with a detailed lumbar spine was developed and validated to estimate L4/L5 spinal loads for symmetrical and asymmetrical lifting tasks. In study 2, spinal loads for the BATT were compared to those of common unsupported one-handed and two-handed lifting techniques in healthy individuals and individuals with LBP. In study 3, the BATT was applied to three common ADLs simulated in the laboratory to compare spinal loads between unsupported self-selected techniques and BATT. Collectively, the findings from these studies demonstrated that the BATT substantially reduced spinal loading, compared to unsupported techniques, both for lifting tasks and other ADLs.

7.2 Summary of outcomes and findings

1. A new full-body model OpenSim was developed and validated to evaluate changes in lumbar loading for symmetrical and asymmetrical lifting tasks.
2. A new method to include the forces created by the box during lifting tasks was developed by incorporating the mass properties of the box with those of the hands.
3. Bracing the hand on the thigh during 2 kg and 10 kg lifts reduced trunk flexion angles and L4/L5 extension moments, and compression and antero-posterior shear forces, compared to unsupported lifting techniques, for healthy individuals and individuals with LBP aged 30-70 years old.
4. Bracing the hand on the thigh during lifting tasks introduced higher asymmetrical trunk motions and moments, in LBP and healthy individuals.
5. A wide variation in thigh bracing force was observed across participants; the bracing force had an effect on the timing of the peak compression force at L4/L5 during the lifting trial for some participants.
6. Bracing the hand on the thigh reduced L4/L5 extension moments, and compression and antero-posterior shear forces in healthy young males, compared to unsupported self-selected

techniques for three common ADLs simulated in the laboratory: weeding (gardening), reaching for objects in low cupboards, and car egress.

7.3 Lifting Full-Body Model

In the pursuit of understanding spinal loading and its link to LBP, musculoskeletal models are used to estimate joint and muscle loads, because direct measurement of these variables is limited to invasive *in vivo* techniques. Musculoskeletal models play an important role in basic science investigations, and have been used in a wide range of applications such as informing surgical decisions via simulations (Steele et al., 2010), or identifying motion patterns that could reduce injury risk in sporting activities (Reinbolt et al., 2011).

The LFB model described in this thesis has several unique features which make it particularly suited for the evaluation of lumbar loads during tasks that involve forward bending and lifting. Although previous spine models with a highly detailed lumbar spine (Christophy et al., 2012, de Zee et al., 2007, Bruno et al., 2015, Shirazi-Adl, 2006) have significantly contributed to detailed knowledge of spinal mechanics, they often lack legs and arms. A full-body model is essential for studies of real-life situations in which interactions with external objects or between non-adjacent body segments (e.g. hand and thigh), and a wider range of arm and leg movements, need to be simulated. Notably, the interaction of the bracing hand with the ipsilateral thigh could be included during simulations for the BATT with the LFB model. This bracing force was applied to the bracing hand and ipsilateral thigh (action-reaction forces), with a changing orientation and magnitude at each time frame of the lifting trial, as measured by the load cell placed on the thigh. Therefore, the LFB model represents an important step forward from previous validated OpenSim models that do not comprise full legs or arms, or cannot analyse lifting tasks from experimental data collected in the laboratory (Bruno et al., 2015, Senteler et al., 2015, Actis et al., 2018).

The development of the methods to include the box in the hands for the lifting tasks, especially for two-handed lifting techniques, highlighted the paucity of spine and lifting related research in OpenSim. The main difficulty associated with simulating lifting tasks is the additional box rigid

body connecting to the model for a finite time period during the trial. A previous study examined shoulder muscle co-activation during one-handed lifts by including an additional box rigid body connected to the hand body (Blache et al., 2015a, Blache et al., 2015b). Although this method is feasible for one-handed lifts, two-handed lifts pose the additional challenge of connecting the box to both hands, thus violating the closed loop (trunk, arms, box) modelling assumption in OpenSim. Instead, a novel method attributing the box mass properties to the hands was developed for the simulations in this thesis. This approach incorporated the linear and rotational inertial properties of the box and produced small pelvis residuals during the simulations (Chapter 3), thus allowing for evaluation of spinal loads and trunk kinematics for one-handed and two-handed lifting techniques.

The LFB model was validated extensively in this thesis, using a range of techniques used in previous studies, including direct comparison with myoelectric signals and indirect comparison with *in vivo* IDP and VBR measurements. In addition, parameters of the model were validated by testing various maximum muscle stress values to evaluate the sensitivity of the compression force estimates to this assumption (Chapter 4) (Bruno et al., 2015) and by comparing the L5/S1 maximum isometric moment generated by the model to experimental data (Raabe and Chaudhari, 2016). A strength of the validation is that a *direct* comparison was made between the model and experimental EMG with the same participants. Although experimental EMG measurements have inherent limitations associated with electrode placement and skin preparation, this *direct* comparison is an improvement over previous studies that used *indirect* comparison (Bruno et al., 2015, Han et al., 2012), comparing the estimated muscle activations by the model to those reported in the literature, with different participants. In addition, a cross-correlation analysis was used to quantitatively evaluate the similarity of EMG with model estimates, improving over a previous qualitative evaluation (Raabe and Chaudhari, 2016). Although VBR studies have reported measurements of *in vivo* intervertebral compression forces in a small patient cohort, the accuracy and reliability of these absolute values must be treated with caution due to load-sharing with the instrumentation and remaining bone, and high variability in surgical procedures and

anthropometry between patients (Dreischarf et al., 2015, Rohlmann et al., 2014a). Nevertheless, they provide an indication on the spine loading trends during lifting tasks for indirect comparison with model estimates. Comparison of model estimates to *in vivo* IDP measurements is another indirect joint loading validation technique; these pressures are correlated with intervertebral compression forces. However, the specific relationship between IDP and compression forces remains unknown due to the heterogeneous composition and the non-uniform load transfer within the disc (Dreischarf et al., 2013) and the intersegmental flexion angle (Ghezelbash et al., 2016). A range of correction factors values (0.55-0.77) (Nachemson, 1960, Brinckmann and Grootenboer, 1991, Bruno et al., 2015) or regression approach (Ghezelbash et al., 2016) have been used to estimate compression forces based on *in vivo* IDP measurements and reported disc cross-sectional area. Similarly to the VBR measurements, this validation technique has limitations related to the validity of the absolute values of the compression force; however it also provides valuable information on spine loading for different postures and tasks. In summary, the LFB model was validated using numerous techniques to moderate the limitations associated with each technique as direct comparison with *in vivo* data is not possible. Overall, it was demonstrated that the LFB was suitable to evaluate changes in lumbar spine loading during lifting (Chapter 4).

The LFB model was used to evaluate three ADLs that included biomechanical risk factors associated with LBP and involved movements beyond lifting (Chapter 6). The simulations for the ADLs were more straightforward than those for lifting as they did not require modifications of the hand properties; the interactions of the hand with the magnet (weeding) and car frame were modelled as external forces acting on the model. These forces were measured using a load cell with a custom hand interface. For car egress, the hand interaction was limited to one location (the door frame), due to the number of sensors available and to limit variability in techniques between participants. Although the kinematics of car egress has been investigated previously, spinal joint loading has not been evaluated. The high residuals at the pelvis obtained during car egress simulations required further investigation as they were much higher than the recommended thresholds (Hicks et al., 2015). Integrating a force place under the car seat substantially reduced

the residuals, but had no effect on spinal loads when using static optimisation in OpenSim. This testing revealed that the residuals corresponded to the interaction between the chair and participant. Consequently, the high values were not inherently problematic, but rather modelled the forces not accounted for in the simulations. These results supported the hypotheses of Caruthers et al. (2016) for sit-to-stand motions, in which large residuals at the pelvis were observed because no force platform was placed under the seat in that study.

The advantage of the LFB model over simple static models is that it incorporates the dynamic properties of lifting tasks, as they result in higher intervertebral forces (Lavender et al., 1999). Static models only evaluate injury risks as a function of the size and position of the load in the hands with respect to the intervertebral lumbar joints. Moreover, the individual contribution of each muscle to the reaction moment can be examined with this model. Although the high level of complexity of the LFB model (six intervertebral lumbar joints and 238 muscles for the trunk) was not fully exploited in this thesis as the individual trunk muscle activations were not investigated, the LFB model allows for participant-specific modifications and evaluations. For example, manipulation of individual muscle properties (maximum isometric force) or lumbar joint kinematics to reflect asymmetric atrophy in the multifidus (Hides et al., 2008, Hodges et al., 2006, Barker et al., 2004) or disturbed spine kinematics (Sihvonen et al., 1997) for individuals with LBP.

In addition to including legs and arms, incorporating dynamic properties of lifting, and having a highly-detailed lumbar spine, a considerable advantage of the LFB model is that it is open source. Although previously developed spine models have made significant contributions to the field of simulation technology for the lumbar spine (McGill and Norman, 1986, Kingma and van Dieen, 2004, Bassani et al., 2017), these models are generally unavailable to other groups (Delp et al., 2007). Many of these models were developed on proprietary software; thus limiting the implementation of new techniques for the broad biomechanical community outside the laboratory (Delp et al., 2007). The AnyBody modelling platform (Damsgaard et al., 2006) uses the same multibody dynamic approach as OpenSim and provides an alternative to proprietary models.

However, it requires an expensive license restricting its availability for technical groups with limited financial resources. The LFB model developed on the OpenSim modelling platform is freely accessible to researchers worldwide, providing the ability to reproduce simulations and to build on existing knowledge.

7.4 Effect of thigh bracing

Overloading of the back structures may result in tissue damage and subsequent back pain (McGill, 2007, Abouhossein et al., 2011). Trunk muscles, ligaments, and other spinal structures are stressed during lifting and bending as they support trunk posture and facilitate movements. Cumulative loading of these structures over time has been identified as an additional risk factor for the development of back pain (Marras et al., 2014, Norman et al., 1998). The majority of the work relating to injury risks and injury thresholds for spinal structures was performed between 1980 and 2005. Although this literature is not recent, it is still considered relevant for biomechanical injury risk factors for low back pain (Marras et al., 2014, McGill, 2007).

The bracing force on the thigh substantially reduced L4/L5 extension moments, and L4/L5 compression and shear forces, compared to unsupported techniques (Chapters 5 and 6), thus reducing the risk of low back injury related to overloading. Biomechanically, these reductions are explained by the spine-sparing mechanism of the BATT, where the hand on the thigh partially redirects forces to the knee, thus bypassing the spine linkage. Therefore, the bracing action reduces the external moments in the lower spine, subsequently also reducing compression and shear forces. This spine-sparing principle also applies to forward bending and lifting techniques where an external object is used to provide support to the trunk (Kingma and van Dieen, 2004, Marras and Davis, 1998, Cook et al., 1990). However, the BATT further reduced spinal loads, likely due to the larger trunk flexion angles generally associated with bracing on an external object rather than the thigh (Chapter 5). The BATT is an effective technique for repeated lifting light-to-moderate objects from floor level as it reduced peak and cumulative spine loading (Chapter 5).

7.4.1 Trunk Kinematics

The BATT significantly reduced trunk flexion when compared to one-handed and two-handed stoop lifting techniques; both stoop lifts had large trunk flexion angles near the end of range (Chapter 5). Avoiding full spine flexion minimises the risk of injury on ligaments and other passive tissues, as large trunk flexion causes ligamentous creep (Adams et al., 1987, McGill and Brown, 1992) and a redistribution of the nucleus within the annulus that can lead to disc herniation (Callaghan and McGill, 2001). Prolonged trunk flexion also modifies the neurological response of the back extensors (Jackson et al., 2001) and reduces the ability of the spine to withstand compressive loads (Adams et al., 1994, Callaghan and McGill, 2001). Although trunk flexion angles for the BATT were larger than those for the squat, they were not at the end of range of motion of the spine, and adopted the same neutral straight back posture with hip flexion, thus recruiting back extensor muscles instead of excessively loading the ligaments (McGill, 2007). While many individuals adhere to the general instructions of bending the knees and keeping the back straight while lifting (essentially emulating the spine posture of weight lifters), they should also consider the spine-conserving benefits of the BATT, as it reduces the risk of ligamentous damage (ligaments remain unstrained) and disc herniation associated with full flexion. The BATT could be preferable to squat for lifting light-to-moderate objects from the floor because squats are physiological demanding (Hagen et al., 1993, Welbergen et al., 1991, Kumar, 1984).

The BATT generally increased lateral bending and axial rotation angles, compared to unsupported techniques (Chapters 5 and 6). Axial rotation has been identified as a risk factor for low back injury (Frymoyer et al., 1983), as the annulus and other passive tissues can be damaged at the end of range of axial rotation (Shirazi-Adl et al., 1986, Duncan and Ahmed, 1991). However, it has been suggested that moderate degrees of axial rotation *without generating high axial rotation torque* is generally not dangerous (McGill, 2007). An elevated risk of injury only arises when the spine is fully rotated and large axial rotation moments are generated (McGill, 2007). This elevated risk occurs because there are no trunk muscles with a primary action designed to create axial rotation torque, thus such an action results in co-activation of all muscles,

and subsequently large compressive forces (McGill, 1997). The axial rotation and lateral bending moments for the BATT were higher than for the other lifting techniques, but still relatively small, therefore not substantially increasing the risk of injury (Figure 5.5 and Figure 6.11). In addition, the effect of the bracing support have not been assessed in *ex vivo* studies, and therefore these guidelines might not hold true in the specific case of BATT.

7.4.2 BATT adapted to activities of daily living

The BATT technique was adapted to three common ADLs, and while reductions in spine loads were observed, trunk flexion angles were not reduced for all tasks (Chapter 6). The study in Chapter 6 demonstrated that the benefits of the BATT may be translated to ADLs, which is promising for individuals with LBP as external objects are rarely available to lean on in everyday life.

The weeding task (in standing posture) was chosen because it combines two risk factors associated with the development of low back pain: large trunk flexion and pulling whilst in a flexed posture. In addition, it often involves prolonged forward bending. The novel method developed to replicate and measure the pulling force allowed for a complete kinetic analysis of the task, which has not been reported previously.

The cupboard task, although it resembles lifting of a light load, was selected because it involves reaching for an object in a constrained space based on the cabinet dimensions. This movement differs from lifting tasks studied in Chapter 5, where the box could be picked up by a handle located on the top of the box.

Car egress was also selected because of the large trunk flexion movements required to exit a car. In addition, local spinal surgeons reported that their patients complained of difficulty performing this particular task and associated pain. Accordingly, the *two-leg out* technique was selected to represent a population with limited mobility. The hand support on the door frame used in both the “self-selected” technique and the BATT was integrated in the simulation as this population often requires additional support to complete the car egress motion. Consequently, car egress with

the BATT provided double bracing support: from the thigh and from the door frame. Bracing on the door involved an additional load cell to measure this force and integrate it into the simulations. Car egress using dash support (load cell moved to dash instead of on door frame) (Chapter 3) and car ingress were also successfully adapted with the BATT; however simulations of these tasks with the current LFB model for these tasks were not possible. Kinetic studies of car egress, involving instrumentation of the car frame to measure the different interactions, are limited in the literature. The study in Chapter 6 not only provided an insight on spinal loads with the BATT for car egress, but also generated new knowledge on spinal loads for car egress in general.

7.4.3 Temporal effect of BATT on peak compression force

The BATT not only reduced spinal loading, it also shifted L4/L5 peak forces to occur at smaller trunk flexion for some participants (Chapter 5). Peak L4/L5 compression forces during unsupported lifting tasks (squat and stoop) typically occurred at large trunk flexion with a load held in the hand(s), when the external moments in the lower back are the greatest. However, this was not always true for the BATT; some participants appeared to spare the spine at peak flexion by effectively using thigh bracing. For those participants, peak L4/L5 compression occurred when the hand was not in contact with the thigh, either as they were standing up in the box pick-up phase, or as they were starting to bend forward in the put-down phase. This temporal shift of peak spinal compression due to thigh bracing was explored for the first time in this thesis (Chapters 5 and 6). This finding influenced the analyses in Chapter 5 as trunk flexion angles at which peak loads occur affect how spinal structures are loaded; large trunk flexion causes ligamentous creep (Adams et al., 1987, McGill and Brown, 1992) and a redistribution of the nucleus within the annulus (Callaghan and McGill, 2001). Rather than using peak loads like most lifting studies (Kingma et al., 2016), spinal loads were compared at the instant of peak trunk flexion during box pick-up and put-down phases. Peak L4/L5 compression forces were then categorised as occurring either *during* or *outside* bracing. The results suggest that participants who had peak L4/L5 compression forces occur *outside* bracing used the BATT more effectively because peak L4/L5 compression forces were lower and peak bracing forces were higher. However, it is not possible

to relate this hypothesis to other studies, as this temporal shift in peak compression loads during lifting due to trunk support (either from thigh bracing or from an external object) has not been studied previously.

Recruiting participants in the 30-70 years old range, including individuals with LBP, instead of the typical young healthy male cohort, better represented the target population that could benefit from the BATT. In addition, the large variation in participant demographics (age, LBP disability, weight, sex, height) likely further highlighted the difference in participant's bracing ability and willingness, thus allowing for the detection of the temporal effect of thigh bracing on peak compression forces.

7.5 Limitations

There are limitations associated with the LFB model used in Chapters 4 to 6 and the measurement of experimental data that drives the model. This section discusses the modelling and experimental limitations of the work in this thesis, as well as their implications for the interpretation of the results.

The LFB model is based on a generic template that is linearly scaled to the anthropometry of each participant. Although the scaled model is personalised for each participant, several properties of the model such as the bone geometry, muscle moment arms, muscle properties, lumbar curvature, joint kinematics, and joint centres are not participant-specific. In addition, the motion of each lumbar vertebra is assumed to be a pure rotation about a fixed centre of rotation in the subadjacent vertebra (Pearcy and Bogduk, 1988). Contrary to this assumption, the location of the centre of rotation varies throughout range of motion and is dependent on the subject and the activity (Zander et al., 2009, Kettler et al., 2004, Wachowski et al., 2009), likely affecting model estimates of joint forces, especially at large flexion angles (Nevins et al., 2014). Further, the amount of rotation in each plane at each intervertebral joint is assumed to be a percentage of the total motion between the thorax and pelvis/sacrum in the model, and this is constant throughout the range of motion. These assumptions are common to all generic models (de Zee et al., 2007, Bassani et al.,

2017), but their effects on model joint force estimates are unclear. In the studies presented in Chapters 4 to 6, and similar to other musculoskeletal model studies in the literature (Kingma et al., 2016, Potvin et al., 1991), the emphasis was placed on relative change in magnitude of lumbar loading, rather than its absolute value. Therefore, errors in the intervertebral joint loading estimates probably had a limited impact on the conclusions drawn. Participant-specific models can predict more accurate values of joint loads; however, these require extensive use of medical imaging techniques and time-consuming image segmentation, which at present is not feasible for studies of this size. In addition, despite the higher biofidelity of participant-specific models, they also have the inherent validation limitation associated with all models, as comparison with reported *in vivo* measurements is limited.

The effect of intra-abdominal pressure was not included in the model due to the challenges associated with modelling the IAP as an elastic membranous pressure vessel in OpenSim (Christophy et al., 2012) and the limited experimental IAP data available in the literature (Marras and Granata, 1995, Marras and Mirka, 1996, De Keulenaer et al., 2009). Generation of appreciable IAP during lifting has been documented (Hemborg et al., 1985, Cresswell and Thorstensson, 1994); however, its role remains uncertain and controversial (Stokes et al., 2010). It has been suggested that abdominal muscle activation and its associated abdominal pressurisation produce spinal unloading during extension efforts (Arjmand and Shirazi-Adl, 2006b, Daggfeldt and Thorstensson, 1997, Hodges et al., 2001), in addition to increasing trunk stability (Cresswell and Thorstensson, 1994, Cholewicki et al., 1999b, Stokes et al., 2000). The unloading effect of IAP, although questioned (McGill and Norman, 1987b), is thought to result from the pressure acting on the diaphragm and pelvic floor (Stokes et al., 2010). The stabilising effect is a consequence of the added stiffness of activated muscles (Bergmark, 1989, Cresswell and Thorstensson, 1994, Cholewicki et al., 1999b, Stokes et al., 2000). Given the controversy surrounding the role of IAP on spinal loading during lifting, it is difficult to interpret how its inclusion in the model would have affected compression loads estimated by the LFB models in Chapters 4 to 6. Nevertheless, relative changes in lumbar loading was the focus of the studies in

Chapters 5 and 6, thus limiting its impact on the conclusions drawn, especially since the trunk extensors are the prime-mover muscles during lifting and their activations are unaffected by IAP (Cresswell and Thorstensson, 1994, McGill et al., 1990).

Ligaments and other passive components were not included in the LFB model, due to the limited experimental data available regarding their mechanical properties. In addition, it is challenging to predict passive tissue forces in full flexion, as their load-displacement responses are non-linear and highly variable between participants (Abouhossein et al., 2011, Arjmand and Shirazi-Adl, 2006a, Kingma et al., 2016). Extension moments during lifting are distributed between the passive and active (muscle) components of the spine (Abouhossein et al., 2011). Passive structure contributions are minimal at moderate trunk flexion angles (BATT and squat) but increase at larger trunk flexion angles (stoop lifts), regardless of the load held in the hands (Potvin et al., 1991, Dolan et al., 1994b). Consequently, intervertebral forces for one-handed and two-handed stoop lifts (1ST and 2ST) might have been slightly overestimated by recruiting muscles instead of ligaments as they had more flexed postures than BATT and squat (2SQ). Nonetheless, the conclusions drawn in Chapter 5 are likely unaffected as muscles provide the dominant contributions to the extension moment in all lifts evaluated.

Tracking spine motion using skin surface markers is a known limitation associated with motion capture studies. It is challenging to measure individual intervertebral motion, given the small size of each vertebra rigid body and the large number of DOFs in the spine. The estimated L4/L5 angles in this thesis were higher than reported physiological ranges of motion for some participants (Chapter 5 & 6). This overestimation can mostly be attributed to the rigid trunk assumption which distributes the motion of the entire trunk (C7 to S1) over the lumbar region (T12-S1), thus increasing the intervertebral motion. Overestimation of trunk flexion is also likely partly due to the difficulty in tracking subtle pelvis tilts during forward bending, thus incorrectly increasing lumbar motion. Axial rotation and lateral bending estimates also likely included some shoulder motion as these movements were tracked using markers placed on the upper trunk, near the scapula and acromion. Nevertheless, as previously mentioned, the emphasis of this thesis was

to evaluate relative changes between lifting tasks and bracing conditions during ADLs. Trunk angles, instead of L4/L5 motion, were compared between lifting techniques and ADLs in an attempt to minimise the impact of these limitations on the conclusions (Chapters 4 to 6).

7.6 Recommendations

Given the paucity of the literature relating to the BATT for lifting and other ADLs, especially in the LBP population, there are many opportunities for improving and extending the work in this thesis. In addition, the current LFB model could be enhanced to provide more participant-specific spinal load estimates and expand the range of tasks it can simulate. This section provides recommendations for future investigations to improve the LFB model and to better understand the effect of the BATT on spinal loads for healthy and LBP populations.

7.6.1 Modelling

The model could be improved to better represent muscle contributions/activations for the healthy and LBP populations, especially considering the known motor defects and differences in muscle activations for LBP individuals (McGill et al., 2003, Hodges et al., 2006). Muscle forces in this thesis were estimated using static optimisation. Although this approach yielded reasonable approximations of lumbar loading (Chapter 4), any motor control issues by LBP participants were not taken into account as no physiological signals were used to determine muscle activation. While not within the scope of this thesis, EMG measurements could be used to provide more physiologically accurate levels of activations for the back muscles. Although EMG-driven models have limitations regarding grouping assumptions for muscle activations, future studies should explore hybrid models that exploit the strengths of both EMG-driven and optimisation approaches to incorporate EMG data into objective functions in order to obtain more realistic muscle force predictions while retaining musculotendon complexity.

The magnitudes of the maximum isometric extensor moments for the erector spinae muscle group produced by the model were within the range of reported experimental data in the literature from upright posture to full flexion (0°-60°). However, the moment did not increase linearly with

length (or flexion angle) as expected for the back extensors (Raschke and Chaffin, 1996). Instead, the model showed a decreasing moment-angle relationship for trunk flexion angles above 20° (Figure 4.4). Consequently, the model muscle force estimates and joint reaction forces were likely underestimated (Chapters 5 and 6), especially for the one-handed (1ST) and two-handed (2ST) stoops that exhibited the largest trunk flexion angles. However, the conclusions of these chapters remain unaffected because significant differences between the BATT and the other three lifting techniques were detected despite these smaller estimates. Future versions of the model should seek to achieve the expected increasing linear relationship between muscle length and force during trunk flexion.

In addition, future versions of the model should seek to include passive components (ligaments, discs, facet joints, etc.). Ligaments have a stabilising effect on the spine over the range of motion (Arjmand and Shirazi-Adl, 2006a), while the disc resists a greater proportion of the applied load as the spine is fully flexed (Abouhossein et al., 2011, Arjmand and Shirazi-Adl, 2006a). Facets and capsular ligaments provide resistance in extension (Abouhossein et al., 2011). Therefore, the integration of these components is relevant for a full understanding of the possible mechanics of LBP during lifting (Panjabi et al., 1982).

Shear forces are especially sensitive to modelling parameters and orientation of the vertebra in the model (Kingma et al., 2016); therefore, small changes in intervertebral motions or changes in muscle lines of action can have large effects on shear forces. This is evident when comparing absolute values of shear force estimates between studies and across spine levels. Future work should perform a sensitivity analysis to investigate the effect of changing the orientation of the L4/L5 joint axes on the intervertebral joint forces.

The transition phases for box pick-up and put-down were not modelled in the current work due to limitations associated with modelling the distribution of mass of the box between the ground and hands at each time frame. Consequently, peak L4/L5 spinal loads were assumed to occur in the loaded portion of the lifting trials, when the boxes mass was completely supported by the

hand(s). The modelling approach used in Chapters 4 and 5 could be improved to examine these transition periods and understand how load pick-up and put-down influence spinal loading.

The shoulder was modelled as a three-DOF rotational joint, without any translational DOF. It is difficult to measure shoulder translations *in vivo*, particularly using skin-mounted markers, and as a result, these translations were not quantified. Shoulder motion was predominantly in the sagittal plane for the lifting techniques studied in Chapter 5, except for the BATT in which the bracing action on the thigh induced motions in the transverse and frontal planes. These motions might have resulted in overestimation of trunk lateral bending and axial rotation angles for the BATT, thus overestimating the observed differences in trunk lateral bending and axial rotation kinematics between BATT and the other lifting techniques. Comparisons with the one-handed stoop (1ST) may have been more affected by this overestimation as this lifting technique is not symmetrical in the sagittal plane, unlike the two-handed stoop (2ST) and squat (2SQ). In the ADLs simulated in Chapter 6, shoulder motion was also predominantly in the sagittal plane for the unsupported condition, but included transverse and frontal plane motion in the supported (bracing) condition. Therefore, the model may have overestimated the kinematic differences between the unsupported and unsupported conditions. This limitation of the model was most evident for the car egress task with dash support that was attempted in this thesis (Chapter 3). It could not be simulated accurately with the current LFB model because trunk axial rotation angles and shoulder motion were too large. Future versions of the model should incorporate a more detailed model of the shoulder that includes translational DOF to better represent these motions.

7.6.2 Lifting tasks

A large dataset of back and abdominal EMG muscle activity was collected for all the participants recruited for the study in Chapter 5. Future projects should utilise these physiological signals to provide a better understanding of the muscle activation between healthy and LBP groups. In addition, these EMG signals could be used to calculate co-contraction indices, defined as the simultaneous activation of antagonist muscles (Lewek et al., 2004), to determine if participants

with LBP had higher muscle activation than healthy participants to protect themselves during different lifting techniques.

Lumbar spinal instability has been linked to causes of LBP (Cholewicki and McGill, 1996). A future exploratory project should assess spinal stability during each of the four lifting tasks studied in Chapter 5 by evaluating the role of muscle co-contraction, using an equation that sums the stability contribution of each muscle acting over a joint based on their geometric parameters (attachment point and moment arm) and activation (Potvin and Brown, 2005). This method has previously been used on the spine in neutral posture (Brown and Potvin, 2007) and on the wrist (Holmes et al., 2015), but has not been used for the evaluation of lifting tasks. Muscle activations and their corresponding geometric properties obtained in Chapter 5 could be used to determine L4/L5 joint stability for the four different lifting tasks between healthy and LBP groups.

Participants' ability to use the thigh bracing force varied substantially in Chapters 5 and 6. In order to remove the training effect associated with same day testing, participants should be trained using visual real-time feedback prior to data collection to investigate the effect of training on spinal loads. In addition, future work should assess knee and shoulder loading associated with the BATT to identify potential injury risks at those joints.

7.6.3 Activity of daily living

The feasibility of simulating three common ADLs was demonstrated in Chapter 6 with ten young healthy male participants. Future work should repeat the protocol with a larger cohort, including LBP participants, to increase the statistical power of the study and to improve the applicability of the results to individuals with LBP.

In line with the recommendation to improve shoulder modelling in the current LFB model, the dataset collected for car egress using the car frame dash could be analysed in a future study to determine the effect of the BATT on this *one-leg first* car egress technique.

This study only included three ADLs to which the BATT could applied. Additional activities should be evaluated and simulated in the laboratory, including tasks where elbow support on the thigh is more appropriate than the hand (shovelling, some gardening and domestics tasks, etc). These tasks would likely require the development of a load cell interface to maintain elbow-thigh contact over a trunk range of motion during forward bending (Kingma et al., 2016).

The ultimate goal of this proposed work would be to develop a musculoskeletal model capable of evaluating the difference in muscle activations between LBP and healthy participants for various forward bending and lifting tasks to understand the mechanism of injury and propose solutions. Based on the results of this thesis, bracing on the thigh appears to be a good solution for low weight lifting and tasks that involve forward bending. However, an enhanced model would provide a better understanding of the effect of bracing on individual muscle activations and contributions, and on spine stability.

7.7 Original contributions

This thesis made a number of original contributions to the biomechanical modelling and clinical research fields:

1. A novel OpenSim full-body model with a detailed lumbar spine was developed and validated to evaluate lumbar spinal loading during symmetrical and asymmetrical lifting techniques (Chapter 4). This model has the potential to help bridge the gap with clinical recommendations of different lifting techniques as it is currently not possible to directly measure *in vivo* intervertebral joint loads.

2. A new method to model the forces created by the box during lifting was developed in OpenSim; the mass properties of the hands are incorporated to those of the hands (Chapters 4 and 5). This method can be used as a template for a wide range of one-handed and two-handed lifting simulations, including non-spine related studies.

3. This thesis presents the first study to include healthy participants and participants with LBP aged 30-70 years old, for the evaluation of the braced arm-to-thigh lifting technique (Chapter 5). This distinct population is underrepresented in lifting studies, as most studies recruit only young healthy males. This specific cohort is representative of the population that could benefit for the braced arm-to-thigh technique.

4. The unique dataset for healthy participants and participants with LBP collected in Chapter 5 enhances the limited existing literature on one-handed lifting techniques, especially supported asymmetrical one-handed lifts. Most one-handed lifting techniques studied in the literature have focused on industrial settings, as opposed to light or moderate weights lifted during activities of daily living.

5. This is the first study to explore the relationship between thigh bracing force and spinal unloading, indicating that training to improve efficacy of the bracing force might be beneficial to further reduce spinal loads (Chapter 5). These results are important because they revealed that thigh bracing not only reduced trunk loading, but could also influence the trunk flexion angles at which peak loads occurred.

6. For the first time, spinal loads were estimated for several activities of daily living that involve reaching, pulling, and sit-to-stand movements, with and without the thigh bracing force (Chapter 6). This study provides an important contribution to the biomechanics literature as spine musculoskeletal models are rarely used to simulate tasks other than lifting.

7. Custom apparatus were designed and built to simulate these activities of daily living in the laboratory (Chapter 6). These designs can be used as prototypes for future studies of activities of daily living.

8. The results of Chapter 6 demonstrated for the first time that the BATT can successfully be used for tasks other than lifting. This finding supports biomechanical hypotheses that this technique could be used in a wide range of activities.

7.8 Conclusion

Biomechanical loading of the spine during lifting and forward bending is a risk factor associated with the development of LBP as these loads might be high enough to damage structures of the spine; this risk increases with repeated loading and cumulative exposure to loads over time.

The findings from the experimental studies, using the novel musculoskeletal model developed in the thesis, revealed that supporting the upper body with the hand on the thigh reduced moments, compression and antero-posterior shear forces at L4/L5 for LBP and healthy populations in two loading conditions (2 kg and 10 kg). The BATT also increased trunk asymmetry (moments and angles) compared to symmetrical two-handed lifting techniques, due to the bracing action. The BATT reduced L4/L5 loads when applied to three common ADLs simulated in the laboratory, compared to unsupported self-selected techniques. In conclusion, the BATT is promising for individuals with LBP, that have a limited ability to perform lifting tasks with low-to-moderate loads and other ADLs that require frequent forward bending.

References

ABOUHOSSEIN, A., WEISSE, B. & FERGUSON, S. J. 2011. A multibody modelling approach to determine load sharing between passive elements of the lumbar spine. *Comput Methods Biomech Biomed Engin,* 14**,** 527-37.

ACTIS, J. A., HONEGGER, J. D., GATES, D. H., PETRELLA, A. J., NOLASCO, L. A. & SILVERMAN, A. K. 2018. Validation of lumbar spine loading from a musculoskeletal model including the lower limbs and lumbar spine. *J Biomech,* 68**,** 107-114.

ADAMS, M., BOGDUK, N., BURTON, K. & DOLAN, P. 2006. *The Biomechanics of Back Pain,* Edinburg, Churchill Livingston.

ADAMS, M. A. & DOLAN, P. 1991. A technique for quantifying the bending moment acting on the lumbar spine in vivo. *J Biomech,* 24**,** 117-26.

ADAMS, M. A., DOLAN, P. & HUTTON, W. C. 1987. Diurnal variations in the stresses on the lumbar spine. *Spine (Phila Pa 1976),* 12**,** 130-7.

ADAMS, M. A., GREEN, T. P. & DOLAN, P. 1994. The strength in anterior bending of lumbar intervertebral discs. *Spine (Phila Pa 1976),* 19**,** 2197-203.

ADAMS, M. A. & HUTTON, W. C. 1982. Prolapsed intervertebral disc. A hyperflexion injury 1981 Volvo Award in Basic Science. *Spine (Phila Pa 1976),* 7**,** 184-91.

ADAMS, M. A., HUTTON, W. C. & STOTT, J. R. 1980. The resistance to flexion of the lumbar intervertebral joint. *Spine (Phila Pa 1976),* 5**,** 245-53.

AIRAKSINEN, O., BROX, J. I., CEDRASCHI, C., HILDEBRANDT, J., KLABER-MOFFETT, J., KOVACS, F., MANNION, A. F., REIS, S., STAAL, J. B., URSIN, H., ZANOLI, G. & PAIN, C. B. W. G. O. G. F. C. L. B. 2006. Chapter 4. European guidelines for the management of chronic nonspecific low back pain. *Eur Spine J,* 15 Suppl 2**,** S192-300.

AIT-HADDOU, R., BINDING, P. & HERZOG, W. 2000. Theoretical considerations on cocontraction of sets of agonistic and antagonistic muscles. *J Biomech,* 33**,** 1105-11.

AN, K. N., KWAK, B. M., CHAO, E. Y. & MORREY, B. F. 1984. Determination of muscle and joint forces: a new technique to solve the indeterminate problem. *J Biomech Eng,* 106**,** 364-7.

ARJMAND, N., GAGNON, D., PLAMONDON, A., SHIRAZI-ADL, A. & LARIVIERE, C. 2009. Comparison of trunk muscle forces and spinal loads estimated by two biomechanical models. *Clin Biomech (Bristol, Avon),* 24**,** 533-41.

ARJMAND, N., PLAMONDON, A., SHIRAZI-ADL, A., PARNIANPOUR, M. & LARIVIERE, C. 2012. Predictive equations for lumbar spine loads in load-dependent asymmetric one- and two-handed lifting activities. *Clin Biomech (Bristol, Avon),* 27**,** 537-44.

ARJMAND, N. & SHIRAZI-ADL, A. 2005. Biomechanics of changes in lumbar posture in static lifting. *Spine (Phila Pa 1976),* 30**,** 2637-48.

ARJMAND, N. & SHIRAZI-ADL, A. 2006a. Model and in vivo studies on human trunk load partitioning and stability in isometric forward flexions. *J Biomech,* 39**,** 510-21.

ARJMAND, N. & SHIRAZI-ADL, A. 2006b. Role of intra-abdominal pressure in the unloading and stabilization of the human spine during static lifting tasks. *Eur Spine J,* 15**,** 1265-75.

ARJMAND, N. & SHIRAZI-ADL, A. 2006c. Sensitivity of kinematics-based model predictions to optimization criteria in static lifting tasks. *Med Eng Phys,* 28**,** 504-14.

ARJMAND, N., SHIRAZI-ADL, A. & BAZRGARI, B. 2006. Wrapping of trunk thoracic extensor muscles influences muscle forces and spinal loads in lifting tasks. *Clin Biomech (Bristol, Avon),* 21**,** 668-75.

ARJMAND, N., SHIRAZI-ADL, A. & PARNIANPOUR, M. 2007. Trunk biomechanical models based on equilibrium at a single-level violate equilibrium at other levels. *Eur Spine J,* 16**,** 701-9.

ARNOLD, A. S., SALINAS, S., ASAKAWA, D. J. & DELP, S. L. 2000. Accuracy of muscle moment arms estimated from MRI-based musculoskeletal models of the lower extremity. *Comput Aided Surg,* 5**,** 108-19.

ARNOLD, E. M., WARD, S. R., LIEBER, R. L. & DELP, S. L. 2010. A model of the lower limb for analysis of human movement. *Ann Biomed Eng,* 38**,** 269-79.

AUSTRALIAN INSTITUTE OF HEALTH AND WELFARE 2016. Impacts of chronic back problems. . Canberra: AIHW.

AUVINEN, J. P., PAANANEN, M. V., TAMMELIN, T. H., TAIMELA, S. P., MUTANEN, P. O., ZITTING, P. J. & KARPPINEN, J. I. 2009. Musculoskeletal pain combinations in adolescents. *Spine (Phila Pa 1976),* 34**,** 1192-7.

AZAR, N. R., ANDREWS, D. M. & CALLAGHAN, J. P. 2005. Accuracy of spine cumulative loading using self-reported duration and frequency information during non-occupational tasks. *International journal of industrial ergonomics,* 35**,** 687-696.

AZAR, N. R., GODIN, C. A., ANDREWS, D. M. & CALLAGHAN, J. P. 2010. Three-dimensional peak and cumulative L4/L5 spine loads and trunk postures during non-occupational tasks. *Occupational Ergonomics,* 9**,** 127-139.

BALAGUE, F., MANNION, A. F., PELLISE, F. & CEDRASCHI, C. 2012. Non-specific low back pain. *Lancet,* 379**,** 482-91.

BARKER, K. L., SHAMLEY, D. R. & JACKSON, D. 2004. Changes in the cross-sectional area of multifidus and psoas in patients with unilateral back pain: the relationship to pain and disability. *Spine (Phila Pa 1976),* 29**,** E515-9.

BASSANI, T., STUCOVITZ, E., QIAN, Z., BRIGUGLIO, M. & GALBUSERA, F. 2017. Validation of the AnyBody full body musculoskeletal model in computing lumbar spine loads at L4L5 level. *J Biomech,* 58**,** 89-96.

BAZRGARI, B. & SHIRAZI-ADL, A. 2007. Spinal stability and role of passive stiffness in dynamic squat and stoop lifts. *Comput Methods Biomech Biomed Engin,* 10**,** 351-60.

BAZRGARI, B., SHIRAZI-ADL, A. & ARJMAND, N. 2007. Analysis of squat and stoop dynamic liftings: muscle forces and internal spinal loads. *Eur Spine J,* 16**,** 687-99.

BEAUCAGE-GAUVREAU, E., BRANDON, S. C. E., ROBERTSON, W. S. P., FRASER, R., FREEMAN, B. J. C., GRAHAM, R. B., THEWLIS, D. & JONES, C. F. 2019. Validation of an OpenSim full-body model with detailed lumbar spine for estimating lower lumbar spine loads during symmetric and asymmetric lifting tasks. *Computer Methods in Biomechanics and Biomedical Engineering,* In press.

BECKER, A., HELD, H., REDAELLI, M., STRAUCH, K., CHENOT, J. F., LEONHARDT, C., KELLER, S., BAUM, E., PFINGSTEN, M., HILDEBRANDT, J., BASLER, H. D., KOCHEN, M. M. & DONNER-BANZHOFF, N. 2010. Low back pain in primary care: costs of care and prediction of future health care utilization. *Spine (Phila Pa 1976),* 35**,** 1714-20.

BERGMARK, A. 1989. Stability of the lumbar spine. A study in mechanical engineering. *Acta Orthop Scand Suppl,* 230**,** 1-54.

BIGOS, S. J., SPENGLER, D. M., MARTIN, N. A., ZEH, J., FISHER, L., NACHEMSON, A. & WANG, M. H. 1986. Back injuries in industry: a retrospective study. II. Injury factors. *Spine (Phila Pa 1976),* 11**,** 246-51.

BLACHE, Y., DAL MASO, F., DESMOULINS, L., PLAMONDON, A. & BEGON, M. 2015a. Superficial shoulder muscle co-activations during lifting tasks: Influence of lifting height, weight and phase. *J Electromyogr Kinesiol,* 25**,** 355-62.

BLACHE, Y., DESMOULINS, L., ALLARD, P., PLAMONDON, A. & BEGON, M. 2015b. Effects of height and load weight on shoulder muscle work during overhead lifting task. *Ergonomics,* 58**,** 748-61.

BLEMKER, S. S. & DELP, S. L. 2005. Three-dimensional representation of complex muscle architectures and geometries. *Ann Biomed Eng,* 33**,** 661-73.

BOGDUK, N. 2005. *Clinical anatomy of the lumbar spine and sacrum,* Elsevier Health Sciences.

BOGDUK, N., JOHNSON, G. & SPALDING, D. 1998. The morphology and biomechanics of latissimus dorsi. *Clin Biomech (Bristol, Avon),* 13**,** 377-385.

BOGDUK, N., MACINTOSH, J. E. & PEARCY, M. J. 1992a. A universal model of the lumbar back muscles in the upright position. *Spine (Phila Pa 1976),* 17**,** 897-913.

BOGDUK, N., PEARCY, M. & HADFIELD, G. 1992b. Anatomy and biomechanics of psoas major. *Clin Biomech (Bristol, Avon),* 7**,** 109-19.

BRAGE, S., IHLEBAEK, C., NATVIG, B. & BRUUSGAARD, D. 2010. [Musculoskeletal disorders as causes of sick leave and disability benefits]. *Tidsskr Nor Laegeforen,* 130**,** 2369-70.

BRINCKMANN, P., BIGGEMANN, M. & HILWEG, D. 1988. Fatigue fracture of human lumbar vertebrae. *Clin Biomech (Bristol, Avon),* 3 Suppl 1**,** i-S23.

BRINCKMANN, P., BIGGEMANN, M. & HILWEG, D. 1989. Prediction of the compressive strength of human lumbar vertebrae. *Spine (Phila Pa 1976),* 14**,** 606-10.

BRINCKMANN, P. & GROOTENBOER, H. 1991. Change of disc height, radial disc bulge, and intradiscal pressure from discectomy. An in vitro investigation on human lumbar discs. *Spine (Phila Pa 1976),* 16**,** 641-6.

BROWN, L. P., NIEHUES, S. L., HARRAH, A., YAVORSKY, P. & HIRSHMAN, H. P. 1988. Upper extremity range of motion and isokinetic strength of the internal and external shoulder rotators in major league baseball players. *Am J Sports Med,* 16**,** 577-85.

BROWN, S. H. & POTVIN, J. R. 2005. Constraining spine stability levels in an optimization model leads to the prediction of trunk muscle cocontraction and improved spine compression force estimates. *J Biomech,* 38**,** 745-54.

BROWN, S. H. & POTVIN, J. R. 2007. Exploring the geometric and mechanical characteristics of the spine musculature to provide rotational stiffness to two spine joints in the neutral posture. *Hum Mov Sci,* 26**,** 113-23.

BRUNO, A. G., BOUXSEIN, M. L. & ANDERSON, D. E. 2015. Development and Validation of a Musculoskeletal Model of the Fully Articulated Thoracolumbar Spine and Rib Cage. *J Biomech Eng,* 137**,** 081003.

BUCHANAN, T. S., LLOYD, D. G., MANAL, K. & BESIER, T. F. 2004. Neuromusculoskeletal modeling: estimation of muscle forces and joint moments and movements from measurements of neural command. *J Appl Biomech,* 20**,** 367-95.

CALLAGHAN, J. P. & MCGILL, S. M. 2001. Intervertebral disc herniation: studies on a porcine model exposed to highly repetitive flexion/extension motion with compressive force. *Clin Biomech (Bristol, Avon),* 16**,** 28-37.

CAMOMILLA, V., CEREATTI, A., VANNOZZI, G. & CAPPOZZO, A. 2006. An optimized protocol for hip joint centre determination using the functional method. *J Biomech,* 39**,** 1096-106.

CAPPELAERE, A., THÉVENON, A. & DELCAMBRE, B. Polyarthrite rhumatoïde et conduite automobile. Essais contrôlés d'un véhicule de série. Annales de Réadaptation et de médecine physique, 1991. Elsevier, 239-244.

CAPPELLO, A., CAPPOZZO, A., LA PALOMBARA, P. F., LUCCHETTI, L. & LEARDINI, A. 1997. Multiple anatomical landmark calibration for optimal bone pose estimation. *Human movement science,* 16**,** 259-274.

CAPPOZZO, A., CATANI, F., DELLA CROCE, U. & LEARDINI, A. 1995. Position and orientation in space of bones during movement: anatomical frame definition and determination. *Clinical biomechanics,* 10**,** 171-178.

CARUTHERS, E. J., THOMPSON, J. A., CHAUDHARI, A. M., SCHMITT, L. C., BEST, T. M., SAUL, K. R. & SISTON, R. A. 2016. Muscle Forces and Their Contributions to Vertical and Horizontal Acceleration of the Center of Mass During Sit-to-Stand Transfer in Young, Healthy Adults. *J Appl Biomech,* 32**,** 487-503.

CAUSSE, J., CHATEAUROUX, E., MONNIER, G., WANG, X. & DENNINGER, L. 2009. Dynamic analysis of car ingress/egress movement: an experimental protocol and preliminary results. *SAE International Journal of Passenger Cars-Mechanical Systems,* 2**,** 1633-1640.

CAUSSE, J., WANG, X. & DENNINGER, L. 2012. An experimental investigation on the requirement of roof height and sill width for car ingress and egress. *Ergonomics,* 55**,** 1596-611.

CAZZOLA, D., HOLSGROVE, T. P., PREATONI, E., GILL, H. S. & TREWARTHA, G. 2017. Cervical Spine Injuries: A Whole-Body Musculoskeletal Model for the Analysis of Spinal Loading. *PLoS One,* 12**,** e0169329.

CHATEAUROUX, E. & WANG, X. 2010. Car egress analysis of younger and older drivers for motion simulation. *Appl Ergon,* 42**,** 169-77.

CHATEAUROUX, E., WANG, X. & TRASBOT, J. 2007. A database of ingress/egress motions of elderly people. SAE Technical Paper.

CHEREDNICHENKO, A., ASSMANN, E. & BUBB, H. 2006. Computational approach for entry simulation. SAE Technical Paper.

CHOLEWICKI, J., JULURU, K. & MCGILL, S. M. 1999a. Intra-abdominal pressure mechanism for stabilizing the lumbar spine. *J Biomech,* 32**,** 13-7.

CHOLEWICKI, J., JULURU, K., RADEBOLD, A., PANJABI, M. M. & MCGILL, S. M. 1999b. Lumbar spine stability can be augmented with an abdominal belt and/or increased intra-abdominal pressure. *Eur Spine J,* 8**,** 388-95.

CHOLEWICKI, J. & MCGILL, S. M. 1994. EMG assisted optimization: a hybrid approach for estimating muscle forces in an indeterminate biomechanical model. *J Biomech,* 27**,** 1287-9.

CHOLEWICKI, J. & MCGILL, S. M. 1996. Mechanical stability of the in vivo lumbar spine: implications for injury and chronic low back pain. *Clin Biomech (Bristol, Avon),* 11**,** 1-15.

CHOLEWICKI, J., MCGILL, S. M. & NORMAN, R. W. 1995. Comparison of muscle forces and joint load from an optimization and EMG assisted lumbar spine model: towards development of a hybrid approach. *J Biomech,* 28**,** 321-31.

CHRISTOPHY, M., FARUK SENAN, N. A., LOTZ, J. C. & O'REILLY, O. M. 2012. A musculoskeletal model for the lumbar spine. *Biomech Model Mechanobiol,* 11**,** 19-34.

COENEN, P., KINGMA, I., BOOT, C. R., BONGERS, P. M. & VAN DIEEN, J. H. 2014. Cumulative mechanical low-back load at work is a determinant of low-back pain. *Occup Environ Med,* 71**,** 332-7.

COHEN, J. 1988. Statistical power analysis for the behavioral sciences 2nd edn. Erlbaum Associates, Hillsdale.

COOK, T. M., MANN, S. & LOVESTED, G. E. 1990. Dynamic comparison of the two-hand stoop and assisted one-hand lift methods. *Journal of Safety Research,* 21**,** 53-59.

COSTA-BLACK, K. M., LOISEL, P., ANEMA, J. R. & PRANSKY, G. 2010. Back pain and work. *Best Pract Res Clin Rheumatol,* 24**,** 227-40.

CRESSWELL, A. G. & THORSTENSSON, A. 1994. Changes in intra-abdominal pressure, trunk muscle activation and force during isokinetic lifting and lowering. *Eur J Appl Physiol Occup Physiol,* 68**,** 315-21.

CRIPTON, P. 1995. Response of the lumbar spine due to shear loading. *Proceedings of the Symposium on Injury Prevention Through Biomechanics, Wayne State University, Detroit, MI, May 4-5, 1995*.

CROFT, P. R., MACFARLANE, G. J., PAPAGEORGIOU, A. C., THOMAS, E. & SILMAN, A. J. 1998. Outcome of low back pain in general practice: a prospective study. *BMJ,* 316**,** 1356-9.

CROWNINSHIELD, R. D. & BRAND, R. A. 1981. A physiologically based criterion of muscle force prediction in locomotion. *J Biomech,* 14**,** 793-801.

DAGENAIS, S., CARO, J. & HALDEMAN, S. 2008. A systematic review of low back pain cost of illness studies in the United States and internationally. *Spine J,* 8**,** 8-20.

DAGGFELDT, K. & THORSTENSSON, A. 1997. The role of intra-abdominal pressure in spinal unloading. *J Biomech,* 30**,** 1149-55.

DAMSGAARD, M., RASMUSSEN, J., CHRISTENSEN, S. T., SURMA, E. & DE ZEE, M. 2006. Analysis of musculoskeletal systems in the AnyBody Modeling System. *Simulation Modelling Practice and Theory,* 14**,** 1100-1111.

DAVIS, K. G., MARRAS, W. S. & WATERS, T. R. 1998. Reduction of spinal loading through the use of handles. *Ergonomics,* 41**,** 1155-68.

DE KEULENAER, B. L., DE WAELE, J. J., POWELL, B. & MALBRAIN, M. L. 2009. What is normal intra-abdominal pressure and how is it affected by positioning, body mass and positive end-expiratory pressure? *Intensive Care Med,* 35**,** 969-76.

DE ZEE, M., HANSEN, L., WONG, C., RASMUSSEN, J. & SIMONSEN, E. B. 2007. A generic detailed rigid-body lumbar spine model. *J Biomech,* 40**,** 1219-27.

DELP, S. L., ANDERSON, F. C., ARNOLD, A. S., LOAN, P., HABIB, A., JOHN, C. T., GUENDELMAN, E. & THELEN, D. G. 2007. OpenSim: open-source software to create and analyze dynamic simulations of movement. *IEEE Trans Biomed Eng,* 54**,** 1940-50.

DELP, S. L., LOAN, J. P., HOY, M. G., ZAJAC, F. E., TOPP, E. L. & ROSEN, J. M. 1990. An interactive graphics-based model of the lower extremity to study orthopaedic surgical procedures. *IEEE Trans Biomed Eng,* 37**,** 757-67.

DOLAN, P. & ADAMS, M. A. 1993. Influence of lumbar and hip mobility on the bending stresses acting on the lumbar spine. *Clin Biomech (Bristol, Avon),* 8**,** 185-92.

DOLAN, P., EARLEY, M. & ADAMS, M. A. 1994a. Bending and compressive stresses acting on the lumbar spine during lifting activities. *J Biomech,* 27**,** 1237-48.

DOLAN, P., MANNION, A. F. & ADAMS, M. A. 1994b. Passive tissues help the back muscles to generate extensor moments during lifting. *J Biomech,* 27**,** 1077-85.

DOORENBOSCH, C. A., HARLAAR, J., ROEBROECK, M. E. & LANKHORST, G. J. 1994. Two strategies of transferring from sit-to-stand; the activation of monoarticular and biarticular muscles. *J Biomech,* 27**,** 1299-307.

DREISCHARF, M., ROHLMANN, A., GRAICHEN, F., BERGMANN, G. & SCHMIDT, H. 2015. In vivo loads on a vertebral body replacement during different lifting techniques. *J Biomech.*

DREISCHARF, M., ROHLMANN, A., ZHU, R., SCHMIDT, H. & ZANDER, T. 2013. Is it possible to estimate the compressive force in the lumbar spine from intradiscal pressure measurements? A finite element evaluation. *Med Eng Phys,* 35**,** 1385-90.

DRISCOLL, T., JACKLYN, G., ORCHARD, J., PASSMORE, E., VOS, T., FREEDMAN, G., LIM, S. & PUNNETT, L. 2014. The global burden of occupationally related low back pain: estimates from the Global Burden of Disease 2010 study. *Ann Rheum Dis,* 73**,** 975-81.

DUNCAN, N. A. & AHMED, A. M. 1991. The role of axial rotation in the etiology of unilateral disc prolapse. An experimental and finite-element analysis. *Spine (Phila Pa 1976),* 16**,** 1089-98.

DVORAK, J., PANJABI, M. M., CHANG, D. G., THEILER, R. & GROB, D. 1991. Functional radiographic diagnosis of the lumbar spine. Flexion-extension and lateral bending. *Spine (Phila Pa 1976),* 16**,** 562-71.

EHRIG, R. M., TAYLOR, W. R., DUDA, G. N. & HELLER, M. O. 2007. A survey of formal methods for determining functional joint axes. *J Biomech,* 40**,** 2150-7.

EL-RICH, M., SHIRAZI-ADL, A. & ARJMAND, N. 2004. Muscle activity, internal loads, and stability of the human spine in standing postures: combined model and in vivo studies. *Spine (Phila Pa 1976),* 29**,** 2633-42.

EL MENCEUR, M. O. A., PUDLO, P., GORCE, P., THÉVENON, A. & LEPOUTRE, F.-X. 2008. Alternative movement identification in the automobile ingress and egress for young and elderly population with or without prostheses. *International Journal of Industrial Ergonomics,* 38**,** 1078-1087.

ERIKSEN, W., BRUUSGAARD, D. & KNARDAHL, S. 2004. Work factors as predictors of intense or disabling low back pain; a prospective study of nurses' aides. *Occup Environ Med,* 61**,** 398-404.

FABER, G. S., KINGMA, I. & VAN DIEEN, J. H. 2011. Effect of initial horizontal object position on peak L5/S1 moments in manual lifting is dependent on task type and familiarity with alternative lifting strategies. *Ergonomics,* 54**,** 72-81.

FAIRBANK, J. C. & PYNSENT, P. B. 2000. The Oswestry Disability Index. *Spine (Phila Pa 1976),* 25**,** 2940-52; discussion 2952.

FERGUSON, S. A., GAUDES-MACLAREN, L. L., MARRAS, W. S., WATERS, T. R. & DAVIS, K. G. 2002. Spinal loading when lifting from industrial storage bins. *Ergonomics,* 45**,** 399-414.

FERGUSON, S. A. & MARRAS, W. S. 1997. A literature review of low back disorder surveillance measures and risk factors. *Clin Biomech (Bristol, Avon),* 12**,** 211-226.

FERNANDEZ, J. W. & PANDY, M. G. 2006. Integrating modelling and experiments to assess dynamic musculoskeletal function in humans. *Exp Physiol,* 91**,** 371-82.

FRAZER, M., NORMAN, R., WELLS, R. & NEUMANN, P. 2003. The effects of job rotation on the risk of reporting low back pain. *Ergonomics,* 46**,** 904-919.

FRITZ, J. M. & GEORGE, S. Z. 2002. Identifying psychosocial variables in patients with acute work-related low back pain: the importance of fear-avoidance beliefs. *Phys Ther,* 82**,** 973-83.

FRYMOYER, J. W., POPE, M. H., CLEMENTS, J. H., WILDER, D. G., MACPHERSON, B. & ASHIKAGA, T. 1983. Risk factors in low-back pain. An epidemiological survey. *J Bone Joint Surg Am,* 65**,** 213-8.

FUJII, R., SAKAURA, H., MUKAI, Y., HOSONO, N., ISHII, T., IWASAKI, M., YOSHIKAWA, H. & SUGAMOTO, K. 2007. Kinematics of the lumbar spine in trunk rotation: in vivo three-dimensional analysis using magnetic resonance imaging. *Eur Spine J,* 16**,** 1867-74.

FUKAYA, T., MUTSUZAKI, H., IDA, H. & WADANO, Y. 2012. Two different protocols for knee joint motion analyses in the stance phase of gait: correlation of the rigid marker set and the point cluster technique. *Rehabil Res Pract,* 2012**,** 586348.

GAGNON, D., ARJMAND, N., PLAMONDON, A., SHIRAZI-ADL, A. & LARIVIERE, C. 2011. An improved multi-joint EMG-assisted optimization approach to estimate joint and muscle forces in a musculoskeletal model of the lumbar spine. *J Biomech,* 44**,** 1521-9.

GALBUSERA, F. & WILKE, H.-J. 2018. *Biomechanics of the Spine: Basic Concepts, Spinal Disorders and Treatments*, Academic Press.

GALLAGHER, S. & MARRAS, W. S. 2012. Tolerance of the lumbar spine to shear: a review and recommended exposure limits. *Clin Biomech (Bristol, Avon),* 27**,** 973-8.

GATTON, M. L., PEARCY, M. J. & PETTET, G. J. 1999. Difficulties in estimating muscle forces from muscle cross-sectional area. An example using the psoas major muscle. *Spine (Phila Pa 1976),* 24**,** 1487-93.

GHEZELBASH, F., ARJMAND, N. & SHIRAZI-ADL, A. 2015. Effect of intervertebral translational flexibilities on estimations of trunk muscle forces, kinematics, loads, and stability. *Comput Methods Biomech Biomed Engin,* 18**,** 1760-7.

GHEZELBASH, F., ESKANDARI, A. H., SHIRAZI-ADL, A., ARJMAND, N., EL-OUAAID, Z. & PLAMONDON, A. 2018. Effects of motion segment simulation and joint positioning on spinal loads in trunk musculoskeletal models. *J Biomech,* 70**,** 149-156.

GHEZELBASH, F., SHIRAZI-ADL, A., ARJMAND, N., EL-OUAAID, Z. & PLAMONDON, A. 2016. Subject-specific biomechanics of trunk: musculoskeletal scaling, internal loads and intradiscal pressure estimation. *Biomech Model Mechanobiol,* 15**,** 1699-1712.

GILL, K. P., BENNETT, S. J., SAVELSBERGH, G. J. & VAN DIEEN, J. H. 2007. Regional changes in spine posture at lift onset with changes in lift distance and lift style. *Spine (Phila Pa 1976),* 32**,** 1599-604.

GLOBAL BURDEN OF DISEASE STUDY, C. 2015. Global, regional, and national incidence, prevalence, and years lived with disability for 301 acute and chronic diseases and injuries in 188 countries, 1990-2013: a systematic analysis for the Global Burden of Disease Study 2013. *Lancet,* 386**,** 743-800.

GORE, M., SADOSKY, A., STACEY, B. R., TAI, K. S. & LESLIE, D. 2012. The burden of chronic low back pain: clinical comorbidities, treatment patterns, and health care costs in usual care settings. *Spine (Phila Pa 1976),* 37**,** E668-77.

GOULART, F. R.-D.-P. & VALLS-SOLÉ, J. 1999. Patterned electromyographic activity in the sit-to-stand movement. *Clinical neurophysiology,* 110**,** 1634-1640.

GRANATA, K. P. & MARRAS, W. S. 1993. An EMG-assisted model of loads on the lumbar spine during asymmetric trunk extensions. *J Biomech,* 26**,** 1429-38.

GRANATA, K. P. & MARRAS, W. S. 1995a. An EMG-assisted model of trunk loading during free-dynamic lifting. *J Biomech,* 28**,** 1309-17.

GRANATA, K. P. & MARRAS, W. S. 1995b. The influence of trunk muscle coactivity on dynamic spinal loads. *Spine (Phila Pa 1976),* 20**,** 913-9.

GRAY, H. 1918. Anatomy of the human body. Philadelphia, PA: Lea & Febiger.

HAGEN, K. B., HALLEN, J. & HARMS-RINGDAHL, K. 1993. Physiological and subjective responses to maximal repetitive lifting employing stoop and squat technique. *Eur J Appl Physiol Occup Physiol,* 67**,** 291-7.

HAMILL, J. & KNUTZEN, K. M. 2006. *Biomechanical basis of human movement*, Lippincott Williams & Wilkins.

HAMNER, S. R., SETH, A. & DELP, S. L. 2010. Muscle contributions to propulsion and support during running. *J Biomech,* 43**,** 2709-16.

HAN, K. S., ZANDER, T., TAYLOR, W. R. & ROHLMANN, A. 2012. An enhanced and validated generic thoraco-lumbar spine model for prediction of muscle forces. *Med Eng Phys,* 34**,** 709-16.

HANSEN, L., DE ZEE, M., RASMUSSEN, J., ANDERSEN, T. B., WONG, C. & SIMONSEN, E. B. 2006. Anatomy and biomechanics of the back muscles in the lumbar spine with reference to biomechanical modeling. *Spine (Phila Pa 1976),* 31**,** 1888-99.

HANSSON, T. H., KELLER, T. S. & SPENGLER, D. M. 1987. Mechanical behavior of the human lumbar spine. II. Fatigue strength during dynamic compressive loading. *J Orthop Res,* 5**,** 479-87.

HEMBORG, B., MORITZ, U. & LOWING, H. 1985. Intra-abdominal pressure and trunk muscle activity during lifting. IV. The causal factors of the intra-abdominal pressure rise. *Scand J Rehabil Med,* 17**,** 25-38.

HEMMERICH, A., BROWN, H., SMITH, S., MARTHANDAM, S. S. & WYSS, U. P. 2006. Hip, knee, and ankle kinematics of high range of motion activities of daily living. *J Orthop Res,* 24**,** 770-81.

HENEWEER, H., STAES, F., AUFDEMKAMPE, G., VAN RIJN, M. & VANHEES, L. 2011. Physical activity and low back pain: a systematic review of recent literature. *Eur Spine J,* 20**,** 826-45.

HEUER, F., SCHMIDT, H., CLAES, L. & WILKE, H. J. 2007. Stepwise reduction of functional spinal structures increase vertebral translation and intradiscal pressure. *J Biomech,* 40**,** 795-803.

HICKS, J. L., UCHIDA, T. K., SETH, A., RAJAGOPAL, A. & DELP, S. L. 2015. Is my model good enough? Best practices for verification and validation of musculoskeletal models and simulations of movement. *J Biomech Eng,* 137**,** 020905.

HIDES, J., GILMORE, C., STANTON, W. & BOHLSCHEID, E. 2008. Multifidus size and symmetry among chronic LBP and healthy asymptomatic subjects. *Manual therapy,* 13**,** 43-49.

HIDES, J. A., JULL, G. A. & RICHARDSON, C. A. 2001. Long-term effects of specific stabilizing exercises for first-episode low back pain. *Spine (Phila Pa 1976),* 26**,** E243-8.

HILL, A. V. 1938. The heat of shortening and the dynamic constants of muscle. *Proc. R. Soc. Lond. B,* 126**,** 136-195.

HODGES, P., HOLM, A. K., HANSSON, T. & HOLM, S. 2006. Rapid atrophy of the lumbar multifidus follows experimental disc or nerve root injury. *Spine (Phila Pa 1976),* 31**,** 2926-33.

HODGES, P. W., CRESSWELL, A. G., DAGGFELDT, K. & THORSTENSSON, A. 2001. In vivo measurement of the effect of intra-abdominal pressure on the human spine. *J Biomech,* 34**,** 347-53.

HODGES, P. W. & MOSELEY, G. L. 2003. Pain and motor control of the lumbopelvic region: effect and possible mechanisms. *J Electromyogr Kinesiol,* 13**,** 361-70.

HODGES, P. W. & RICHARDSON, C. A. 1996. Inefficient muscular stabilization of the lumbar spine associated with low back pain. A motor control evaluation of transversus abdominis. *Spine (Phila Pa 1976),* 21**,** 2640-50.

HODGES, P. W. & RICHARDSON, C. A. 1999. Altered trunk muscle recruitment in people with low back pain with upper limb movement at different speeds. *Arch Phys Med Rehabil,* 80**,** 1005-12.

HOLMES, M. W., TAT, J. & KEIR, P. J. 2015. Neuromechanical control of the forearm muscles during gripping with sudden flexion and extension wrist perturbations. *Comput Methods Biomech Biomed Engin,* 18**,** 1826-34.

HOLZBAUR, K. R., MURRAY, W. M. & DELP, S. L. 2005. A model of the upper extremity for simulating musculoskeletal surgery and analyzing neuromuscular control. *Ann Biomed Eng,* 33**,** 829-40.

HOOGENDOORN, W. E., BONGERS, P. M., DE VET, H. C., DOUWES, M., KOES, B. W., MIEDEMA, M. C., ARIENS, G. A. & BOUTER, L. M. 2000. Flexion and rotation of the trunk and lifting at work are risk factors for low back pain: results of a prospective cohort study. *Spine (Phila Pa 1976),* 25**,** 3087-92.

HSIANG, S., BROGMUS, G. & COURTNEY, K. 1997. Low back pain (LBP) and lifting technique-A review. *International Journal of Industrial Ergonomics,* 19**,** 59-74.

HUGHES, M. A. & SCHENKMAN, M. L. 1996. Chair rise strategy in the functionally impaired elderly. *J Rehabil Res Dev,* 33**,** 409-12.

HUGHES, R. E., CHAFFIN, D. B., LAVENDER, S. A. & ANDERSSON, G. B. 1994. Evaluation of muscle force prediction models of the lumbar trunk using surface electromyography. *J Orthop Res,* 12**,** 689-98.

IGNASIAK, D., DENDORFER, S. & FERGUSON, S. J. 2016a. Thoracolumbar spine model with articulated ribcage for the prediction of dynamic spinal loading. *J Biomech,* 49**,** 959-966.

IGNASIAK, D., FERGUSON, S. J. & ARJMAND, N. 2016b. A rigid thorax assumption affects model loading predictions at the upper but not lower lumbar levels. *J Biomech,* 49**,** 3074-3078.

JACKSON, M., SOLOMONOW, M., ZHOU, B., BARATTA, R. V. & HARRIS, M. 2001. Multifidus EMG and tension-relaxation recovery after prolonged static lumbar flexion. *Spine (Phila Pa 1976),* 26**,** 715-23.

JEFFRIES, L. J., MILANESE, S. F. & GRIMMER-SOMERS, K. A. 2007. Epidemiology of adolescent spinal pain: a systematic overview of the research literature. *Spine (Phila Pa 1976),* 32**,** 2630-7.

JOHN, C. T., SETH, A., SCHWARTZ, M. H. & DELP, S. L. 2012. Contributions of muscles to mediolateral ground reaction force over a range of walking speeds. *J Biomech,* 45**,** 2438-43.

JUNG, N. H., KIM, H. & CHANG, M. 2015. Discomfort and muscle activation during car egress in drivers with hemiplegia following stroke. *J Phys Ther Sci,* 27**,** 3775-7.

KATZ, J. N. 2006. Lumbar disc disorders and low-back pain: socioeconomic factors and consequences. *J Bone Joint Surg Am,* 88 Suppl 2**,** 21-4.

KELLER, T. S. & ROY, A. L. 2002. Posture-dependent isometric trunk extension and flexion strength in normal male and female subjects. *J Spinal Disord Tech,* 15**,** 312-8.

KETTLER, A., MARIN, F., SATTELMAYER, G., MOHR, M., MANNEL, H., DURSELEN, L., CLAES, L. & WILKE, H. J. 2004. Finite helical axes of motion are a useful tool to describe the three-dimensional in vitro kinematics of the intact, injured and stabilised spine. *Eur Spine J,* 13**,** 553-9.

KHALAF, K. A., PARNIANPOUR, M., SPARTO, P. J. & SIMON, S. R. 1997. Modeling of functional trunk muscle performance: interfacing ergonomics and spine rehabilitation in response to the ADA. *J Rehabil Res Dev,* 34**,** 459-69.

KIM, H. K. & ZHANG, Y. 2017. Estimation of lumbar spinal loading and trunk muscle forces during asymmetric lifting tasks: application of whole-body musculoskeletal modelling in OpenSim. *Ergonomics,* 60**,** 563-576.

KINGMA, I., BUSSCHER, I., VAN DER VEEN, A. J., VERKERKE, G. J., VELDHUIZEN, A. G., HOMMINGA, J. & VAN DIEEN, J. H. 2018. Coupled motions in human and porcine thoracic and lumbar spines. *J Biomech,* 70**,** 51-58.

KINGMA, I., DE LOOZE, M. P., TOUSSAINT, H. M., KLIJNSMA, H. G. & BRUIJNEN, T. B. 1996. Validation of a full body 3-D dynamic linked segment model. *Human Movement Science,* 15**,** 833-860.

KINGMA, I., FABER, G. S., BAKKER, A. J. & VAN DIEEN, J. H. 2006. Can low back loading during lifting be reduced by placing one leg beside the object to be lifted? *Phys Ther,* 86**,** 1091-105.

KINGMA, I., FABER, G. S. & VAN DIEEN, J. H. 2010. How to lift a box that is too large to fit between the knees. *Ergonomics,* 53**,** 1228-38.

KINGMA, I., FABER, G. S. & VAN DIEEN, J. H. 2016. Supporting the upper body with the hand on the thigh reduces back loading during lifting. *J Biomech,* 49**,** 881-889.

KINGMA, I. & VAN DIEEN, J. H. 2004. Lifting over an obstacle: effects of one-handed lifting and hand support on trunk kinematics and low back loading. *J Biomech,* 37**,** 249-55.

KINGMA, I., VAN DIEEN, J. H., DE LOOZE, M., TOUSSAINT, H. M., DOLAN, P. & BATEN, C. T. 1998. Asymmetric low back loading in asymmetric lifting movements is not prevented by pelvic twist. *J Biomech,* 31**,** 527-34.

KRISMER, M., VAN TULDER, M., LOW BACK PAIN GROUP OF THE, B. & JOINT HEALTH STRATEGIES FOR EUROPE, P. 2007. Strategies for prevention and management of musculoskeletal conditions. Low back pain (non-specific). *Best Pract Res Clin Rheumatol,* 21**,** 77-91.

KUMAR, S. 1984. The physiological cost of three different methods of lifting in sagittal and lateral planes. *Ergonomics,* 27**,** 425-33.

KUMAR, S., DUFRESNE, R. M. & VAN SCHOOR, T. 1995a. Human trunk strength profile in flexion and extension. *Spine (Phila Pa 1976),* 20**,** 160-8.

KUMAR, S., DUFRESNE, R. M. & VAN SCHOOR, T. 1995b. Human trunk strength profile in lateral flexion and axial rotation. *Spine (Phila Pa 1976),* 20**,** 169-77.

LAMBRECHT, J. M., AUDU, M. L., TRIOLO, R. J. & KIRSCH, R. F. 2009. Musculoskeletal model of trunk and hips for development of seated-posture-control neuroprosthesis. *J Rehabil Res Dev,* 46**,** 515-28.

LARIVIERE, C., ARSENAULT, A. B., GRAVEL, D., GAGNON, D. & LOISEL, P. 2003. Surface electromyography assessment of back muscle intrinsic properties. *J Electromyogr Kinesiol,* 13**,** 305-18.

LARIVIERE, C., GAGNON, D. & LOISEL, P. 2002. A biomechanical comparison of lifting techniques between subjects with and without chronic low back pain during freestyle lifting and lowering tasks. *Clin Biomech (Bristol, Avon),* 17**,** 89-98.

LAVENDER, S. A., LI, Y. C., ANDERSSON, G. B. & NATARAJAN, R. N. 1999. The effects of lifting speed on the peak external forward bending, lateral bending, and twisting spine moments. *Ergonomics,* 42**,** 111-25.

LEWEK, M. D., RUDOLPH, K. S. & SNYDER-MACKLER, L. 2004. Control of frontal plane knee laxity during gait in patients with medial compartment knee osteoarthritis. *Osteoarthritis Cartilage,* 12**,** 745-51.

LLOYD, D. G. & BESIER, T. F. 2003. An EMG-driven musculoskeletal model to estimate muscle forces and knee joint moments in vivo. *J Biomech,* 36**,** 765-76.

MACDONALD, D., MOSELEY, G. L. & HODGES, P. W. 2009. Why do some patients keep hurting their back? Evidence of ongoing back muscle dysfunction during remission from recurrent back pain. *Pain,* 142**,** 183-8.

MACINTOSH, J. E. & BOGDUK, N. 1986. The biomechanics of the lumbar multifidus. *Clin Biomech (Bristol, Avon),* 1**,** 205-13.

MACINTOSH, J. E. & BOGDUK, N. 1987. 1987 Volvo award in basic science. The morphology of the lumbar erector spinae. *Spine (Phila Pa 1976),* 12**,** 658-68.

MACINTOSH, J. E., VALENCIA, F., BOGDUK, N. & MUNRO, R. R. 1986. The morphology of the human lumbar multifidus. *Clin Biomech (Bristol, Avon),* 1**,** 196-204.

MAGANARIS, C. N., BALTZOPOULOS, V., BALL, D. & SARGEANT, A. J. 2001. In vivo specific tension of human skeletal muscle. *J Appl Physiol (1985),* 90**,** 865-72.

MAK, M. K., LEVIN, O., MIZRAHI, J. & HUI-CHAN, C. W. 2003. Joint torques during sit-to-stand in healthy subjects and people with Parkinson's disease. *Clinical Biomechanics,* 18**,** 197-206.

MANIADAKIS, N. & GRAY, A. 2000. The economic burden of back pain in the UK. *Pain,* 84**,** 95-103.

MANTOAN, A., PIZZOLATO, C., SARTORI, M., SAWACHA, Z., COBELLI, C. & REGGIANI, M. 2015. MOtoNMS: A MATLAB toolbox to process motion data for neuromusculoskeletal modeling and simulation. *Source Code Biol Med,* 10**,** 12.

MARRAS, W. 1987. Trunk motion during lifting: temporal relations among loading factors. *International journal of industrial ergonomics,* 1**,** 159-167.

MARRAS, W. S. & DAVIS, K. G. 1998. Spine loading during asymmetric lifting using one versus two hands. *Ergonomics,* 41**,** 817-34.

MARRAS, W. S., DAVIS, K. G., FERGUSON, S. A., LUCAS, B. R. & GUPTA, P. 2001. Spine loading characteristics of patients with low back pain compared with asymptomatic individuals. *Spine (Phila Pa 1976),* 26**,** 2566-74.

MARRAS, W. S., FERGUSON, S. A., LAVENDER, S. A., SPLITTSTOESSER, R. E. & YANG, G. 2014. Cumulative spine loading and clinically meaningful declines in low-back function. *Hum Factors,* 56**,** 29-43.

MARRAS, W. S. & GRANATA, K. P. 1995. A biomechanical assessment and model of axial twisting in the thoracolumbar spine. *Spine (Phila Pa 1976),* 20**,** 1440-51.

MARRAS, W. S., LAVENDER, S. A., LEURGANS, S. E., FATHALLAH, F. A., FERGUSON, S. A., ALLREAD, W. G. & RAJULU, S. L. 1995. Biomechanical risk factors for occupationally related low back disorders. *Ergonomics,* 38**,** 377-410.

MARRAS, W. S. & MIRKA, G. A. 1996. Intra-abdominal pressure during trunk extension motions. *Clin Biomech (Bristol, Avon),* 11**,** 267-274.

MARRAS, W. S. & SOMMERICH, C. M. 1991. A three-dimensional motion model of loads on the lumbar spine: I. Model structure. *Hum Factors,* 33**,** 123-37.

MARTELLI, S., CALVETTI, D., SOMERSALO, E. & VICECONTI, M. 2015. Stochastic modelling of muscle recruitment during activity. *Interface Focus,* 5**,** 20140094.

MCGILL, S. 2007. *Low back disorders: evidence-based prevention and rehabilitation,* Human Kinetics.

MCGILL, S. & BROWN, S. 1992. Creep response of the lumbar spine to prolonged full flexion. *Clinical Biomechanics,* 7**,** 43-46.

MCGILL, S., JUKER, D. & KROPF, P. 1996. Quantitative intramuscular myoelectric activity of quadratus lumborum during a wide variety of tasks. *Clinical biomechanics,* 11**,** 170-172.

MCGILL, S., NORMAN, R. & SHARRATT, M. 1990. The effect of an abdominal belt on trunk muscle activity and intra-abdominal pressure during squat lifts. *Ergonomics,* 33**,** 147-160.

MCGILL, S. M. 1991a. Electromyographic activity of the abdominal and low back musculature during the generation of isometric and dynamic axial trunk torque: implications for lumbar mechanics. *J Orthop Res,* 9**,** 91-103.

MCGILL, S. M. 1991b. Electromyographic activity of the abdominal and low back musculature during the generation of isometric and dynamic axial trunk torque: implications for lumbar mechanics. *Journal of Orthopaedic Research,* 9**,** 91-103.

MCGILL, S. M. 1992. A myoelectrically based dynamic three-dimensional model to predict loads on lumbar spine tissues during lateral bending. *J Biomech,* 25**,** 395-414.

MCGILL, S. M. 1997. The biomechanics of low back injury: implications on current practice in industry and the clinic. *J Biomech,* 30**,** 465-75.

MCGILL, S. M., GRENIER, S., KAVCIC, N. & CHOLEWICKI, J. 2003. Coordination of muscle activity to assure stability of the lumbar spine. *J Electromyogr Kinesiol,* 13**,** 353-9.

MCGILL, S. M. & NORMAN, R. W. 1985. Dynamically and statically determined low back moments during lifting. *Journal of Biomechanics,* 18**,** 877-885.

MCGILL, S. M. & NORMAN, R. W. 1986. Partitioning of the L4-L5 dynamic moment into disc, ligamentous, and muscular components during lifting. *Spine (Phila Pa 1976),* 11**,** 666-78.

MCGILL, S. M. & NORMAN, R. W. 1987a. Effects of an anatomically detailed erector spinae model on L4/L5 disc compression and shear. *J Biomech,* 20**,** 591-600.

MCGILL, S. M. & NORMAN, R. W. 1987b. Reassessment of the role of intra-abdominal pressure in spinal compression. *Ergonomics,* 30**,** 1565-88.

MCGILL, S. M., NORMAN, R. W., YINGLING, V. R., WELLS, R. P. & NEUMANN, P. 1998. Shear Happens! Suggested guidelines for ergonomists to reduce the risk of low back injury from shear loading. *The 30th Annual Conference of the Human Factors Association of Canada (HFAC).* Mississauga, Ontario, Canada.

MILBURN, P. D. & BARRETT, R. S. 1999. Lumbosacral loads in bedmaking. *Appl Ergon,* 30**,** 263-73.

MILLARD, M., UCHIDA, T., SETH, A. & DELP, S. L. 2013. Flexing computational muscle: modeling and simulation of musculotendon dynamics. *J Biomech Eng,* 135**,** 021005.

NACHEMSON, A. 1960. Lumbar intradiscal pressure. Experimental studies on post-mortem material. *Acta Orthop Scand Suppl,* 43**,** 1-104.

NACHEMSON, A. 1965. The Effect of Forward Leaning on Lumbar Intradiscal Pressure. *Acta Orthop Scand,* 35**,** 314-28.

NASERKHAKI, S., ARJMAND, N., SHIRAZI-ADL, A., FARAHMAND, F. & EL-RICH, M. 2018. Effects of eight different ligament property datasets on biomechanics of a lumbar L4-L5 finite element model. *J Biomech,* 70**,** 33-42.

NELSON-WONG, E., HOWARTH, S., WINTER, D. A. & CALLAGHAN, J. P. 2009. Application of autocorrelation and cross-correlation analyses in human movement and rehabilitation research. *J Orthop Sports Phys Ther,* 39**,** 287-95.

NEVINS, D. D., ZHENG, L. & VASAVADA, A. N. 2014. Inter-individual variation in vertebral kinematics affects predictions of neck musculoskeletal models. *J Biomech,* 47**,** 3288-94.

NIOSH 1981. Work Practices Guide for Manual Lifting. Cincinnati, OH: National Institute for Occupational Safety and Health.

NORMAN, R., WELLS, R., NEUMANN, P., FRANK, J., SHANNON, H. & KERR, M. 1998. A comparison of peak vs cumulative physical work exposure risk factors for the reporting of low back pain in the automotive industry. *Clin Biomech (Bristol, Avon),* 13**,** 561-573.

NYGÅRD, C.-H., MERISALO, T., AROLA, H., MANKA, M.-L. & HUHTALA, H. 1998. Effects of work changes and training in lifting technique on physical strain: A pilot study among female workers of different ages. *International Journal of Industrial Ergonomics,* 21**,** 91-98.

O'BRIEN, T. D., REEVES, N. D., BALTZOPOULOS, V., JONES, D. A. & MAGANARIS, C. N. 2010. In vivo measurements of muscle specific tension in adults and children. *Exp Physiol,* 95**,** 202-10.

OCHIA, R. S., INOUE, N., RENNER, S. M., LORENZ, E. P., LIM, T. H., ANDERSSON, G. B. & AN, H. S. 2006. Three-dimensional in vivo measurement of lumbar spine segmental motion. *Spine (Phila Pa 1976),* 31**,** 2073-8.

OXLAND, T. R., CRISCO, J. J., 3RD, PANJABI, M. M. & YAMAMOTO, I. 1992. The effect of injury on rotational coupling at the lumbosacral joint. A biomechanical investigation. *Spine (Phila Pa 1976),* 17**,** 74-80.

PANDY, M. G. 2001. Computer modeling and simulation of human movement. *Annu Rev Biomed Eng,* 3**,** 245-73.

PANJABI, M. M., GOEL, V. K. & TAKATA, K. 1982. Physiologic strains in the lumbar spinal ligaments. An in vitro biomechanical study 1981 Volvo Award in Biomechanics. *Spine (Phila Pa 1976),* 7**,** 192-203.

PEARCY, M., PORTEK, I. & SHEPHERD, J. 1984. Three-dimensional x-ray analysis of normal movement in the lumbar spine. *Spine (Phila Pa 1976),* 9**,** 294-7.

PEARCY, M. J. 1985. Stereo radiography of lumbar spine motion. *Acta Orthop Scand Suppl,* 212**,** 1-45.

PEARCY, M. J. & BOGDUK, N. 1988. Instantaneous axes of rotation of the lumbar intervertebral joints. *Spine (Phila Pa 1976),* 13**,** 1033-41.

PEARCY, M. J. & TIBREWAL, S. B. 1984. Axial rotation and lateral bending in the normal lumbar spine measured by three-dimensional radiography. *Spine (Phila Pa 1976),* 9**,** 582-7.

PEREY, O. 1957. Fracture of the vertebral end-plate in the lumbar spine; an experimental biochemical investigation. *Acta Orthop Scand Suppl,* 25**,** 1-101.

PHILLIPS, S., MERCER, S. & BOGDUK, N. 2008. Anatomy and biomechanics of quadratus lumborum. *Proc Inst Mech Eng H,* 222**,** 151-9.

POLGA, D. J., BEAUBIEN, B. P., KALLEMEIER, P. M., SCHELLHAS, K. P., LEW, W. D., BUTTERMANN, G. R. & WOOD, K. B. 2004. Measurement of in vivo intradiscal pressure in healthy thoracic intervertebral discs. *Spine (Phila Pa 1976),* 29**,** 1320-4.

POLLINTINE, P., PRZYBYLA, A. S., DOLAN, P. & ADAMS, M. A. 2004. Neural arch load-bearing in old and degenerated spines. *J Biomech,* 37**,** 197-204.

POTVIN, C. & TOUSIGNANT, D. 1996. Evolutionary consequences of simulated global change: genetic adaptation or adaptive phenotypic plasticity. *Oecologia,* 108**,** 683-693.

POTVIN, J. R. & BROWN, S. H. 2005. An equation to calculate individual muscle contributions to joint stability. *J Biomech,* 38**,** 973-80.

POTVIN, J. R., MCGILL, S. M. & NORMAN, R. W. 1991. Trunk muscle and lumbar ligament contributions to dynamic lifts with varying degrees of trunk flexion. *Spine (Phila Pa 1976),* 16**,** 1099-107.

PUA, Y. H., WRIGLEY, T. V., COWAN, S. M. & BENNELL, K. L. 2008. Intrarater test-retest reliability of hip range of motion and hip muscle strength measurements in persons with hip osteoarthritis. *Arch Phys Med Rehabil,* 89**,** 1146-54.

RAABE, M. E. & CHAUDHARI, A. M. 2016. An investigation of jogging biomechanics using the full-body lumbar spine model: Model development and validation. *J Biomech,* 49**,** 1238-43.

RAJAGOPAL, A., DEMBIA, C. L., DEMERS, M. S., DELP, D. D., HICKS, J. L. & DELP, S. L. 2016. Full-Body Musculoskeletal Model for Muscle-Driven Simulation of Human Gait. *IEEE Trans Biomed Eng,* 63**,** 2068-79.

RASCHKE, U. & CHAFFIN, D. B. 1996. Support for a linear length-tension relation of the torso extensor muscles: an investigation of the length and velocity EMG-force relationships. *J Biomech,* 29**,** 1597-604.

REINBOLT, J. A., SETH, A. & DELP, S. L. 2011. Simulation of human movement: applications using OpenSim. *Procedia Iutam,* 2**,** 186-198.

ROBERTSON, G., CALDWELL, G., HAMILL, J., KAMEN, G. & WHITTLESEY, S. 2013. *Research methods in biomechanics, 2E*, Human Kinetics.

ROHLMANN, A., GRAICHEN, F., KAYSER, R., BENDER, A. & BERGMANN, G. 2008. Loads on a telemeterized vertebral body replacement measured in two patients. *Spine (Phila Pa 1976),* 33**,** 1170-9.

ROHLMANN, A., POHL, D., BENDER, A., GRAICHEN, F., DYMKE, J., SCHMIDT, H. & BERGMANN, G. 2014a. Activities of everyday life with high spinal loads. *PLoS One,* 9**,** e98510.

ROHLMANN, A., SCHWACHMEYER, V., GRAICHEN, F. & BERGMANN, G. 2014b. Spinal loads during post-operative physiotherapeutic exercises. *PLoS One,* 9**,** e102005.

RUBIN, D. I. 2007. Epidemiology and risk factors for spine pain. *Neurol Clin,* 25**,** 353-71.

SANTAGUIDA, P. L. & MCGILL, S. M. 1995. The psoas major muscle: a three-dimensional geometric study. *J Biomech,* 28**,** 339-45.

SATO, K., KIKUCHI, S. & YONEZAWA, T. 1999. In vivo intradiscal pressure measurement in healthy individuals and in patients with ongoing back problems. *Spine (Phila Pa 1976),* 24**,** 2468-74.

SCHIPPLEIN, O. D., REINSEL, T. E., ANDERSSON, G. B. & LAVENDER, S. A. 1995. The influence of initial horizontal weight placement on the loads at the lumbar spine while lifting. *Spine (Phila Pa 1976),* 20**,** 1895-8.

SCHOFIELD, D. J., SHRESTHA, R. N., CUNICH, M., TANTON, R., KELLY, S., PASSEY, M. E. & VEERMAN, L. J. 2015. Lost productive life years caused by chronic conditions in Australians aged 45-64 years, 2010-2030. *Med J Aust,* 203**,** 260 e1-6.

SCHULTZ, A., ANDERSSON, G., ORTENGREN, R., HADERSPECK, K. & NACHEMSON, A. 1982a. Loads on the lumbar spine. Validation of a biomechanical analysis by measurements of intradiscal pressures and myoelectric signals. *J Bone Joint Surg Am,* 64**,** 713-20.

SCHULTZ, A. B., ANDERSSON, G. B., HADERSPECK, K., ORTENGREN, R., NORDIN, M. & BJORK, R. 1982b. Analysis and measurement of lumbar trunk loads in tasks involving bends and twists. *J Biomech,* 15**,** 669-75.

SELYA, A. S., ROSE, J. S., DIERKER, L. C., HEDEKER, D. & MERMELSTEIN, R. J. 2012. A Practical Guide to Calculating Cohen's f(2), a Measure of Local Effect Size, from PROC MIXED. *Front Psychol,* 3**,** 111.

SENTELER, M., WEISSE, B., ROTHENFLUH, D. A. & SNEDEKER, J. G. 2015. Intervertebral reaction force prediction using an enhanced assembly of OpenSim models. *Comput Methods Biomech Biomed Engin***,** 1-11.

SHAHVARPOUR, A., SHIRAZI-ADL, A., LARIVIERE, C. & BAZRGARI, B. 2015a. Computation of trunk stability in forward perturbations: effects of preload, perturbation load, initial flexion and abdominal preactivation. *J Biomech,* 48**,** 716-20.

SHAHVARPOUR, A., SHIRAZI-ADL, A., LARIVIERE, C. & BAZRGARI, B. 2015b. Trunk active response and spinal forces in sudden forward loading: analysis of the role of perturbation load and pre-perturbation conditions by a kinematics-driven model. *J Biomech,* 48**,** 44-52.

SHIRAZI-ADL, A. 1991. Finite-element evaluation of contact loads on facets of an L2-L3 lumbar segment in complex loads. *Spine (Phila Pa 1976),* 16**,** 533-41.

SHIRAZI-ADL, A. 2006. Analysis of large compression loads on lumbar spine in flexion and in torsion using a novel wrapping element. *J Biomech,* 39**,** 267-75.

SHIRAZI-ADL, A., AHMED, A. M. & SHRIVASTAVA, S. C. 1986. Mechanical response of a lumbar motion segment in axial torque alone and combined with compression. *Spine (Phila Pa 1976),* 11**,** 914-27.

SHIRAZI-ADL, A., EL-RICH, M., POP, D. G. & PARNIANPOUR, M. 2005. Spinal muscle forces, internal loads and stability in standing under various postures and loads--application of kinematics-based algorithm. *Eur Spine J,* 14**,** 381-92.

SHIRAZI-ADL, A., SADOUK, S., PARNIANPOUR, M., POP, D. & EL-RICH, M. 2002. Muscle force evaluation and the role of posture in human lumbar spine under compression. *Eur Spine J,* 11**,** 519-26.

SIGNORILE, J. F., KACSIK, D., PERRY, A., ROBERTSON, B., WILLIAMS, R., LOWENSTEYN, I., DIGEL, S., CARUSO, J. & LEBLANC, W. G. 1995. The effect of knee and foot position on the electromyographical activity of the superficial quadriceps. *J Orthop Sports Phys Ther,* 22**,** 2-9.

SIHVONEN, T., LINDGREN, K. A., AIRAKSINEN, O. & MANNINEN, H. 1997. Movement disturbances of the lumbar spine and abnormal back muscle electromyographic findings in recurrent low back pain. *Spine (Phila Pa 1976),* 22**,** 289-95.

SMEDLEY, J., EGGER, P., COOPER, C. & COGGON, D. 1995. Manual handling activities and risk of low back pain in nurses. *Occup Environ Med,* 52**,** 160-3.

STAUDENMANN, D., POTVIN, J. R., KINGMA, I., STEGEMAN, D. F. & VAN DIEEN, J. H. 2007. Effects of EMG processing on biomechanical models of muscle joint systems: sensitivity of trunk muscle moments, spinal forces, and stability. *J Biomech,* 40**,** 900-9.

STEELE, K. M., SETH, A., HICKS, J. L., SCHWARTZ, M. S. & DELP, S. L. 2010. Muscle contributions to support and progression during single-limb stance in crouch gait. *J Biomech,* 43**,** 2099-105.

STOKES, I. A. & GARDNER-MORSE, M. 1995. Lumbar spine maximum efforts and muscle recruitment patterns predicted by a model with multijoint muscles and joints with stiffness. *J Biomech,* 28**,** 173-86.

STOKES, I. A. & GARDNER-MORSE, M. 1999. Quantitative anatomy of the lumbar musculature. *J Biomech,* 32**,** 311-6.

STOKES, I. A., GARDNER-MORSE, M., HENRY, S. M. & BADGER, G. J. 2000. Decrease in trunk muscular response to perturbation with preactivation of lumbar spinal musculature. *Spine (Phila Pa 1976),* 25**,** 1957-64.

STOKES, I. A., GARDNER-MORSE, M. G. & HENRY, S. M. 2010. Intra-abdominal pressure and abdominal wall muscular function: Spinal unloading mechanism. *Clin Biomech (Bristol, Avon),* 25**,** 859-66.

STOKES, I. A., WILDER, D. G., FRYMOYER, J. W. & POPE, M. H. 1981. 1980 Volvo award in clinical sciences. Assessment of patients with low-back pain by biplanar radiographic measurement of intervertebral motion. *Spine (Phila Pa 1976),* 6**,** 233-40.

STRATFORD, P. W., BINKLEY, J., SOLOMON, P., FINCH, E., GILL, C. & MORELAND, J. 1996. Defining the minimum level of detectable change for the Roland-Morris questionnaire. *Phys Ther,* 76**,** 359-65; discussion 366-8.

SULLIVAN, M. J. L., BISHOP, S. R. & PIVIK, J. 1995. The Pain Catastrophizing Scale: Development and validation. *Psychological Assessment,* 7**,** 524-532.

TAKAHASHI, I., KIKUCHI, S., SATO, K. & SATO, N. 2006. Mechanical load of the lumbar spine during forward bending motion of the trunk-a biomechanical study. *Spine (Phila Pa 1976),* 31**,** 18-23.

THELEN, D. G. 2003. Adjustment of muscle mechanics model parameters to simulate dynamic contractions in older adults. *J Biomech Eng,* 125**,** 70-7.

THELEN, D. G., CHUMANOV, E. S., SHERRY, M. A. & HEIDERSCHEIT, B. C. 2006. Neuromusculoskeletal models provide insights into the mechanisms and rehabilitation of hamstring strains. *Exerc Sport Sci Rev,* 34**,** 135-41.

VAN DEN BOGERT, A., GEIJTENBEEK, T. & EVEN-ZOHAR, O. Real-time estimation of muscle forces from inverse dynamics. Annual Meeting of the American Society of Biomechanics (NACOB), 2008.

VAN DIEEN, J. H. 1997. Are recruitment patterns of the trunk musculature compatible with a synergy based on the maximization of endurance? *J Biomech,* 30**,** 1095-100.

VAN DIEËN, J. H., HOOZEMANS, M. J. M. & TOUSSAINT, H. M. 1999. Stoop or squat: a review of biomechanical studies on lifting technique. *Clinical Biomechanics,* 14**,** 685-696.

VAN DIEEN, J. H. & KINGMA, I. 2005. Effects of antagonistic co-contraction on differences between electromyography based and optimization based estimates of spinal forces. *Ergonomics,* 48**,** 411-26.

VAN DIEEN, J. H., THISSEN, C. E., VAN DE VEN, A. J. & TOUSSAINT, H. M. 1991. The electro-mechanical delay of the erector spinae muscle: influence of rate of force development, fatigue and electrode location. *Eur J Appl Physiol Occup Physiol,* 63**,** 216-22.

VAN DIEEN, J. H., VAN DER BURG, P., RAAIJMAKERS, T. A. & TOUSSAINT, H. M. 1998. Effects of repetitive lifting on kinematics: inadequate anticipatory control or adaptive changes? *J Mot Behav,* 30**,** 20-32.

VASAVADA, A. N., LI, S. & DELP, S. L. 1998. Influence of muscle morphometry and moment arms on the moment-generating capacity of human neck muscles. *Spine (Phila Pa 1976),* 23**,** 412-22.

WACHOWSKI, M., MANSOUR, M., LEE, C., ACKENHAUSEN, A., SPIERING, S., FANGHÄNEL, J., DUMONT, C., KUBEIN-MEESENBURG, D. & NÄGERL, H. 2009. How do spinal segments move? *Journal of biomechanics,* 42**,** 2286-2293.

WADDELL, G., NEWTON, M., HENDERSON, I., SOMERVILLE, D. & MAIN, C. J. 1993. A Fear-Avoidance Beliefs Questionnaire (FABQ) and the role of fear-avoidance beliefs in chronic low back pain and disability. *Pain,* 52**,** 157-68.

WADDELL, G. & SCHOENE, M. 2004. *The back pain revolution*, Elsevier Health Sciences.

WATERS, T. R., PUTZ-ANDERSON, V., GARG, A. & FINE, L. J. 1993. Revised NIOSH equation for the design and evaluation of manual lifting tasks. *Ergonomics,* 36**,** 749-76.

WELBERGEN, E., KEMPER, H. C., KNIBBE, J. J., TOUSSAINT, H. M. & CLYSEN, L. 1991. Efficiency and effectiveness of stoop and squat lifting at different frequencies. *Ergonomics,* 34**,** 613-24.

WILKE, H., NEEF, P., HINZ, B., SEIDEL, H. & CLAES, L. 2001. Intradiscal pressure together with anthropometric data--a data set for the validation of models. *Clin Biomech (Bristol, Avon),* 16 Suppl 1**,** S111-26.

WILKE, H. J., NEEF, P., CAIMI, M., HOOGLAND, T. & CLAES, L. E. 1999. New in vivo measurements of pressures in the intervertebral disc in daily life. *Spine (Phila Pa 1976),* 24**,** 755-62.

WILKENFELD, A. J., AUDU, M. L. & TRIOLO, R. J. 2006. Feasibility of functional electrical stimulation for control of seated posture after spinal cord injury: A simulation study. *J Rehabil Res Dev,* 43**,** 139-52.

WILSON, D. J., HICKEY, K. M., GORHAM, J. L. & CHILDERS, M. K. 1997. Lumbar spinal moments in chronic back pain patients during supported lifting: a dynamic analysis. *Arch Phys Med Rehabil,* 78**,** 967-72.

WONG, K. W., LUK, K. D., LEONG, J. C., WONG, S. F. & WONG, K. K. 2006. Continuous dynamic spinal motion analysis. *Spine (Phila Pa 1976),* 31**,** 414-9.

WOO, S. L., GOMEZ, M. A. & AKESON, W. H. 1985. *Mechanical behaviors of soft tissues: Measurements, modifications, injuries and treatment*, Norwalk.

WOOLF, A. D. & PFLEGER, B. 2003. Burden of major musculoskeletal conditions. *Bull World Health Organ,* 81**,** 646-56.

WRETENBERG, P. & ARBORELIUS, U. P. 1994. Power and work produced in different leg muscle groups when rising from a chair. *Eur J Appl Physiol Occup Physiol,* 68**,** 413-7.

WRIGLEY, A. T., ALBERT, W. J., DELUZIO, K. J. & STEVENSON, J. M. 2005. Differentiating lifting technique between those who develop low back pain and those who do not. *Clin Biomech (Bristol, Avon),* 20**,** 254-63.

ZAJAC, F. E. 1989. Muscle and tendon: properties, models, scaling, and application to biomechanics and motor control. *Crit Rev Biomed Eng,* 17**,** 359-411.

ZANDER, T., ROHLMANN, A. & BERGMANN, G. 2009. Influence of different artificial disc kinematics on spine biomechanics. *Clin Biomech (Bristol, Avon),* 24**,** 135-42.

Appendix A Screening questionnaire

Government of South Australia
SA Health

University of South Australia

THE UNIVERSITY of ADELAIDE

Adelaide Centre for Spinal Research

PO BOX 14, Rundle Mall
Adelaide SA 5000
Australia

T 08 8222 3056
F 08 8222 3064
www.sapathology.sa.gov.au

PARTICIPANT SCREENING FORM

Biomechanics of one-handed reaching and lifting tasks in people with low back pain.

Thank you for expressing an interest in participating in this study.

In order to ensure that you meet the criteria required to be a participant in this study, please answer the following questions.

1. What is your name? *(first, family)*		
2. What is your age? *(in years)*		
3. What is your date of birth? *(dd/mm/yyyy)*		
4. What is your sex? *(circle one)*	M☐	F☐
5. Are you comfortable following simple verbal and/or written instructions in English?	Yes☐	No☐
6. Weight *(kg or lb, please indicate)*		
7. Height *(cm or feet/inch, please indicate)*		
8. What is your dominant hand *(i.e. the hand you write with)*	Right☐	Left☐
9. Are you in general good health? *<u>If no, please specify the cause of your ill-health:</u>*	Yes☐	No☐
10. Do you suffer from, or have you been diagnosed, with chronic low back pain? *(pain persisting for over 3 months)* *<u>If yes, please specify the approximate duration of your low back pain:</u>*	Yes☐	No☐

11. Have you ever been diagnosed with a spinal condition called degenerative spondylolisthesis? *If yes, have you had spine surgery to address this diagnosis?:*	Yes☐	No☐
12. Have you ever been diagnosed with any other spinal condition, disease or injury? *If yes, please specify:* *Approximate date of occurrence:* *Is this condition, disease or injury ongoing:*	Yes☐	No☐
13. Have you ever had back (spine) surgery? *If yes, please specify:*	Yes☐	No☐
14. Have you been diagnosed with Spinal tumor(s)?	Yes☐	No☐
15. Have you been diagnosed with Cauda Equina Syndrome?	Yes☐	No☐
16. Have you been diagnosed with a muscle or nerve disease(s)?	Yes☐	No☐
17. Have you been diagnosed with a balance disorder(s)?	Yes☐	No☐
18. Are you currently taking any medications that affect your balance?	Yes☐	No☐
19. Do you have a history of falls? (i.e. falling/tripping over)	Yes☐	No☐
20. Have you been diagnosed with heart disease or cancer, or suffered a stroke? *If yes, please specify:*	Yes☐	No☐
21. Have you been diagnosed with osteoarthritis or rheumatoid arthritis of the hips or knees? *If yes, please specify:*	Yes☐	No☐
22. Do you have any disease or condition affecting your body that would limit your ability to bend down, and lift a small-to-medium weight from the floor?	Yes☐	No☐

If yes, please specify:		
23. Are you, or could you be, pregnant?	Yes☐	No☐
24. Do you have a pending or ongoing workers compensation claim?	Yes☐	No☐

Additional Comments *(please comment on any other information you think may help the investigators determine if you are suitable to participate)* :

Office use only:	ELIGIBLE – idiopathic low back pain
	ELIGIBLE – degenerative spondylolisthesis
	ELIGIBLE – other lumbar degeneration
	ELIGIBLE – healthy normal (age match)
	INELIGIBLE

Thank you for your time. We will contact you in 2-4 weeks to let you know if you are eligible for the study.

Appendix B Load cell Assembly and parts drawings

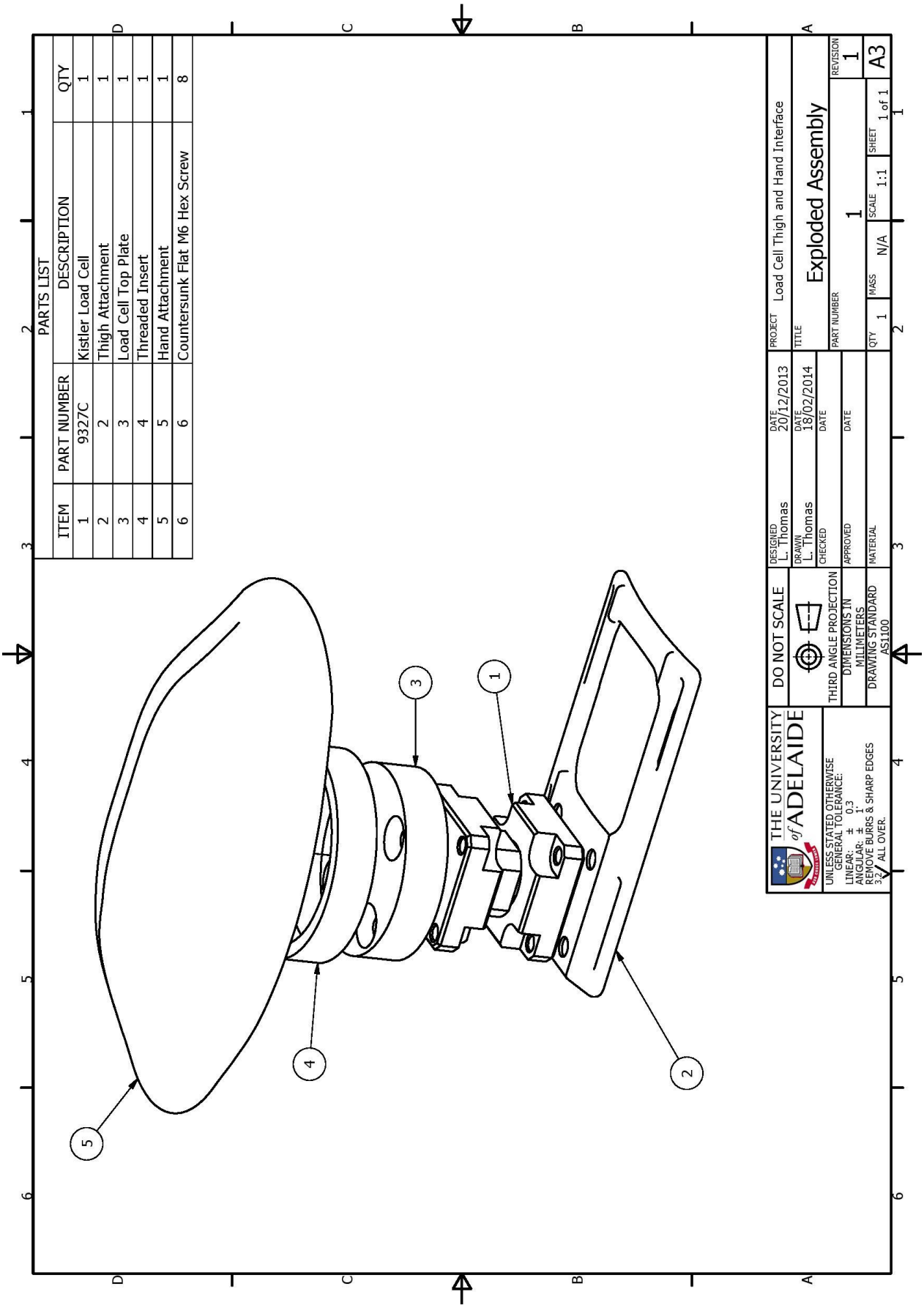

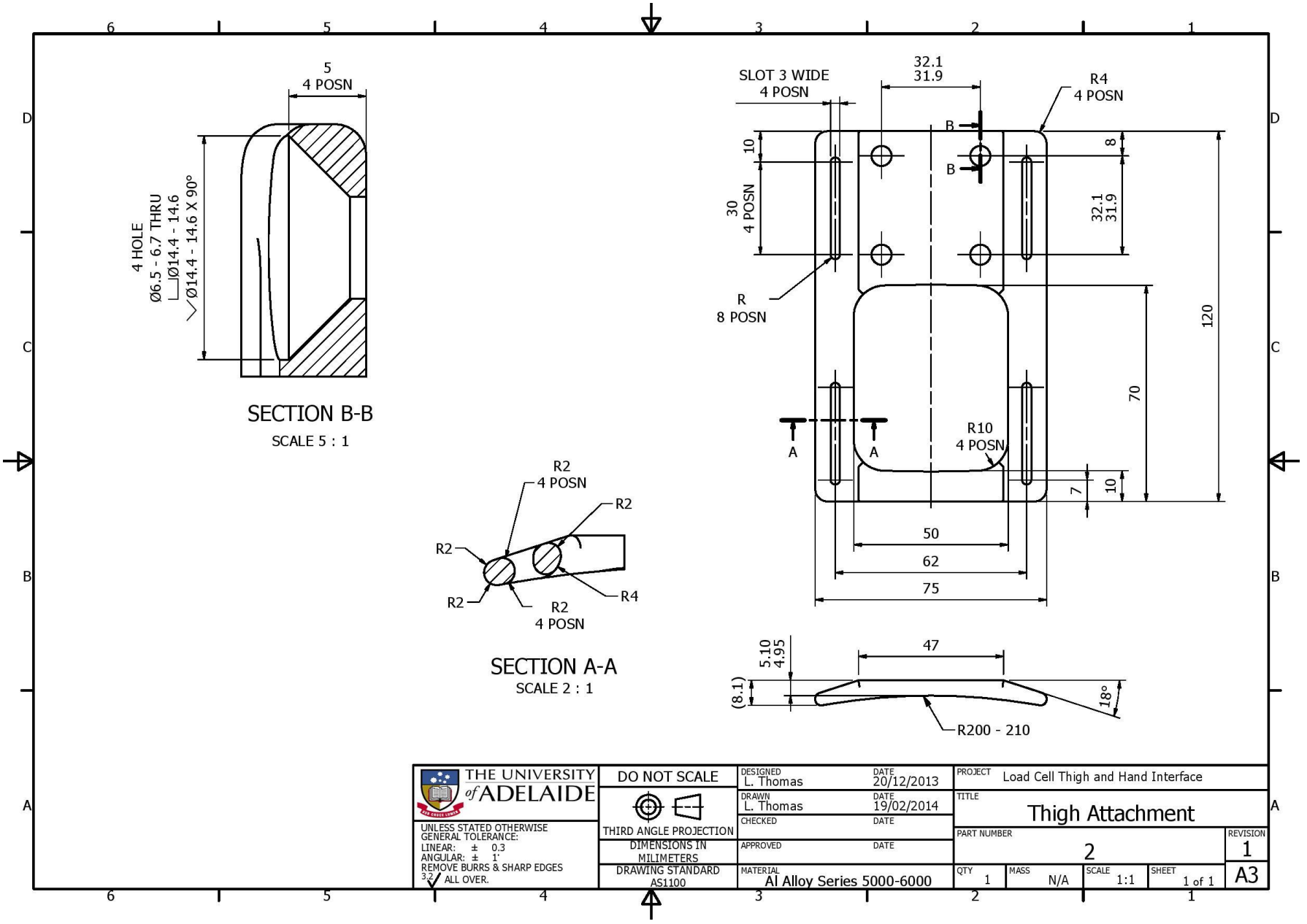

THE UNIVERSITY of ADELAIDE	DO NOT SCALE	DESIGNED L. Thomas	DATE 20/12/2013	PROJECT Load Cell Thigh and Hand Interface
UNLESS STATED OTHERWISE GENERAL TOLERANCE: LINEAR: ± 0.3 ANGULAR: ± 1° REMOVE BURRS & SHARP EDGES 3.2 ALL OVER.	THIRD ANGLE PROJECTION	DRAWN L. Thomas	DATE 19/02/2014	TITLE Thigh Attachment
	DIMENSIONS IN MILIMETERS	CHECKED	DATE	PART NUMBER 2 / REVISION 1
	DRAWING STANDARD AS1100	APPROVED	DATE	MATERIAL Al Alloy Series 5000-6000 / QTY 1 / MASS N/A / SCALE 1:1 / SHEET 1 of 1 / A3

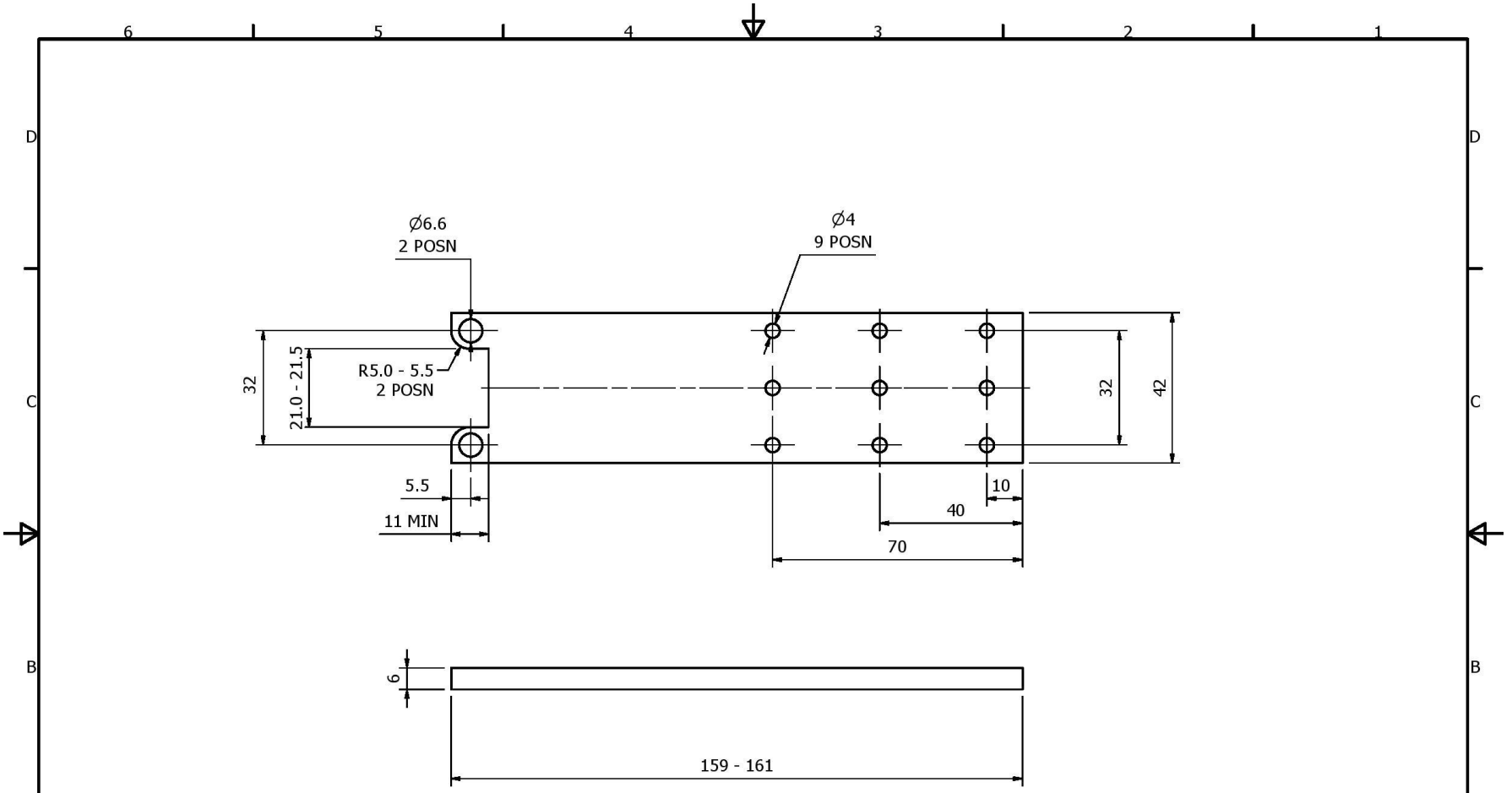

THE UNIVERSITY of ADELAIDE	DO NOT SCALE	DESIGNED L. Thomas DATE 14/05/2014	PROJECT FYP 1697 - LIFTING TECHNIQUES	
UNLESS STATED OTHERWISE GENERAL TOLERANCE: LINEAR: ± 0.3 ANGULAR: ± 1° REMOVE BURRS & SHARP EDGES 3.2 ALL OVER.	THIRD ANGLE PROJECTION	DRAWN L. Thomas DATE 16/05/2014	TITLE MARKER ATTACHMENT	
	DIMENSIONS IN MILIMETERS	CHECKED DATE	PART NUMBER 1	REVISION 1
	DRAWING STANDARD AS1100	APPROVED DATE	QTY 1 / MASS N/A / SCALE 1:1 / SHEET 1 of 1	A3
		MATERIAL PMMA Plastic		

SECTION A-A

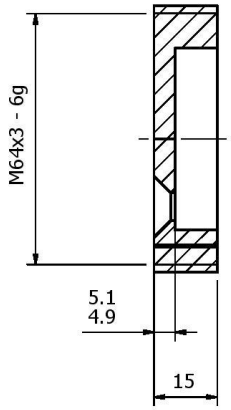

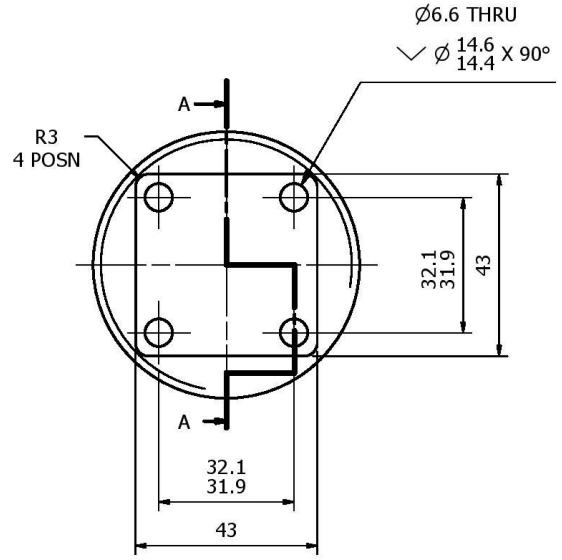

NOTE:
FINISH
ANODISE - CLEAR TO 20µm

THE UNIVERSITY of ADELAIDE	DO NOT SCALE	DESIGNED L. Thomas DATE 20/12/2013	PROJECT Load Cell Thigh and Hand Interface	
UNLESS STATED OTHERWISE GENERAL TOLERANCE: LINEAR: ± 0.3 ANGULAR: ± 1° REMOVE BURRS & SHARP EDGES 3.2 ALL OVER.	THIRD ANGLE PROJECTION	DRAWN L. Thomas DATE 19/02/2014	TITLE Load Cell Top Plate	
	DIMENSIONS IN MILIMETERS	CHECKED DATE	PART NUMBER 3	REVISION 1
	DRAWING STANDARD AS1100	APPROVED DATE	MATERIAL Al Alloy Series 5000-6000	QTY 1 / MASS N/A / SCALE 1:1 / SHEET 1 of 1 / A3

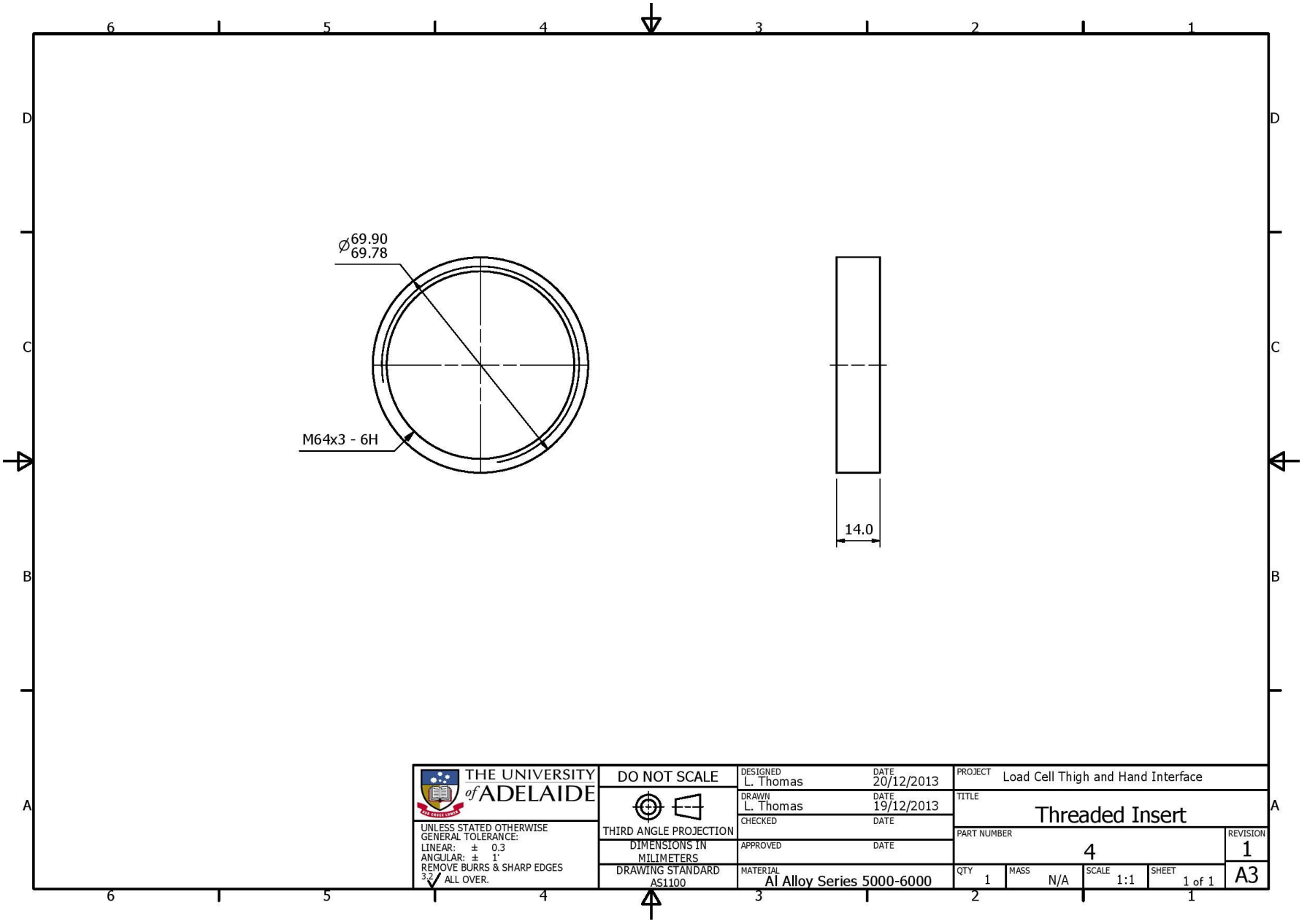

THE UNIVERSITY of ADELAIDE

UNLESS STATED OTHERWISE
GENERAL TOLERANCE:
LINEAR: ± 0.3
ANGULAR: ± 1°
REMOVE BURRS & SHARP EDGES
3.2 ALL OVER.

DO NOT SCALE

THIRD ANGLE PROJECTION

DIMENSIONS IN MILIMETERS

DRAWING STANDARD AS1100

DESIGNED	L. Thomas	DATE 20/12/2013
DRAWN	L. Thomas	DATE 19/12/2013
CHECKED		DATE
APPROVED		DATE
MATERIAL	Al Alloy Series 5000-6000	

PROJECT: Load Cell Thigh and Hand Interface

TITLE: Threaded Insert

PART NUMBER: 4

REVISION: 1

QTY	MASS	SCALE	SHEET
1	N/A	1:1	1 of 1

A3

SECTION B-B (1 : 1)

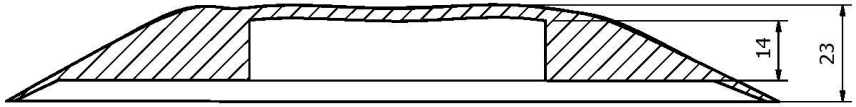

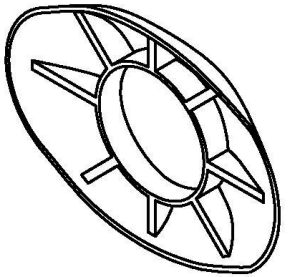

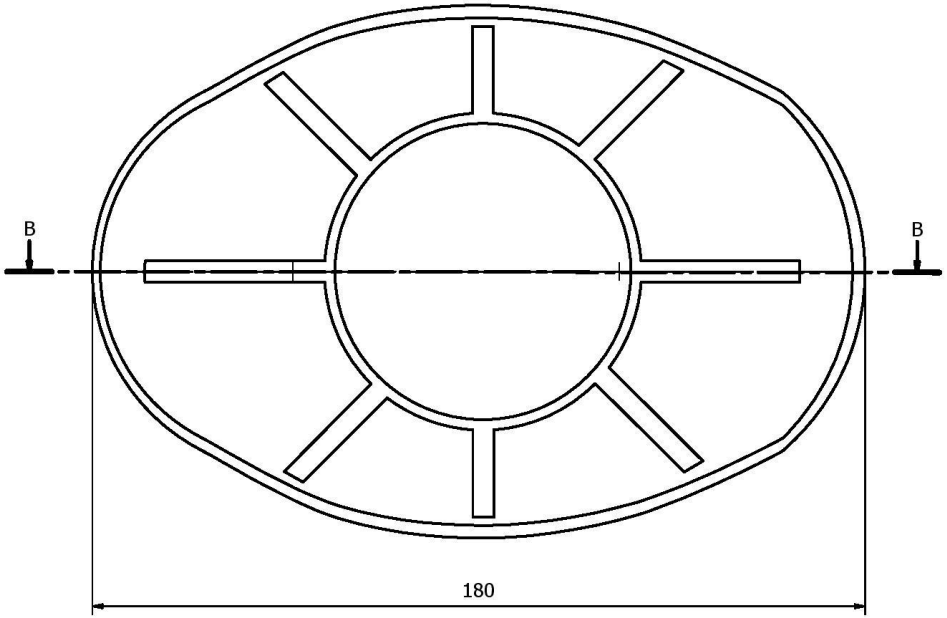

THE UNIVERSITY of ADELAIDE	DO NOT SCALE	DESIGNED L. Thomas DATE 18/02/2014	PROJECT Load Cell Thigh and Hand Interface
UNLESS STATED OTHERWISE GENERAL TOLERANCE: LINEAR: ± 0.3 ANGULAR: ± 1° REMOVE BURRS & SHARP EDGES 3.2 ALL OVER.	THIRD ANGLE PROJECTION	DRAWN L. Thomas DATE 4/03/2014	TITLE Hand Interface
	DIMENSIONS IN MILIMETERS	CHECKED DATE	PART NUMBER 5 REVISION 1
	DRAWING STANDARD AS1100	APPROVED DATE	QTY 1 MASS N/A SCALE 1:1 SHEET 1 of 1 A3
		MATERIAL Generic	

Appendix C Cupboard drawings

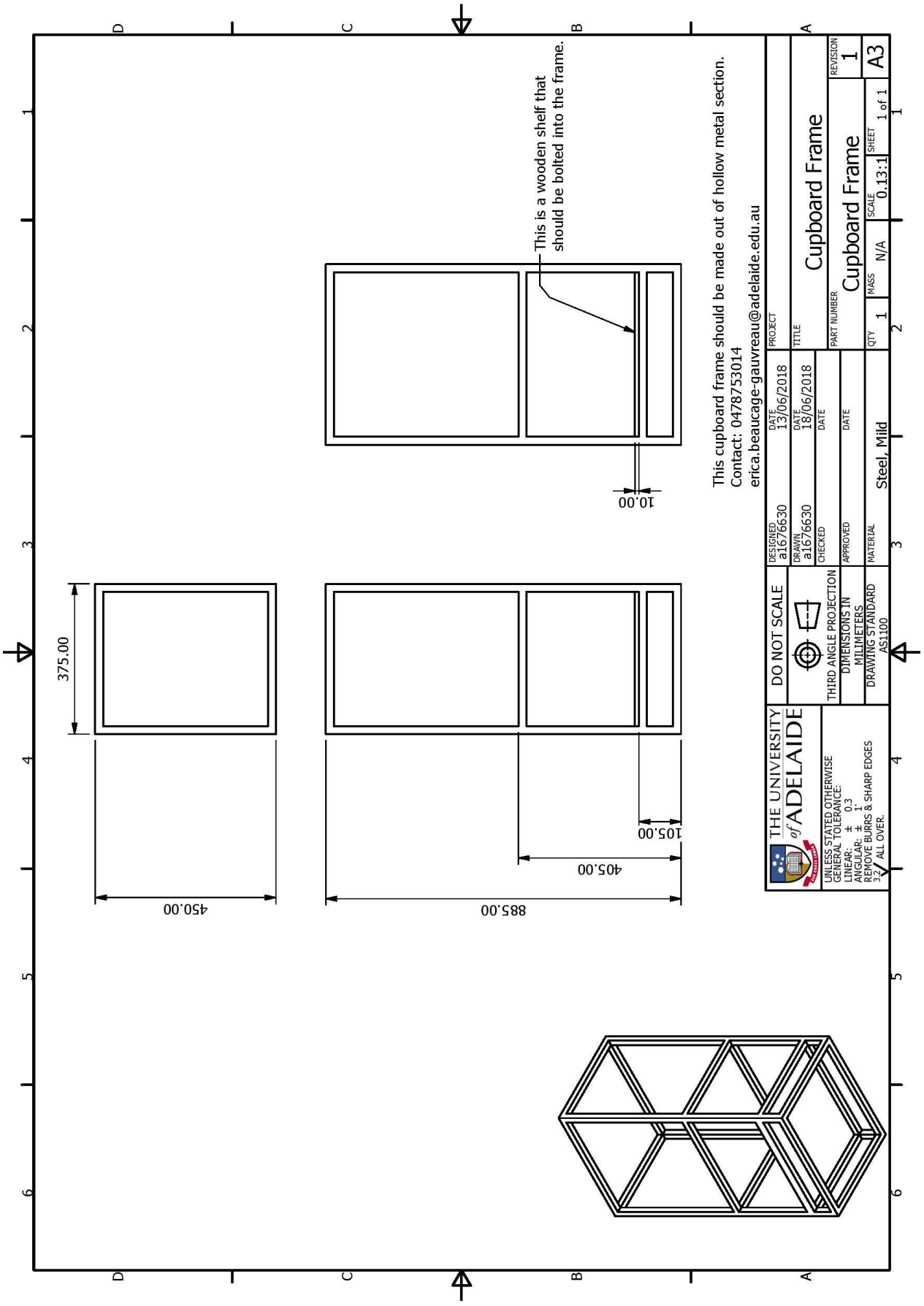

Appendix D Car Egress Drawings

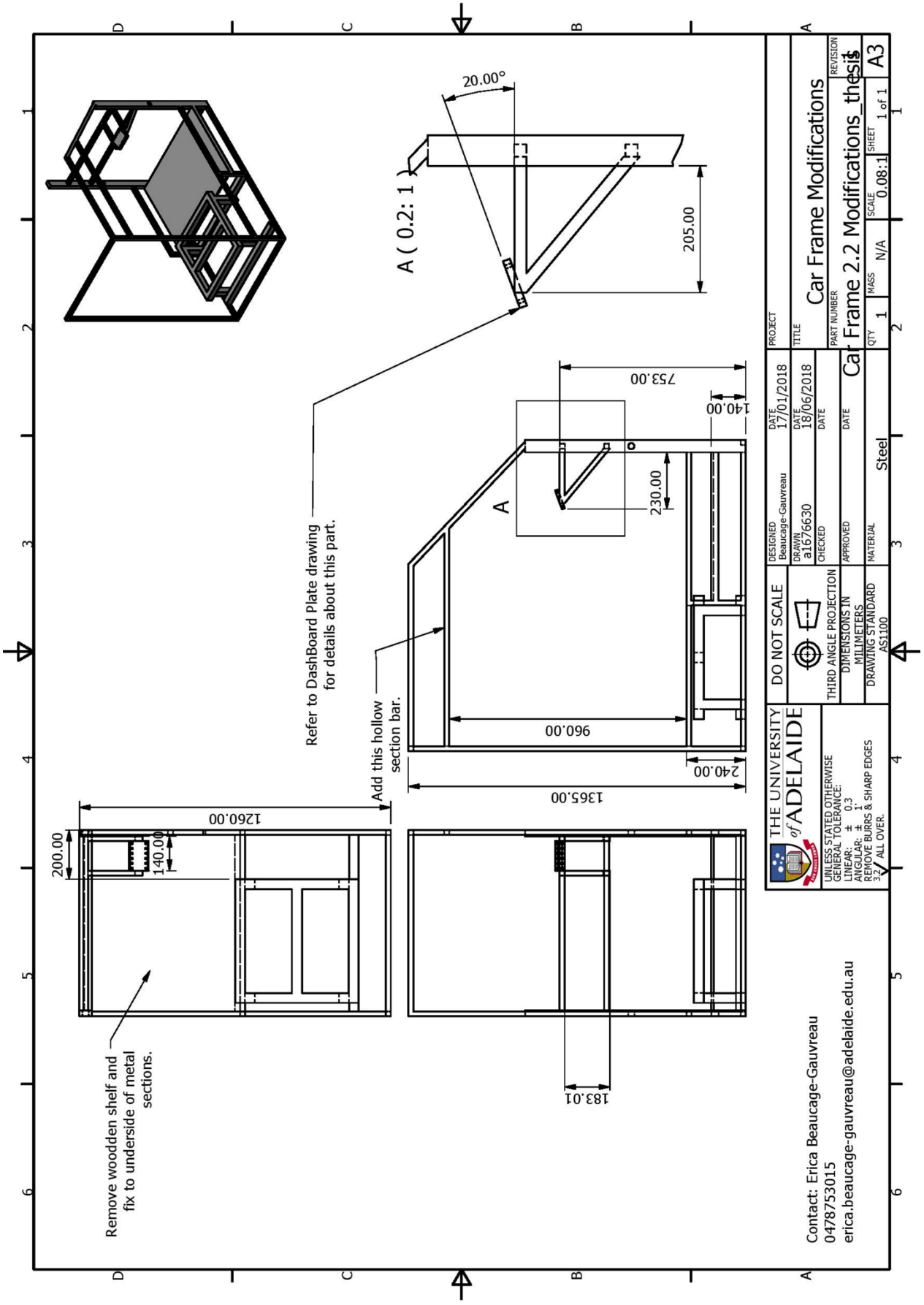

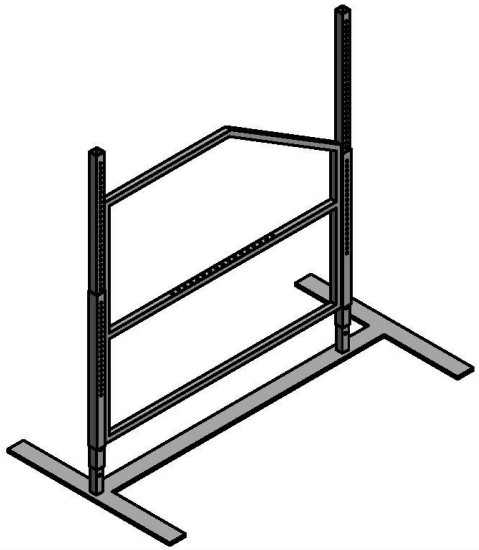

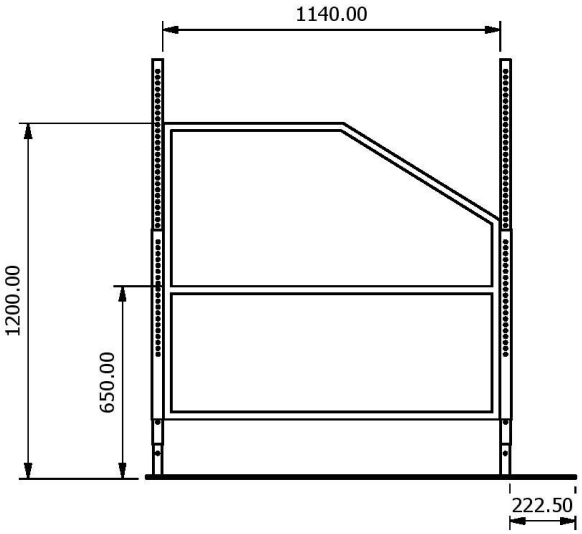

THE UNIVERSITY of ADELAIDE	DO NOT SCALE	DESIGNED Beaucage-Gauvreau DATE 7/06/2017	PROJECT
UNLESS STATED OTHERWISE GENERAL TOLERANCE: LINEAR: ± 0.3 ANGULAR: ± 1' REMOVE BURRS & SHARP EDGES 3.2 ALL OVER.	THIRD ANGLE PROJECTION	DRAWN a1676630 DATE 19/02/2019	TITLE Braced arm-to-thigh
	DIMENSIONS IN MILIMETERS	CHECKED DATE	PART NUMBER REVISION 1
	DRAWING STANDARD AS1100	APPROVED DATE	QTY 1 MASS N/A SCALE 0.07:1 SHEET 1 of 1 A3
		MATERIAL	

Appendix E Final linear mixed-effects models for peak loaded values

Final linear mixed-effects models for the peak loaded value at each outcome parameter at peak trunk flexion angle (maximum between phases 2 and 3). Where the Lift Type*Category interaction was significant, the Estimated Marginal Means (EMM) are presented for each participant category and the p-Value for the post-hoc comparison is reported. The reference category is indicated by *.

Compression force at L4/L5 (N):				
Variable:	*EMM (95% CI):*		*p-Value:*	*Estimate (95% CI):*
Lift Type			**<0.001**	
1ST	-3026.5 (-3151.7, -2907.3)		**<0.001**	-899.3 (-984.8, -813.8)
2SQ	-3309.1 (-3434.7, -3183.5)		**<0.001**	-1181.9 (-1268.0, -1095.7)
2ST	-3106.6 (-3231.7,-2981.6)		**<0.001**	-979.4 (-1064.7,-894.1)
BATT*	-2127.3 (-2252.4, -2002.2)		-	-
Gender			**<0.001**	
Female	-2661.4 (-2823.4, -2499.5)		**<0.001**	461.9 (232.8, 690.9)
Male*	-3123.3 (-3285.3, -2961.3)		-	-
Mass lifted			**<0.001**	
10 kg	-2661.4 (-2823.4, -2499.5)		**<0.001**	-900.8 (-961.4, -840.2)
2 kg*	-3123.3 (-3285.3, -2961.3)		-	-
Antero-posterior shear force at L4/L5 (N):				
Variable:	*EMM (95% CI):*		*p-Value:*	*Estimate (95% CI):*[β]
Lift Type	LBP	Healthy*	**0.006**	
1ST	-480.6 (-544.1, -417.2)	-530.5 (-590.7, -470.3)	**0.258**	-81.5 (-143.2, -19.8)
2SQ	-542.6 (-606.6, -478.7)	-689.1 (-749.3, -628.9)	**0.001**	15.2 (-47.1, 77.4)
2ST	-598.8 (-662.2, -535.4)	-674.3 (-734.5, -614.2)	**0.089**	-55.8 (-117.4, -5.8)
BATT*	-197.2 (-260.6, -133.8)	-328.5 (-388.7, -268.4)	**0.004**	-
Mass lifted			**<0.001**	
10 kg	-612.7 (-653.8, -571.6)		**<0.001**	-214.9 (-236.8, -193.1)
2 kg*	-397.8 (-438.8, -356.7)		-	-
Age was a significant predictor. Covariates appearing in the model are evaluated at Age = 47.91.				
Medio-lateral shear force at L4/L5 (N):				
Variable:	*EMM (95% CI):*		*p-Value:*	*Estimate (95% CI):*[β]
Lift Type			**<0.001**	
1ST	-279.6 (-306.8, -252.4)		**0.611**	-7.9 (-38.3, 22.5)
2SQ	35.9 (8.4, 63.4)		**<0.001**	307.7 (277.0, 338.3)
2ST	14.1 (-13.1, 41.3)		**<0.001**	285.9 (255.5, 316.2)
BATT*	-271.8 (-298.9, -244.6)		-	-
Category			**0.023**	
LBP	-101.6 (-131.0, -72.2)		**0.023**	47.5 (7.0, 87.9)
Healthy*	-149.1 (-176.9, -121.3)		-	-
Mass lifted			**<0.001**	
10 kg	-150.1 (-172.8, -127.3)		**<0.001**	-49.4 (-71.0, -27.9)

2 kg*	-100.6 (-123.4, -77.9)		-	-
Extension Moment (Nm):				
Variable:	*EMM (95% CI):*		*p-Value:*	*Estimate (95% CI):*
Lift Type			**<0.001**	
1ST	113.8 (108.4, 119.2)		**<0.001**	34.4 (31.2, 37.6)
2SQ	121.2 (115.8, 126.7)		**<0.001**	41.9 (38.6, 45.1)
2ST	125.0 (119.6, 130.4)		**<0.001**	45.6 (42.4, 48.8)
BATT*	79.4 (74.0, 84.8)		-	-
Gender			**<0.001**	
Female	98.0 (90.8, 105.1)		**<0.001**	-23.8 (-33.9, -13.6)
Male*	121.7 (114.5, 128.9)		-	-
Mass lifted			**<0.001**	
10 kg	126.0 (120.9, 131.2)		**<0.001**	32.4 (30.1, 34.7)
2 kg*	93.7 (88.5, 98.8)		-	-
Lateral bending Moment (Nm):				
Variable:	*EMM (95% CI):*		*p-Value:*	*Estimate (95% CI):*
Lift Type			**<0.001**	
1ST	-14.2 (-16.7, -11.7)		**<0.001**	16.4 (13.5, 19.3)
2SQ	-2.8 (-5.3, -0.3)		**<0.001**	27.8 (24.8, 30.7)
2ST	-0.8 (-3.3, 1.7)		**<0.001**	29.8 (26.9, 32.7)
BATT*	-30.6 (-33.1, -28.1)		-	-
Gender			**<0.001**	
Female	-7.6 (-10.1, -5.1)		**<0.001**	9.0 (5.5, 12.5)
Male*	-16.6 (-19.1, -14.1)		-	-
Mass lifted			**<0.001**	
10 kg	-14.5 (-16.5, -12.5)		**<0.001**	-4.8 (-6.8, -2.7)
2 kg*	-9.7 (-11.8, -7.7)		-	-
Category			**0.015**	
LBP	-14.4 (-16.9, -11.8)		**0.015**	-4.5 (-8.0, -1.0)
Healthy	-10.0 (-12.3, -7.4)			
Age was a significant predictor. Covariates appearing in the model are evaluated at Age = 47.91.				
Axial rotation Moment (Nm):				
Variable:	*EMM (95% CI):*		*p-Value:*	*Estimate (95% CI):*
Lift Type	LBP	Healthy*	**<0.033**	
1ST	-0.1 (-3.7, 3.6)	0.3 (-3.1, 3.8)	**0.878**	5.9 (-0.1, 11.9)
2SQ	3.6 (-0.1, 7.3)	2.2 (-1.2, 5.6)	**0.576**	7.7 (1.7, 13.7)
2ST	3.7 (0.1, 7.3)	2.1 (-1.3, 5.6)	**0.530**	7.9 (1.9, 13.8)
BATT*	-21.3 (-25.1, -17.9)	-15.3 (-18.7, -11.8)	**0.014**	-
Gender			**<0.001**	
Female	13.8 (12.1, 15.4)		**<0.001**	-2.5 (-4.9, -0.01)
Male*	16.3 (14.6, 18.0)		-	-
Mass lifted			**<0.001**	
10 kg	18.9 (17.5, 20.3)		**<0.001**	7.8 (6.2, 9.3)
2 kg*	11.1 (9.7, 12.5)		-	-
Trunk flexion angle (°):				
Variable:	*EMM (95% CI):*		*p-Value:*	*Estimate (95% CI):*
Lift Type			**<0.001**	

1ST	53.8 (50.5, 57.1)		**<0.001**	4.5 (2.9, 6.1)
2SQ	41.3 (38.0, 44.6)		**<0.001**	-8.0 (-9.6, -6.4)
2ST	59.1 (55.8, 62.4)		**<0.001**	9.8 (8.2, 11.4)
BATT*	49.3 (46.0, 52.6)		-	-
Gender			**0.048**	
Female	47.7 (43.3, 52.1)		**0.048**	-6.3 (-12.5, -0.1)
Male*	54.0 (49.6, 58.4)		-	-
Age was a significant predictor. Covariates appearing in the model are evaluated at Age = 47.91.				
Trunk Lateral bending angle (Towards lifting hand) (°):				
Variable:	*EMM (95% CI):*		*p-Value:*	*Estimate (95% CI):*
Lift Type			**<0.001**	
1ST	5.4 (3.8, 7.0)		**<0.001**	-6.9 (-8.6, -5.3)
2SQ	-1.9 (-3.5, -0.2)		**<0.001**	-14.2 (-15.8, -12.6)
2ST	-1.1 (-2.7, 0.5)		**<0.001**	-13.4 (-15.0, -11.8)
BATT*	12.3 (10.7, 13.9)		-	-
Gender			**0.021**	
Female	2.2 (0.4, 4.0)		**0.021**	-3.1 (-5.6, -0.5)
Male*	5.2 (3.4, 7.1)		-	-
Trunk axial rotation angle (Towards lifting hand) (°):				
Variable:	*EMM (95% CI):*		*p-Value:*	*Estimate (95% CI):*
Lift Type			**<0.001**	
1ST	26.7 (24.9, 28.6)		**0.002**	-2.8 (-4.6, -1.0)
2SQ	-0.5 (-2.4, 1.4)		**<0.001**	-30.0 (-31.8, -28.2)
2ST	0.4 (-1.5, 2.2)		**<0.001**	-29.1 (-30.9, -27.3)
BATT*	29.5 (27.7, 31.4)		-	-
VAS:				
Variable:	*EMM (95% CI):*		*p-Value:*	*Estimate (95% CI):*
Lift Type	LBP	Healthy*	**<0.001**	
1ST	1.3 (0.7, 1.6)	0.4 (0.02, 0.8)	**<0.001**	0.8 (0.001, 0.09)
2SQ	0.4 (-0.1, 0.8)	0.4 (-0.004, 0.8)	**<0.001**	0.02 (0.4, 1.1)
2ST	1.0 (0.6, 1.4)	0.4 (-0.1, 0.8)	**<0.001**	0.6 (0.3, 1.0)
BATT*	0.4 (-0.1, 0.8)	0.4 (-0.02, 0.8)	-	-
Mass lifted			**<0.001**	
10 kg	0.8 (0.6, 1.0)		**<0.001**	0.4 (0.3, 0.5)
2 kg*	0.4 (0.2, 0.6)		-	-

Appendix F Final linear mixed-effects models for peak values in phase 2

Final linear mixed-effects models for each outcome parameter at peak trunk flexion angle in phase 2 (box pick-up). Where the Lift Type*Category interaction was significant, the Estimated Marginal Means (EMMs) are presented for each participant category and the p-Value for the post-hoc comparison is reported. The reference category is indicated by *.

Compression force at L4/L5 (N):			
Variable:	*EMM (95% CI):*	*p-Value:*	*Estimate (95% CI):*
Lift Type		**<0.001**	
1ST	-2930.7 (-3063.1, -2798.4)	**<0.001**	-945.4 (-1045.8, -844.9)
2SQ	-3225.3 (-3358.1, -3092.5)	**<0.001**	-1239.9 (-1341.0, -1138.8)
2ST	-3025.8 (-3158.0, -2893.7)	**<0.001**	-1040.5 (-1040.7, -940.2)
BATT*	-1985.4 (-2117.6, -1853.2)	-	-
Gender		**<0.001**	
Female	-2545.3 (-2712.4, -2378.3)	**<0.001**	493.0 (256.7, 729.3)
Male*	-3038.3 (-3205.5, -2871.1)	-	-
Mass lifted		**<0.001**	
10kg	-3175.9 (-3298.9, -3052.8)	**<0.001**	-768.1 (-839.3, -696.9)
2kg*	-2407.8 (-2530.7, -2284.8)	-	-
Antero-posterior shear force at L4/L5 (N):			
Variable:	*EMM (95% CI):*	*p-Value:*	*Estimate (95% CI):*[β]
Lift Type		**<0.001**	
1ST	-471.8 (-517.6, -426.1)	**<0.001**	-242.6 (-276.4, -208.7)
2SQ	-583.6 (-629.5, -537.6)	**<0.001**	-354.3 (-388.4, 320.2)
2ST	-609.4 (-655.1, -563.7)	**<0.001**	-380.1 (-413.9, -346.3)
BATT*	-229.3 (-275.0, -183.6)	-	-
Category			
LBP	-424.9 (-484.6, -365.3)	**0.022**	97.1 (14.9, 179.4)
Healthy*	-522.1 (-578.7, -465.5)	-	
Mass lifted		**<0.001**	
10kg	-560.2 (-602.9, -517.4)	**<0.001**	-173.3 (-197.3, -149.3)
2kg*	-386.9 (-429.6, -344.2)	-	-
Medio-lateral shear force at L4/L5 (N):			
Variable:	*EMM (95% CI):*	*p-Value:*	*Estimate (95% CI):*[β]
Lift Type		**<0.001**	
1ST	-258.7 (-285.3, -232.0)	**0.001**	-62.9 (-100.6, -25.2)
2SQ	30.3 (3.4, 57.1)	**<0.001**	339.3 (301.3, 377.3)
2ST	13.4 (-13.3, 40.0)	**<0.001**	314.6 (277.0, 352.3)
BATT*	-253.0 (-279.6, -226.4)	-	-
Category		**0.017**	
LBP	-95.0 (-124.1, -65.9)	**0.017**	59.7 (8.2, 111.3)
Healthy*	-139.0 (-166.5, -111.5)	-	-
Mass lifted		**<0.001**	

10kg	-137.7 (-160.1, -115.3)		**<0.001**	-81.0 (-107.7, -54.2)
2kg*	-96.3 (-118.7, -73.9)		-	-
Extension Moment (Nm):				
Variable:	*EMM (95% CI):*		*p-Value:*	*Estimate (95% CI):*
Lift Type			**<0.001**	
1ST	110.6 (104.9, 116.2)		**<0.001**	36.7 (32.9, 40.5)
2SQ	118.3 (112.6, 123.9)		**<0.001**	44.4 (40.6, 48.2)
2ST	122.5 (116.8, 128.1)		**<0.001**	48.6 (44.8, 52.3)
BATT*	73.9 (68.3, 79.5)		-	-
Gender			**<0.001**	
Female	94.1 (86.8, 101.4)		**<0.001**	-24.4 (-34.8, -14.1)
Male*	118.5 (111.2, 125.8)		-	-
Mass lifted			**<0.001**	
10kg	120.2 (114.9, 125.5)		**<0.001**	27.8 (25.1, 30.5)
2kg*	92.4 (87.1, 97.7)		-	-
Lateral bending Moment (Nm):				
Variable:	*EMM (95% CI):*		*p-Value:*	*Estimate (95% CI):*
Lift Type			**<0.001**	
1ST	-12.5 (-14.9, -10.2)		**<0.001**	16.4 (13.6, 19.3)
2SQ	-2.5 (-4.9, -0.1)		**<0.001**	26.5 (23.6, 29.3)
2ST	-0.8 (-3.2, 1.6)		**<0.001**	28.2 (25.4, 31.0)
BATT*	-29.0 (-31.4, -26.6)		-	-
Mass lifted			**<0.001**	
10kg	-13.2 (-15.2, -11.3)		**<0.001**	-4.0 (-6.0, -2.0)
2kg*	-9.2 (-11.1, -7.2)		-	-
Category			**0.012**	
LBP	-13.4 (-15.8, -10.9)		**0.012**	-4.0 (-6.0, -2.0)
Healthy*	-9.0 (-11.3, -6.7)		-	-
Gender			**<0.001**	
Female	-7.1 (-9.5, -4.7)		**<0.001**	8.2 (4.9, 11.6)
Male*	-15.3 (-17.7, -12.9)		-	-
Repetition#			**0.043**	
1	-11.4 (-13.1, -9.7)		**0.049**	-0.7 (-1.4, -0.0)
2	-11.5 (-13.2, -9.8)		**0.020**	-0.8 (-1.5, -0.1)
3*	-10.7 (-12.4, -9.0)		-	-
Age was a significant predictor. Covariates appearing in the model are evaluated at Age = 47.91.				
Axial rotation Moment (Nm):				
Variable:	*EMM (95% CI):*		*p-Value:*	*Estimate (95% CI):*
Lift Type	LBP	Healthy*	**0.046**	
1ST	-0.1 (-3.5, 3.3)	-0.0 (-3.3, 3.2)	**0.036**	6.0 (0.4, 11.7)
2SQ	2.6 (-0.9, 6.1)	2.1 (-1.1, 5.3)	**0.023**	6.6 (0.9, 12.3)
2ST	3.1 (-0.3, 6.5)	2.0 (-1.2, 5.3)	**0.013**	7.2 (1.5, 12.8)
BATT*	-20.1 (-23.5, -16.8)	-14.0 (-17.2, -10.8)	-	-
Trunk flexion angle (°):				

Variable:	*EMM (95% CI):*	*p-Value:*	*Estimate (95% CI):*
Lift Type		**<0.001**	
1ST	-52.7 (-56.1, -49.3)	**<0.001**	-5.2 (-6.9, -3.5)
2SQ	-39.0 (-42.4, -35.6)	**<0.001**	8.5 (6.7, 10.2)
2ST	-57.8 (-61.2, -54.4)	**<0.001**	-10.3 (-12.0, -8.6)
BATT*	-47.4 (-50.9, -44.1)	-	-
Gender		**0.049**	
Female	-46.0 (50.6, -41.3)	**0.049**	6.6 (0.0, 13.1)
Male*	-52.5 (-57.2, -47.9)	-	-
Age was a significant predictor. Covariates appearing in the model are evaluated at Age = 47.91.			
Trunk Lateral Bending angle (Towards lifting hand) (°):			
Variable:	*EMM (95% CI):*	*p-Value:*	*Estimate (95% CI):*
Lift Type		**<0.001**	
1ST	5.1 (3.7, 6.5)	**<0.001**	-6.7 (-8.2, -5.3)
2SQ	-1.5 (-3.0, -0.1)	**<0.001**	-13.4 (-14.8, -12.0)
2ST	-1.0 (-2.4, 0.4)	**<0.001**	-12.9 (-14.3, -11.5)
BATT*	11.8 (10.4, 13.3)	-	-
Gender		**0.031**	
Female	2.3 (0.7, 3.9)	**0.031**	-2.5 (-4.8, -0.2)
Male*	4.9 (3.2, 6.5)	-	-
Trunk axial rotation angle (Towards lifting hand) (°):			
Variable:	*EMM (95% CI):*	*p-Value:*	*Estimate (95% CI):*
Lift Type		**<0.001**	
1ST	25.9 (24.1, 27.7)	**0.025**	-2.0 (-3.7, -0.2)
2SQ	-0.3 (-2.1, 1.5)	**<0.001**	-28.2 (-29.9, -26.4)
2ST	0.4 (-1.4, 2.2)	**<0.001**	-27.5 (-29.3, -25.7)
BATT*	27.9 (26.1, 29.7)	-	-

Appendix G Final linear mixed-effects models for peak values in phase 3

Final linear mixed-effects models for each outcome parameter at peak trunk flexion angle for phase 3 (box put-down). Where the Lift Type*Category interaction was significant, the Estimated Marginal Means (EMM) are presented for each participant category and the p-Value for the post-hoc comparison is reported. The reference category is indicated by *.

Compression force at L4/L5 (N):				
Variable:	*EMM (95% CI):*		*p-Value:*	*Estimate (95% CI):*
Lift Type			**<0.001**	
1ST	-2799.1 (-2919.2, -2679.0)		**<0.001**	-826.2 (-908.7, -743.7)
2SQ	-3131.6 (-3252.1, -3011.1)		**<0.001**	-1158.7 (-1241.8, -1075.5)
2ST	-2932.0 (-3052.0, -2812.0)		**<0.001**	-959.1 (-1041.5, -876.7)
BATT*	-1972.9 (-2093.0, -1852.9)		-	-
Gender			**<0.001**	
Female	-2493.9 (-2649.0, -2338.7)		**<0.001**	430.1 (210.6, 649.5)
Male*	-2923.9 (-3079.2, -2768.7)		-	-
Mass lifted			**<0.001**	
10kg	-3177.5 (-3290.8, -3064.2)		**<0.001**	-937.2 (-995.7, -878.7)
2kg*	-2240.3 (-2353.6, -2127.1)		-	-
Antero-posterior shear force at L4/L5 (N):				
Variable:	*EMM (95% CI):*		*p-Value:*	*Estimate (95% CI):*[β]
Lift Type	LBP	Healthy	**0.006**	
1ST	-426.1 (-485.9, -366.3)	-481.6 (-538.3, -424.9)	**<0.001**	-242.6 (-276.4, -208.7)
2SQ	-502.0 (-563.2, -442.6)	-649.4 (-706.2, -592.7)	**<0.001**	-354.3 (-388.4, 320.2)
2ST	-558.0 (-617.7, -498.2)	-627.3 (-684.0, -570.6)	**<0.001**	-380.1 (-413.9, -346.3)
BATT*	-168.4 (-228.2, -108.7)	-294.7 (-351.4, -238.0)	-	-
Mass lifted			**<0.001**	
10kg	-571.0 (-609.7, -532.4)		**<0.001**	-215.0 (-236.0, -194.0)
2kg*	-356.1 (-394.7, -317.4)		-	-
Medio-lateral shear force at L4/L5 (N):				
Variable:	*EMM (95% CI):*		*p-Value:*	*Estimate (95% CI):*[β]
Lift Type			**<0.001**	
1ST	-237.3 (-261.1, -213.4)		**0.001**	-3.2 (-24.1, 30.6)
2SQ	29.6 (5.5, 53.6)		**<0.001**	270.1 (242.6, 297.6)
2ST	11.6 (-12.3, 35.4)		**<0.001**	252.1 (224.7, 279.4)
BATT*	-240.5 (-264.3, -216.7)		-	-
Category			**0.017**	
LBP	-87.7 (-112.9, -62.5)		**0.017**	42.9 (8.2, 77.6)
Healthy*	-130.6 (-154.5, -106.8)		-	-
Mass lifted			**<0.001**	
10kg	-135.0 (-154.7, -115.3)		**<0.001**	-51.6 (-71.0, -32.3)
2kg*	-83.3 (-103.1, -63.6)		-	-
Extension Moment (Nm):				

Variable:	*EMM (95% CI):*		*p-Value:*	*Estimate (95% CI):*
Lift Type			**<0.001**	
1ST	105.4 (100.1, 110.7)		**<0.001**	31.5 (28.2, 34.8)
2SQ	114.4 (109.1, 119.8)		**<0.001**	40.5 (37.2, 43.9)
2ST	117.6 (112.3, 122.9)		**<0.001**	43.7 (40.4, 46.9)
BATT*	73.9 (68.6, 79.2)		-	-
Gender			**<0.001**	
Female	91.7 (84.7, 98.6)		**<0.001**	-22.3 (-32.2, -12.5)
Male*	114.0 (107.0, 121.0)		-	-
Mass lifted			**<0.001**	
10kg	120.0 (114.9, 125.5)		**<0.001**	34.3 (32.0, 36.7)
2kg*	85.7 (80.6, 90.7)		-	-
Lateral bending Moment (Nm):				
Variable:	*EMM (95% CI):*		*p-Value:*	*Estimate (95% CI):*
Lift Type			**<0.001**	
1ST	-12.2 (-14.5, -10.0)		**<0.001**	14.7 (12.1, 17.3)
2SQ	-2.4 (-4.7, -0.1)		**<0.001**	24.5 (21.8, 27.2)
2ST	-0.7 (-3.0, 1.5)		**<0.001**	26.2 (23.6, 28.8)
BATT*	-27.0 (-29.2, -24.7)		-	-
Mass lifted			**<0.001**	
10kg	-12.8 (-14.7, -11.0)		**<0.001**	-4.5 (-6.4, -2.6)
2kg*	-8.3 (-10.2, -6.5)		-	-
Category			**0.012**	
LBP	-12.4 (-14.8, -10.1)		**0.012**	-3.7 (5.0, 11.5)
Healthy*	-8.7 (-10.9, -6.5)		-	-
Gender			**<0.001**	
Female	-6.4 (-8.7, -4.2)		**<0.001**	8.3 (5.0, 11.5)
Male*	-14.7 (-17.0, -12.4)		-	-
Age was a significant predictor. Covariates appearing in the model are evaluated at Age = 47.91.				
Axial rotation Moment (Nm):				
Variable:	*EMM (95% CI):*		*p-Value:*	*Estimate (95% CI):*
Lift Type	LBP	Healthy*	**0.047**	
1ST	1.5 (-1.2, 4.2)	0.7 (-1.8, 3.3)	**<0.001**	5.2 (0.6, 9.9)
2SQ	2.8 (0.0, 5.6)	1.6 (-0.9, 4.2)	**<0.001**	5.6 (1.0, 10.3)
2ST	2.3 (-0.4, 5.0)	1.3 (-1.2, 3.9)	**<0.001**	5.4 (0.8, 10.0)
BATT*	-16.2 (-18.9, -13.5)	-11.8 (-14.3, -9.2)	-	-
Trunk flexion angle (°):				
Variable:	*EMM (95% CI):*		*p-Value:*	*Estimate (95% CI):*
Lift Type			**<0.001**	
1ST	-51.8 (-55.1, -48.4)		**<0.001**	-5.5 (-7.2, -3.8)
2SQ	-38.9 (-42.3, -35.6)		**<0.001**	7.4 (5.7, 9.1)
2ST	-56.8 (-60.1, -53.4)		**<0.001**	-10.5 (-12.2, -8.8)
BATT*	-46.3 (-49.7, -43.0)		-	-
Gender			**0.036**	

Female	-45.0 (-49.6, -40.6)	**0.036**	6.8 (0.5, 13.2)
Male*	-51.9 (-56.4, -47.4)	-	-
Age was a significant predictor. Covariates appearing in the model are evaluated at Age = 47.91.			
Trunk Lateral Bending angle (Towards lifting hand) (°):			
Variable:	*EMM (95% CI):*	*p-Value:*	*Estimate (95% CI):*
Lift Type		**<0.001**	
1ST	4.4 (3.0, 5.9)	**<0.001**	-5.6 (-7.1, -4.0)
2SQ	-1.6 (-3.1, -0.1)	**<0.001**	-11.6 (-13.1, -10.0)
2ST	-0.9 (-2.4, 0.6)	**<0.001**	-10.9 (-12.4, -9.4)
BATT*	10.0 (8.5, 11.5)	-	-
Mass lifted		**0.020**	
10kg	2.3 (0.7, 3.9)	**0.020**	-1.3 (-2.4, -0.2)
2kg*	4.9 (3.2, 6.5)	-	-
Gender		**0.012**	
Female	1.5 (-0.2, 3.1)	**0.012**	-3.0 (-5.3, -0.7)
Male*	4.5 (2.8, 6.1)	-	-
Trunk axial rotation angle (Towards lifting hand) (°):			
Variable:	*EMM (95% CI):*	*p-Value:*	*Estimate (95% CI):*
Lift Type		**<0.001**	
1ST	24.9 (23.2, 26.7)	**0.094**	-1.5 (-3.3, 0.3)
2SQ	-0.6 (-2.3, 1.2)	**<0.001**	-27.0 (-28.8, -25.2)
2ST	0.2 (-1.6, 1.9)	**<0.001**	-26.3 (-28.0, -24.5)
BATT*	26.4 (24.7, 28.2)	-	-
Category		**0.034**	
LBP	11.2 (9.2, 13.2)	**0.034**	-3.0 (-5.8, -0.2)
Healthy*	14.2 (12.3, 16.1)	-	-

Appendix H Final linear mixed-effects models for peak value over the entire trial

Final linear mixed-effects models for each outcome parameter for the peak value over the entire trial. Marginal Means (EMM) are presented for each significant variable with their corresponding p-Value. The reference category is indicated by *.

Compression force at L4/L5 (N):			
Variable:	*EMM (95% CI):*	*p-Value:*	*Estimate (95% CI):*
Lift Type		**<0.001**	
1ST	-3466.4 (-3602.8, -3330.1)	**<0.001**	-775.1 (-849.4, -700.7)
2SQ	-3643.8 (-3780.5, -3507.2)	**<0.001**	-952.5 (-1027.3, -877.6)
2ST	-3476.4 (-3612.8, -3340.1)	**<0.001**	-785.1 (-859.3, -710.8)
BATT*	-2691.4 (-2827.7, -2555.1)	-	-
Gender		**<0.001**	
Female	-3037.9 (-3220.5, -2855.2)	**<0.001**	563.3 (304.9, 821.6)
Male*	-3601.2 (-3783.9, -3418.5)	-	-
Mass lifted		**<0.001**	
10kg	-3886.8 (-4018.4, -3755.2)	**<0.001**	-1134.6 (-1187.3, -1081.9)
2kg*	-2752.2 (-2883.8, -2620.6)	-	-
Age was a significant predictor. Covariates appearing in the model are evaluated at Age = 47.91.			
Antero-posterior shear force at L4/L5 (N):			
Variable:	*EMM (95% CI):*	*p-Value:*	*Estimate (95% CI):*[β]
Lift Type		**0.006**	
1ST	-620.3 (-666.1, -574.4)	**<0.001**	-242.6 (-276.4, -208.7)
2SQ	-675.9 (-721.9, -629.9)	**<0.001**	-354.3 (-388.4, 320.2)
2ST	-726.1 (-771.9, -680.3)	**<0.001**	-380.1 (-413.9, -346.3)
BATT*	-457.7 (-503.5, -411.9)	-	-
Category		**0.006**	
LBP	-559.6 (-620.4, -498.7)	**0.006**	42.9 (8.2, 77.6)
Healthy*	-680.4 (-738.1, -622.7)	-	-
Mass lifted		**<0.001**	
10kg	-571.0 (-609.7, -532.4)	**<0.001**	-215.0 (-236.0, -194.0)
2kg*	-356.1 (-394.7, -317.4)	-	-
Medio-lateral shear force at L4/L5 (N):			
Variable:	*EMM (95% CI):*	*p-Value:*	*Estimate (95% CI):*[β]
Lift Type		**<0.001**	
1ST	-356.0 (-390.3, -321.7)	**0.001**	-62.9 (-100.6, 25.2)
2SQ	46.2 (11.7, 80.8)	**<0.001**	339.3 (301.3, 377.3)
2ST	21.5 (-12.7, 55.7)	**<0.001**	314.6 (277.0, 352.3)
BATT*	-293.1 (-327.3, -258.9)	-	-
Category		**0.024**	
LBP	-115.5 (-152.9, -78.0)	**0.024**	59.7 (8.2, 11.3)
Healthy*	-175.2 (-210.6, -139.8)	-	-
Mass lifted		**<0.001**	

10kg	-185.8 (-214.7, -157.0)	<**0.001**	-81.0 (-107.7, -54.2)
2kg*	-104.9 (-133.7, -76.0)	-	-
Extension Moment (Nm):			
Variable:	*EMM (95% CI):*	*p-Value:*	*Estimate (95% CI):*
Lift Type		<**0.001**	
1ST	129.6 (123.4, 135.8)	<**0.001**	31.8 (29.0, 34.7)
2SQ	133.2 (127.0, 139.4)	<**0.001**	35.4 (32.5, 38.3)
2ST	137.9 (131.7, 144.1)	<**0.001**	40.1 (37.2, 43.0)
BATT*	97.8 (91.6, 104.0)	-	-
Gender		<**0.001**	
Female	110.8 (102.4, 119.2)	<**0.001**	-27.7 (-39.6, -15.8)
Male*	138.5 (130.1, 146.9)	-	-
Mass lifted		<**0.001**	
10kg	145.1 (139.1, 151.1)	<**0.001**	41.0 (38.9, 43.0)
2kg*	104.1 (98.1, 110.2)	-	-
Lateral bending Moment (Nm):			
Variable:	*EMM (95% CI):*	*p-Value:*	*Estimate (95% CI):*
Lift Type		<**0.001**	
1ST	20.3 (18.0, 22.7)	<**0.001**	-16.2 (-18.7, -13.7)
2SQ	9.9 (7.6, 12.3)	<**0.001**	-26.7 (-29.2, -24.1)
2ST	8.7 (6.3, 11.0)	<**0.001**	-27.9 (-30.4, -25.4)
BATT*	36.6 (34.2, 38.9)	-	-
Mass lifted		<**0.001**	
10kg	22.4 (20.4, 24.4)	<**0.001**	7.1 (5.3, 8.8)
2kg*	15.3 (13.4, 17.3)	-	-
Gender		<**0.001**	
Female	14.6 (12.0, 17.1)	<**0.001**	-8.6 (-12.2, -5.0)
Male*	23.2 (20.6, 25.7)	-	-
Age was a significant predictor. Covariates appearing in the model are evaluated at Age = 47.91.			
Axial rotation Moment (Nm):			
Variable:	*EMM (95% CI):*	*p-Value:*	*Estimate (95% CI):*
Lift Type		<**0.001**	
1ST	13.8 (12.0, 15.6)	<**0.001**	-15.7 (-17.9, -13.5)
2SQ	8.5 (6.7, 10.3)	<**0.001**	-21.1 (-23.3,-18.9)
2ST	8.2 (6.5, 10.0)	<**0.001**	-21.3 (-23.5, -19.1)
BATT*	29.5 (27.8, 31.3)	-	-
Mass lifted		<**0.001**	
10kg	18.9 (17.5, 20.3)	<**0.001**	7.8 (6.2, 9.3)
2kg*	11.1 (9.7, 12.5)	-	-
Gender		<**0.001**	
Female	13.8 (12.1, 15.4)	<**0.001**	-2.5 (-4.9, -0.1)
Male*	16.3 (14.6, 18.0)	-	-
Trunk flexion angle (°):			
Variable:	*EMM (95% CI):*	*p-Value:*	*Estimate (95% CI):*

Lift Type		**<0.001**	
1ST	-53.8 (-50.5, -57.1)	**<0.001**	-4.5 (2.9, 6.1)
2SQ	-41.3 (-38.0, -44.6)	**<0.001**	-8.0 (-9.6, -6.4)
2ST	-59.1 (-55.8, -62.4)	**<0.001**	9.8 (8.2, 11.4)
BATT*	-49.3 (-46.0, -52.6)	-	-
Gender		**0.048**	
Female	47.7 (43.3, 52.1)	**0.048**	-6.3 (-12.5, -0.1)
Male*	54.0 (49.6, 58.4)	-	-
Age was a significant predictor. Covariates appearing in the model are evaluated at Age = 47.91.			
Trunk Lateral Bending angle (Towards lifting hand) (°):			
Variable:	*EMM (95% CI):*	*p-Value:*	*Estimate (95% CI):*
Lift Type		**<0.001**	
1ST	9.1 (7.9, 10.3)	**<0.001**	-5.6 (-6.8, -4.3)
2SQ	2.8 (1.6, 4.1)	**<0.001**	-11.8 (-13.0, -10.6)
2ST	2.7 (1.5, 3.9)	**<0.001**	-12.0 (-13.2, -10.8)
BATT*	14.6 (13.4, 15.8)	-	-
Gender		**0.026**	
Female	6.2 (4.9, 7.6)	**0.026**	-2.2 (-4.1, -0.3)
Male*	8.4 (7.1, 9.8)	-	-
Trunk Lateral Bending angle (Towards bracing hand) (°):			
Variable:	*EMM (95% CI):*	*p-Value:*	*Estimate (95% CI):*
Lift Type		**<0.001**	
1ST	-4.6 (-5.5, -3.6)	**<0.001**	9.0 (8.0, 10.0)
2SQ	-4.5 (-5.5, -3.6)	**<0.001**	9.1 (8.1, 10.1)
2ST	-3.9 (-4.8, -2.9)	**<0.001**	9.7 (8.8, 10.7)
BATT*	-14.0 (-14.5, -12.7)	-	-
Mass lifted		**0.014**	
10kg	-7.1 (-7.8, -6.2)	**0.014**	-0.9 (-1.5, -0.2)
2kg*	-6.2 (-7.0, -5.4)	-	-
Trunk axial rotation angle (Towards lifting hand) (°):			
Variable:	*EMM (95% CI):*	*p-Value:*	*Estimate (95% CI):*
Lift Type		**<0.001**	
1ST	2.0 (0.5, 3.4)	**<0.001**	6.5 (5.5, 7.5)
2SQ	-3.3 (-4.8, -1.9)	**0.017**	1.2 (0.2, 2.2)
2ST	-2.6 (-4.1, -1.2)	**<0.001**	1.9 (0.9, 2.9)
BATT*	-4.6 (-6.0, -3.1)	-	-
Trunk axial rotation angle (Towards bracing hand) (°):			
Variable:	*EMM (95% CI):*	*p-Value:*	*Estimate (95% CI):*
Lift Type		**<0.001**	
1ST	27.8 (26.0, 29.6)	**<0.001**	-3.1 (-4.7, -1.5)
2SQ	5.7 (3.9, 7.5)	**<0.001**	-25.2 (-26.8, -23.6)
2ST	6.1 (4.3, 7.9)	**<0.001**	-24.8 (-26.4, -23.2)
BATT*	30.9 (29.1, 32.7)	-	-

Appendix I Final multi-variable linear mixed-effects models for BATT trials

Final linear mixed-effects models for peak bracing force during braced arm-to-thigh (BATT) lifting technique. Estimated Marginal Means (EMMs) are presented for each significant predictor. The reference category is indicated by *.

Bracing Force (N):			
Variable:	*EMM (95% CI):*	*p-Value:*	*Estimate (95% CI):*
Category		0.305	
LBP	132.8 (108.1, 157.5)	0.305	17.4 (-16.6, 51.4)
Healthy*	115.4 (92.0, 138.8)	-	-
Gender		**0.047**	
Female	106.9 (82.9, 130.9)	-	-34.4 (-68.4, -0.5)
Male*	141.2 (117.3, 165.3)	-	-
Mass lifted		**<0.001**	-
10 kg	131.4 (114.3, 148.6)	-	14.7 (9.3, 20.2)
2 kg*	116.7 (99.5, 133.9)	-	-
Age was a significant predictor. Covariates appearing in the model are evaluated at Age = 47.91.			

Final linear mixed-effects models for the effect of the bracing category (During or Outside) on peak bracing force during braced arm-to-thigh (BATT) lifting technique. Estimated Marginal Means (EMM) are presented for each significant predictor. The reference category is indicated by *.

Bracing Force (N):			
Variable:	*EMM (95% CI):*	*p-Value:*	*Estimate (95% CI):*
Bracing Category		**<0.001**	
During	107.3 (91.1, 123.5)	**<0.001**	-
Outside*	117.6 (101.5, 133.7)	-	10.3 (5.8, 14.8)
Lifting Phase		**<0.001**	
Pick-up	101.3.9 (85.2, 117.4)	**<0.001**	-22.2 (-25.3, -19.2)
Put-down*	123.5 (107.5, 139.6)	-	-
Mass lifted		**<0.001**	-
10 kg	120.8 (104.6, 137.0)	**<0.001**	16.8 (11.5, 22.1)
2 kg*	104.0 (87.8, 120.3)	-	-

Final linear mixed-effects models for the effect of the bracing category (During or Outside) on compression force at L4/L5 at peak trunk flexion angle during braced arm-to-thigh (BATT) lifting technique. Estimated Marginal Means (EMMs) are presented for each significant predictor. The reference category is indicated by *.

Compression force at L4/L5 at peak trunk flexion angle (N):			
Variable:	*EMM (95% CI):*	*p-Value:*	*Estimate (95% CI):*
Bracing Category		**<0.001**	
During	-2087.0 (-2242.9, -1931.2)	**<0.001**	-
Outside*	-1907.6 (-2060.2, -1755.0)	-	179.4 (108.0, 250.9)
Mass lifted		**<0.001**	-
10 kg	-2378.6 (-2533.0, -2224.2)	**<0.001**	-762.5 (-841.3, -683.6)
2 kg*	-1616.1 (-1771.3, -1460.9)	-	-

Appendix J Ethics Approval for Chapters 4 & 6

Approval Date: 12 September 2017

CALHN Reference number: R20170816
please quote this number in all future correspondence

Government of South Australia
SA Health

Central Adelaide Local Health Network
Royal Adelaide Hospital Human Research Ethics Committee
Level 4, Women's Health Centre
Royal Adelaide Hospital
North Terrace
Adelaide, South Australia, 5000
Telephone: +61 8 8222 4139
Email: Health.CALHNResearchEthics@sa.gov.au

Dr Claire F Jones
School of Mechanical Engineering
University of Adelaide

Dear Dr Jones,

Project Title: A novel 'arm-to-thigh' bracing technique for one-handed reaching and bending tasks adapted for car ingress and car egress.

Thank you for submitting the above project for ethical review. This project was considered by the Chairman of the Royal Adelaide Hospital Research Ethics Committee. I am pleased to advise that your protocol has been granted full ethics approval and meets the requirements of the *National Statement on Ethical Conduct in Human Research* (2007) incorporating all updates. The documents reviewed and approved include:

Document	***Version***	***Date***
LNR Ethics and Governance Application Form	-	-
Protocol	2	9 September 2017
Participant Information Sheet and Consent Form	3	12 September 2017
Short Form McGill Pain Questionnaire	-	-
Oswestry Low Back Pain Disability Questionnaire	-	-
Roland-Morris Disability Questionnaire MAPI 2005	-	-
FAB Questionnaire	-	-
Newsletter Advert	2	-
Noticeboard Advert	2	-
Noticeboard Advert – Healthy Study	2	-

Sites covered by this approval:

- Royal Adelaide Hospital, SA: CPI – Dr Claire Jones
- SA Pathology, SA: CPI – Dr Claire Jones
- University of Adelaide, SA: CPI – Dr Claire Jones
- University of South Australia, SA: CPI – Dr Claire Jones

GENERAL TERMS AND CONDITIONS OF ETHICAL APPROVAL:

1. This HREC is the South Australian 'lead HREC' for the purpose of this ethics approval. Any study sites that are not listed on this letter are not covered by this ethics approval. For any SA study-sites within the public health system that are proposed to be added, the CPI must write formally to this HREC requesting the additional study site and a separate formal letter will be issued.
2. Adequate record-keeping must be maintained in accordance with GCP, NHMRC and state and national guidelines. The duration of record retention for all clinical research data is 15 years from the date of publication.
3. Researchers are required to immediately report to this HREC anything which might warrant review of ethical approval of the study, including:
   (a) adverse events which warrant protocol change or notification to research participants;
   (b) changes to the protocol;
   (c) changes to the safety or efficacy of the investigational product, device or method;
   (d) premature termination of the study.
4. The Committee must be notified within 72 hours of any Urgent Safety Measures (USMs) occurring at this or any approved sites.
5. Confidentiality of the research participants shall be maintained at all times as required by law.
6. Approval is valid for **5 years** from the date of this letter, after which an extension must be applied for.

7. Investigators are responsible for providing an annual review to the RAH REC Executive Officer each anniversary of the above approval date, within 10 workings days, using the Annual Review Form available at: https://www.rahresearchfund.com.au/rah-research-institute/for-researchers/human-research-ethics/
8. The REC must be advised with a report or in writing within 30 days of completion.

Should you have any queries about the HREC's consideration of your project, please contact Ms Heather O'Dea on 08 8222 4139, or Health.CALHNResearchEthics@sa.gov.au.

You are reminded that this letter constitutes ethical approval only. You must not commence this research project at a SA Health site until governance authorisation at that site has been obtained. Please contact the CALHN Research Office Health.CALHNResearchLNR@sa.gov.au

This Committee is constituted in accordance with the NHMRC's *National Statement on the Ethical Conduct of Human Research* (2007).

The HREC wishes you every success in your research.

Yours sincerely,

A/Prof A Thornton
CHAIRMAN
RESEARCH ETHICS COMMITTEE

Appendix K Ethics Approval for Chapter 5

Government of South Australia
SA Health

Central Adelaide Local Health Network
Royal Adelaide Hospital Human Research Ethics Committee
Level 3, Hanson Institute, IMVS Building
Royal Adelaide Hospital
North Terrace
Adelaide, South Australia, 5000
Telephone: +61 8 8222 4139
Fax: +61 8 8222 3035
Email: rah.ethics@health.sa.gov.au

Approval Date: 6 March 2014

Dr C Jones
Adelaide Centre for Spinal Research
SA PATHOLOGY

Dear Dr Jones,

HREC reference number: **HREC/14/RAH/87**

Project Title: **"A novel "arm-to-thigh" bracing technique for one-handed reaching and lifting tasks in patients with chronic low back pain and spinal degeneration: biomechanical evaluation of spine and knee loads, and patient reported pain."**

RAH Protocol No: 140307.

Thank you for submitting the above project for ethical review. This project was considered by the Chairman of the Royal Adelaide Hospital Human Research Ethics Committee. I am pleased to advise that your protocol has been granted full ethics approval and meets the requirements of the *National Statement on Ethical Conduct in Human Research*. The documents reviewed and approved include:

- **Study Protocol Version 1, 17 February 2014**
- **Participant Information Sheet & Consent Form, Version 1, 4 March 2014**
- **Participant Screening Form, Version 1, 17 February 2014**
- **Participant Identification Form, Version 1, 17 February 2014**
- **Participant Data Sheet, Including Roland Morris Disability Questionnaire & Short Form McGill Pain Questionnaire, Version 1, 17 February 2014**
- **Advertisement for notice boards, Version 1, 17 February 2014**
- **Advertisement, for electronic Newsletters and/or local Newspaper, Version 1, 17 February 2014**
- **Talent Release Form, Version 1, 17 February 2014**

The committee expects that the main study will only proceed if the pilot study shows that the method is feasible and safe.

Please quote the RAH Protocol Number allocated to your study on all future correspondence.

GENERAL TERMS AND CONDITIONS OF ETHICAL APPROVAL:

- Adequate record-keeping is important. If the project involves signed consent, you should retain the completed consent forms which relate to this project and a list of all those participating in the project, to enable contact with them in the future if necessary. The duration of record retention for all clinical research data is 15 years.
- You must notify the Research Ethics Committee of any events which might warrant review of the approval or which warrant new information being presented to research participants, including:
  (a) serious or unexpected adverse events which warrant protocol change or notification to research participants,
  (b) changes to the protocol,
  (c) premature termination of the study.
- The Committee must be notified within 72 hours of any serious adverse event occurring at this site.
- Approval is valid for **5 years** from the date of this letter, after which an extension must be applied for. Investigators are responsible for providing an annual review to the RAH REC Executive Officer each anniversary of the above approval date, within 10 workings days, using the Annual Review Form available at: http://www.rah.sa.gov.au/rec/index.php
- The REC must be advised with a report or in writing within 30 days of completion.

Should you have any queries about the HREC's consideration of your project, please contact Ms Heather O'Dea on 08 8222 4139, or rah.ethics@health.sa.gov.au .

You are reminded that this letter constitutes ethical approval only. You must not commence this research project at a SA Health site until separate authorisation from the Chief Executive or delegate of that site has been obtained.

This Committee is constituted in accordance with the NHMRC's *National Statement on the Ethical Conduct of Human Research* (2007). The HREC wishes you every success in your research.

Yours sincerely,

A/Prof A Thornton
CHAIRMAN
RESEARCH ETHICS COMMITTEE